Designed Construction of Hydrogen-bonded Host Lattices with Urea/Thiourea, Guanidinium and Selected Anions

HAN, Jie

A Thesis Submitted in Partial Fulfillment of the Requirements for the Degree of Doctor of Philosophy in Chemistry

March, 2009

Thesis/Assessment Committee

Prof. Tony K. M. Shing (Chair)

Prof. Ken C. F. Leung (Committee Member)

Prof. Thomas C. W. Mak (Thesis Supervisor)

Prof. Wing Hong Chan (External Examiner)

Prof. Michael D. Ward (External Examiner)

Acknowledgment

I should like to express my sincere thanks to Prof. Thomas C. W. Mak for his kind guidance, invaluable advice and continuous encouragement during my PhD study in the past three years. I deeply appreciate the time and effort that he spent in introducing me to the wonderful world of crystal engineering.

I am also grateful to Prof. Xiao-Li Zhao, Dr. Xu-Dong Chen, Dr. Shuang-Quan Zang, Dr. Chong-Qing Wan, Dr. Guang-Gang Gao, Ms. Hoi-Shan Chan, Mr. Minji Wang, and Mr. Ping-Shing Cheng for their kind assistance and encouragement.

In particular, I wish to thank Prof. Chi-Keung Lam (Sun Yat-Sen University), Dr. Liang Zhao and Mr. Chung-Wah Yau for their helpful discussion and suggestions.

I should also like to acknowledge the award of a studentship by The Chinese University of Hong Kong and financial support by The Hong Kong Research Grant Council (GRF CUHK 402003 and 402206).

Lastly, and most importantly, I wish to thank and honor my parents. They brought me into this world, raised me, supported me, taught me, and loved me. To them I dedicate this thesis.

December, 2008

Jie Han

Department of Chemistry

The Chinese University of Hong Kong

Abstract

This thesis reports a systematic investigation on the generation of new inclusion compounds by the combined use of urea/thiourea, guanidinium ion and various organic anions as building blocks of hydrogen-bonded host lattices and selected quaternary ammonium ion as the enclosed guests.

Various acids bearing specific functional groups have been explored as structure building components, including boric acid, Kemp's triacid, heterocyclic (thio)urea derivatives, aryl and *N*-heteroaryl carboxylic acids and (dithio)squaric acid. All the co-crystals and inclusion compounds built of molecular components in the afore-mentioned categories have been characterized by single-crystal X-ray analysis. As a result, the complexes exhibit a rich variety of inclusion topologies, such as networks containing isolated cages, open channels, intersecting tunnels, double-layer systems, and sandwich-like as well as wave-like layer structures.

Self-assembly of two-dimensional hydrogen-bonded honeycomb grids exhibiting the rosette motif has been conducted with the guanidinium cation and various anions as the building blocks, tetraalkylammonium ions of suitable bulk being employed as interlayer templates. It is noteworthy that the rosette layer constructed from three different trigonal-planar molecular components has been achieved. In addition, deviating from conventional topological design, the generation of new rosette layers, albeit highly distorted, has also been accomplished with 1,2-dithiosquarate and the dianionic form of 1,1'-biphenyl-2,2',6,6'-tetracarboxylate that do not conform to C_3-symmetry. Although threefold molecular symmetry is regarded as a sacrosanct requirement for molecular building blocks in the construction of hydrogen-bonded rosette motif, this study shows that rosette

motifs can be generated even if one of the building blocks does not have inherent threefold symmetry.

Study of compounds containing the deprotonated forms of Kemp's triacid (H_3KTA) has revealed the chair or twist-boat conformation in six crystal structures. X-ray structural analysis showed that $[C(NH_2)_3^+] \cdot [C_6H_6(CH_3)_3(COOH)_2(COO^-)]$ (**2.2.2**) exhibits a corrugated layer structure which mimics the rosette motif constructed from the guanidinium ion and the hydrogen carbonate dimer. The tricarboxylate form of Kemp's triacid KTA^{3-} in $3[C(NH_2)_3^+] \cdot [C_6H_6(CH_3)_3(COO^-)_3]$ (**2.2.4**) registers a record number of eighteen acceptor hydrogen bonds involving the convergent N–H donor sites from nine guanidinium ions. The crystal structure of $3[(C_2H_5)_4N^+] \cdot 20[C(NH_2)_3^+] \cdot 11[C_6H_6(CH_3)_3(COOH)\ (COO^-)_2] \cdot [C_6H_6(CH_3)_3(COOH)_2(COO^-)] \cdot 17H_2O$ (**2.2.3**) features a hydrogen-bonded aggregate with a centrosymmetric pseudo-octahedral arrangement of H_2KTA^- anions surrounding an inner core composed of eight guanidinium ions. The unusual twist-boat conformation of KTA^{3-} is found in $[(CH_3)_4N^+] \cdot 2[C(NH_2)_3^+] \cdot [C_6H_6(CH_3)_3(COO^-)_3] \cdot 2H_2O$ (**2.2.6**), which is stabilized by the co-existence of guanidinium and tetramethylammonium cations.

Systematic investigation on hydrogen-bonded supramolecular assembly using aromatic carboxylic acids bearing linear or bent skeletons with urea/guanidinium resulted in the formation of mainly $R_2^2(8)$ and $R_2^1(6)$ synthon motifs. In addition, isostructures were also constructed by varying the length of the linker between two carboxylate groups, as in naphthalene-2,6-dicarboxylate (**2.3.2**) and biphenyl dicarboxylate (**2.3.3**).

Investigation on a series of hydrogen-bonded networks constructed with *N*-heteroaryl acids is described in Section 3.4. In this section, we focused on the

connection modes within the heteroaryl dimer. The study of co-crystals and inclusion compounds based on 2-thiobarbituric acid (TBA) or trithiocyanuric acid (TCA) indicated that the dimer of TBA is present in all three crystals in the forms of ribbon, tetramer or separated dimer. In the case of 5-nitrobarbiturate, its dimer occurs in two ammonium salts and in three of its four thiourea complexes, but is absent in all three urea complexes.

摘　　要

本論文報導並討論了一系列新穎包合物的製備及其單晶結構。該類包合物均由有機陰離子（如：方酸根、順式-1,3,5-三甲基環己烷-1,3,5-三羧基酸根、巴比妥酸根、對/間苯二甲酸根等）以及脲/硫脲、胍基作爲晶格的主體建築材料，配合不同大小的四正烷基銨陽離子作爲客體範本而生成。這些包合物顯示出豐富的拓撲幾何結構， 如隔離的籠狀結構、雙管道、交叉管道、單/雙層狀結構等。

胍基和碳酸根可以通過氫鍵形成二維的超分子玫瑰花狀結構，在該二組分玫瑰花體系中引入具有類似 C_3 對稱性的硼酸，首次成功合成了新穎的三組分層狀玫瑰花結構。此外，偏離傳統的拓撲互補理論，利用非 C_3 對稱性的1,2-硫代方酸根和聯苯四酸根與 C_3 對稱性的胍基結合，輔助正烷基銨陽離子作爲客體範本，成功合成了准玫瑰花層狀結構。

通過對順式-1,3,5-三甲基環己烷-三羧基酸根作爲主要碳氧陰離子的六個晶體結構研究表明，該酸在晶體中展現出船式（**2.2.1** ~ **2.1.5**）或扭船式（**2.2.6**）的構型。晶體 **2.2.2** 由三羧基酸根和胍基組成的玫瑰花狀的結構單元構成。而包合物 **2.2.3** 則由 8 個胍基組成的八面體核與周圍六個酸根相連而構成。

研究結果還發現，利用不同長度和角度的連接臂的苯/萘二羧酸，與脲、胍基的氫鍵連接模式都以產生 $R_2^2(8)$ 和 $R_2^1(6)$ 結構單元爲主。其中，2,6-萘二羧酸和 1,4-聯苯二酸作爲主體建築材料與胍基形成的晶體結構具有相同氫鍵連接模式。此外， 通過 9 個有關 5-硝基巴比妥酸的晶體結構研究發現， 5-硝基巴比妥酸二聚體出現在相關的硫脲類包合物中，但在脲類包合物中則不存在。

Table of Contents

Acknowledgment.....i

Abstract.....ii

Table of contents.....vi

Index of compounds.....ix

Chapter 1. Introduction.....1

1.1 Inclusion compounds.....1

1.1.1 Development of inclusion chemistry.....1

1.1.2 Urea/thiourea inclusion compounds.....6

1.2 The significance of hydrogen bonds in crystal engineering.....10

1.2.1 Nature of hydrogen bonding.....10

1.2.2 Graph-set encoding of hydrogen-bonding pattern.....11

1.2.3 Supramolecular synthons.....12

1.3 Hydrogen-bonded rosette motifs.....17

1.3.1 Rosette motif based on C_3-symmetric molecular building blocks.....17

1.3.2 Use of non-C_3-symmetric molecules to build up a rosette motif.....23

1.4 Research strategies.....24

1.4.1 Complementarity in hydrogen-bonded network.....24

1.4.2 Changeable number of hydrogen-bond donors and acceptors.....27

1.4.3 Kemp's triacid as a building unit.....28

1.4.4 Urea derivatives as build blocks.....29

1.4.5 Quaternary ammonium guest templates.....30

Chapter 2. Description of Crystal Structures.....31

2.1 Strategies in designing new supramolecular rosette motifs.....31

2.1.1 Crystalline compounds constructed with boric acid.....31

2.1.2 Crystalline compounds constructed with squaric acid.....41

2.1.3 Crystalline compounds constructed with 1,1'-biphenyl-2,2',6,6'-tetracarboxylic acid.....54

2.2 Hydrogen-bonded molecular complexes based on Kemp's triacid 69

2.3 Supramolecular hydrogen bonding motifs based on aromatic carboxylic acids.....86

2.4 Supramolecular hydrogen bonding motifs based on *N*-heteroaryl acids.....105

2.4.1 Inclusion compounds containing anions of 2-thiobarbituric acid/ trithiocyanuric acid.....105

2.4.2 Inclusion compounds containing anions of 5-nitrobarbituric acid.....126

2.4.3 Inclusion compounds containing anions of imidazole-4,5-dicarboxylic acid 151

Chapter 3. Summary and Discussion..... 161

3.1 Strategies in designing new supramolecular rosette motifs..... 161

3.2 Hydrogen-bonded molecular complexes based on Kemp's triacid.....173

3.3 Supramolecular hydrogen bonding motifs based on the aromatic carboxylic acids.....176

3.4 Supramolecular hydrogen bonding motifs based on *N*-heteroaryl acids.....180

3.4.1 Discussion about inclusion compounds containing anions of 2-thiobarbituric acid/trithiocyanuric acid.....180

3.4.2 Discussion about inclusion compounds containing anions of 5-nitrobarbituric acid.....181

3.4.3 Discussion about inclusion compounds containing anions of imidazole-4,5-dicarboxylic acid.....187

3.5 Conclusions.....189

Chapter 4. Experimental.....193

4.1 Preparation.....193

4.1.1 Materials and physical measurements.....193

4.1.2 Preparation of complexes.....193

4.2 X-ray crystallography.....202

References.....203

Appendix I. Publications.....218

Appendix II. Crystal data.....220

Appendix III. Final atomic coordinates, thermal parameters, bond lengths and bond angles, along with their estimated standard deviations (available as an electronic file).

Index of Compounds

Number	Formula	Page*
2.1.1	$2[C(NH_2)_3^+] \cdot (H_4B_4O_9^{2-}) \cdot 2H_2O$	31
2.1.2	$[C(NH_2)_3^+] \cdot (H_4B_5O_{10}^-) \cdot H_2O$	34
2.1.3	$[2(Et_4N^+)] \cdot 2(H_3BO_3) \cdot CO_3^{2-} \cdot 5H_2O$	36
2.1.4	$[(n\text{-}C_3H_7)_4N^+] \cdot [C(NH_2)_3^+] \cdot 2(H_3BO_3) \cdot CO_3^{2-}$	38
2.1.5	$[(n\text{-}C_4H_9)_4N^+] \cdot [C_4O_4H^-] \cdot [H_3BO_3]$	41
2.1.6	$2[(n\text{-}C_3H_7)_4N^+] \cdot 4[CS(NH_2)_2] \cdot [C_4O_2S_2^{2-}] \cdot 2H_2O$	43
2.1.7	$2[(n\text{-}C_4H_9)_4N^+] \cdot 4[CS(NH_2)_2] \cdot [C_4O_2S_2^{2-}]$	45
2.1.8	$2[(n\text{-}C_4H_9)_4N^+] \cdot 6[CS(NH_2)_2] \cdot [C_4O_2S_2^{2-}] \cdot H_2O$	48
2.1.9	$[(n\text{-}C_4H_9)_4N^+] \cdot [C(NH_2)_3^+] \cdot [C_4O_2S_2^{2-}]$	51
2.1.10	$2[(CH_3)_4N^+] \cdot 2[(C_6H_3)_2(COOH)_3(COO^-)] \cdot H_2O$	54
2.1.11	$2[(C_2H_5)_4N^+] \cdot 2[CS(NH_2)_2] \cdot [(C_6H_3)_2(COOH)_2(COO^-)_2]$	57
2.1.12	$[(CH_3)_4N^+] \cdot [C(NH_2)_3^+] \cdot [(C_6H_3)_2(COOH)_2(COO^-)_2]$	60
2.1.13	$[(C_2H_5)_4N^+] \cdot [C(NH_2)_3^+] \cdot [(C_6H_3)_2(COOH)_2(COO^-)_2]$	62
2.1.14	$[(n\text{-}C_3H_7)_4N^+] \cdot [C(NH_2)_3^+] \cdot [(C_6H_3)_2(COOH)_2(COO^-)_2]$	65
2.2.1	$[(CH_3)_4N^+] \cdot [H_2KTA^-] \cdot H_2O$ (H_3KTA = Kemp's triacid)	69
2.2.2	$[C(NH_2)_3^+] \cdot [H_2KTA^-]$	70
2.2.3	$3[(C_2H_5)_4N^+] \cdot 20[C(NH_2)_3^+] \cdot 11[HKTA^{2-}] \cdot [H_2KTA^-] \cdot 17H_2O$	73
2.2.4	$3[C(NH_2)_3^+] \cdot [KTA^{3-}]$	78
2.2.5	$[(n\text{-}C_3H_7)_4N^+] \cdot 2[C(NH_2)_3^+] \cdot [KTA^{3-}]$	80
2.2.6	$[(CH_3)_4N^+] \cdot 2[C(NH_2)_3^+] \cdot [KTA^{3-}] \cdot 2H_2O$	83
2.3.1	$3[(n\text{-}C_4H_9)_4N^+] \cdot 2[C(NH_2)_3^+] \cdot 3[1,4\text{-}C_6H_4(COOH)(CO_2^-)] \cdot [1,4\text{-}C_6H_4(CO_2^-)_2] \cdot 2H_2O$	86
2.3.2	$2[C(NH_2)_3^+] \cdot [2,6\text{-}C_{10}H_4(CO_2^-)_2] \cdot 4H_2O$	88
2.3.3	$2[C(NH_2)_3^+] \cdot [(4\text{-}C_6H_4CO_2^-)_2] \cdot 4H_2O$	91
2.3.4	$[(CH_3)_4N^+] \cdot 5[C(NH_2)_3^+] \cdot 3[(4\text{-}C_6H_4CO_2^-)_2] \cdot 2.5H_2O$	93

* First occurrence in page

Index of Compounds

Number	Formula	Page*
2.3.5	$4[(n\text{-}C_4H_9)_4N^+] \cdot 2[C(NH_2)_3^+] \cdot 2[C(NH_2)_2{}^+NHCO_2^-] \cdot 3[(4\text{-}C_6H_4CO_2^-)_2] \cdot 8H_2O$	96
2.3.6	$[(n\text{-}C_3H_7)_4N^+] \cdot [C(NH_2)_3^+] \cdot [1,3\text{-}C_6H_4(CO_2^-)_2] \cdot 3H_2O$	99
2.3.7	$(C_5H_4N^+CH_2COO^-)_2 \cdot 2H_2O$	101
2.3.8	$[C(NH_2)_3^+] \cdot (C_5H_4N^+CH_2COOH)_2 \cdot CO_3^{2-} \cdot H_2O$	102
2.4.1	$[(Et_4N^+)] \cdot [C_4N_2O_2H_4S^-] \cdot H_2O$	106
2.4.2	$[(Et_4N^+)] \cdot [C_4N_2O_2H_4S^-] \cdot 2H_2O$	107
2.4.3	$2[(n\text{-}C_3H_7)_4N^+] \cdot 2[C_4N_2O_2H_4S^-] \cdot 2[CO(NH_2)_2] \cdot 5H_2O$	109
2.4.4	$[(CH_3)_4N^+] \cdot [C_3N_3S_3H_2^-]$	112
2.4.5	$[(n\text{-}C_4H_9)_4N^+][C_3N_3S_3H_2^-] \cdot 2H_2O$	114
2.4.6	$2[(CH_3)_4N^+] \cdot [C_3N_3S_3H^{2-}] \cdot 5[CO(NH_2)_2] \cdot H_2O$	116
2.4.7	$[(n\text{-}C_3H_7)_4N^+] \cdot [C_3N_3S_3H_2^-] \cdot [CS(NH_2)_2]$	119
2.4.8	$[(n\text{-}C_3H_7)_4N^+] \cdot [C(NH_2)_3^+] \cdot [C_3N_3S_3H^{2-}]$	122
2.4.9	$[(n\text{-}C_4H_9)_4N^+] \cdot [C(NH_2)_3^+] \cdot [C_3N_3S_3H^{2-}]$	124
2.4.10	$[(CH_3)_4N^+] \cdot [(C_4H_2N_3O_5)^-]$	128
2.4.11	$[(n\text{-}C_3H_7)_4N^+] \cdot [(C_4H_2N_3O_5)^-] \cdot H_2O$	130
2.4.12	$2[(CH_3)_4N^+] \cdot 2[(C_4H_2N_3O_5)^-] \cdot (NH_2)_2CS$	133
2.4.13	$2[(C_2H_5)_4N^+] \cdot [(C_4HN_3O_5)^{2-}] \cdot 2(NH_2)_2CS \cdot H_2O$	136
2.4.14	$[(n\text{-}C_3H_7)_4N^+] \cdot [(C_4H_2N_3O_5)^-] \cdot (NH_2)_2CS \cdot 2H_2O$	138
2.4.15	$2[(n\text{-}C_4H_9)_4N^+] \cdot 2[(C_4H_2N_3O_5)^-] \cdot (NH_2)_2CS \cdot H_2O$	140
2.4.16	$[(C_2H_5)_4N^+] \cdot [(C_4H_2N_3O_5)^-] \cdot 2(NH_2)_2CO \cdot 2H_2O$	143
2.4.17	$[(n\text{-}C_3H_7)_4N^+] \cdot [(C_4H_2N_3O_5)^-] \cdot 2(NH_2)_2CO$	146
2.4.18	$[(n\text{-}C_4H_9)_4N^+] \cdot [(C_4H_2N_3O_5)^-] \cdot (NH_2)_2CO \cdot 2H_2O$	148
2.4.19	$3[(C_2H_5)_4N^+] \cdot (H^+)[C_3HN_2^-(CO_2^-)(CO_2H)]_2 \cdot 8H_2O$	151
2.4.20	$2[(C_2H_5)_4N^+] \cdot [C_3HN_2^-(CO_2^-)(CO_2H)] \cdot 2[(NH_2)_2CS]$	153
2.4.21	$[(n\text{-}C_4H_9)_4N^+] \cdot [C_3HN_2H(CO_2^-)(CO_2H)] \cdot [(NH_2)_2CS] \cdot 2H_2O$	155
2.4.22	$[(n\text{-}C_3H_7)_4N^+] \cdot [C_3HN_2^-(CO_2^-)(CO_2H)] \cdot [C(NH_2)_3^+] \cdot H_2O$	158

* First occurrence in page

Chapter 1. Introduction

1.1 Inclusion compounds

1.1.1 Development of inclusion chemistry

Sixty years ago, H. M. Powell wrote the first page of a new fascinating chapter in inclusion chemistry.[1] Early advances on inclusion complexes that contain layer-, channel-, or cage-type (clatharate) host structures were summarized in a monograph in 1964.[2] In 1980s, a five-volume set entitled *Inclusion Compounds* appeared, in which developments in various areas of inclusion chemistry were systematically described.[3] The phenomena of inclusion complexation and molecular recognition are of current interest in the context of host-guest chemistry and supramolecular assembly.[4] Nowadays, the designed construction of new inclusion compounds and investigation of their properties, including porosity,[5] ferroelasticity,[6] and nonlinear optical effects,[7] are keenly pursued. Some selected examples are described in the following paragraphs.

The simple tripodal ligand tris-[2-(naphthalen-2-yloxy)-ethyl]-amine forms inclusion complexes with several electron-deficient aromatic compounds which show interesting fluorescent properties (Scheme 1.1.1).[8]

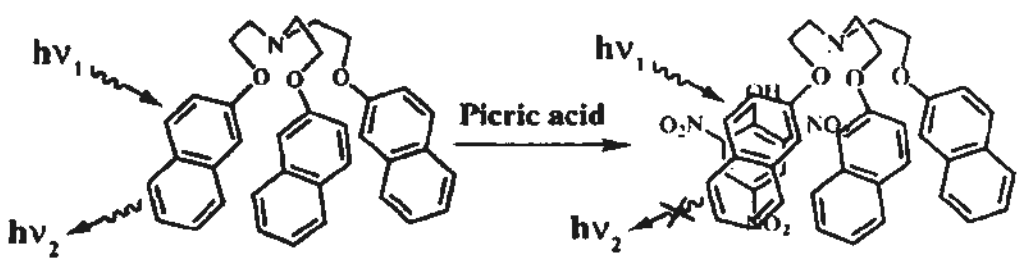

Scheme 1.1.1 Pictorial representation of fluorescence quenching of tris-[2-(naphthalen-2-yloxy)-ethyl]-amine and formation of an inclusion complex in the presence of picric acid.

In another example, advantage is taken of the self-inclusion behavior of mono-substituted *N*-alkyl-*N'*-dimethylammonium-β-cyclodextrins (DMA–C_n–CD). Adamantanecarboxylic acid (Adac) can be used to determine the association constant between the alkyl moiety and the cyclodextrins (CD), as illustrated in Scheme 1.1.2.[9]

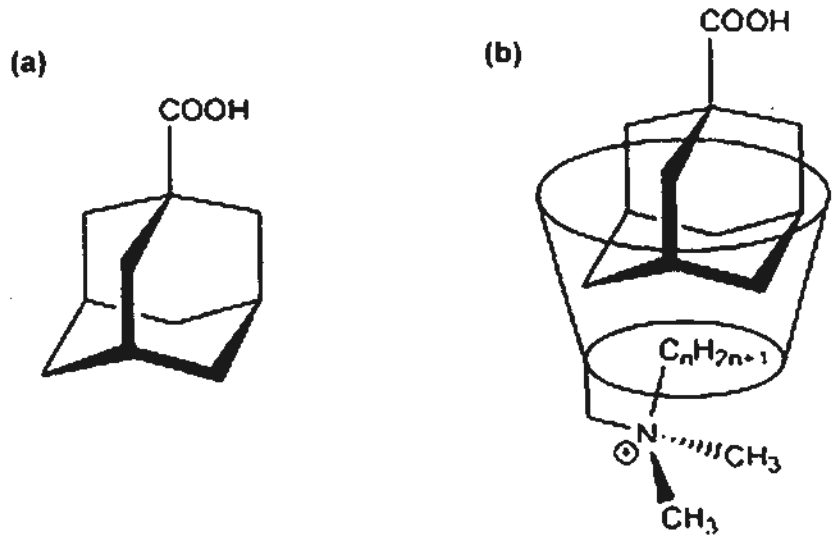

Scheme 1.1.2 (a) 1-Adamantanecarboxylic acid (Adac); (b) inclusion complex between DMA–C_n–CD (n >2) and Adac.

The zeolite-like form of an inclusion compound was demonstrated to be formed by a solid-to-solid transformation from micrometer-sized particles of the rhombohedral modification of 2,4,6-tris-(4-bromophenoxy)-1,3,5-triazine (BrPOT), which features an open pore size of 12 Å that takes up gaseous CS_2 (Scheme 1.1.3). Functionalization of the pore volume of BrPOT by including aromatic amines allowed sorption of molecular iodine.[10]

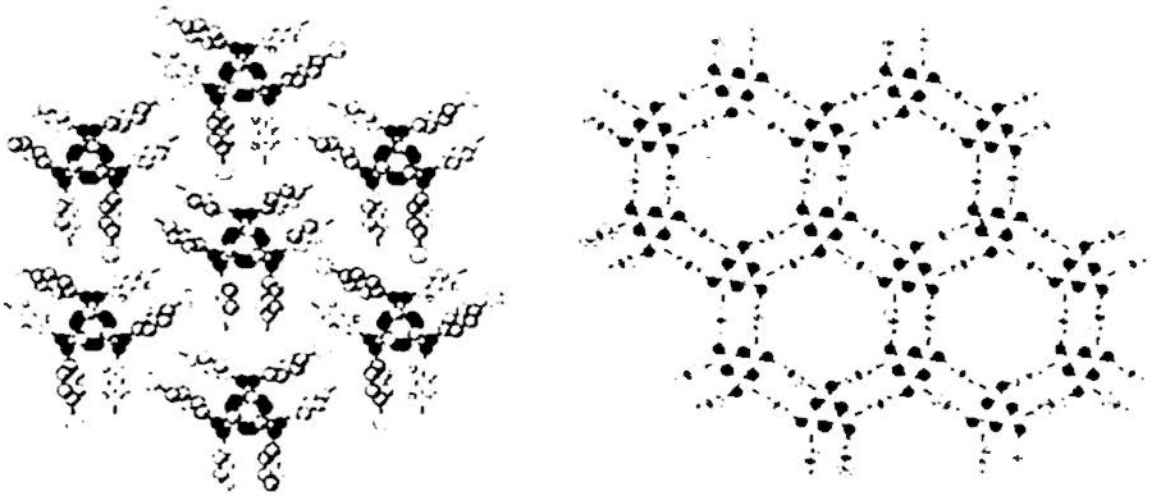

(a) (b)

Scheme 1.1.3 (a) Crystal structure of guest-free BrPOT; (b) channel structure of BrPOT · $(CS_2)_2$ (guests not shown).

The group of O. M. Yaghi has reported highly porous crystalline Zn_4O(1,3,5-benzenetribenzoate)$_2$ (MOF-177, Scheme 1.1.4) combined with a wider opening of the windows up to 14 nm, which is capable of binding large organic guest molecules like C_{60}.[11] In related work, MOF-177 was also loaded with organometallic compounds, e.g. [Cp_2Fe], [$Cu(OCHMeCH_2NMe_2)_2$] and [$CpPd(\eta^3\text{-}C_3H_5)$] via solvent-free adsorption from the gas-phase to form $[L_nM]_a$@MOF-177 inclusion compounds. Remarkably high effective loadings of up to 11 molecules [Cp_2Fe] and 10 molecules [$CpPd(\eta^3\text{-}C_3H_5)$] per cavity were reported in the most recent literature.[12]

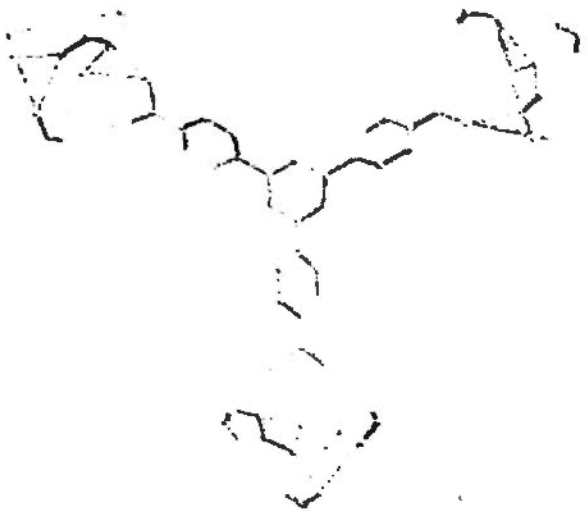

Scheme 1.1.4 The Structure of MOF-177 (Tetrahedral unit is represent ZnO_4 and hydrogen atoms are omitted for clarity).

The relationship between the dihedral angle (Φ) and the chromic behavior of salicylicdeneaniline (SA) was studied by including it in a porous coordination network.[13] Thermochromic SA becomes photochromic when trapped inside the $[\{(ZnI_2)_3(L)_2 \cdot 1.4(o\text{-}HOC_6H_4)CH{=}N(p\text{-}ClC_6H_4)\} \cdot 1.0(^tBuOH)]_n$ (L=tris(4-pyridyl) triazine) host network because the dihedral angle of the chromophore is significantly twisted as a result of inclusion (Scheme 1.1.5).

Scheme 1.1.5 Thermo-to-photo-switching of salicylideneanilines by inclusion.

An interesting example that produces polar host frameworks that are preordained by the structure and symmetry of the molecular components was reported by M. D. Ward's group in 2001.[14] The polar "brick" host frameworks were constructed by connecting flexible hydrogen-bonded guanidinium-sulfonate (GS) sheets which has banana-shaped pillars. These polar frameworks guide the alignment of selected guest molecules into polar arrays, affording inclusion compounds that exhibit second harmonic generation activity.

In addition, new tubular inclusion compounds with guest-filled cylinders[15] (Scheme 1.1.6) were constructed from the quasihexagonal GS motif which has proven to be remarkably robust toward the introduction of various organic pendant groups attached to the sulfonate moieties.[16] The cylinders assemble into hexagonal arrays through interdigitation of the organosulfonate residues that project from their outer surfaces, crystallizing in high-symmetry trigonal or hexagonal space groups.

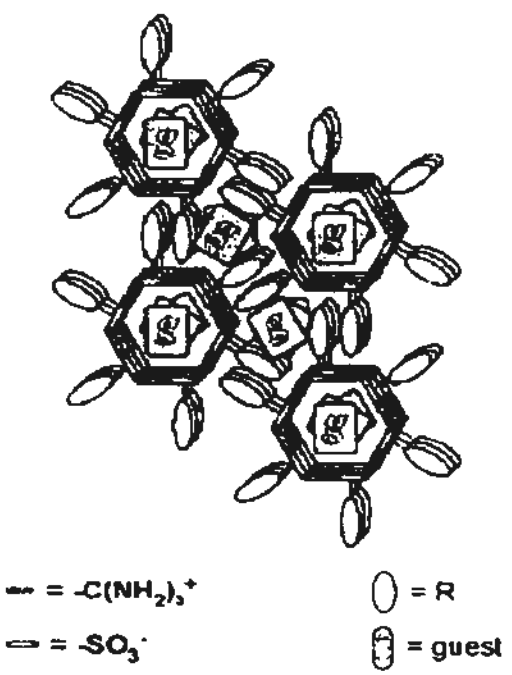

Scheme 1.1.6 Tubular inclusion compounds contain guest molecules within the cylinders.

1.1.2 Urea/thiourea inclusion compounds

Urea was the first organic compound synthesized in the laboratory in 1828. Since it is a small molecule with high symmetry and crystal of good quality can be easily grown, its crystal structure is the earliest to be determined by X-ray crystallography.[17] W. Schlenk's works during 1945 to 1950 laid the foundation of channel inclusion compounds of urea and thiourea (Scheme 1.1.7a).[18]

The similar though different channel-type host frameworks of urea and thiourea that accommodate straight- (Scheme 1.1.7b) and branched-chain aliphatic guest molecules,[3.6a,19] respectively, in their inclusion compounds serve as classical examples in the historical development of host-guest chemistry[20] and crystal engineering.[21]

These phases may be either commensurate, poorly commensurate, or incommensurate with respect to the guest and host repeat distances along the channel direction. Atomic force microscopy research has shown that the degree of commensurism influences crystal growth on the (001) faces, which is the plane perpendicular to the channel direction.[19e,22]

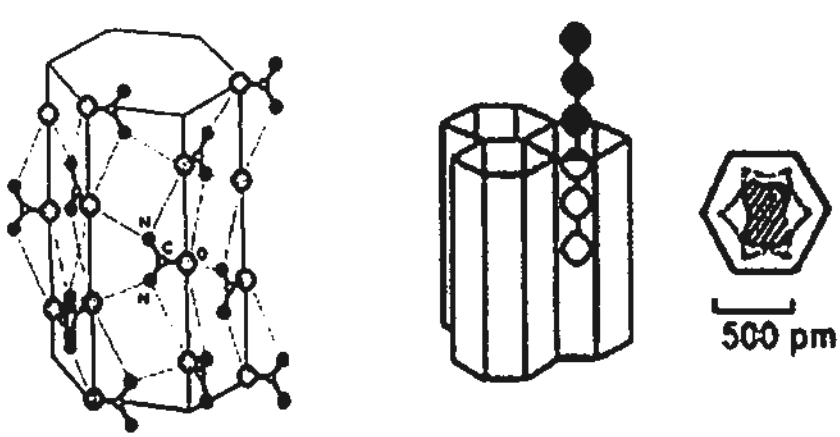

(a) (b)

Scheme 1.1.7 (a) Channel structure in the urea lattice; (b) with a guest *n*-hexane.

With the introduction of various anionic species as an additional host component and hydrophobic peralkylated ammonium ions as guest templates, a series of urea/thiourea/selenourea-anion inclusion compounds can be generated that exhibit a rich variety of host lattices with different topological features.[23]

In previous studies our group have utilized the cooperative effect exerted by the hydrogen bond[24] to stabilize elusive anionic molecular species such as allophanate[25] (Scheme 1.1.8), dihydrogen borate,[26] and the non-benzenoid aromatic D_{6h} and enediolate C_{6v} valence tautomeric forms of the rhodizonate dianion $C_6O_6^{2-}$[27] in the host lattices of some urea-anion inclusion compounds (Scheme 1.1.9).

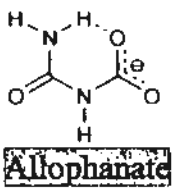

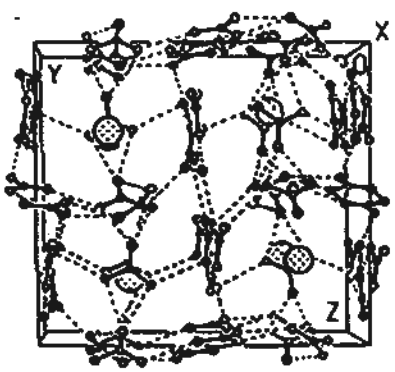

(a)

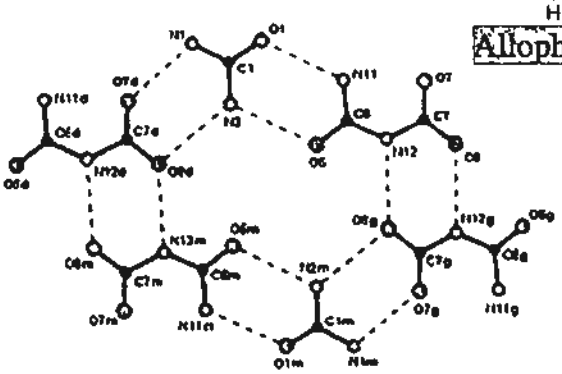

(b)

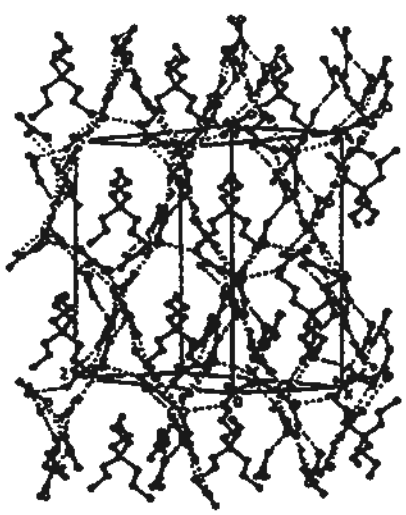

(c)

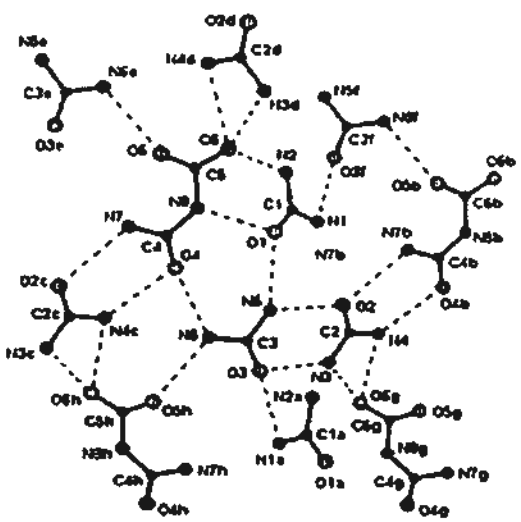

(d)

Scheme 1.1.8 Crystal structure of (a) $[(CH_4)_4N^+] \cdot [NH_2CONHCO_2^-] \cdot 5(NH_2)_2CO$ and (b) a portion of a wide urea-allophanate ribbon in it. (c) Crystal structure of $[(n\text{-}C_3H_7)_4N^+] \cdot [NH_2CONHCO_2^-] \cdot 3(NH_2)_2CO$ and (d) a portion of a wide urea-allophanate ribbon in it.

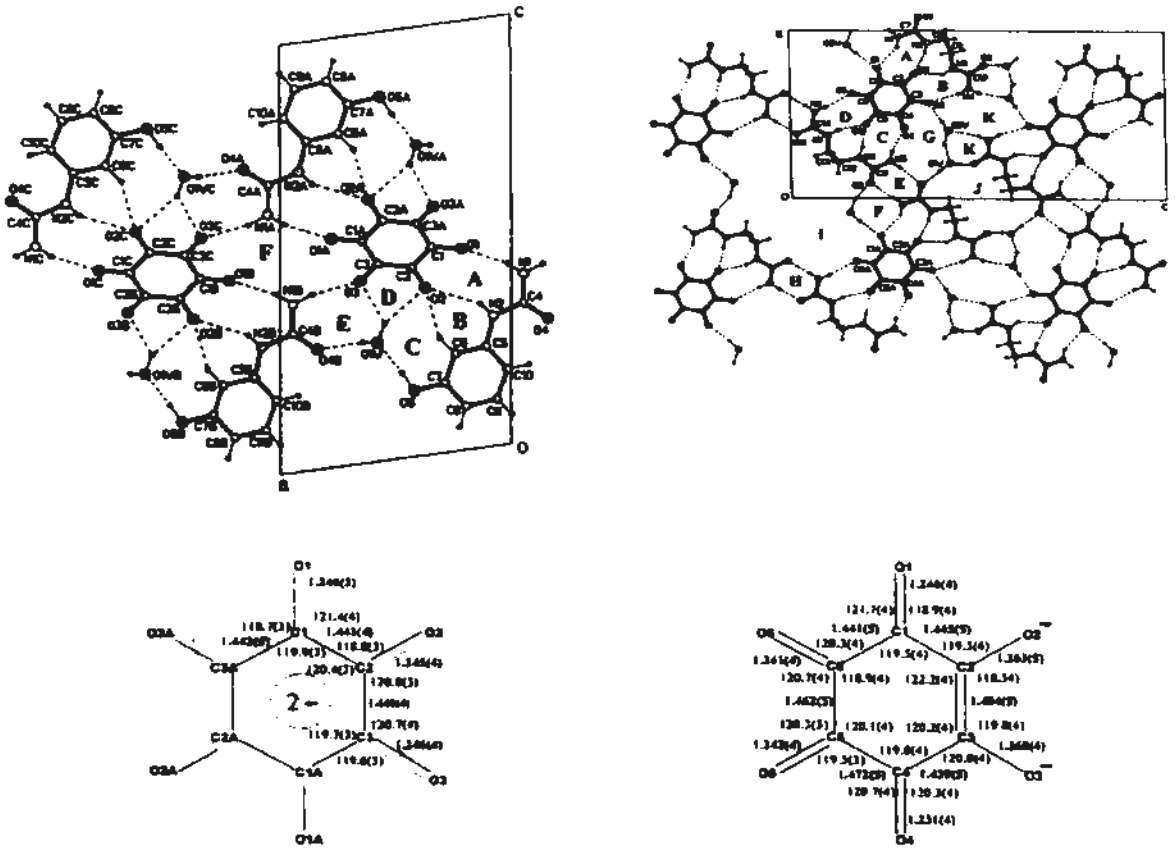

(a) (b)

Scheme 1.1.9 Bond lengths and angles of the (a) D_{6h} and (b) C_{2v} valence tautomers of the rhodizonate dianion in $2[(n\text{-}C_4H_9)_4N^+] \cdot [C_6O_6^{2-}] \cdot 2(m\text{-}OHC_6H_4NHCONH_2) \cdot 2H_2O$ and $[(n\text{-}C_4H_9)_4N^+] \cdot [C_6O_6^{2-}] \cdot 2(NH_2CONHCH_2CH_2NHCONH_2) \cdot 3H_2O$, respectively.

We then showed that the analogous D_{5h} and C_{5v} valence tautomers of croconate $C_5O_5^{2-}$ can be trapped in hydrogen-bonded host lattices constructed with urea and 1,3-dimethylurea, repectively.[28]

Employing thiourea in place of urea, our group subsequently generated a new layer-type inclusion complex $[(n\text{-}C_4H_9)_4N^+] \cdot H_2NCSNHCO_2^- \cdot (NH_2)_2CS$ containing the elusive 3-thioallophanate anion, as well as its precursor $[(n\text{-}C_4H_9)_4N^+] \cdot HCO_3^- \cdot (NH_2)_2CS$.[29] In the majority of the above compounds, the urea or thiourea molecules are inter-connected in the head-to-tail or shoulder-to-shoulder mode by N–H···X (X = O or S) hydrogen bonds (Scheme 1.1.10).

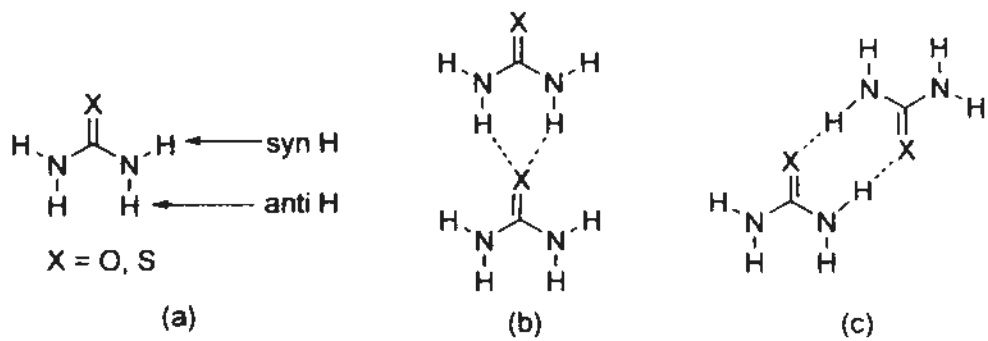

Scheme 1.1.10 (a) Structure of (thio)urea showing *syn* and *anti* hydrogens, (b) conventional head-to-tail mode of (thio)urea, and (c) conventional shoulder-to-shoulder mode of (thio)urea.

Besides the structural analysis in the solid state, the urea inclusion compounds have also received particular attention in view of the wide range of fundamental physicochemical phenomena that they exhibit, e.g. order-disorder phase transitions,[30] molecular motion,[31] and ferroelastic properties.[32] In 2002, M. D. Hollingsworth reported the observation of guest motion during a phase transition in a inclusion compound of urea containing $Cl(CH_2)_6CN$.[6c] This inclusion compound undergo reversible single crystal to single crystal phase transitions in which small conformational changes of guests give rise to guest transitions of

approximately 5.5 Å and exhibit ferroelastic domain reorientation at relatively high forces at different low temperatures.

In a recent example, thiourea crystals with pyridinium iodide and with pyridinium nitrate have been proven to show ferroelectric properties.[6b] In addition, a new thiourea thiazolium bromide inclusion compound undergoes a second order phase transition at 190.5 K.[30a]

1.2 The significance of hydrogen bonds in crystal engineering

1.2.1 Nature of hydrogen bonding

The intermolecular forces that are relevant to the generation and stabilization of host-guest systems have been systematically reviewed.[33] Among all known intermolecular interactions, the hydrogen bond has always been recognized as being particularly significant, especially in biomolecular structures.[34] It is known that the strongest intermolecular interactions are stronger than the weakest covalent bonds.[35] In addition, the directionality of hydrogen bond is particular important, and a number of studies describing the geometries of various hydrogen-bonding systems have appeared.[36] Hydrogen bonding is the most often used as principal tool in design strategies in crystal engineering, generating specific supramolecular architectures.

The hydrogen bond, usually characterized as D–H···A, is mainly an electrostatic interaction that forms between a hydrogen atom (H) [covalently bonded to an electronegative atom (D), hydrogen bond donor] and another atom (hydrogen bond acceptor, A) that has a lone pair of electrons and is fairly electronegative.[24a] The properties of strong, moderate and weak hydrogen bonds D–H···A are listed in Table 1.2.1.

Table 1.2.1 Properties of strong, moderate and weak hydrogen bonds D–H···A.

Types of hydrogen bond	Strong	Moderate	Weak
D–H···A interaction type	Mostly covalent	Mostly electrostatic	Electrostatic/dispersion
D–H···A versus H···A	D–H ≈ H···A	D–H < H···A	D–H << H···A
D···A (Å)	2.2–2.5	2.5–3.2	>3.2
H···A (Å)	~1.2–1.5	~1.5–2.2	>2.2
Lengthening of D–H (Å)	0.08–0.25	0.02–0.08	<0.02
Directionality	Strong	Moderate	Weak
Bond angles (°)	175–180	130–180	90–150
Bond energy (kcal mol^{-1})	14–40	4–15	<4
Types of hydrogen bond	Strong	Moderate	Weak
Relative IR *vs* vibration shift (cm^{-1})	25%	10-25%	<10%
^{1}H downfield shift (ppm)	14–22	<14	-
Examples	(i) Gas-phase dimers with strong acids or strong bases (ii) Acid salts (iii) Proton sponges (iv) Pseudohydrates (v) HF complexes	(i) Acids (ii) Alcohols (iii) Phenols (iv) Hydrates (v) All biological molecules	(i) Gas phase dimers with weak acids or weak bases (ii) Minor components of 3-centre bonds (iii) C–H···O/N bonds (iv) O/N–H···π bonds

1.2.2 Graph-set encoding of hydrogen-bonding pattern

In 1990, M. C. Etter introduced the concept of graph-set analysis for the description of hydrogen-bond patterns in organic crystals.[37] These patterns can be classified according to one of four descriptors: chains (C), rings (R), dimers (D), or intramolecular (self-associating) ring (S). In a graph-set descriptor, the number of hydrogen-bond acceptors (superscript) and donors (subscript) are designated and the total number of atoms involved in the motif is enclosed in parentheses. Examples of the use of these quantitative descriptors are given in Scheme 1.2.1.

$$G_d^a(n)$$

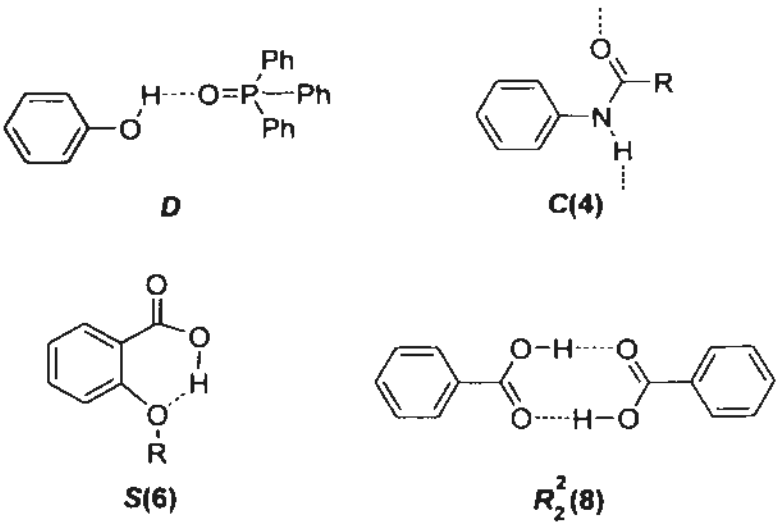

Scheme 1.2.1 Examples of graph-set notation in hydrogen-bonded structural motifs.

1.2.3 Supramolecular synthons

1.2.3.1 Introduction of supramolecular synthons

The term *supramolecular synthons*, as introduced by Desiraju in 1995[3b] refers to structural units within supramolecules which can be formed and/or assembled by known or conceivable synthetic operations involving intermolecular interactions. They may be understood as basic building blocks whose structural motifs remain intact in supramolecular self-assembly, by analogy with Corey's definition of a synthon in traditional organic synthesis.[38]

Noting that all organic crystal structures may be considered to be networks with the supramolecular synthons acting as connections between molecules in the network structures, the dissection of a crystal structure into supramolecular synthons enables a certain structural simplification that is essential in the planning of a synthetic strategy towards a new or modified target network. This strategy is very similar to the retrosynthetic analysis method in organic synthesis.[39]

The observed supramolecular synthons involve motifs held by various intermolecular attractive interactions such as hydrogen bonding, halogen-halogen

interaction, nitro-iodo interaction, and aromatic π-π interaction, as shown in Scheme 1.2.2.[3d,20j,40]

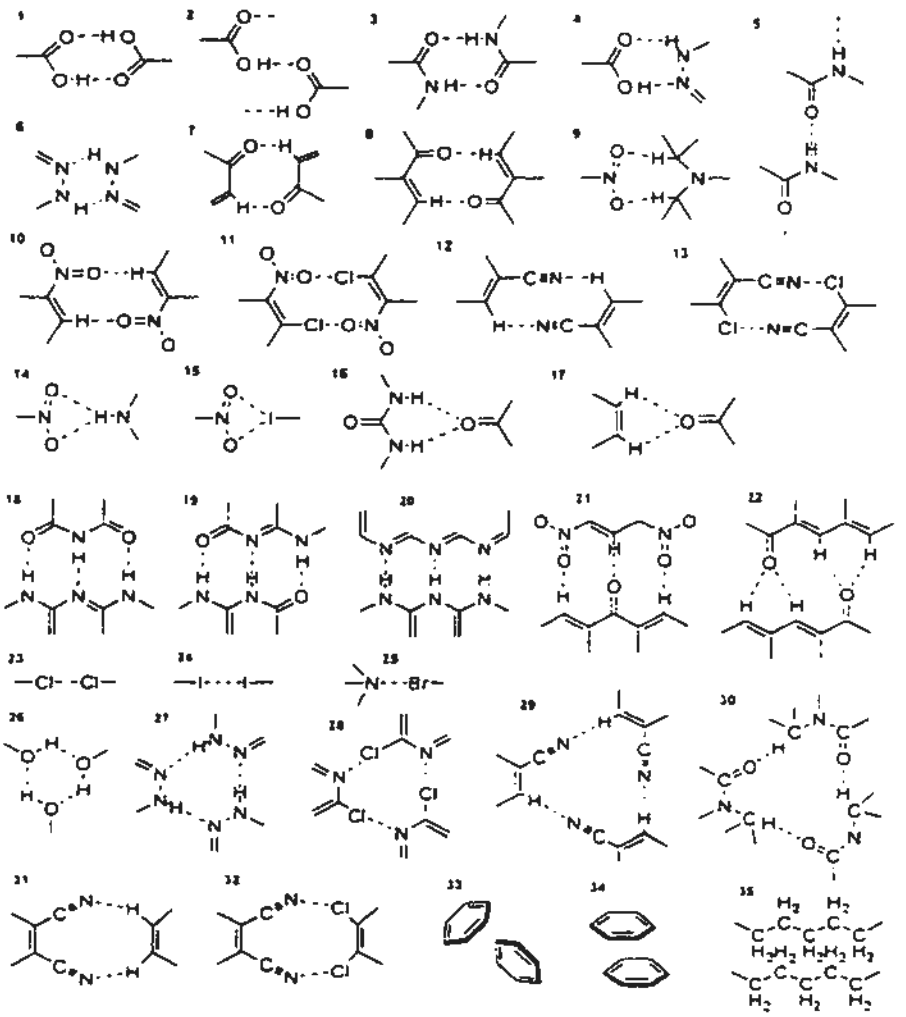

Scheme 1.2.2 Representative supramolecular synthons.

In addition, hydrogen-bonded supramolecular synthons based on intermolecular interactions can either be homomeric or heteromeric motifs. *Homomeric* refer to the presence of two or more identical hydrogen-bond patterns, and *heteromeric* means co-existence of two or more different hydrogen-bond patterns. A homomeric supramolecular synthon containing self-complementary hydrogen bonds in the squarate dimer and a heteromeric supramolecular synthon

containing two different types of hydrogen bonds in the carboxylic acid···carboxamide dimer are shown in Scheme1.2.3.

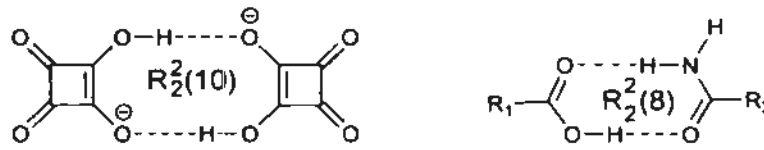

Homomeric synthon Heteromeric synthon

Scheme 1.2.3 Examples of hydrogen-bonded homomeric and heteromeric supramolecular synthons.

1.2.3.2 Supramolecular architecture based on carboxylic dimer or catemer synthons

Carboxylic acids are commonly used as pattern-controlling functional groups for the purpose of crystal engineering. Both in solution[41] and in the solid-state,[42] carboxylic acids generally interact through intermolecular hydrogen bonding to form dimeric or catemeric entities. Hydrogen bonds in these dimers or catemers are highly directive and of considerable strength, and therefore di- and polycarboxylic acids have been extensively used as building blocks for the construction of hydrogen-bonded supramolecular entities.[43,44] Terephthalic acid and isophthalic acid[45] form linear and zigzag ribbons or tapes, respectively. Trimesic acid with its threefold molecular symmetry forms a hexagonal rosette structure,[46] and a three-dimensional diamondoid structure is generated from adamantane tetracarboxylic acid (Scheme 1.2.4).[47]

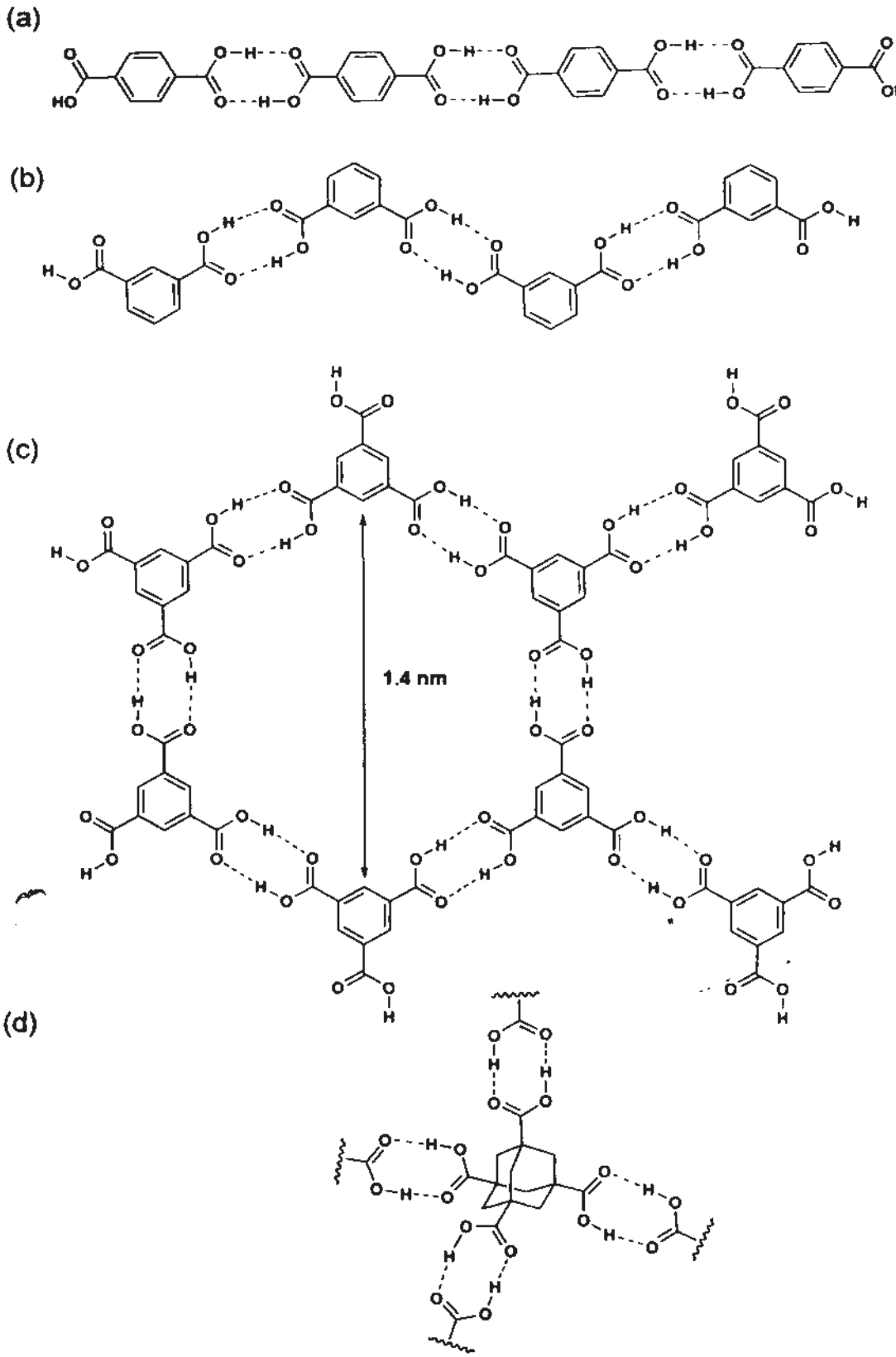

Scheme 1.2.4 (a) Infinite linear tape, (b) crinkled tape, (c) rosette sheet and (d) three-dimensional diamondoid structure network held together by the carboxylic acid dimer synthon.

Recently, G. R. Desiraju reported *syn*, *anti* catemers in a particular family of mono- and di-substituted phenylpropiolic acids. Scheme 1.2.5 shows related one-dimensional catemer motifs.[48]

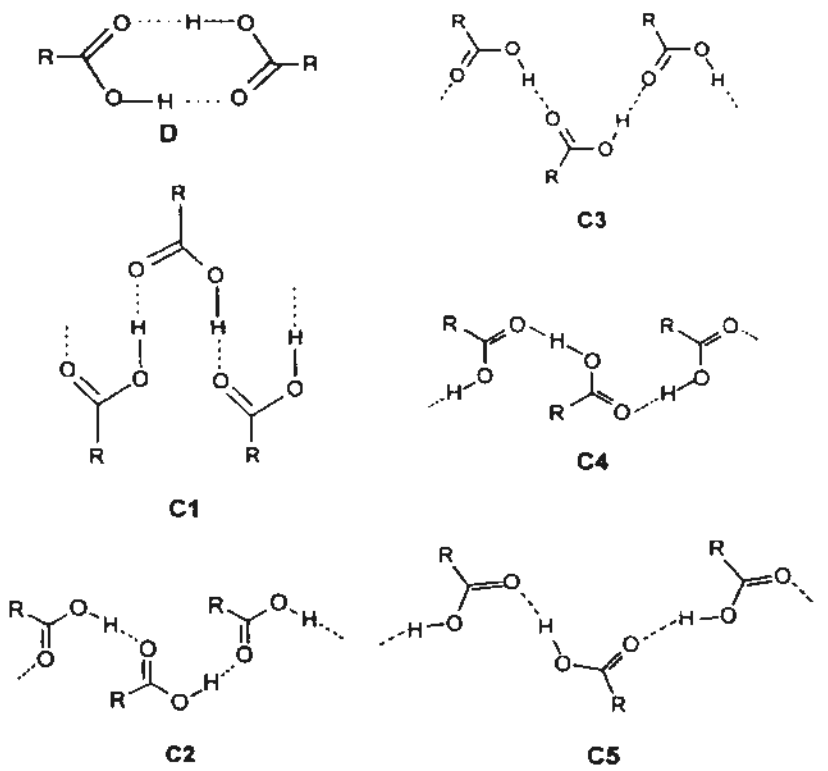

Scheme 1.2.5 Six kinds of carboxylic acid catemer supramolecular synthons: zero-dimensional (D), open chains of various types (C1–C5).

Since charged species form stronger hydrogen bonds,[34a] carboxylate ions have also been used for this purpose.[49] Relative orientation of the carboxylate groups in a dicarboxylate anion and planarity of the whole molecule are crucial factors in determining both the molecular and the supramolecular structure, especially in building layer structures. The planar linear carboxylic acids, such as terephthalic acid and naphthalene-2,6-dicarboxylic acid, and acids with a flexible skeleton, such as Kemp's triacid, are employed for the construction of hydrogen-bonded complexes, as described in the following chapter.

1.3 Hydrogen-bonded rosette motifs

1.3.1 Rosette motif based on C_3-symmetric molecular building blocks

Over the years, chemical entities bearing a rosette motif have attracted considerable interest in connection with supramolecular self-assembly of potentially useful organic functional materials,[50] and many studies have been conducted using computational methods[51] and a plethora of modern instrumental techniques.[52-59] In the context of crystal engineering, an effective strategy of constructing a hydrogen-bonded rosette layer (often described as hexagonal honeycomb grid or sheet) is to make use of C_3-symmetric molecular building blocks of different shapes and sizes such that their donor and acceptor sites are perfectly matched.

The sheet structure of orthoboric acid is the archetypal example of a single-component hydrogen-bonded rosette layer in which the boron atoms are arranged in a planar hexagonal array, and adjacent $B(OH)_3$ molecules are symmetrically linked by a pair of O–H···O hydrogen bonds.[53] Another single-component example is trimesic acid (1,3,5-benzenetricarboxylic acid, H_3TMA), which self-assembles through the carboxylic acid dimer motif into a honeycomb grid, whose stacking generates tunnels of net diameter *ca.* 14 Å for the accommodation of organic guest molecules (Scheme 1.2.4c).[54]

The most notable example of a binary hydrogen-bonded rosette supramolecular structure in the 1:1 complex of melamine with cyanuric acid,[55,56] which has three hydrogen bonds linking every adjacent pair of its two molecular components (Scheme 1.3.1).

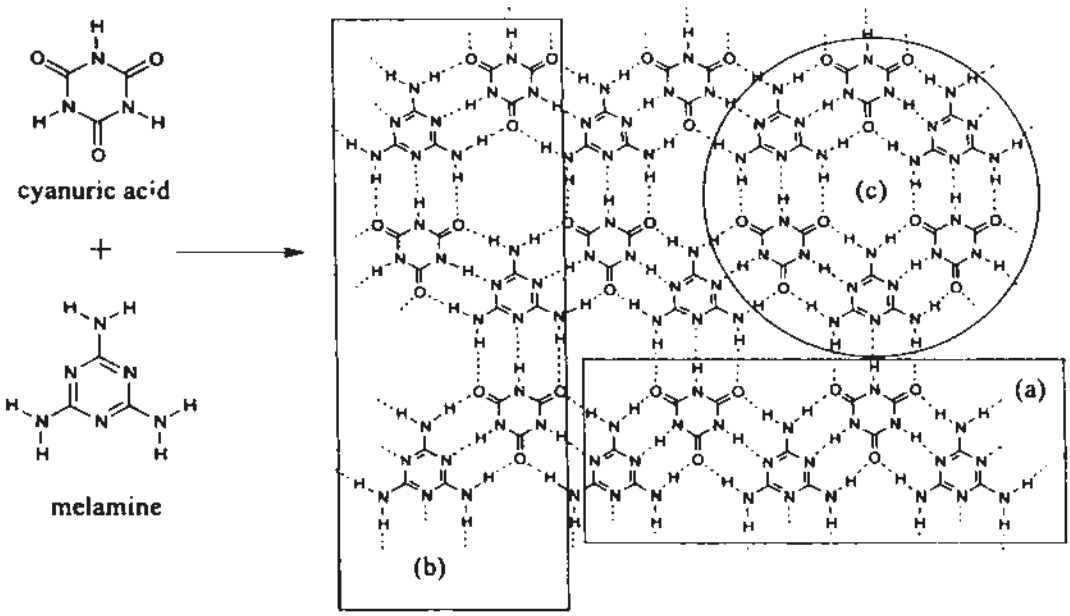

Scheme 1.3.1 Hexagonal layer structure of the 1:1 complex of melamine and cyanuric acid. Three kinds of assembly in lower dimensions are possible: (a) linear tape, (b) crinkled tape and (c) rosette motif.

The same structure is also formed when cyanuric acid is replaced by thiocyanuric acid[56] or using barbituric acid derivatives and 2,4,6-triaminopyrimidine derivatives (Scheme 1.3.2). Interestingly, recent work has demonstrated that the pet food contaminant responsible for the deaths of dogs and cats is caused by the reaction of melamine with cyanuric acid to form insoluble crystalline deposits in the animals' kidneys.[60]

Planar guanidinium cation (GM^+) bearing a particularly C_3 symmetry is a potential structure-determining template in the formation of both coordination polymeric networks[61] and hydrogen-bonded networks.[62] Its internal C_3 symmetry enables the formation of three pairs of strong hydrogen bonds to various oxyanions, generating a stable supramolecular synthon,[13,63] e.g. it is internally prefer associated

with three oxy-anions by three pairs of strong hydrogen bonds as shown in Scheme 1.3.3.

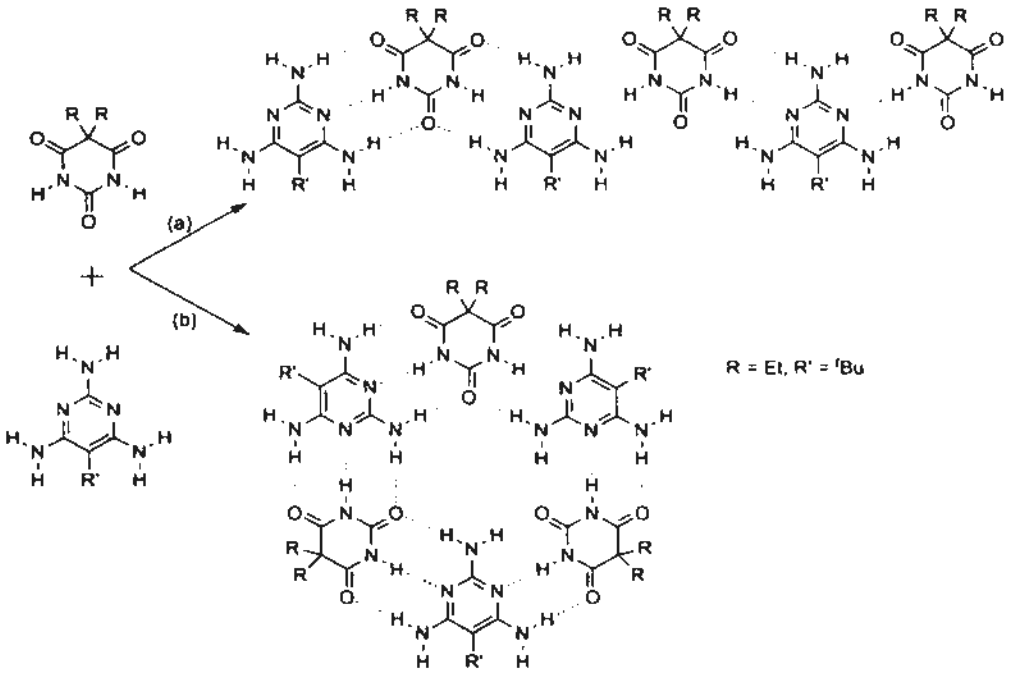

Scheme 1.3.2 (a) Linear tape and (b) rosette 1:1 complexes constructed with barbituric acid derivatives and 2,4,6-triaminopyrimidine derivatives.

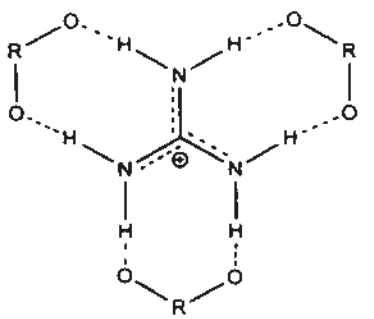

Scheme 1.3.3 Schematic bonding diagram of guanidinium cation with oxy-anions.

Roughly at the same time of Whiteside's work, M. D. Ward systematically reported inclusion compounds based on host frameworks constructed from guanidinium and organodisulfonate ions in the solid state.[14,15,58] The equal number of separate hydrogen-bond donor and acceptor sites with matched geometry allows the formation of persistent guanidinium/sulfonate six-member modular "rosettes"

periodically extended into saturated two dimensional hydrogen-bonded networks (Scheme 1.3.4).

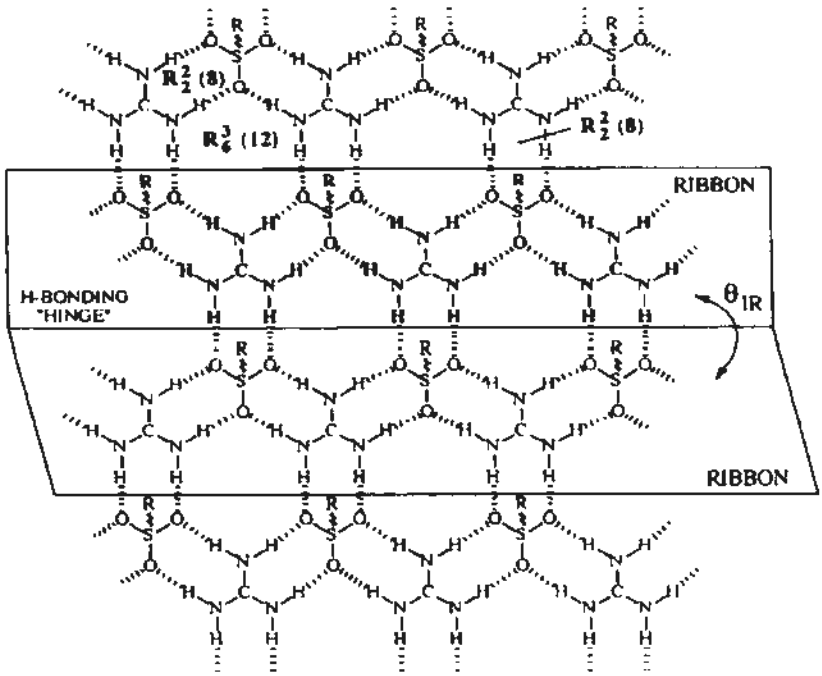

Scheme 1.3.4 Rosette motif constructed by guanidinium and organic sulfonate ions.

The guanidinium monosulfonates display variable mono- and bilayer structures dependent upon the auxiliary *R* group. The inter-ribbon dihedral angle θ_{IR} changes according to the nature of the *R* group, ranging from 171° for small *R* (methyl) to 146° for large *R* (2-naphthyl).

There are several successful examples to separate isomer by forming inclusion compound, such as using tetraphenylhexa-2,4-diynediol to separate aminobenzonitrile isomers,[64] cyclophane to separate picoline and lutidine isomers,[65] 1,1,2,2-tetraphenyl-1,2-ethane diol to separate picoline isomers,[66] and phosphonium salt to separate cyclohexanepolyols.[67] Most recently, the principle of selective guest inclusion by using guanidinium and organic sulfonate ions host frame has been used for xylene isomer separation.[68] In a pair-wise competition of

xylene isomers, *m*-xylene was most favored for inclusion into guanidinium *p*-toluenesulfonate host frame over other xylene isomers.

By analogy to the guanidinium sulfonate structures of Ward, we contrived new structures based on topological equivalence. We have reported a hydrogen-bonded, anionic two-dimensional rosette network assembled with guanidinium and carbonate ions [69,70] (Scheme 1.3.5 and 1.3.6). In the inclusion compounds $4[(C_2H_5)_4N^+] \cdot 8[C(NH_2)_3^+]\cdot 3CO_3^{2-} \cdot 3(C_2O_4)^{2-} \cdot 2H_2O$[69], the guanidinium–carbonate (1:1) rosette layer is folded into a pronounced plane-wave configuration via binding to other guanidinium ions in former crystal structure (Scheme 1.3.7a), as each of its two independent carbonate ions forms 11 acceptor hydrogen bonds, only one fewer than the maximum allowable number.[71]

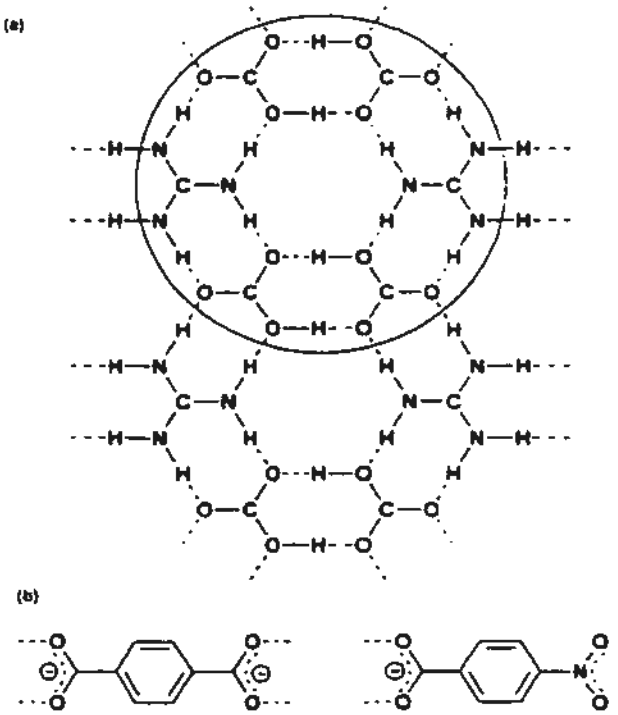

Scheme 1.3.5 (a) Rosette networks composed of guanidinium and dimer of hydrogen carbonate; (b) terephthalate anion and 4-nitrobenzoate anion as suitable "molecular connector" linked with adjacent parallel ribbons into a two dimensional sheet-like rosette work.

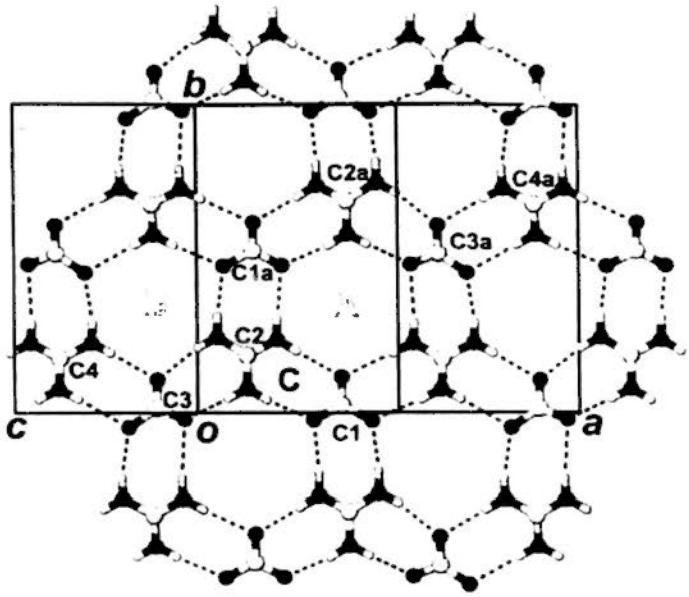

Scheme 1.3.6 Guanidinium cation and carbonate dimer (GM^{+}–CO_3^{-}) rosettes motif.

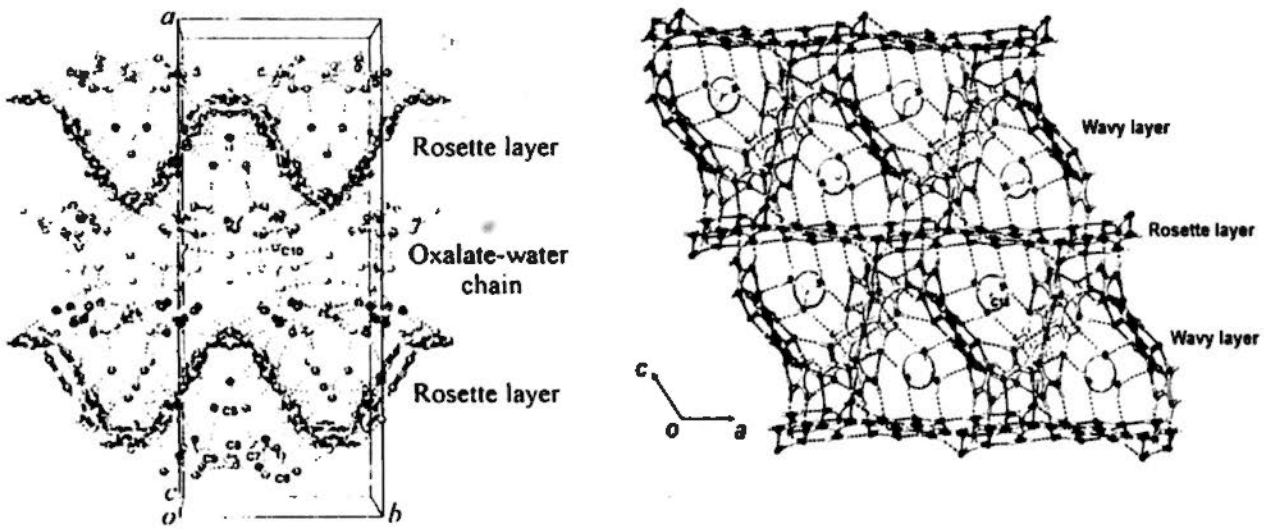

(a) (b)

Scheme 1.3.7 (a) Highly distorted oxalate water layer as a linker to connect the rosette layers of $4[(C_2H_5)_4N^+] \cdot 8[C(NH_2)_3^+] \cdot 3CO_3^{2-} \cdot 3(C_2O_4)^{2-} \cdot 2H_2O$; (b) Wavy layers composed of guanidinium–carbonate–1*H*-imidazole-4,5-dicarboxylate as a linker to join adjacent rosette layers of $[(C_2H_5)_4N^+] \cdot 7[C(NH_2)_3^+] \cdot 3CO_3^{2-} \cdot [C_3N_2H_2(COO^-)_2]$.

In the case of the complex $[(C_2H_5)_4N^+] \cdot 7[C(NH_2)_3^+] \cdot 3CO_3^{2-} \cdot [C_3N_2H_2(COO^-)_2]$, introduction of an ancillary anion, namely 1*H*-imidazole-4,5-dicarboxylate, as an auxiliary template and interlayer spacer suffices to convert the sinusoidal guanidinium–carbonate (1:1) rosette layer to a nearly planar configuration (Scheme 1.3.7b).[70]

1.3.2 Use non-C_3-symmetric molecules to build up a rosette motif

The cyclic oxocarbon acids ($C_nO_nH_2$) and their dianions $(C_nO_n)^{2-}$ have been widely investigated both theoretically and experimentally due to their highly functionalized and interesting structures.[72] The squarate dianion $C_4O_4^{2-}$ has unique electronic and chemical properties in view of its idealized D_{4h} symmetry, and its charged oxygen atoms can function as strong hydrogen-bond acceptor sites. In our previous studies, the squarate dianion has been shown to exhibit a tendency to hydrogen-bond with adjacent urea/thiourea molecules along two or four coplanar directions (Scheme 1.3.8).[73]

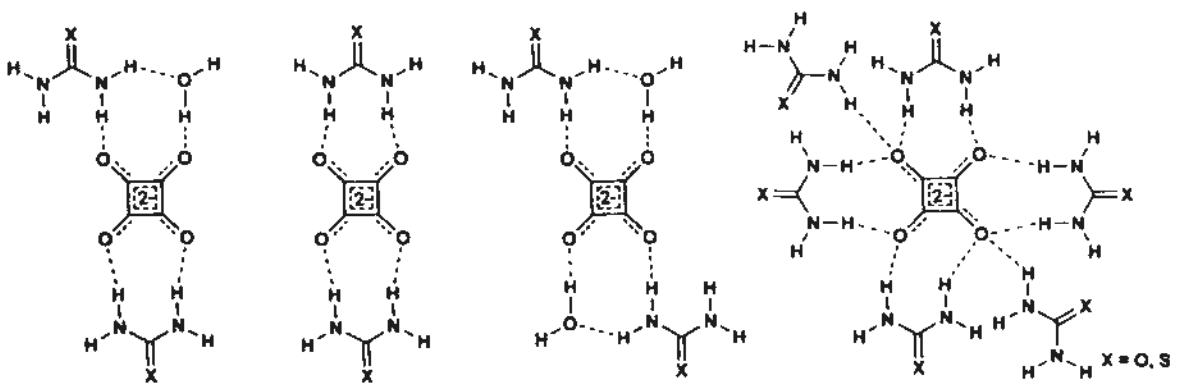

Scheme 1.3.8 Hydrogen bonding schemes between urea/thiourea and squarate dianion.

Substitution of one or more of the O atoms by heteroatoms like S or N leads to the so-called "pseudooxocarbons" (Fatiadi, 1980) in which the symmetry is partly destroyed. Substitution of oxygen atom at the 1,2 positions of the squarate dianion by sulfur atoms yields 1,2-dithiosquarate $C_4O_2S_2^{2-}$, in which the charges are located mainly at sulfur atoms. In hydrogen-bonded systems, sulfur is often overlooked as a hydrogen-bond acceptor[74] and concluded to be a poor hydrogen-bond acceptor from a statistical analysis of the early crystallographic data.[75]

However, owing to the weakness of the (guanidinium)N–H···S hydrogen bond compared to N–H···O, the thio analog 1,2-dithiosquarate was selected to ascertain if it can function as a hydrogen-bond acceptor in three principal directions for the generation of a rosette network.

1,1'-Biphenyl-2,2',6,6'-tetracarboxylic acid, possessing idealized D_{2d} symmetry, is known to constitute a self-complementary hydrogen-bonding tecton with multiple donor and acceptor sites. Its dianion BPTC has a rigid non-planar molecular skeleton held by a pair of intramolecular hydrogen bonds, so that the two phenyl rings are nearly orthogonal to each other.[76] Nevertheless, although the carboxyl and carboxylate groups are widely used in forming hydrogen-bonded adducts, there are few reports of such crystal structures based on BPTC. Here, the non-planar molecule was also explored as a building block to construct a rosette network, as reported in the following chapter.

1.4 Research strategies

1.4.1 Complementarity in hydrogen-bonded network

The most important chemical concept in constructing hydrogen-bonded network is complementarity, i.e. the hydrogen-bonding donor and acceptors should

match in terms of number, shape and interatomic distances. On the other hand, the relevant crystallographic concept is the symmetry operator that interrelates the two molecules of each intermolecular hydrogen bond. A successful design requires a persistent hydrogen-bonded pattern that maintain both the chemical connectivity and the associated symmetry operator.[77]

(a). Hydrogen-bonded rosette network

The most notable and cited examples using this complement rule to design rosette layer motif have been mentioned in Section 1.3. An effective strategy of constructing a new hydrogen-bonded rosette layer is to make use of C_3-symmetric molecular building blocks of different shapes and sizes such that their donor and acceptor sites are perfectly matched.

In our ongoing design of anionic supramolecular rosette host networks using hydrophobic quaternary ammonium ions as guest templates,[23] we aimed at the self-assembly of the rosette layer from more than two molecular components, which their donor and acceptor sites are perfectly matched. In the context of crystal engineering, the carbonate ion and the hydrogen carbonate dimer serves as useful building blocks for the construction of the rosette layer [69,70] and rosette ribbon, [49b] respectively. Therefore, our interest focuses on the generation of new host lattices featuring rosette motifs using guanidinium cation, carbonate anions in combination with the third rosette component, here, namely boric acid, as the building block, leading to the formation of three component rosette layers.

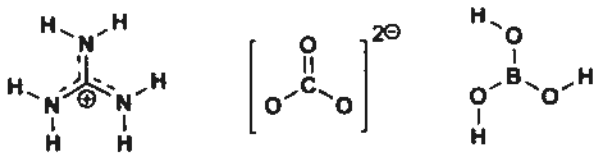

We also tried to extend the conventional topological design of supramolecular rosette layer structures by relaxing the requirement of exact or near C_3 symmetry of the molecular building blocks. In this instance, 1,2-dithiosquaric acid and non-planar 1,1'-biphenyl-2,2',6,6'-tetracarboxylate proved to be suitable starting materials for the construction of distorted hydrogen-bonded rosette layers.

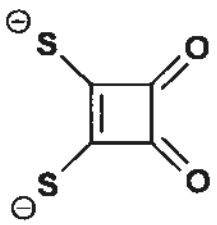

1,2-Dithiosquarate dianion

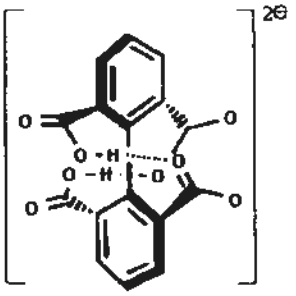

1,1'-Biphenyl-2,2',6,6'-tetracarboxylate dianion

(b). Hydrogen bonded network based on carboxylic acids

We are interested in the design and construction of ordered hydrogen-bonded supramolecular networks which rely on appropriate topological synthons to obtain the desired packing motif. Various supramolecular synthons based on guanidinium and carboxylate,[78] through changing of the position of carboxylate, altering the length of linker between carboxylate groups, or increasing the flexibility of the linker, have been explored in the generation of hydrogen-bonded supramolecular structures.

Here terephthalate (a), naphthalene-2,6-dicarboxylate (b), and 4,4'-biphenyldicarboxlate (c), which possess rigid molecular skeletons and strong *exo* acceptor groups with different linker lengths, are selected as building blocks for the construction of hydrogen-bonded complexes.

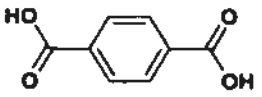

Terephthalic acid
(a)

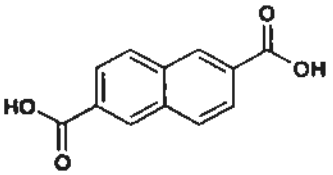

Naphthalene-2,6-dicarboxylic acid
(b)

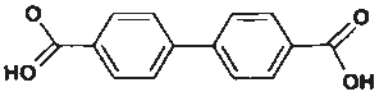

4,4'-Biphenyldicarboxylic acid
(c)

Besides using the above linear bicarboxylic acid, the following angular carboxylate have also been employed as the major building blocks.

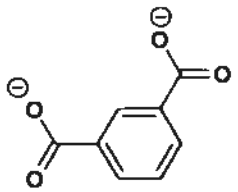

Isophthalate
(d)

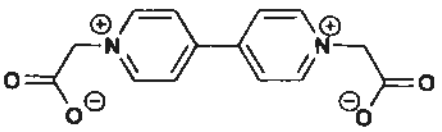

N,N'-bis(carboxymethyl)-4,4'-bipyridinium
(e)

1.4.2 Changeable number of hydrogen-bond donors and acceptors

Heterocyclic compounds are important in both pharmaceutical materials and biological systems and often interact with other molecular components in the system in a manner dependent upon their hydrogen bonding properties.[79]

In the last decade, trithiocyanuric acid (2,4,6-trimercapto-1,3,5-triazine) and its sodium salt are widely applied in industry, analytical chemistry and biochemistry.[80] Barbituric acid is also of particular interest in view of its pharmacological, biochemical and biological capabilities.[81] For example, the thymine group of deoxyribonucleic acid (DNA) gives barbituric acid upon biological oxidation.[82]

Herein we make use of the monoanion or dianion of cyclic ureas such as trithiocyanuric acid and 2-thiobaribiturate (processing a planar and alternating set of hydrogen-bond donor and acceptor sites) to incorporate urea/thiourea/guanidinium as additional components to construct new supramolecular inclusion structures.

In the proposed study, 5-nitrobarbituric acid (also named dilituric acid or 5-nitro-2,4,6-trihydroxypyrimidine) is also selected as a structural component instead of barbituric acid because presence of the nitro group provides additional hydrogen-bonding acceptor sites for supramolecular assembly of the host lattice. In addition, although the nitro group is a weak acceptor, its recognition pattern involves a combination of electronic properties and directionality of the lone pair electrons on the oxygen atoms, which can be modulated by the character of the hydrogen atom donating groups.[83]

The anions or dianions of the following *N*-heteroaryl acids, from which one or two protons can be readily detached, are selected as ingredients for supramolecular assembly through hydrogen bonding in the Chapter 2.

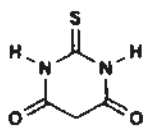

Thiobarbituric acid

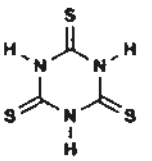

Trithiocyanuric acid

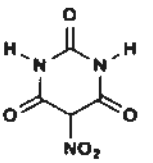

5-Nitrobarbituric acid

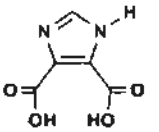

1*H*-imidazole-4,5-dicarboxylic acid

1.4.3 Kemp's triacid as a building unit

Kemp's triacid has three carboxylic groups alternately arranged at the 1,3,5 position of the conformationally flexible cyclohexane ring (Scheme 1.4.1). In solution[84,85] or the solid state,[84,86] the *chair* conformation of Kemp's triacid made up of head-to-tail cyclic hydrogen bonded units, with two at the head and one at the tail predominates, and the three methyl groups are in equatorial positions. However, the trianion is an exception, with its acid groups in equatorial positions due to electrostatic repulsion.[87,88] Six new crystal structures based on mono, di or tri-protonated kemp's triacid are described in the present thesis.

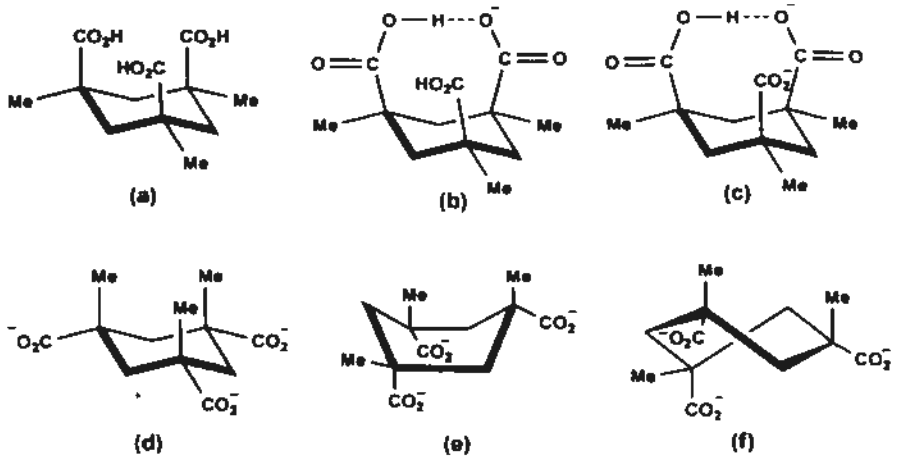

Scheme 1.4.1 Schematic representation of possible conformations of neutral and deprotonated forms of Kemp's triacid: (a) H_3KTA chair form; (b) chair H_2KTA^-; (c) chair H_2KTA^{2-}; (d) chair KTA^{3-} with carboxylate groups in equatorial positions; (e) boat KTA^{3-}; and (f) twist-boat KTA^{3-}.

1.4.4 Urea derivatives as build blocks

Urea and thiourea are suitable candidates for the construction of hydrogen-bonded lattices since both are known to form channel-type inclusion complexes with a wide range of neutral compounds, such as medium-sized alicyclic or highly branched hydrocarbons, ketones, esters, alkane, halides, and even organometallics.[3,19] Here urea, thiourea and guanidinium ion are selected as additional main building blocks to construct new inclusion complexes that may exhibit new interesting topologies.

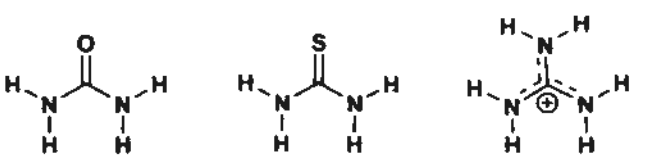

1.4.5 Quaternary ammonium guest templates

Hydrophobic tetra-*n*-alkylammonium cations of different sizes have been used as cationic guest templates for the generation of new host lattices, in order to gauge the influence of the changing shapes and sizes of the enclosed guests. The quaternary ammonium cations shown below are used in the present research project.

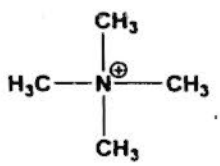

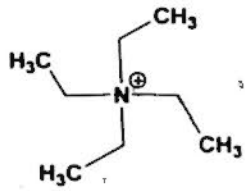

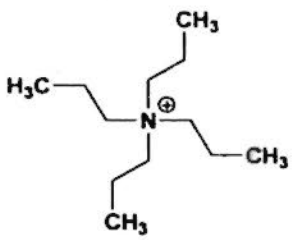

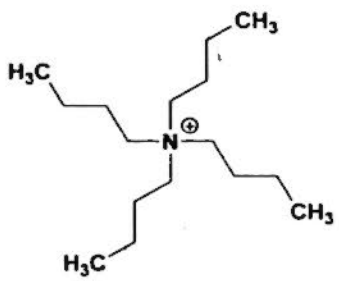

In this thesis, a series of co-crystals and inclusion complexes built of the above molecular species have been prepared and characterized by X-ray crystallography. These inclusion complexes exhibit rich inclusion topologies with new hydrogen bonding patterns and their structural features are presented and discussed in the following chapters.

Chapter 2. Description of Crystal Structures

2.1 Strategies in designing new supramolecular rosette motifs

2.1.1 Crystalline compounds constructed with boric acid

Crystal structure of $2[C(NH_2)_3^+] \cdot H_4B_4O_9^{2-} \cdot 2H_2O$ (2.1.1)

In the crystal structure of $2[C(NH_2)_3^+] \cdot H_4B_4O_9^{2-} \cdot 2H_2O$ (**2.1.1**), there are two guanidiniums C1 and C2 (each GM denoted by the label of its carbon atom), one tetraborate anion ($H_4B_4O_9^{2-}$) and two water molecules in the asymmetric unit. Adjacent tetraborate anions ($H_4B_4O_9^{2-}$) are joined by one O3–H···O4b hydrogen bond to form an infinite chain along the *a* axis (Figure 2.1.1).

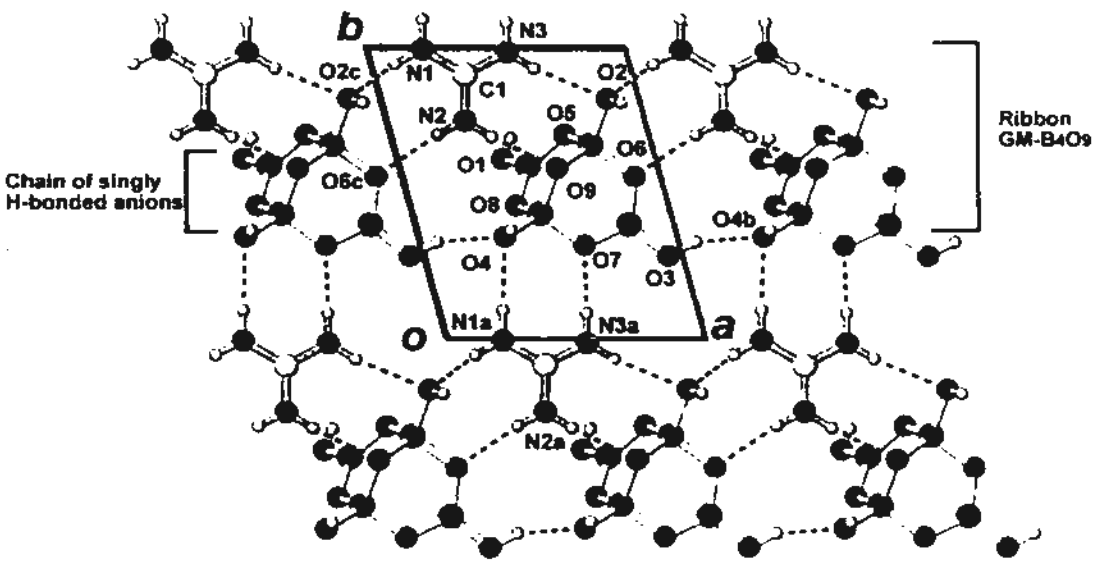

Figure 2.1.1 Projection diagram showing a portion of the neutral skew pseudo-rosette network in the crystal structure of **2.1.1**. *Symmetry transformations*: (a) $x, -1 + y, z$; (b) $1 + x, y, z$; (c) $-1 + x, y, z$.

This chain is further connected by the guanidinium ion C1 through N3–H···O2, N2–H···O9, N1–H···O2c and N2–H···O6c hydrogen bonds to create a

$(GM–B_4O_9)_\infty$ ribbon along the *a* axis. Further cross-linkage between parallel $(GM–B_4O_9)_\infty$ ribbons (N1a–H···O4 and N3a–H···O7) generates a neutral skew pseudo-rosette layer. Detailed hydrogen-bonding geometries are listed in Table 2.1.1.

Table 2.1.1 Hydrogen bonds for **2.1.1** [Å and deg.].

D-H...A	d(D-H)	d(H...A)	d(D...A)	∠(DHA)
O(1)-H(1O)...O(1W)#1	0.85	1.92	2.766(2)	170.0
O(2)-H(2O)...O(3)#2	0.79	2.31	3.088(2)	169.0
O(3)-H(3O)...O(4)#3	0.89	1.84	2.682(2)	157.0
O(4)-H(4O)...O(9)#4	0.85	1.90	2.741(2)	172.0
N(1)-H(1A)...O(2)#5	0.86	2.12	2.883(2)	147.7
N(1)-H(1B)...O(4)#6	0.86	2.08	2.906(2)	162.2
N(2)-H(2A)...O(9)	0.86	1.98	2.837(2)	171.2
N(2)-H(2B)...O(6)#5	0.86	2.07	2.920(2)	172.4
N(3)-H(3A)...O(2)	0.86	2.16	3.009(2)	171.8
N(3)-H(3B)...O(7)#6	0.86	1.97	2.831(2)	174.3
N(4)-H(4A)...O(1)#7	0.86	2.00	2.855(2)	170.1
N(4)-H(4B)...O(5)#5	0.86	2.43	3.059(2)	130.1
N(5)-H(5A)...O(8)#7	0.86	2.20	2.935(2)	142.9
N(5)-H(5B)...O(2W)#1	0.86	2.05	2.909(2)	173.7
N(6)-H(6A)...N(1)	0.86	2.33	3.179(2)	167.8
N(6)-H(6B)...O(1W)#6	0.86	2.18	2.943(2)	148.3
O(1W)-H(1WA)...O(8)	0.86	2.21	3.071(2)	179.3
O(1W)-H(1WB)...O(2W)	0.86	1.94	2.804(2)	179.1
O(2W)-H(2WA)...O(3)	0.86	1.95	2.812(2)	179.8
O(2W)-H(2WB)...O(5)#8	0.84	2.08	2.802(2)	142.5

Symmetry transformations used to generate equivalent atoms:
#1 -x+1,-y+1,-z #2 -x+2,-y+1,-z+1 #3 x+1,y,z #4 -x+1,-y+1,-z+1 #5 x-1,y,z
#6 x,y+1,z #7 -x,-y+1,-z #8 x,y-1,z

Viewed along the [1 1 0] direction, pseudo-rosette layers are further bridged by water molecules O1w, O2w and guanidinium ion C2 (lying almost perpendicular to the pseudo-rosette layer, and the dihedral angle between guanidinium ions C1 and C2 is about 88.3 °, Figure 2.1.2) to create a double layer structure (Figure 2.1.3).

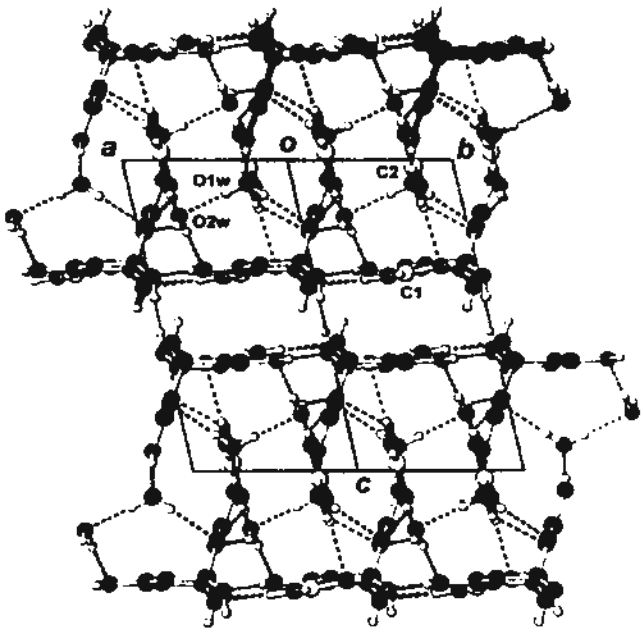

Figure 2.1.2 Projection diagram showing a portion of double layer network in the crystal structure of **2.1.1** viewed along the [1 1 0] direction. Dihedral angle between guanidinium ion C1 and C2 is about 88.3 °.

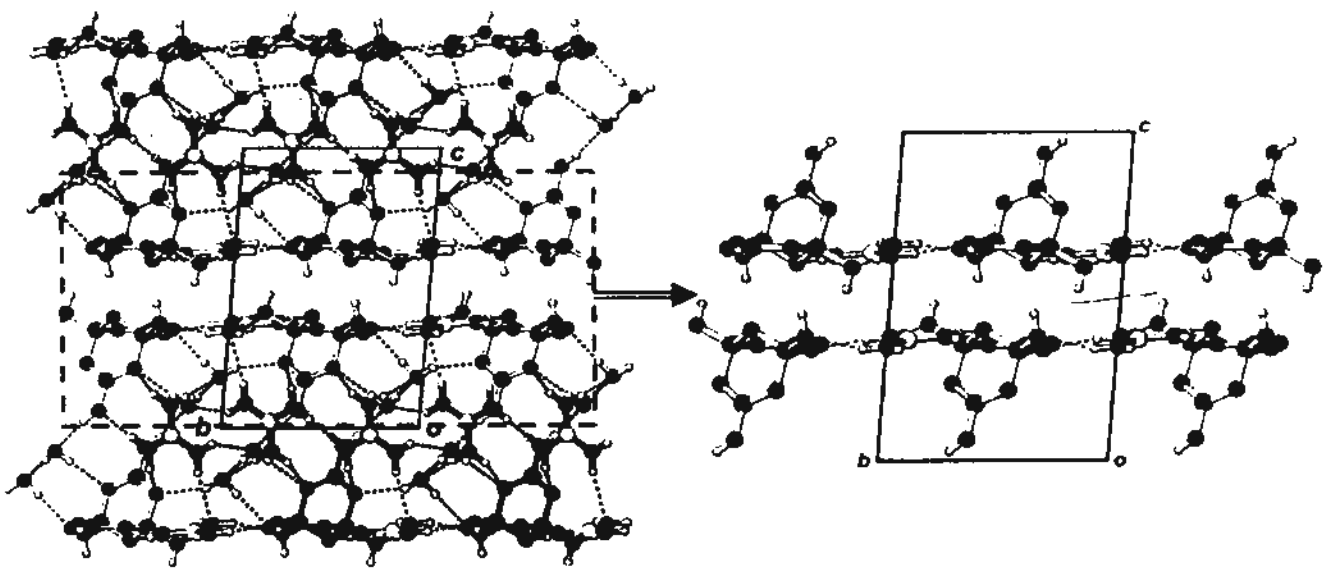

(a) (b)

Figure 2.1.3 (a) Projection diagram showing a double layer framework in the crystal structure of **2.1.1** viewed along the *a* axis; (b) projection diagram of one layer viewed along the *c* axis.

Crystal structure of $[C(NH_2)_3^+] \cdot H_4B_5O_{10}^- \cdot H_2O$ (2.1.2)

In the crystal structure of $[C(NH_2)_3^+] \cdot H_4B_5O_{10}^- \cdot H_2O$ (**2.1.2**), each pentaborate ions has two perpendicular B_3O_3 rings (designated as type **I** and **II**) sharing a common B3 atom to form a zigzag $(H_4B_5O_{10}^-)_\infty$ ribbon along the *c* axis with pairwise hydrogen bonds between type **II** rings (Figure 2.1.4a).

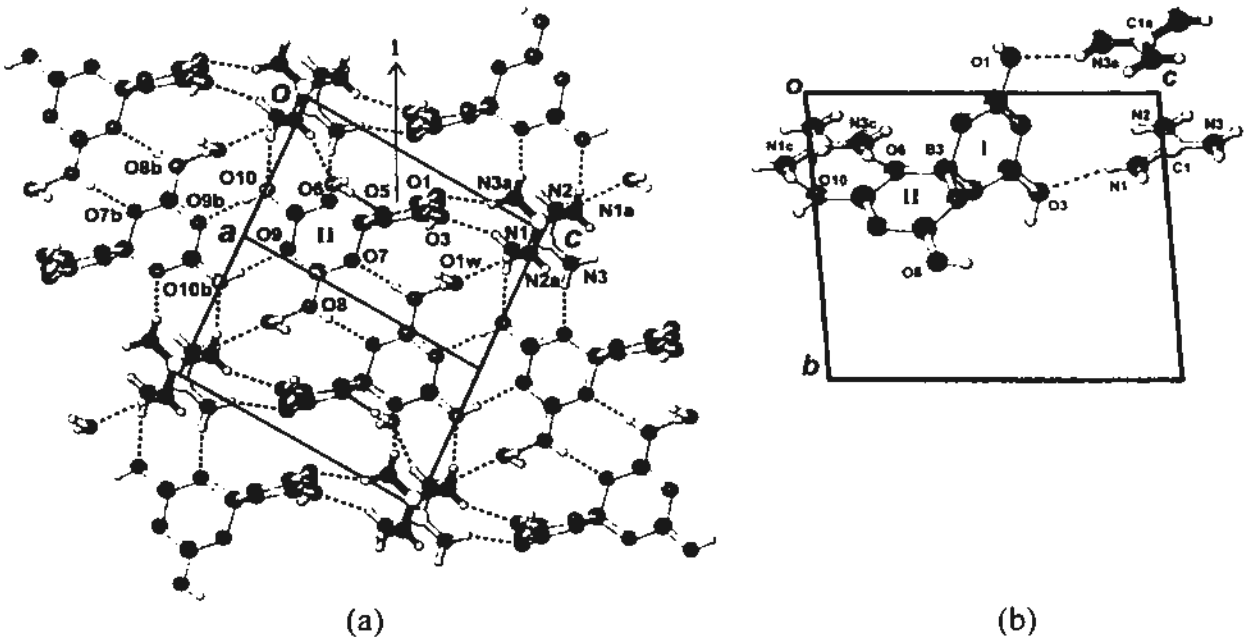

Figure 2.1.4 (a) Projection along the [$\bar{1}$ 1 0] direction showing the hydrogen-bonding framework of **2.1.2**. (b) The connection mode between three surrounding guanidinium ion and $H_4B_5O_{10}^-$. *Symmetry transformations*: (*a*) $-x, -y, 2-z$, (*b*) $1-x, 1-y, -z$.

Adjacent ribbons are bridged by guanidinium cations and bridging water molecules. In this crystal structure, the two perpendicular rings of $H_4B_5O_{10}^-$ are responsible for connection with guanidinium ions along different directions. Ring **I** is linked with two parallel, centrosymmetrically-related guanidiniums by single N3a–H···O1 or N1–H···O3 hydrogen bonds, respectively, almost along the *c* axis, while ring **II** is joined with one guanidinium ion by a pair of hydrogen bonds

N3c–H···O6 and N1c–H···O10 directed nearly parallel to the *a* axis (Figure 2.1.4b). Detailed hydrogen-bonding geometries are listed in Table 2.1.2.

Table 2.1.2 Hydrogen bonds for **2.1.2** [Å and deg.].

D-H...A	d(D-H)	d(H...A)	d(D...A)	∠(DHA)
O(1)-H(1O)...O(7)#1	0.83	2.29	2.968(1)	138.0
O(1)-H(1O)...O(5)#1	0.83	2.46	3.132(1)	138.0
O(3)-H(3O)...O(4)#2	0.88	1.85	2.727(1)	175.0
O(10)-H(10O)...O(9)#3	0.83	1.96	2.793(1)	173.0
N(3)-H(3A)...O(6)#4	0.86	2.07	2.900(2)	163.0
N(3)-H(3B)...O(1)#5	0.86	2.15	2.937(2)	151.9
N(3)-H(3B)...O(2)#5	0.86	2.63	3.311(2)	137.1
N(2)-H(2A)...O(1W)#5	0.86	2.15	2.992(2)	165.6
N(2)-H(2B)...O(1W)#6	0.86	2.11	2.930(2)	158.8
N(1)-H(1A)...O(10)#4	0.86	2.19	3.030 (2)	166.1
N(1)-H(1B)...O(3)	0.86	2.19	2.997(2)	156.0
O(1W)-H(1WA)...O(8)#7	0.85	2.10	2.951(2)	173.5
O(1W)-H(1WB)...O(5)#1	0.85	2.05	2.896(1)	169.4

Symmetry transformations used to generate equivalent atoms:
#1 -x+1,-y,-z+1 #2 -x,-y+1,-z+1 #3 -x+1,-y+1,-z #4 x,y,z+1 #5 -x,-y,-z+2
#6 x-1,y,z #7 -x+1,-y+1,-z+1

The packing diagram of complex **2.1.2** shows its robust hydrogen-bonding framework viewed almost along the [2 $\bar{1}$ 0] direction (Figure 2.1.5). The size of the open channel (separation between guanidinium walls is about 3.5 Å) is too small to accommodate even the smallest Me_4N^+ cations.

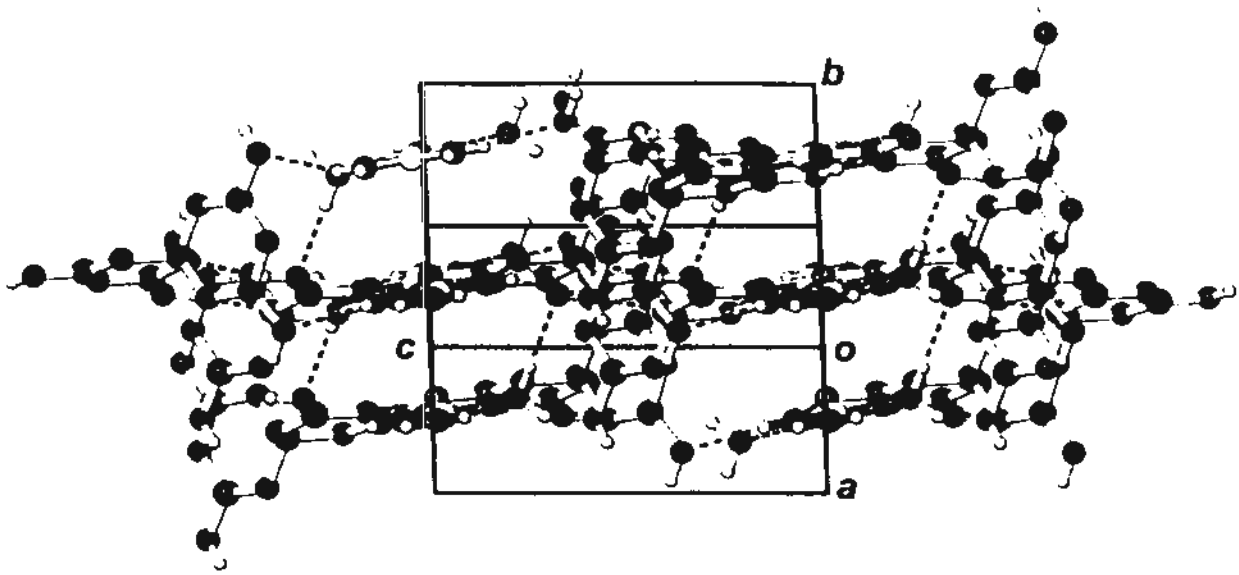

Figure 2.1.5 Projection almost along the [2 $\bar{1}$ 0] direction showing the open channels in the three-dimensional hydrogen-bonded framework of **2.1.2**.

Crystal structure of $2(Et_4N^+) \cdot 2(H_3BO_3) \cdot CO_3^{2-} \cdot 5H_2O$ (2.1.3)

In the crystal structure of $2(Et_4N^+) \cdot 2(H_3BO_3) \cdot CO_3^{2-} \cdot 5H_2O$ (**2.1.3**), boric acid dimers, motif [**C**], are hydrogen-bonded to the carbonate ion to generate zigzag ribbons by forming motifs [**A**] and [**B**]. Parallel ribbons composed of motifs [**A**], [**B**] and [**C**] are further connected by water molecules O1w~O5w to generate hydrogen-bonded layer exhibiting a petal-like motif, where center is a centrosymmetric hexameric water cluster (Figure 2.1.6). Detailed hydrogen-bonding geometries are listed in Table 2.1.3.

Figure 2.1.7 shows that the almost planar layer structure with an interlayer spacing of *b*/2 = 7.25 Å viewed along the *a* axis. Well-ordered Et_4N^+ ions are sandwiched between the neighboring layers.

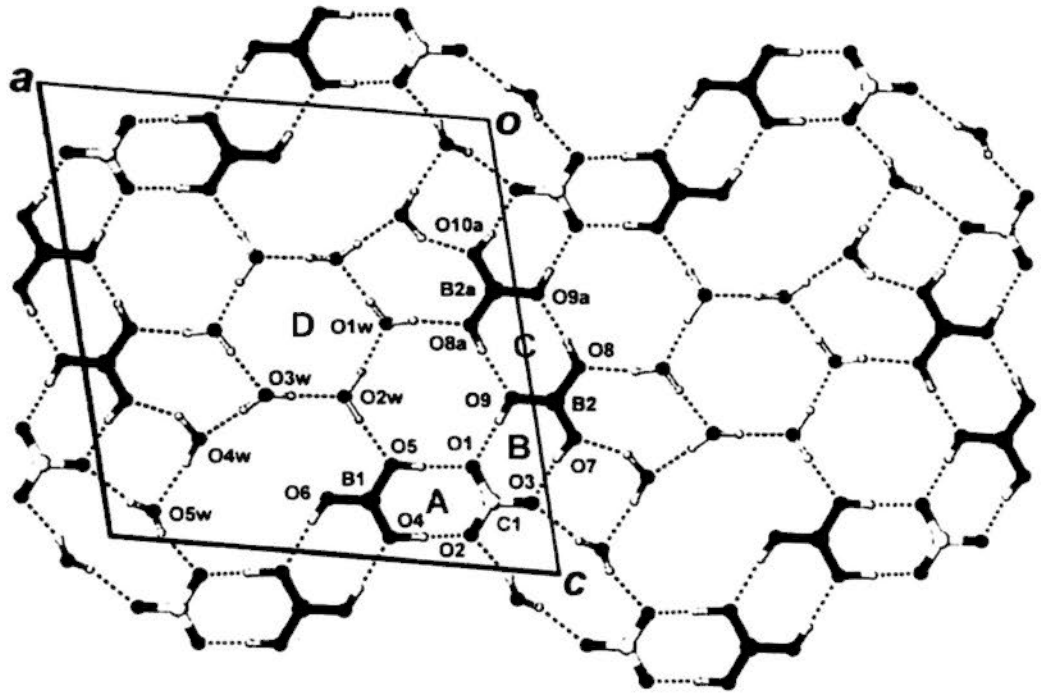

Figure 2.1.6 Projection along the *b* axis showing quasi-hexagonal hydrogen-bonded layer in **2.1.3**. The centrosymmetric petal-like motif has a hexameric water cluster at its center. *Symmetry transformations*: (a) $-x$, $1-y$, $1-z$.

Table 2.1.3 Hydrogen bonds for **2.1.3** [Å and deg.].

D-H...A	d(D-H)	d(H...A)	d(D...A)	∠(DHA)
O(4)-H(4O)...O(2)	0.98	1.62	2.598(2)	176.0
O(5)-H(5O)...O(1)	0.99	1.60	2.591(2)	177.0
O(6)-H(6O)...O(4)#1	0.82	1.99	2.809(2)	176.0
O(7)-H(7O)...O(3)	0.93	1.60	2.528(2)	170.0
O(8)-H(8O)...O(9)#2	0.86	1.88	2.735(2)	178.0
O(9)-H(9O)...O(1)	0.92	1.66	2.577(2)	174.0
O(5W)-H(5WA)...O(2)#1	0.84	1.97	2.769(2)	158.7
O(5W)-H(5WB)...O(3)#3	0.85	2.02	2.837(2)	158.1
O(2W)-H(2WA)...O(5)	0.91	1.88	2.796(2)	175.5
O(2W)-H(2WB)...O(1W)	0.97	1.78	2.755(2)	172.2
O(4W)-H(4WA)...O(5W)	0.89	1.88	2.770(2)	173.2
O(4W)-H(4WB)...O(7)#3	0.98	1.88	2.755(2)	146.6
O(1W)-H(1WA)...O(8)#2	0.94	1.93	2.863(2)	169.7
O(1W)-H(1WB)...O(3W)#4	0.90	1.86	2.761(3)	179.0
O(3W)-H(3WA)...O(2W)	0.89	1.88	2.772(3)	178.1
O(3W)-H(3WB)...O(4W)	0.89	1.85	2.744(3)	178.3

Symmetry transformations used to generate equivalent atoms:
#1 -x+1,-y+1,-z+2 #2 -x,-y+1,-z+1 #3 x+1,y,z #4 -x+1,-y+1,-z+1

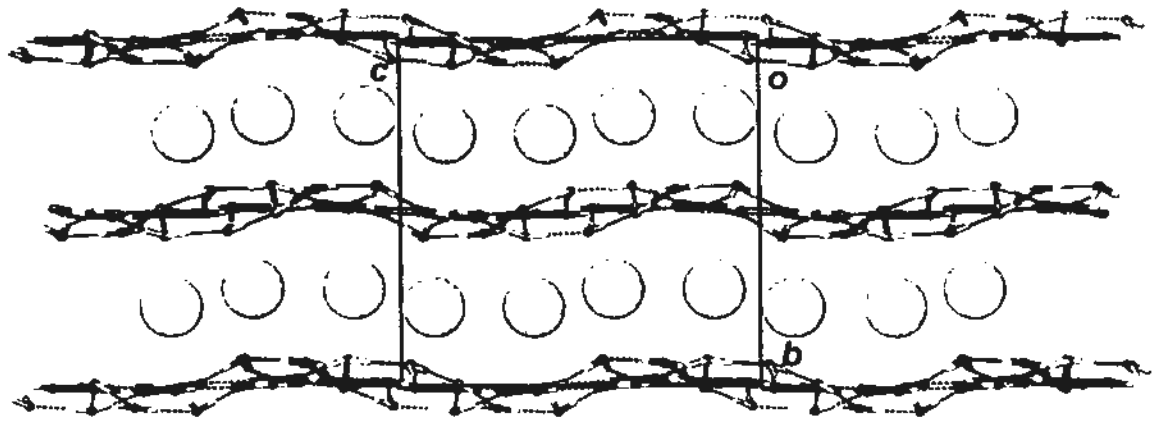

Figure 2.1.7 Planar layer structure of complex **2.1.3** viewed along the *a* axis with an interlayer spacing of *b*/2 = 7.25 Å. The Et_4N^+ ion is represented by a large sphere.

Crystal structure of $[(n\text{-}C_3H_7)_4N^+] \cdot [C(NH_2)_3^+] \cdot 2(H_3BO_3) \cdot CO_3^{2-}$ (2.1.4)

In the crystal structure of $[(n\text{-}C_3H_7)_4N^+] \cdot [C(NH_2)_3^+] \cdot 2(H_3BO_3) \cdot CO_3^{2-}$ (**2.1.4**), three differently charged molecular components are used to construct a hydrogen-bonded rosette layer: guanidinium ion C1, boric acid B1 and carbonate C2. The centrosymmetrically-related boric acid molecules B1a and B1c are joined together through a pair of O–H···O hydrogen bonds of about 2.72 Å to form dimer [**C**] (Figure 2.1.8). Detailed hydrogen-bonding geometries are listed in Table 2.1.4.

Carbonate C2 and guanidinium ion C1 both have site symmetry *m* and are connected pairwise through charge-assisted N^+–H···O^- hydrogen bonds of about 2.80 Å to form motif [**D**]. Notably, motifs [**C**] and [**D**] are linked together in two ways by pairs of O_{BA}–H···O_{CB}^- (2.56 and 2.59 Å) or N_{GM}^+–H···O_{BA} (2.89 and 2.93 Å) hydrogen bonds to generate motif [**E**] and [**F**], respectively. Thus three C_3-symmetric but differently charged molecular components, namely guanidinium cation, boric acid and carbonate dianion, coexist in 1:2:1 ratio in one rosette layer with the first and last serving as hydrogen-bonding donor and acceptor, respectively. However, each boric acid molecule functions as both donor and acceptor, such that a

pair of adjacent hydroxyl groups is orientated *syn-syn*, *syn-anti* and *anti-anti*, respectively, with respect to its proximal carbonate, boric acid and guanidinium neighbors (Figure 2.1.8). In this tertiary guanidinium–boric acid–carbonate (1:2:1) system, dimeric motifs [**C**], [**D**], [**E**] and [**F**] are interlinked to generate two distinguishable rosette motifs [**A**] and [**B**] in the same layer.

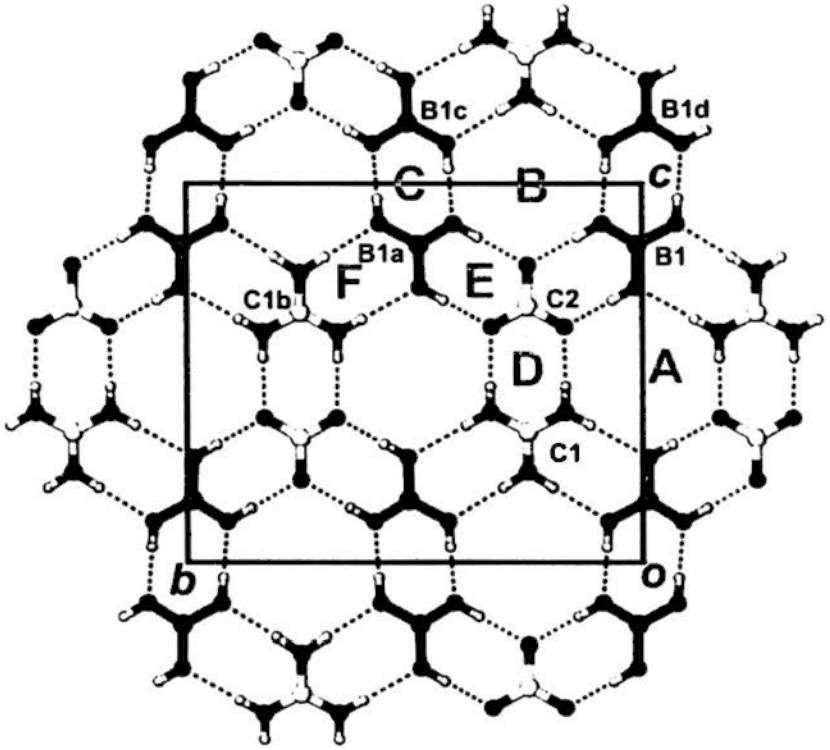

Figure 2.1.8 Projection diagram showing a portion of the guanidinium–boric acid–carbonate rosette network viewed along the *a* axis at x = ½ in the crystal structure of **2.1.4**. The layer is composed of independent guanidinium ion C1 (labeled by the central carbon atom), boric acid B1 and carbonate ion C2 in the ratio of (1:2:1). *Symmetry transformations*: (a) x, 0.5 – y, z; (b) 1 – x, 1 – y, 1 – z; (c) 1 – x, 0.5 + y, 2 – z; (d) 1 – x, – y, 2 + z. Mean atomic deviation from rosette plane: [**A**], 0.12 Å; [**B**], 0.29 Å.

The mean atomic deviation from the mean plane is 0.12 and 0.29 Å for rosette **[A]** and **[B]**, respectively. The dihedral angle between [A] and [B] is about 24.3 °, which reflects the wavy characteristics of the rosette layer.

In the crystal lattice of **2.1.4**, the well-ordered tetra-*n*-propylammonium cation occupies a special position of symmetry *m*. The hydrophobic cations are located at $x \approx ¼$ and ¾ and hence sandwiched between the sinusoidal rosette layers (Figure 2.1.9).

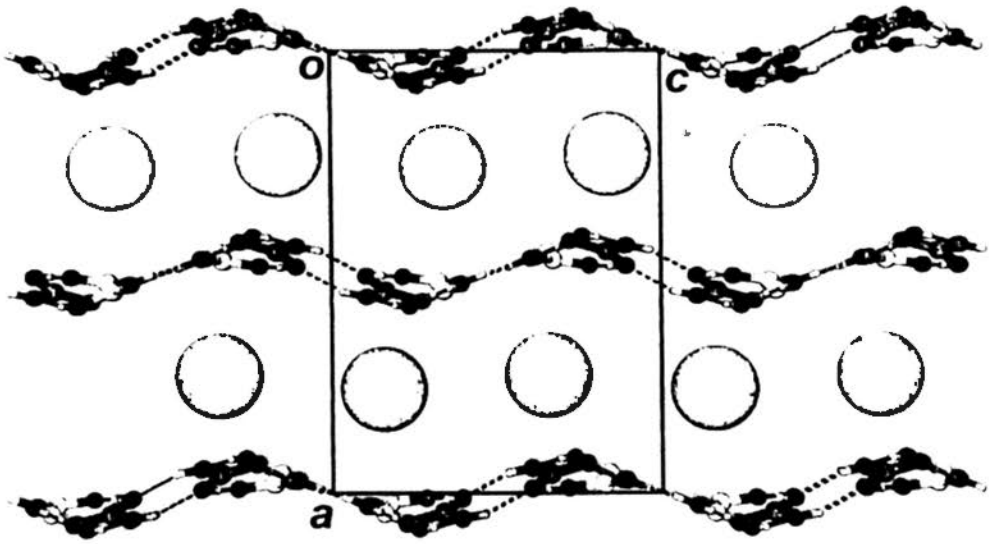

Figure 2.1.9 Packing diagram of **2.1.4** projected along the *b* axis, with large spheres representing the well-ordered hydrophobic $(n\text{-Pr})_4N^+$ cations positioned regularly between adjacent wrinkled layers with an interlayer spacing of 8.01 Å.

Table 2.1.4 Hydrogen bonds for **2.1.4** [Å and deg.].

D-H...A	d(D-H)	d(H...A)	d(D...A)	∠(DHA)
O(1)-H(1O)...O(4)	1.01	1.55	2.561(3)	173.1
O(2)-H(2O)...O(3)#1	0.84	1.90	2.716(3)	162.0
O(3)-H(3O)...O(5)	0.92	1.69	2.591(2)	169.1
N(1)-H(1A)...O(4)	0.86	1.94	2.799(3)	175.9
N(1)-H(1B)...O(1)#2	0.86	2.07	2.933(3)	177.9
N(2)-H(2A)...O(2)#2	0.94	1.95	2.884(3)	172.0

Symmetry transformations used to generate equivalent atoms:
#1 -x+1,-y,-z+2 #2 -x+1,-y,-z+1

2.1.2 Crystalline compounds constructed with squaric acid

Crystal structure of $[(n\text{-}Bu_4N^+)] \cdot [C_4O_4H^-] \cdot [H_3BO_3]$ (2.1.5)

In the crystal structure of $[(n\text{-}C_4H_9)_4N^+] \cdot [C_4O_4H^-] \cdot [H_3BO_3]$ (**2.1.5**), boric acid (BA) and hydrogen squarate (SA) are each organized into cyclic hydrogen-bonded dimers that occupy separate inversion centers. Pairwise donor hydrogen bonds from the boric acid dimer to its adjacent hydrogen squarate dimers gives rise to a zigzag ribbons along the [0 1 1] direction (Figure 2.1.10).

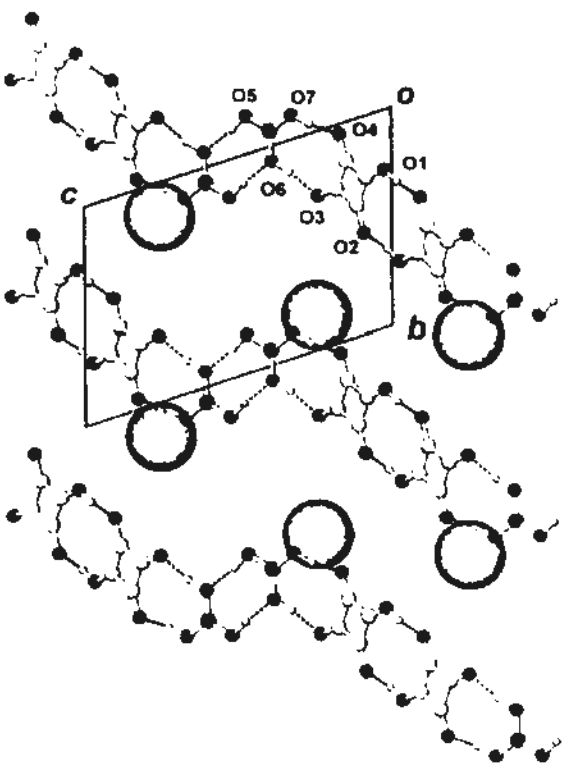

Figure 2.1.10 Projection diagram showing separated ribbons in a layer-type arrangement in the crystal structure of **2.1.5**. Large spheres representing the well-ordered hydrophobic $(n\text{-}Bu)_4N^+$ cations.

The distances of O–H···O hydrogen bond between different molecules are slightly different (O_{SA}–H···O_{SA} = 2.48, O_{BA}–H···O_{SA} = 2.69 and O_{BA}–H···O_{BA} = 2.78 Å). Detailed hydrogen-bonding geometries are listed in Table 2.1.5.

Table 2.1.5 Hydrogen bonds for **2.1.5** [Å and deg.].

D-H...A	d(D-H)	d(H...A)	d(D...A)	∠(DHA)
O(1)-H(1O)...O(2)#1	0.90	1.59	2.481(4)	169.1
O(5)-H(5O)...O(6)#2	1.03	1.76	2.784(4)	171.5
O(6)-H(6O)...O(3)	1.01	1.70	2.692(4)	169.7
O(7)-H(7O)...O(4)	1.08	1.62	2.695(4)	171.9

Symmetry transformations used to generate equivalent atoms:
#1 -x+1,-y+1,-z #2 -x+2,-y,-z+1

The ribbons are arranged in layers with an interlayer distance of about 7.99 Å and the tetra-*n*-butylammonium cations are accommodated between them (Figure 2.1.11).

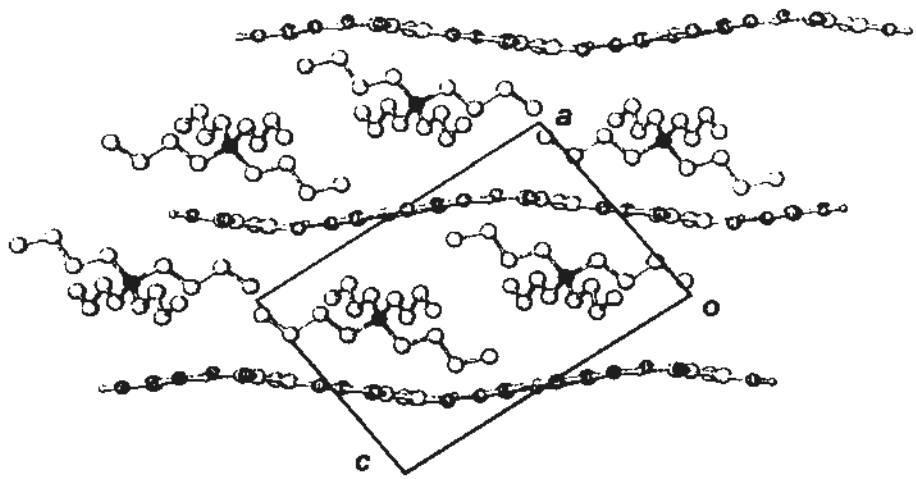

Figure 2.1.11 Crystal structure of complex **2.1.5** viewed along the *b* axis with the well-ordered hydrophobic $(n\text{-Bu})_4N^+$ cations positioned regularly between adjacent wavy layers with an interlayer spacing of 7.99 Å.

Crystal structure of $2[(n\text{-}C_3H_7)_4N^+] \cdot 4[CS(NH_2)_2] \cdot [C_4O_2S_2^{2-}] \cdot 2H_2O$ (2.1.6)

In the crystal complex **2.1.6**, 1,2-dithiosquarate dianion is disordered around an inversion center. Thiourea S3 and S4a are connected in a shoulder-to-shoulder fashion to form a zigzag chain with torsion angles C3–N1···S4a–C4a = 51.0 ° and

C4a–N4a···S3–C3 = 46.6 °. The ribbons are arranged side by side and further cross-linked by water molecule O1w to form a double thiourea–H_2O ribbon (Figure 2.1.12).

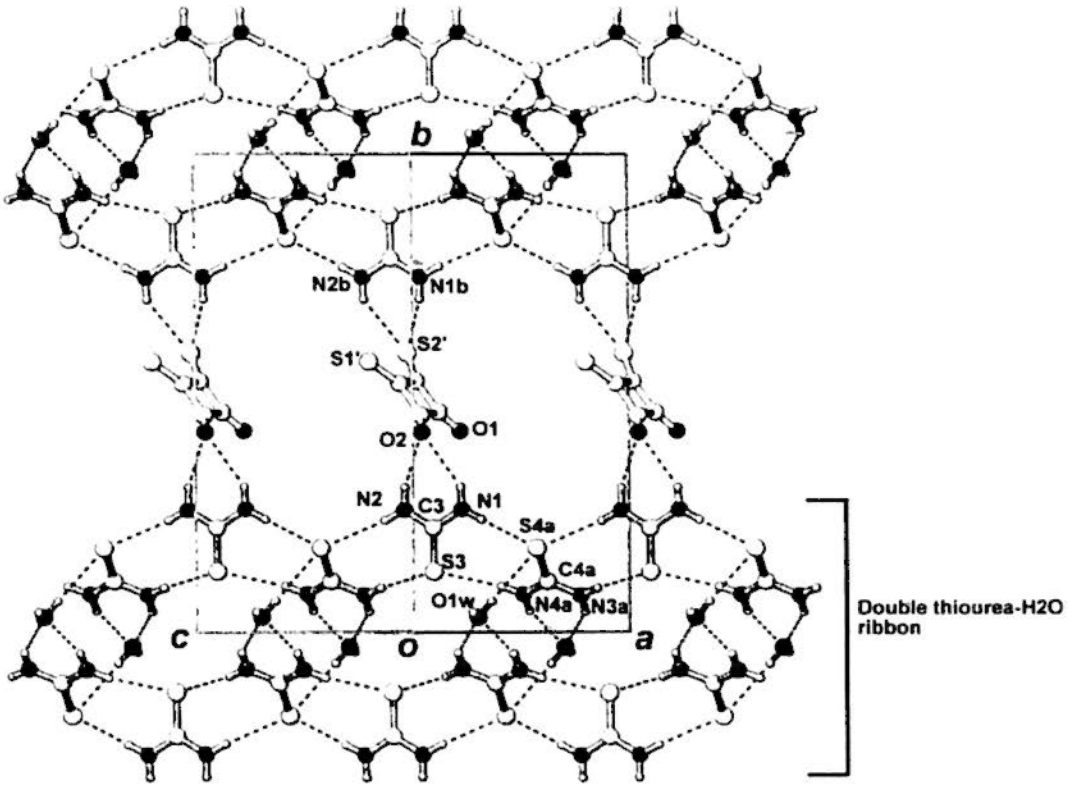

Figure 2.1.12 Crystal structure of **2.1.6** showing a layer constructed of double thiourea–H_2O ribbons and bridging dithiosquarate ions, leading to channels running parallel to [$\bar{1}$ 0 $\bar{1}$]. *Symmetry transformations*: (a) 1.5 – *x*, –0.5 – *y*, 0.5 – *z*; (b) 1– *x*, 1 – *y*, 1 – *z*.

In addition, each 1,2-dithiosquarate dianions (DTS) servers as a linker to join the separated double thioure–H_2O ribbons by chelating hydrogen bonds N1b–H···S2', N2b–H···S2', N1–H···O2 and N2–H···O2 to create channels running parallel to [$\bar{1}$ 0 $\bar{1}$].

Figure 2.1.13 shows the packing diagram viewed along the *a* axis. It can be seen that each DTS is linked with double thiourea–H_2O ribbons along four

directions through single hydrogen bonds to create channels where well-ordered tetra-*n*-propylammonium cations are accommodated.

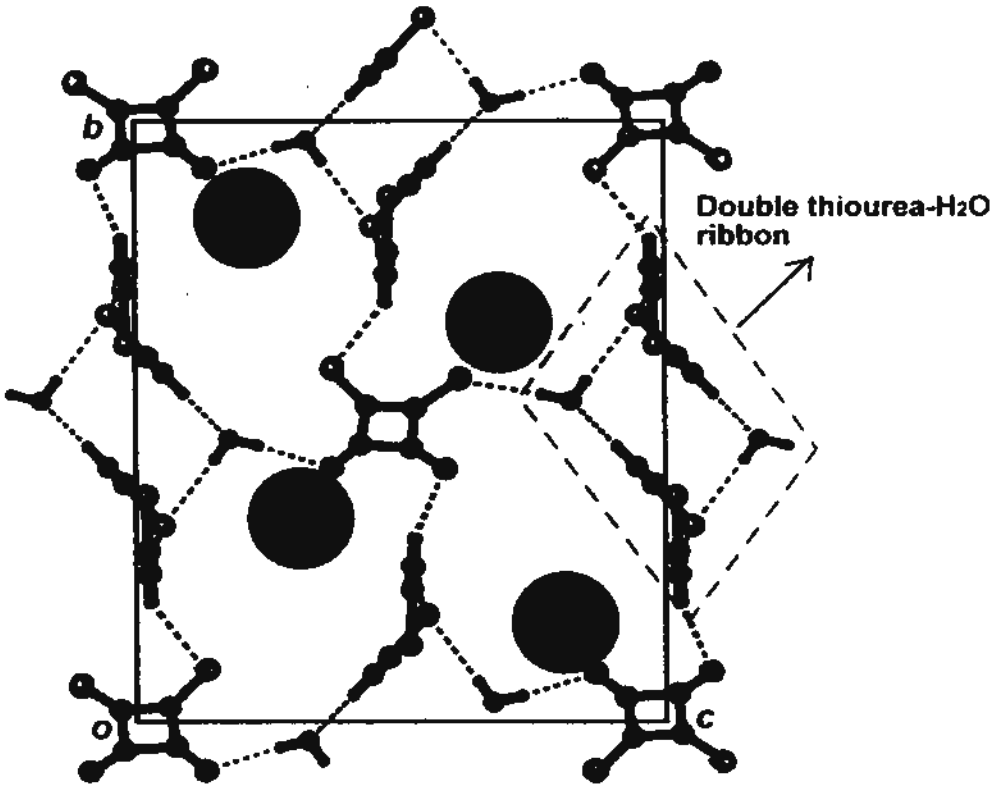

Figure 2.1.13 Crystal structure of **2.1.6**, with large spheres representing the ordered $(n\text{-Pr})_4N^+$ cations that are accommodated in each channel.

The length of hydrogen bonds between the thiourea and 1,2-dithiosquarate N–H···O(S) is uncertain due to the disordered dithiosquarate molecules. Detailed hydrogen-bonding geometries without uncertain N(thiourea)–H···O(S) (DTS) are listed in Table 2.1.6 for reference.

Table 2.1.6 Hydrogen bonds for **2.1.6** [Å and deg.].

D-H...A	d(D-H)	d(H...A)	d(D...A)	∠(DHA)
N(1)-H(1A)...O(2)	0.86	2.56	3.325(9)	149.0
N(2)-H(2A)...O(2)	0.86	2.48	3.265(9)	152.4
N(1)-H(1B)...S(4)#2	0.86	2.66	3.501(4)	165.4
N(2)-H(2B)...S(4)#3	0.86	2.65	3.507(4)	171.9
N(3)-H(3A)...O(1W)	0.86	2.30	3.068(7)	148.4
N(3)-H(3B)...S(3)#4	0.86	2.61	3.472(5)	174.4
N(4)-H(4A)...O(1W)	0.86	2.13	2.935(7)	156.3
N(4)-H(4B)...S(3)#5	0.86	2.56	3.412(4)	171.8
O(1W)-H(1WA)...S(4)#1	0.85	2.80	3.658(7)	178.4
O(1W)-H(1WB)...O(1)	0.87	2.23	3.10(2)	174.9

Symmetry transformations used to generate equivalent atoms:
#1 -x+1,-y+1,-z #2 -x+3/2,y-1/2,-z+1/2 #3 -x+1/2,y-1/2,-z+1/2 #4 -x+1/2,y+1/2,-z+1/2
#5 -x+3/2,y+1/2,-z+1/2

Crystal structure of $2[(n\text{-}C_4H_9)_4N^+] \cdot 4[CS(NH_2)_2] \cdot [C_4O_2S_2^{2-}]$ (2.1.7)

As illustrated in Figure 2.1.14, pairwises donor hydrogen bonds from DTS are linked with adjacent thiourea ribbons **I** and **II** to form a of DTS–thiourea layer. Thiourea molecules S6 connected in a shoulder-to-shoulder fashion create ribbon **I** along the *b* axis, and ribbon **II** constituted of thioureas molecules S4 and S5 in the same fashion as **I** runs parallel to it. The distance of hydrogen bonds between the DTS and thioureas are N5–H···O1 = 3.036(3), N6–H···S2 = 3.375(3), N7–H···O2 = 3.173(3) and N8–H···S1 = 3.533(3) Å.

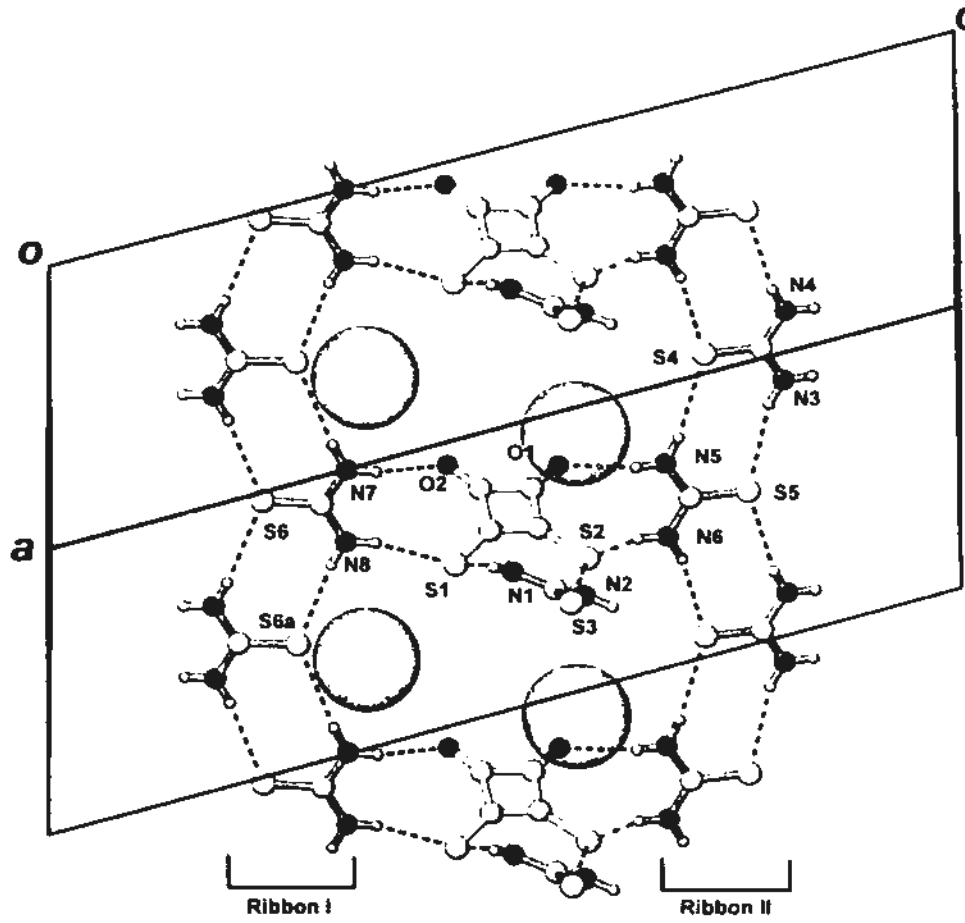

Figure 2.1.14 Crystal structure of **2.1.7** showing DTS are bridged two thiourea ribbon **I** and **II** together and the accommodation of channel of $(n\text{-Bu})_4N^+$ ions in each channel running parallel to the [$\bar{1}$ 1 0] direction. *Symmetry transformations*: (a) $-x, -0.5 + y, 0.5 - z$.

DTS–thiourea layer and dimeric thiourea (S3) are alternately linked together to generate channels with different sizes along the *b* axis (Figure 2.1.15). Detailed hydrogen-bonding geometries are listed in Table 2.1.7.

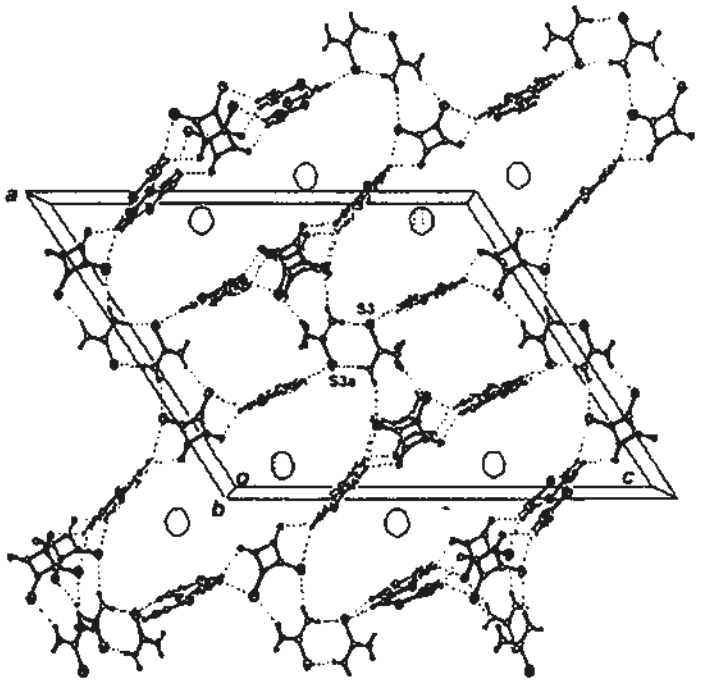

Figure 2.1.15 Perspective view of the crystal structure of **2.1.7** shows two different sizes of channels. *Symmetry transformations*: (a) $1 - x, -y, 1 - z$.

Table 2.1.7 Hydrogen bonds for **2.1.7** [Å and deg.].

D-H...A	d(D-H)	d(H...A)	d(D...A)	∠(DHA)
N(7)-H(7A)...O(2)	0.86	2.48	3.173(3)	138.7
N(7)-H(7B)...S(6)#1	0.86	2.80	3.660(3)	173.5
N(8)-H(8A)...S(1)	0.86	2.74	3.533(3)	153.2
N(8)-H(8B)...S(6)#2	0.86	2.71	3.559(3)	171.1
N(1)-H(1A)...S(1)	0.86	2.59	3.402(3)	158.1
N(1)-H(1B)...S(3)#3	0.86	2.57	3.407(3)	166.1
N(2)-H(2A)...S(2)	0.86	2.50	3.300(3)	154.9
N(2)-H(2B)...N(3)#4	0.86	2.56	3.354(4)	153.4
N(3)-H(3A)...S(3)#5	0.86	2.58	3.381(3)	155.5
N(3)-H(3B)...S(5)	0.86	2.67	3.498(3)	163.3
N(4)-H(4A)...S(3)#5	0.86	2.61	3.404(3)	154.4
N(4)-H(4B)...S(5)#6	0.86	2.70	3.543(3)	165.8
N(5)-H(5A)...O(1)	0.86	2.25	3.036(3)	152.3
N(5)-H(5B)...S(4)	0.86	2.68	3.533(3)	169.2
N(6)-H(6A)...S(2)	0.86	2.69	3.375(3)	137.3
N(6)-H(6B)...S(4)#7	0.86	2.67	3.512(3)	165.6

Symmetry transformations used to generate equivalent atoms:
#1 -x,y-1/2,-z+1/2 #2 -x,y+1/2,-z+1/2 #3 -x+1,-y,-z+1, #4 -x+1,y+1/2,-z+3/2
#5 -x+1,y-1/2,-z+3/2 #6 x,y-1,z #7 x,y+1,z

Crystal structure of $2[(n\text{-}C_4H_9)_4N^+] \cdot 6[CS(NH_2)_2] \cdot [C_4O_2S_2^{2-}] \cdot H_2O$ (2.1.8)

In the complex $2[(n\text{-}C_4H_9)_4N^+] \cdot 6[CS(NH_2)_2] \cdot [C_4O_2S_2^{2-}] \cdot H_2O$ (**2.1.8**), the host structure is built from corrugated thiourea layers (Wall **II**) and bridging dithiosquarate (DTS) ions (Wall **I**), generating channels with a peanut-shaped cross-section (Figure 2.1.16). The $(n\text{-}C_4H_9)_4N^+$ ions are well-ordered and arranged in a zigzag double column within each channel.

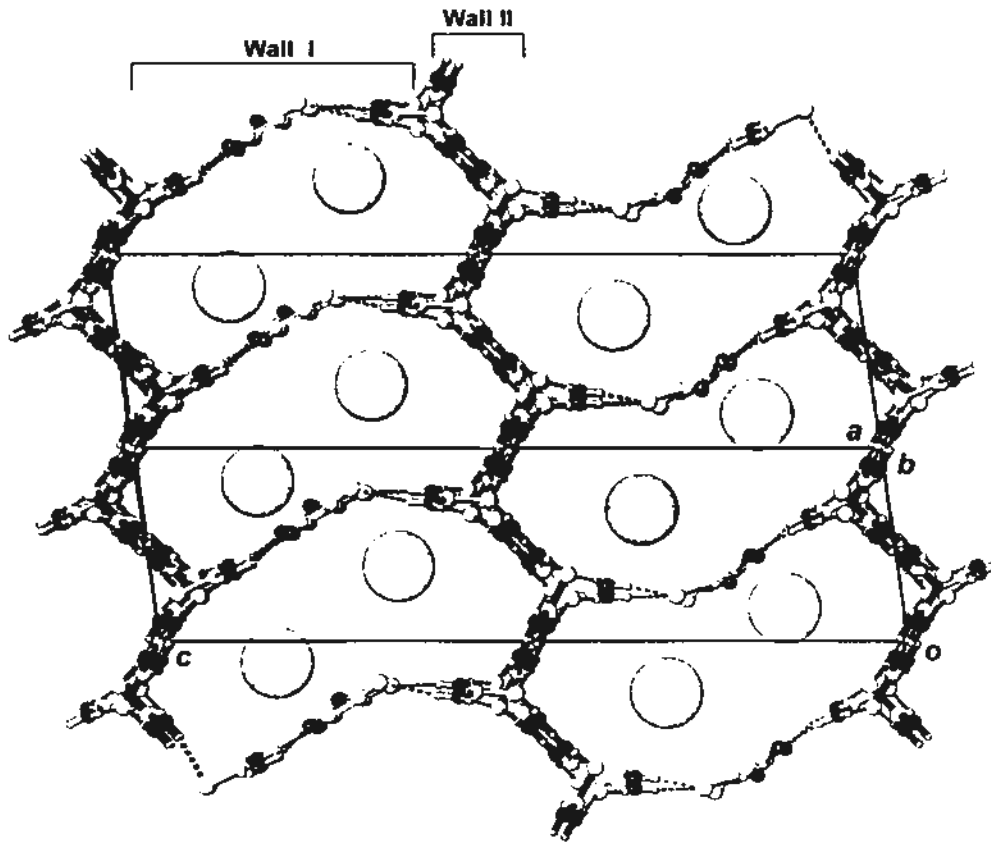

Figure 2.1.16 Stereodrawing of the crystal structure of **2.1.8**, showing the accommodation of zigzag column of $(n\text{-}Bu_4)N^+$ ions in each channel running parallel to the [1 $\bar{1}$ 0] direction.

Two thioureas (S3 and S8) are responsible for connection with DTS anions to form Wall **I**, while the other four thioureas (S4, S5, S6 and S7) are used to build Wall **II** of the channel. In Figure 2.1.17, the DTS anions are connected with thioureas S3 and S8 by pairs of hydrogen bonds N1–H···S2, N2–H···S1 and N11–H···O1, N12–H···O2. The distances of N–H···S hydrogen bonds are around 3.32~3.37 Å, while the distances of N1–H···O hydrogen bonds are about 2.83~2.87 Å. Water molecules bridge the oxygen atom and sulfur atom of DTS. Detailed hydrogen-bonding geometries are listed in Table 2.1.8.

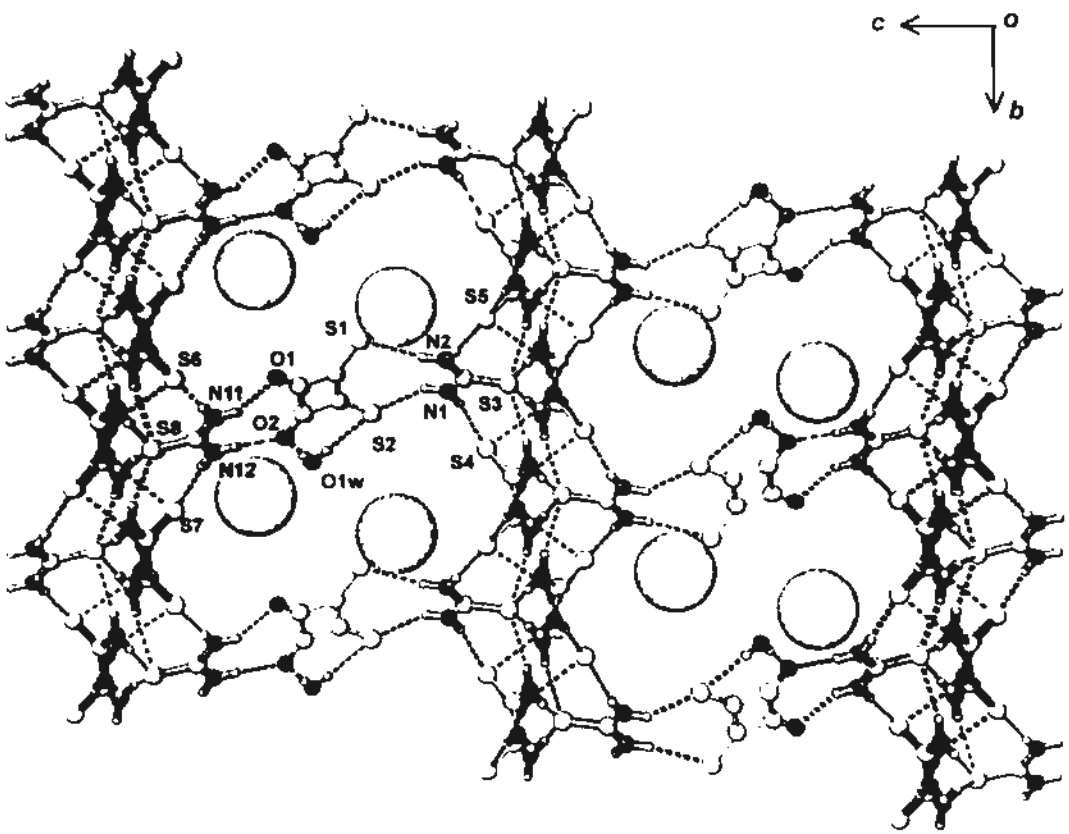

Figure 2.1.17 Channel structure of **2.1.8** formed by wide thiourea ribbons and dithiosquarate dianion.

Table 2.1.8 Hydrogen bonds for **2.1.8** [Å and deg.].

D-H...A	d(D-H)	d(H...A)	d(D...A)	∠(DHA)
N(1)-H(1A)...S(2)	0.86	2.52	3.374(5)	170.6
N(1)-H(1B)...S(5)#1	0.86	2.61	3.468(5)	174.1
N(2)-H(2A)...S(1)	0.86	2.61	3.319(5)	140.8
N(2)-H(2B)...S(4)	0.86	2.57	3.418(5)	168.4
N(3)-H(3A)...S(5)#2	0.86	2.53	3.330(5)	156.2
N(3)-H(3B)...S(5)	0.86	2.61	3.460(5)	169.4
N(4)-H(4A)...S(3)#3	0.86	2.64	3.371(5)	143.8
N(4)-H(4B)...S(3)	0.86	2.60	3.443(5)	166.7
N(5)-H(5A)...S(4)#4	0.86	2.57	3.372(5)	155.1
N(5)-H(5B)...S(4)	0.86	2.61	3.460(5)	169.6
N(6)-H(6A)...S(3)#4	0.86	2.62	3.370(5)	145.9
N(6)-H(6B)...S(3)#5	0.86	2.58	3.421(5)	167.7
N(7)-H(7A)...S(7)#6	0.86	2.64	3.401(5)	147.8
N(7)-H(7B)...S(7)	0.86	2.64	3.493(5)	170.3
N(8)-H(8A)...S(8)#7	0.86	2.61	3.404(5)	153.5
N(8)-H(8B)...S(8)#8	0.86	2.67	3.517(5)	170.1
N(9)-H(9A)...S(6)#7	0.86	2.56	3.402(5)	166.4
N(9)-H(9B)...S(6)	0.86	2.60	3.447(5)	170.0
N(10)-H(10A)...S(8)#9	0.86	2.73	3.405(4)	136.9
N(10)-H(10B)...S(8)#10	0.86	2.63	3.461(4)	163.8
N(11)-H(11A)...O(1)	0.86	2.03	2.827(5)	153.6
N(11)-H(11B)...S(6)#11	0.86	2.55	3.408(4)	176.8
N(12)-H(12A)...O(2)	0.86	2.02	2.870(5)	168.2
N(12)-H(12B)...S(7)#12	0.86	2.61	3.465(4)	175.0
O(1W)-H(1WB)...S(1)	0.87	2.48	3.349(6)	175.6
O(1W)-H(1WA)...O(2)	0.89	1.99	2.881(7)	176.3

Symmetry transformations used to generate equivalent atoms:
#1 x-1,y+1,z #2 -x+2,-y+1,-z+1 #3 -x+1,-y+2,-z+1 #4 -x+1,-y+1,-z+1 #5 x+1,y-1,z #6 -x,-y+1,-z #7 -x+1,-y+1,-z #8 x,y-1,z #9 -x+1,-y+2,-z #10 x-1,y,z #11 x,y+1,z #12 x+1,y,z

In Wall **II**, two independent thiourea molecules S6 and S7 are connected by a pair of N9–H···S6 and N7–H···S7 hydrogen bonds to form a dimer. The dimers are arranged in a broadside manner and interlinked by pairs of lateral hydrogen bonds to generate a puckered, wide ribbon running parallel to the *a* axis. These wide ribbons are arranged side by side and cross-linked by other thiourea molecules derived from S3, each forming two N–H···S donor and four S···H–N acceptor

hydrogen bonds to four thiourea molecules in adjacent ribbons to generate a corrugated layer (Figure 2.1.18).

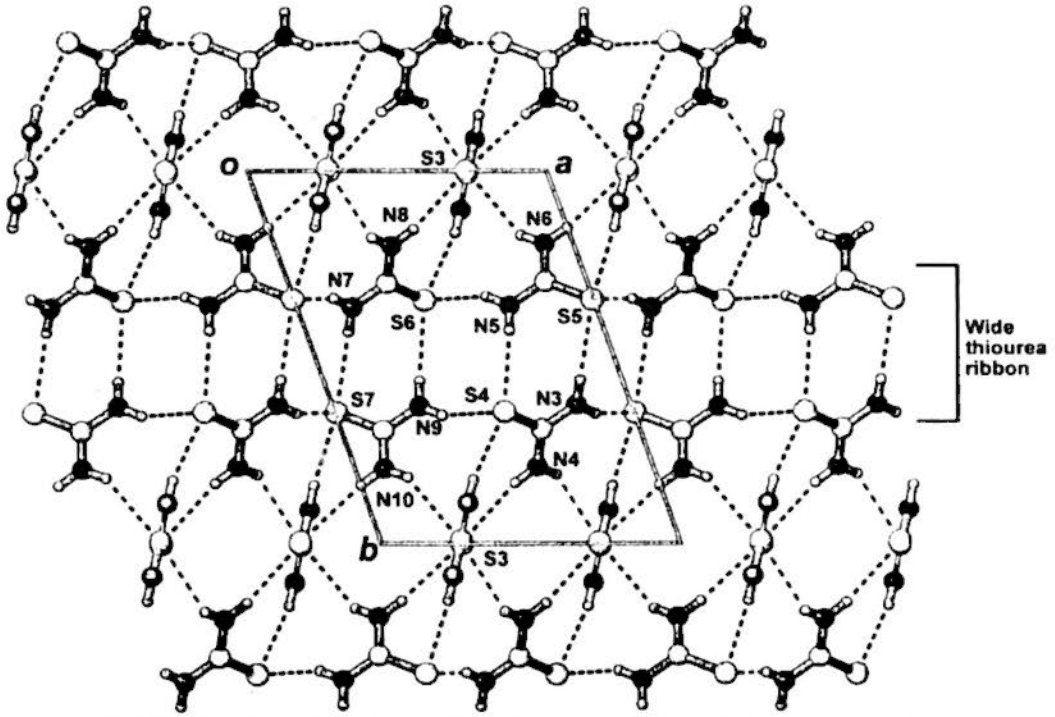

Figure 2.1.18 Projection drawing of the hydrogen-bonded corrugated thiourea layer in **2.1.8** comprising wide thiourea ribbons derived from dimeric thiourea and bridging thiourea molecules S3, which point alternately up and down in the ribbons direction.

Crystal structure of $[(n\text{-}C_4H_9)_4N^+] \cdot [C(NH_2)_3^+] \cdot [C_4O_2S_2^{2-}]$ (2.1.9)

The complex $[(n\text{-}C_4H_9)_4N^+] \cdot [C(NH_2)_3^+] \cdot [C_4O_2S_2^{2-}]$ **2.1.9** has an anionic host network exhibiting a distorted quasi-hexagonal supramolecular rosette motif [**A**] = $R_6^6(21)$ (Figure 2.1.19). The dithiosquarate dianion carries a negative charge on each sulfur atom. It is connected to guanidinium cations C5 and C5a by chelating hydrogen bonds with the respective carbonyl oxygen atom serving as a bifurcated acceptor to form motif [**B**] and [**C**], both being $R_2^1(6)$, and also to C5b via a pair of N^+–H···S^- hydrogen bonds to form $R_2^2(9)$ motif [**D**]. The measured distances of

N^+–H···S^- hydrogen-bonds involving atoms S1 and S2 are 3.36 and 3.46 Å, respectively, and those of geminal N^+–H···O hydrogen-bonds are 2.86 and 3.05 Å at O1, and 2.81 and 2.87 Å at O2, respectively. Thus the guanidinium cations and dithiosquarate dianions are alternately linked to form the highly asymmetrical quasi-rosette motif [A] = $R_6^6(21)$, and the mean atomic deviation from its least-squares plane is 0.31 Å. Detailed hydrogen-bonding geometries are listed in Table 2.1.9.

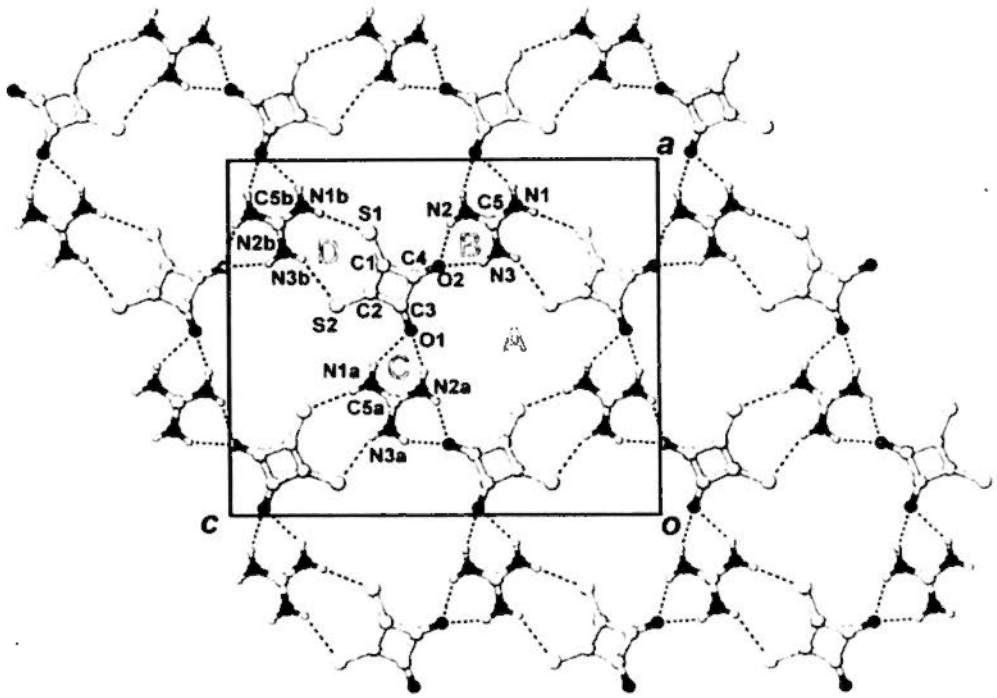

Figure 2.1.19 Projection diagram along the *b* axis showing a portion of the anionic rosette network at y = ¼ in the crystal structure of **2.1.9**. *Symmetry transformations*: (a) $-0.5 + x$, $0.5 - y$, $1 - z$; (b) x, $0.5 - y$, $0.5 + z$. Mean atomic deviation from least-squares plane calculated from the coordinates of three GM carbon atoms plus those of one O–C–C–O fragment and two O–C–C–S fragments that constitute the interior boundary of the deformed rosette unit = 0.31 Å.

Figure 2.1.20a shows the stacking of slightly wavy rosette layers in the crystal structure of **2.1.9**, with an interlayer spacing of 8.45 Å (= *b*/2). Well-ordered

tetra-*n*-butylammonium cations with the terminal methyl carbon atoms of one butyl group pointing toward the central void of rosette motif [**A**] (Figure 2.1.20b) are sandwiched between the sinusoidal rosette layers (Figure 2.1.20a).

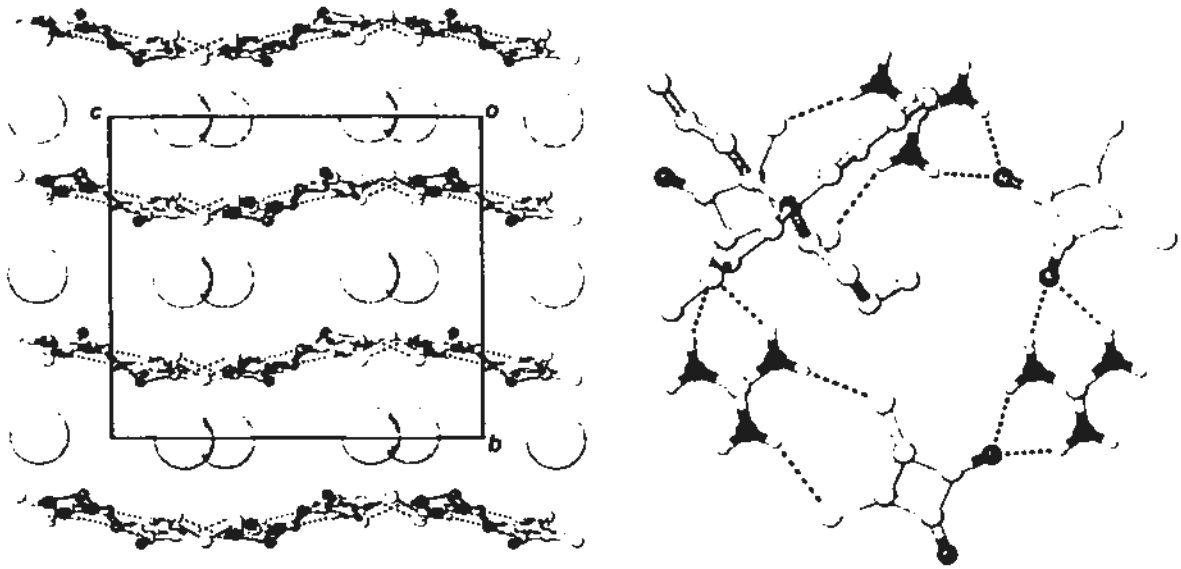

(a) (b)

Figure 2.1.20 (a) Layer structure of **2.1.9** viewed along the *a* axis, with large spheres representing the ordered $(n\text{-}Bu_4)N^+$ cations that are accommodated between sinusoidal layers. (b) Terminal methyl group deviating from the main plane points to the central void of rosette motif, as viewed along the *b* axis.

Table 2.1.9 Hydrogen bonds for **2.1.9** [Å and deg.].

D-H...A	d(D-H)	d(H...A)	d(D...A)	∠(DHA)
N(1)-H(1A)...S(1)#1	0.86	2.56	3.363(3)	156.8
N(1)-H(1B)...O(1)#2	0.86	2.32	3.048(4)	143.1
N(2)-H(2A)...O(2)	0.86	2.12	2.865(4)	144.2
N(2)-H(2B)...O(1)#2	0.86	2.07	2.863(4)	154.0
N(3)-H(3A)...O(2)	0.86	2.04	2.806(4)	147.6
N(3)-H(3B)...S(2)#1	0.86	2.73	3.461(3)	143.9

Symmetry transformations used to generate equivalent atoms:
#1 x,-y+1/2,z-1/2 #2 x+1/2,-y+1/2,-z+1

2.1.3 Crystalline compounds constructed with 1,1'-biphenyl-2,2',6,6'-tetracarboxylic acid

Crystal structure of $2[(CH_3)_4N^+] \cdot 2[(C_6H_3)_2(COOH)_3(COO^-)] \cdot H_2O$ (2.1.10)

Complex $2[(CH_3)_4N^+] \cdot 2[(C_6H_3)_2(COOH)_3(COO^-)] \cdot H_2O$ (**2.1.10**) is composed of two independent HBPTCs (C1 and C17), two $[(CH_3)_4N^+]$ and one water molecule O1w in the asymmetric unit. The HBPTC and water molecules are used to construct two different layers, designated as type **I** and **II**, in the crystal structure. Figure 2.1.21 shows that the layer **I** is built up with mono-deprotonated HBPTC and water molecules. Intramolecular linkage occurs between carboxyl and carboxylate groups attached to different phenyl rings in each tetracarboxylate anion, and adjacent HBPTCs are bridged by the intermolecular water O1–H···O3a hydrogen bond to form a $(HBPTC–H_2O)_\infty$ ribbon along the *b* axis. These ribbons are further joined together by O1wb–H···O2, O1wb–H···O7a and O8b–H···O1wb hydrogen bonds to form a layer structure by generating motif [**A**] and [**B**]. Centrosymmetric motif [**A**] is similar to a tetrameric water cluster, and motif [**B**] is composed of two water molecules and four HBPTCs to form a large void.

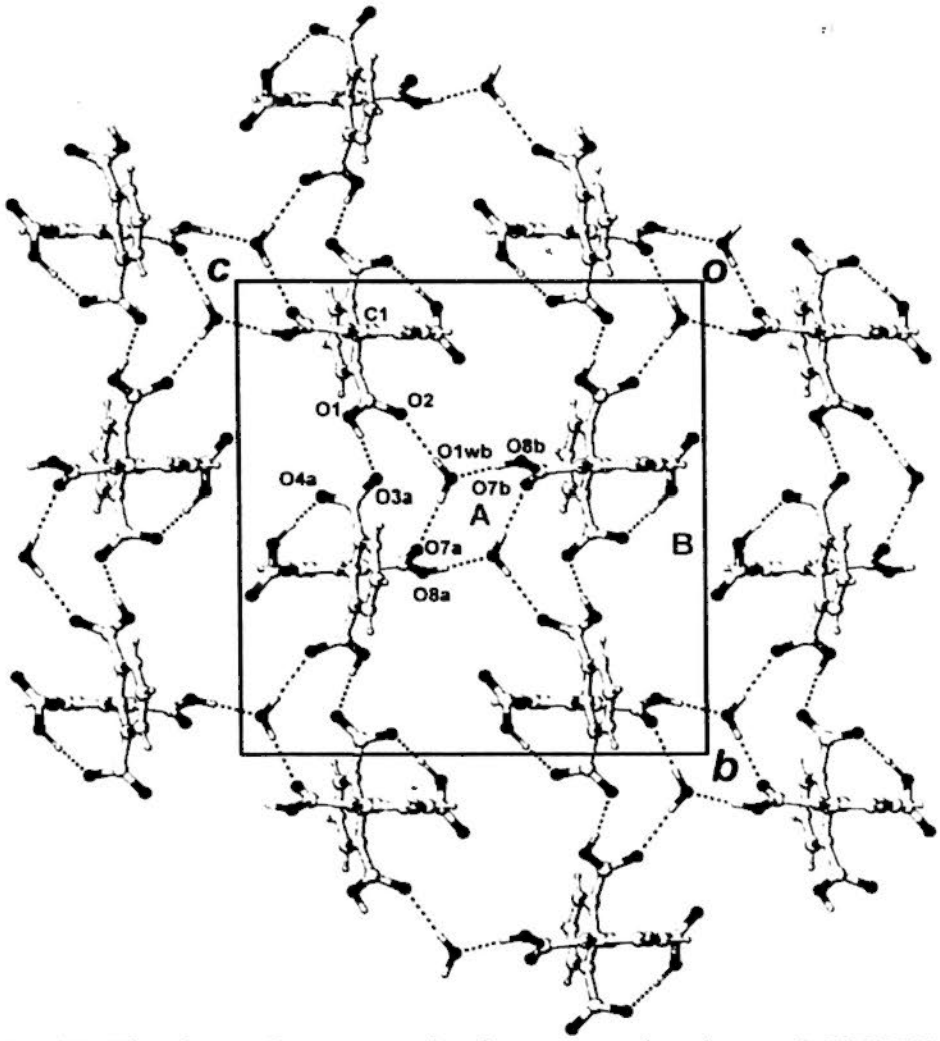

Figure 2.1.21 The layer **I** composed of water molecules and HBPTC (C1) of complex **2.1.10** viewed along the *a* axis. *Symmetry transformations*: (a) $1 - x$, $\frac{1}{2} + y$, $1.5 - z$; (b) x, $0.5 - y$, $-0.5 + z$.

Layer **II** is constructed from mono-deprotonated acid HBPTC (C17) alone. The HBPTC molecules are organized into centrosymmetric hydrogen-bonded dimers, which are then connected together by the O9–H···O12a hydrogen bond to generate layer exhibiting the centrosymmetric HBPTC hexamer, motif **[C]** (Figure 2.1.22). Detailed hydrogen-bonding geometries are listed in Table 2.1.10.

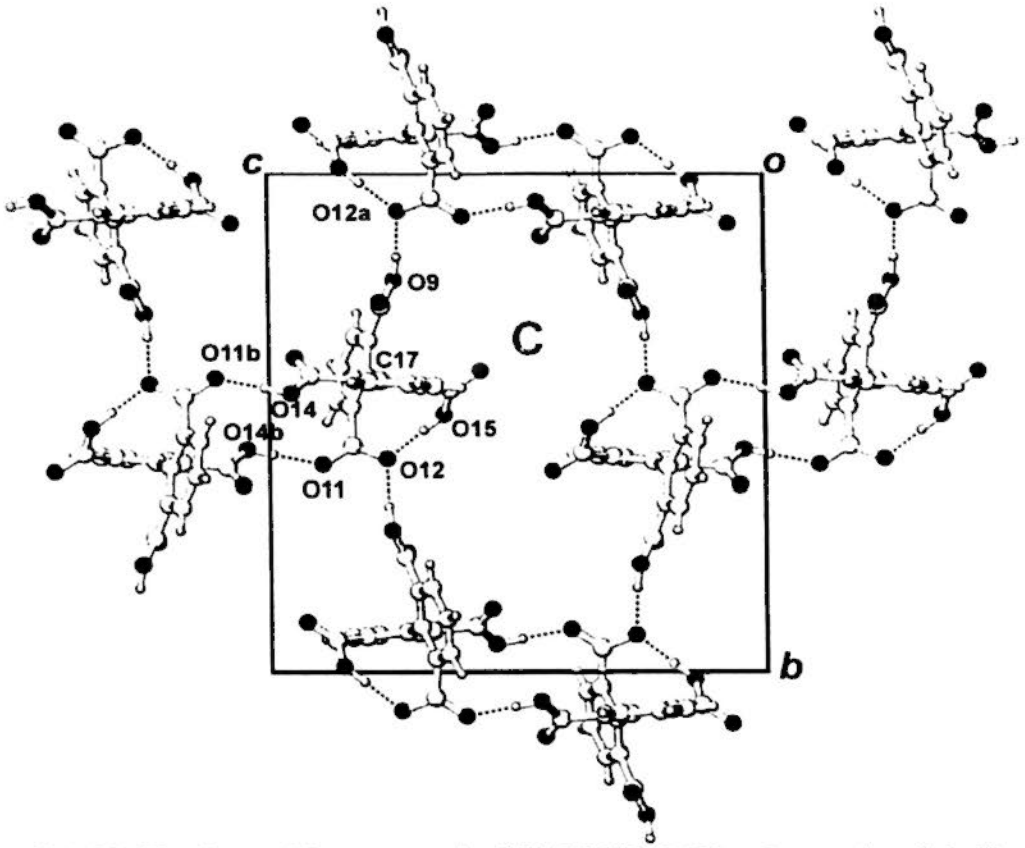

Figure 2.1.22 The layer **II** composed of HBPTC (C17) of complex **2.1.10** viewed along the *a* axis. In this layer, no water molecules are involved in. *Symmetry transformations*: (a) $-x, -0.5 - y, 1.5 - z$; (b) $-x, 1 - y, 2 - z$.

Table 2.1.10 Hydrogen bonds for **2.1.10** [Å and deg.].

D-H...A	d(D-H)	d(H...A)	d(D...A)	∠(DHA)
O(6)-H(6O)...O(4)	0.9	1.65	2.550(5)	179.9
O(8)-H(8O)...O(1W)	0.9	1.73	2.634(5)	179.6
O(14)-H(14O)...O(11)#1	0.9	1.72	2.618(4)	179.9
O(15)-H(15O)...O(12)	0.9	1.64	2.542(4)	179.8
O(1W)-H(1WA)...O(2)#2	0.85	2.15	3.01(1)	179.1
O(1)-H(1O)...O(3)#3	0.9	1.73	2.63(1)	179.9
O(1)-H(1O)...O(4)#3	0.9	2.57	3.15(1)	122.9
O(1W)-H(1WB)...O(7)#4	0.84	2.05	2.897(7)	179.7
O(9)-H(9O)...O(12)#5	0.9	1.79	2.68(1)	174.3

Symmetry transformations used to generate equivalent atoms:
#1 -x,-y+1,-z+2 #2 x,-y+1/2,z+1/2 #3 -x+1,y+1/2,-z+3/2 #4 -x+1,-y,-z+2
#5 -x,y-1/2,-z+3/2

The packing diagram (Figure 2.1.23) shows that layer **I** and **II** are alternately stacked along the *a* axis and the $(CH_3)_4N^+$ cations are accommodated between the layers.

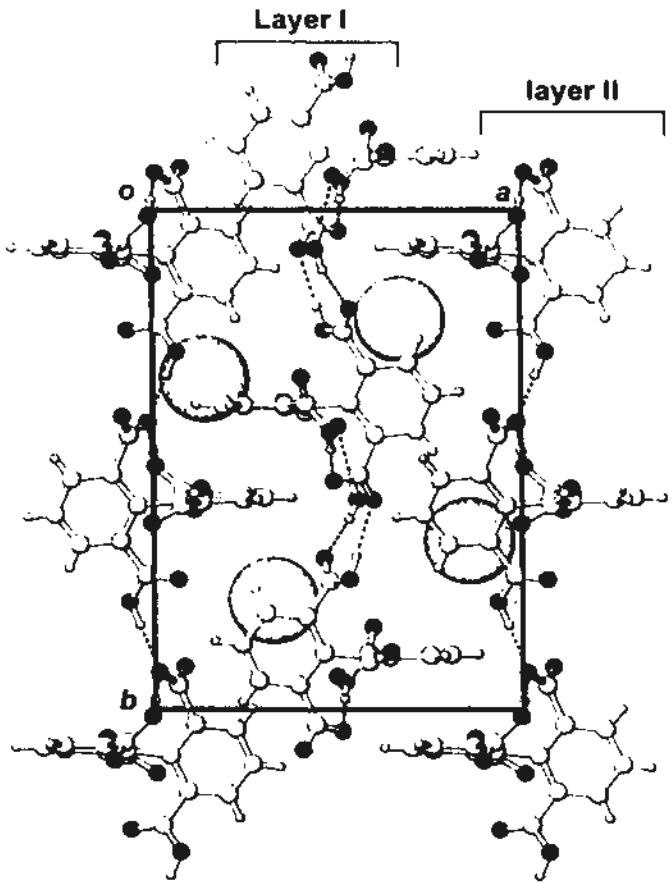

Figure 2.1.23 Packing diagram of **2.1.10** shows that two independent layers **I** and **II** are arranged alternately.

Crystal structure of $2[(C_2H_5)_4N^+] \cdot 2[CS(NH_2)_2] \cdot [(C_6H_3)_2(COOH)_2(COO^-)_2]$ (2.1.11)

In the crystal structure of **2.1.11**, the present of thiourea in the system prohibits the formation of dimeric BPTC species (Figure 2.1.24). Di-deprotonated BPTCs, with intramolecular hydrogen bonds O8–H···O3 and O5–H···O2, are joined together by thiourea dimers (torsion angle between the independent thiourea molecules: C17–N2···S2–C18 = 35.4 and C18–N4···S1–C17 = 31.4 °) through N2–H···O3, N1–H···O4, N3b–H···O1, N4b–H···O2 hydrogen bonds to form a

BPTC–(thiourea)$_2$ ribbon along the *c* axis. The ribbons are further connected by hydrogen bond N3a–H···O7 to create six-membered rosette motif [**A**] and four-membered motif [**B**] located at separate $\bar{1}$ sites, yielding a layer structure. Detailed hydrogen-bonding geometries are listed in Table 2.11.

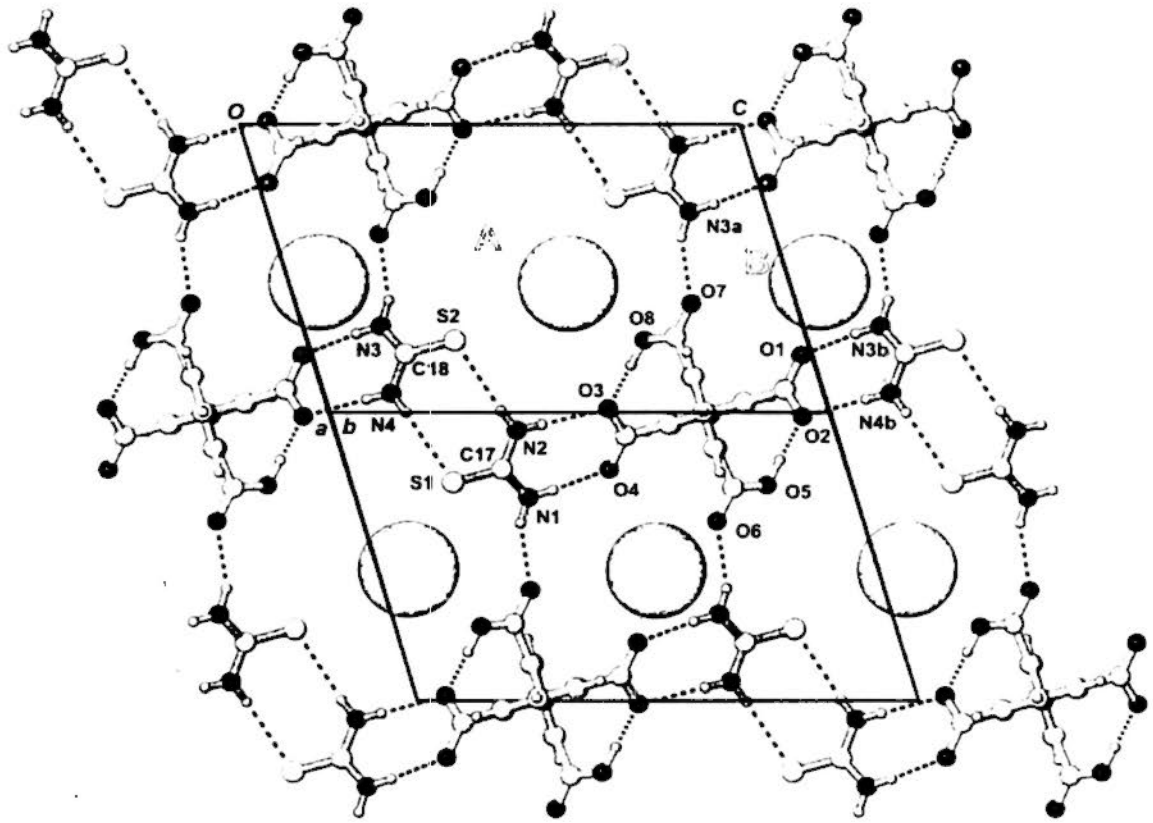

Figure 2.1.24 Projection diagram showing a portion of the anionic rosette network in the crystal structure of **2.1.11** viewed along the [$\bar{1}$ 1 0] direction. *Symmetry transformations*: (a) $-x$, $1-y$, $1-z$; (b) x, y, $1+z$.

The tetraethylammonium cations are located in each void of motif [**A**] and [**B**]. The packing diagram viewed along the *c* axis is shown in Figure 2.1.25.

Table 2.1.11 Hydrogen bonds for **2.1.11** [Å and deg.].

D-H...A	d(D-H)	d(H...A)	d(D...A)	∠(DHA)
N(1)-H(1A)...O(4)	0.86	2.06	2.919(4)	173.9
N(1)-H(1B)...O(6)#1	0.86	2.19	2.988(4)	155.1
N(2)-H(2A)...O(3)	0.86	2.14	2.991(4)	167.9
N(2)-H(2B)...S(2)	0.86	2.67	3.509(3)	163.7
N(3)-H(3B)...O(1)#2	0.86	2.07	2.921(4)	173.2
N(3)-H(3C)...O(7)#3	0.86	2.16	2.960(4)	155.1
N(4)-H(4B)...O(2)#2	0.86	2.10	2.955(4)	171.7
N(4)-H(4C)...S(1)	0.86	2.67	3.480(3)	158.3
O(5)-H(5O)...O(2)	0.90	1.56	2.457(4)	179.8
O(8)-H(8O)...O(3)	0.90	1.56	2.460(3)	179.7

Symmetry transformations used to generate equivalent atoms:
#1 -x+1,-y+2,-z+1 #2 x,y,z-1 #3 -x,-y+1,-z+1

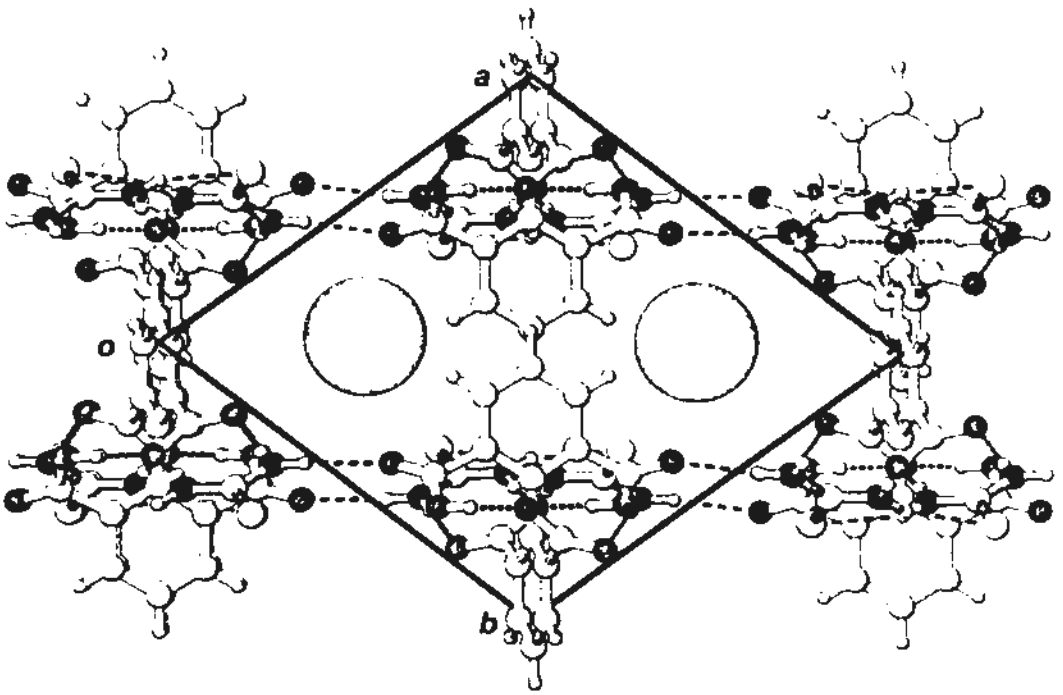

Figure 2.1.25 Packing diagram of **2.1.11** shows that almost planar layer structures viewed along the *c* axis.

Crystal structure of $[(CH_3)_4N^+] \cdot [C(NH_2)_3^+] \cdot [(C_6H_3)_2(COOH)_2(COO^-)_2]$ (2.1.12)

In the complex **2.1.12**, the guanidinium cation replaces the neutral thiourea molecule to enhance the number of hydrogen-bond donors. Each di-deprotonated BPTC is connected by a chelating hydrogen bond and two single hydrogen bonds to separate adjacent guanidinium ion to form an infinite zigzag chain running parallel to the *c* axis. Neighboring chains are further joined by pairwise hydrogen bonds between the carboxylate group of BPTC and guanidinium to generate a ten-membered large void (Figure 2.1.26), which accommodate the small tetramethylammonium cations.

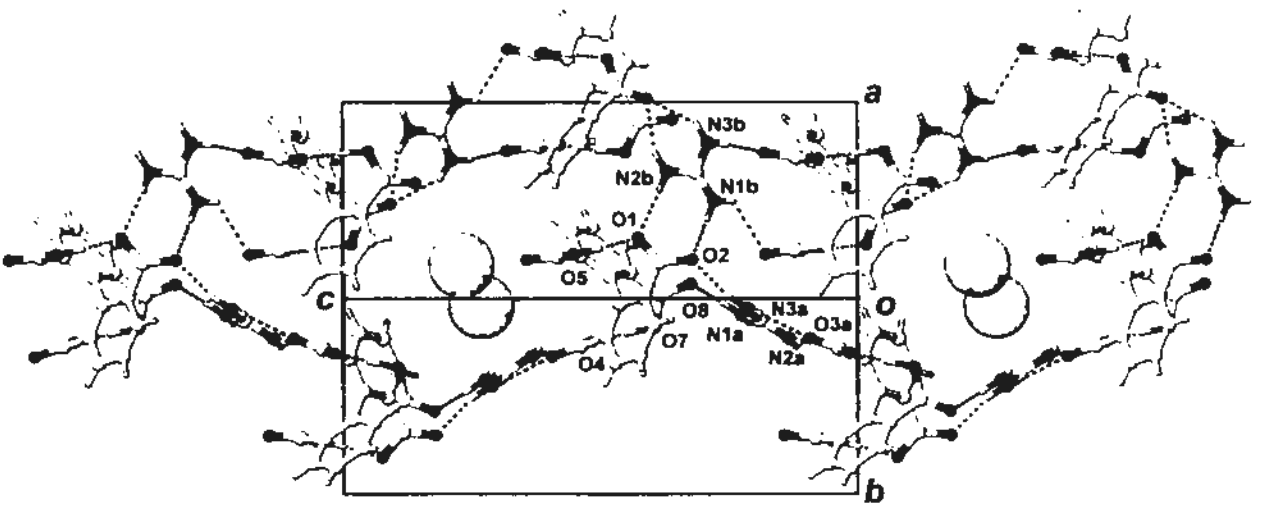

Figure 2.1.26 Ten-membered large voids built up with guanidiniums and BPTCs of complex **2.1.12** viewed along the [1 1 0] direction. *Symmetry transformations*: (a) $0.5 - x, 1 - y, -0.5 + z$; (b) $0.5 + x, 0.5 - y, 1 - z$.

In this structure, hydrogen-bonding interaction around a BPTC is different from that in the thiourea adduct **2.1.11**. Guanidinium is a typical hydrogen bond donor while thiourea can server as both donor and acceptor. In complex **2.1.12**, BPTC is linked with its three guanidinium neighbors by a pair of hydrogen bonds,

two single hydrogen bonds and a chelating hydrogen bond. However, in the thiourea–BPTC system (**2.1.11**), BPTC is joined with surrounding thioureas by two pairs of hydrogen bonds and two single hydrogen bonds along four perpendicular directions. The changeable hydrogen-bonding directions around each BPTC in the thiourea versus guanidinium systems should be considered in the design of pseudo C_3 molecules to build networks exhibiting the rosette motif (Figure 2.1.27). Detailed hydrogen-bonding geometries are listed in Table 2.1.12.

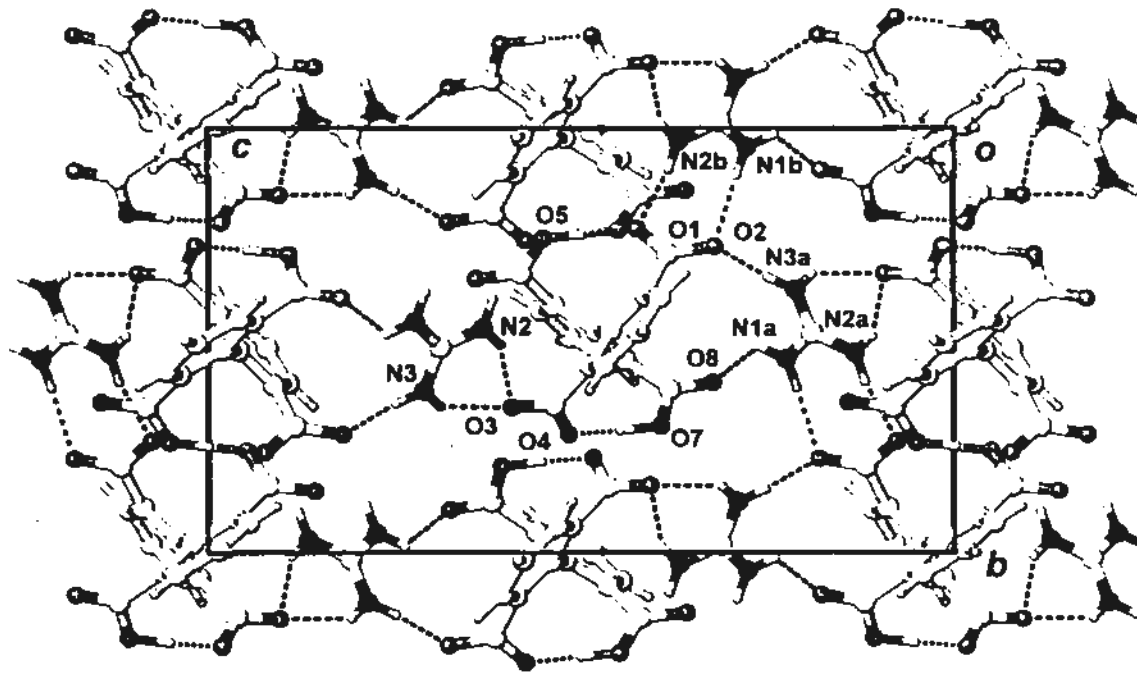

Figure 2.1.27 Packing diagram of complex **2.1.12** viewed along the *a* axis. *Symmetry transformations*: (a) 0.5 – *x*, 1 – *y*, –0.5 + *z*; (b) 0.5 + *x*, 0.5 – *y*, 1 – *z*.

Table 2.1.12 Hydrogen bonds for **2.1.12** [Å and deg.].

D-H...A	d(D-H)	d(H...A)	d(D...A)	∠(DHA)
O(5)-H(5O)...O(1)	0.90	1.68	2.577(3)	173.9
O(7)-H(7O)...O(4)	0.90	1.60	2.497(3)	175.6
N(1)-H(1A)...O(2)#1	0.86	2.03	2.887(4)	173.5
N(1)-H(1B)...O(8)#2	0.86	2.43	2.997(4)	124.2
N(2)-H(2A)...O(1)#1	0.86	2.08	2.924(3)	165.2
N(2)-H(2B)...O(3)	0.86	2.14	2.929(3)	152.6
N(3)-H(3A)...O(3)	0.86	2.30	3.046(3)	145.4
N(3)-H(3B)...O(2)#2	0.86	2.02	2.862(3)	165.1

Symmetry transformations used to generate equivalent atoms:
#1 x-1/2,-y+1/2,-z+1 #2 -x+1/2,-y+1,z+1/2

Crystal structure of $[(C_2H_5)_4N^+]\cdot[C(NH_2)_3^+]\cdot[(C_6H_3)_2(COOH)_2(COO^-)_2]$ (2.1.13)

In the crystal structure of **2.1.13**, a supramolecular rosette layer (Figure 2.1.28) is generated by introducing the larger tetraalkylammonium. The asymmetric unit contains pairs of crystallographically independent BPTC dianions (C1, C17), guanidinium cations (C33, C34) and tetraethylammonium cations. Intramolecular linkage occurs between carboxyl and carboxylate groups attached to different phenyl rings in each tetracarboxylate dianion, forming hydrogen bonds O4–H···O6, O8–H···O2 in BPTC C1, and O16–H···O10, O12–H···O14 in BPTC C17. The distances of these intramolecular hydrogen bonds lie in the range of 2.50 to 2.54 Å. In Figure 2.1.28, carboxylate oxygen atoms O1 and O2 come from the lower phenyl ring (view along *a* axis) of BPTC C1, and carboxylate oxygen atoms O5 and O6 belong to the upper phenyl ring. The pair of carboxylate groups of BPTC C1 are linked with adjacent guanidinium cations C33 and C33b by charge-assisted hydrogen bonds N2–H···O1, N3–H···O2, N1b–H···O5 and N3b–H···O6 to form $R_2^2(8)$ motif **[C]** and **[D]**, yielding an infinite twisted ribbon **I** running parallel to the *b* axis. Similarly, motif **[E]** and **[F]** are generated by connecting guanidinium cations C34 with BPTC C17 and C17b, and further extension gives rise to ribbon **II** (Figure 2.1.28).

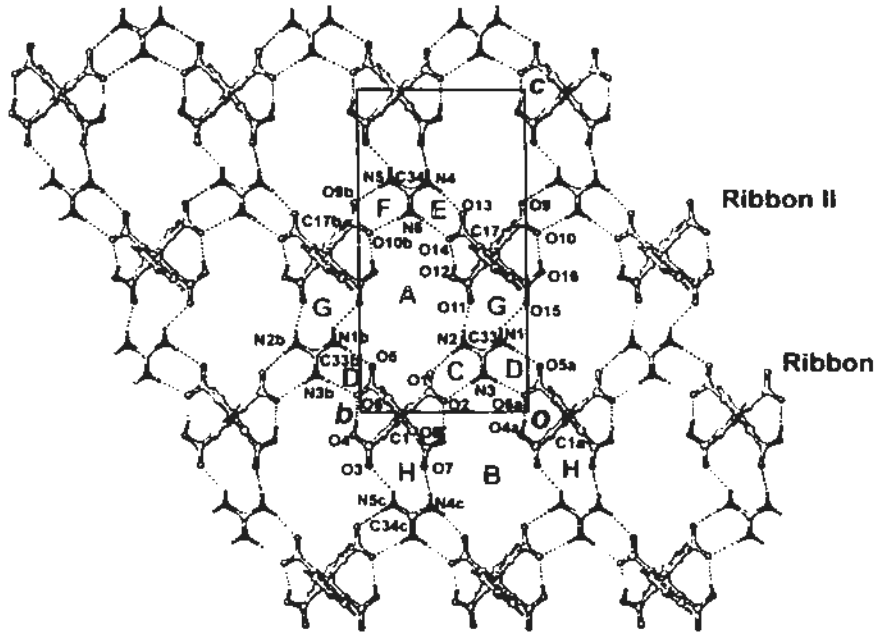

Figure 2.1.28 Projection diagram showing a portion of the anionic rosette network at x = ¼ in the crystal structure of **2.1.13**. *Symmetry transformations*: (a) x, 1 − y, z; (b) x, 1 + y, z; (c) x, y, 1 − z.

Ribbons of type **I** and **II** are cross-linked by pairwise N–H···O hydrogen bonds ranging from 2.80 to 3.02 Å between the carbonyl group of carboxylic acid and guanidinium cation via $R_2^2(13)$ motif [**G**] and [**H**] to generate similar distorted quasi-rosettes designated as [**A**] and [**B**] that exhibit the $R_6^8(27)$ motif. Rosette [**A**] is composed of two GM (C33), one GM (C34) and three BPTCs (one C1 and two C17), while rosette [**B**] is composed of one C33, two C34 and three BPTCs (two C1 and one C17). Figure 2.1.29 shows the packing of the approximately planar rosette layers in the crystal structure of **2.1.13**. In fact, there is no significant π–π interaction between phenyl rings belonging to adjacent rosette layers. Both independent tetraethylammonium cations occupy the interlayer region; the well-

ordered one is located at $x \approx 0$, and the other is disordered and located at $x \approx ½$. Detailed hydrogen-bonding geometries are listed in Table 2.1.13.

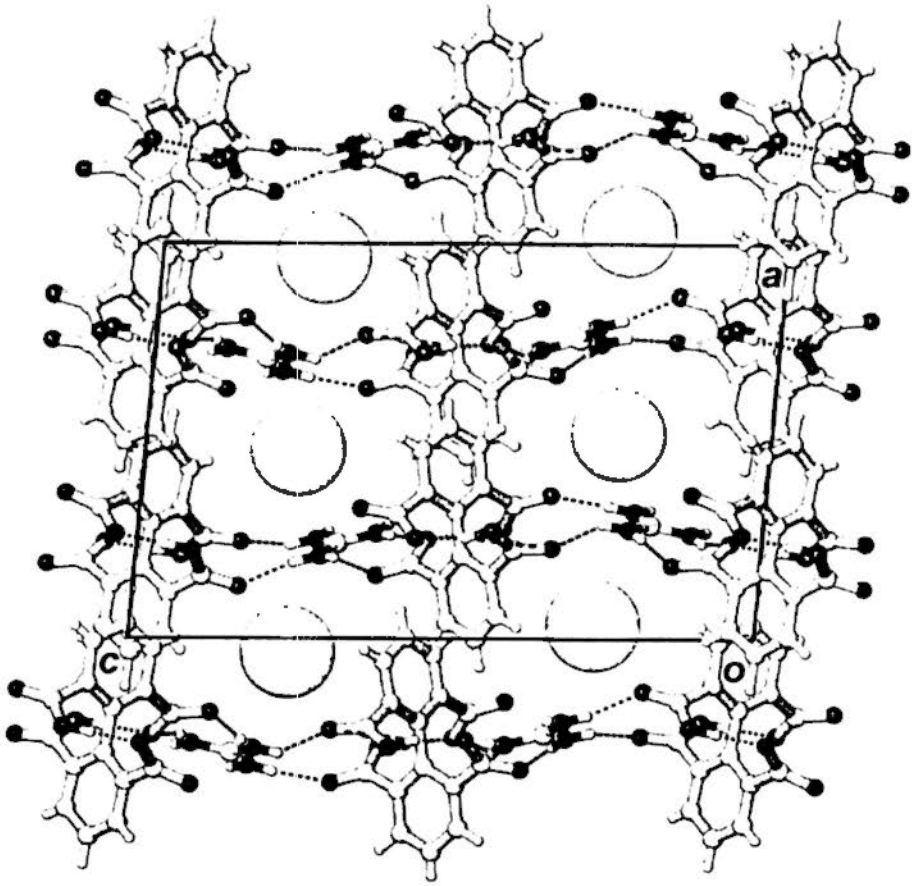

Figure 2.1.29 Approximately planar layer structure of **2.1.13** viewed along the *b* axis. No significant π–π interaction occurs between the phenyl rings belonging to adjacent rosette layers. Both independent tetraethylammonium cations represented by the large spheres occupy the interlayer region; the well-ordered Et_4N^+ is located at $x \approx 0$, and the disordered one is located at $x \approx ½$.

Table 2.1.13 Hydrogen bonds for **2.1.13** [Å and deg.].

D-H...A	d(D-H)	d(H...A)	d(D...A)	∠(DHA)
O(4)-H(4O)...O(6)	0.85	1.65	2.503(5)	179.9
O(8)-H(8O)...O(2)	0.85	1.73	2.536(5)	156.8
O(12)-H(12O)...O(14)	0.85	1.65	2.499(5)	179.9
O(16)-H(16O)...O(10)	0.85	1.68	2.529(6)	179.9
N(1)-H(1A)...O(15)	0.86	2.42	3.019(6)	126.7
N(1)-H(1A)...O(11)	0.86	2.64	3.294(6)	134.2
N(1)-H(1B)...O(5)#1	0.86	2.11	2.963(6)	173.0

N(2)-H(2A)...O(1)	0.86	1.98	2.819(6)	166.6
N(2)-H(2B)...O(11)	0.86	1.96	2.793(5)	163.8
N(3)-H(3A)...O(2)	0.86	2.05	2.908(5)	171.9
N(3)-H(3B)...O(6)#1	0.86	1.94	2.770(5)	160.7
N(4)-H(4A)...O(13)	0.86	2.01	2.841(6)	161.8
N(4)-H(4B)...O(7)#2	0.86	2.02	2.866(6)	166.2
N(5)-H(5A)...O(3)#2	0.86	2.19	2.884(6)	137.4
N(5)-H(5B)...O(9)#3	0.86	2.01	2.871(6)	174.6
N(6)-H(6A)...O(14)	0.86	2.03	2.892(5)	175.7
N(6)-H(6B)...O(10)#3	0.86	2.03	2.809(6)	149.7

Symmetry transformations used to generate equivalent atoms:
#1 x,y-1,z #2 x,y,z+1 #3 x,y+1,z

Crystal structure of $[(n\text{-}C_3H_7)_4N^+] \cdot [C(NH_2)_3^+] \cdot [(C_6H_3)_2(COOH)_2(COO^-)_2]$ (2.1.14)

The crystal structure of **2.1.14** is similar to that of complex **2.1.13**, but there is only one BPTC that possesses a pair of intramolecular hydrogen bonds, one guanidinium cation and one tetra-*n*-propylammonium cation in the asymmetric unit. In complex **2.1.14**, guanidinium C17a is linked with the upper phenyl carboxylate oxygen atoms O1 and O2 (viewed along the *c* axis) to form motif **[B]** = $R_2^2(8)$ (Figure 2.1.30). In addition, guanidinium cation C17a forms two donor hydrogen-bonds with two carbonyl groups of adjacent BPTC C1b to create motif **[C]** = $R_2^2(13)$. These two motifs **[B]** and **[C]** extend along the *a* axis to generate a parallel array of twisted ribbons. Such ribbons are consolidated by pairs of charge-assisted N1–H···O5 and N2–H···O6 hydrogen bonds to form the asymmetric quasi-rosette motif **[A]** = $R_6^8(27)$. Detailed hydrogen-bonding geometries are listed in Table 2.1.14.

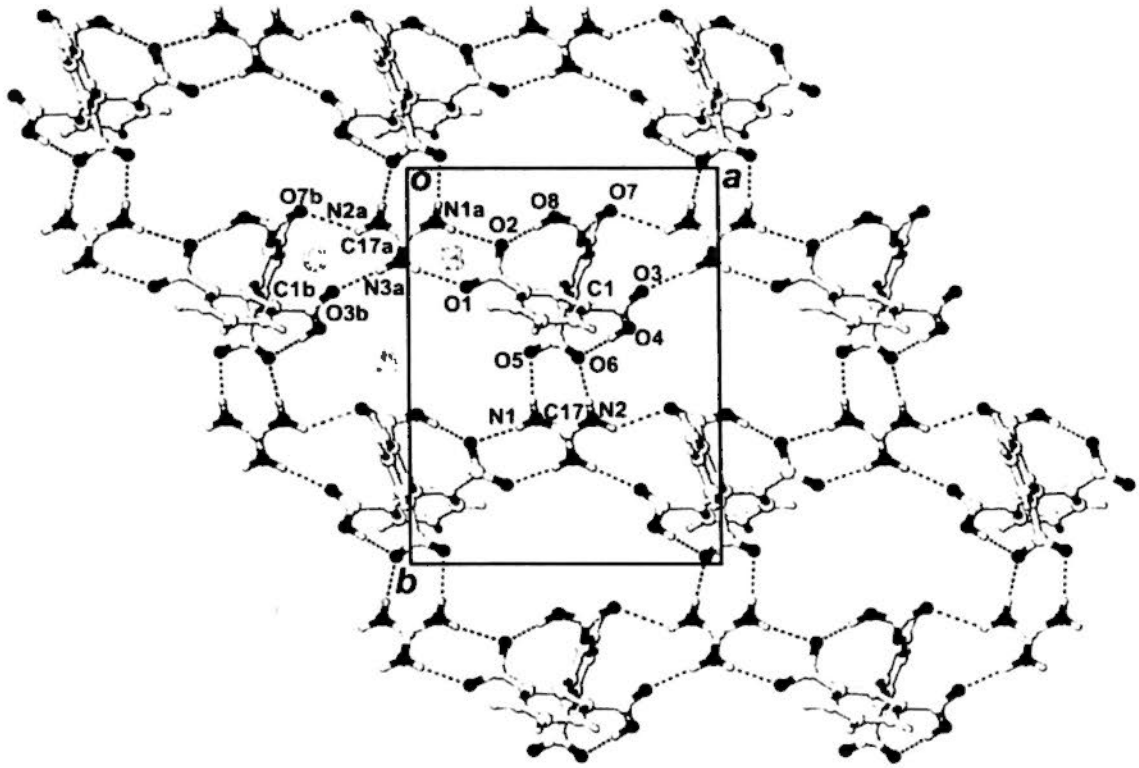

Figure 2.1.30 Projection along the *c* showing the quasi-hexagonal supramolecular rosette motif of **2.1.14**. *Symmetry transformations*: (a) $0.5 - x, -0.5 + y, 1.5 - z$; (b) $-1 + x, y, z$.

The distorted rosette layer of **2.1.14** takes the form of a pleated sheet, in contrast to the nearly planar configuration observed in **2.1.13**. Such sheets are concentrated at $z \approx ¼$ and ¾ with the well-ordered tetra-*n*-propylammonium cation sandwiched in between (Figure 2.1.31).

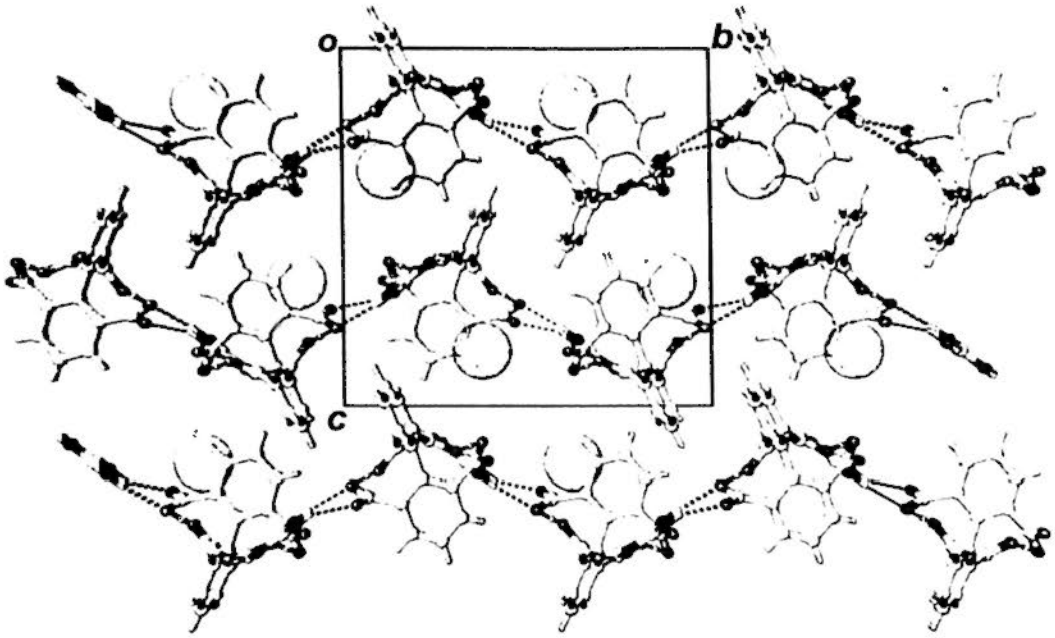

Figure 2.1.31 Crystal structure of **2.1.14**, with large spheres representing the ordered (n-Pr_4)N^+ cations that are accommodated between the pleated sheets.

One alkyl leg of the tetra-*n*-propylammonium cation extends into the central void of a rosette motif to stabilize the pleated sheet structure (Figure 2.1.32).

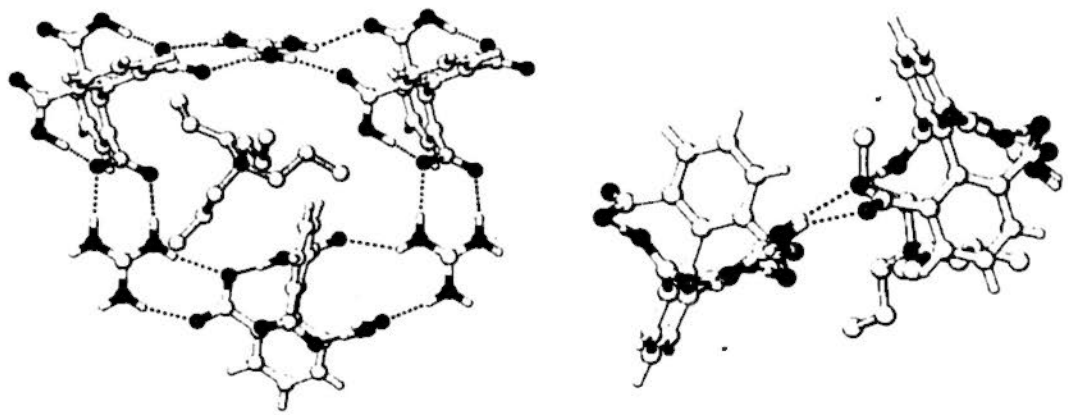

(a) (b)

Figure 2.1.32 An alkyl leg of the tetra-*n*-propylammonium cation is inserted into the central void of the rosette motif in **2.1.14** as viewed (a) along the *c* axis and (b) along the *a* axis.

Table 2.1.14 Hydrogen bonds for **2.1.14** [Å and deg.].

D-H...A	d(D-H)	d(H...A)	d(D...A)	∠(DHA)
O(4)-H(4O)...O(6)	0.85	1.67	2.520(2)	179.9
O(8)-H(8O)...O(2)	0.85	1.66	2.507(2)	180.0
N(1)-H(1A)...O(2)#1	0.86	2.18	3.026(2)	167.5
N(1)-H(1B)...O(5)	0.86	2.02	2.826(2)	155.0
N(2)-H(2A)...O(6)	0.86	2.08	2.936(2)	171.8
N(2)-H(2B)...O(7)#2	0.86	2.37	3.046(2)	135.8
N(3)-H(3A)...O(1)#1	0.86	2.08	2.895(2)	158.2
N(3)-H(3B)...O(3)#2	0.86	2.06	2.902(2)	167.0

Symmetry transformations used to generate equivalent atoms:
#1 -x+1/2,y+1/2,-z+3/2 #2 x+3/2,y+1/2,-z+3/2

2.2 Hydrogen-bonded molecular complexes based on Kemp's triacid

Crystal structure of $[(CH_3)_4N^+] \cdot [C_6H_6(CH_3)_3(COOH)_2(COO^-)] \cdot H_2O$ (2.2.1)

In $[(CH_3)_4N^+] \cdot [C_6H_6(CH_3)_3(COOH)_2(COO^-)] \cdot H_2O$ (**2.2.1**), Kemp's triacid (H_3KTA) takes the H_2KTA^- form with an intramolecular hydrogen bond O5–H···O4. These acids are bridged by water molecules O1w to form zigzag $H_2KTA^- –H_2O$ chains along the [1 0 1] direction (Figure 2.2.1a). Intermolecular hydrogen bonding between pairs of H_2KTA^- ion in adjacent chains generates a wide ribbon containing a large void motif [**A**] (Figure 2.2.1b). Detailed hydrogen-bonding geometries are listed in Table 2.2.1.

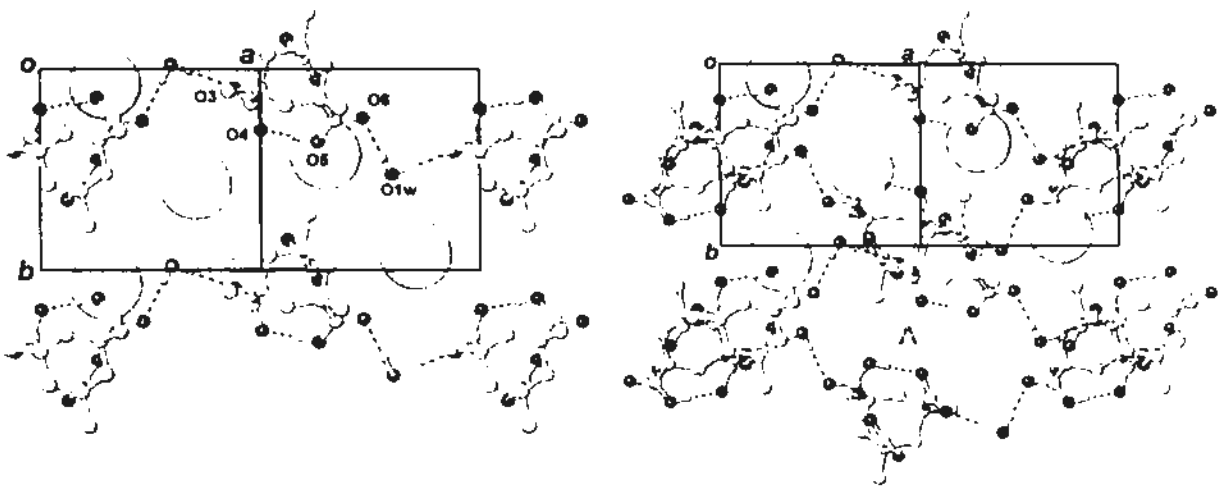

(a) (b)

Figure 2.2.1 Crystal structure of **2.1.1** viewed along the [$\bar{1}$ 0 1] direction: (a) two H_2KTA^-–H_2O zigzag chains formed by hydrogen bonding between the anions and bridging water molecules; (b) double chains formed by linkage between single $H_2KTA^- –H_2O$ chains. The $(CH_3)_4N^+$ ions are shown as large spheres. For clarity, hydrogen atoms of $–CH_2$ and $–CH_3$ groups are omitted.

Figure 2.2.2 shows the packing of ribbons viewed along the *b* axis, and the well-ordered tetramethylammonium cations are fitted to the voids.

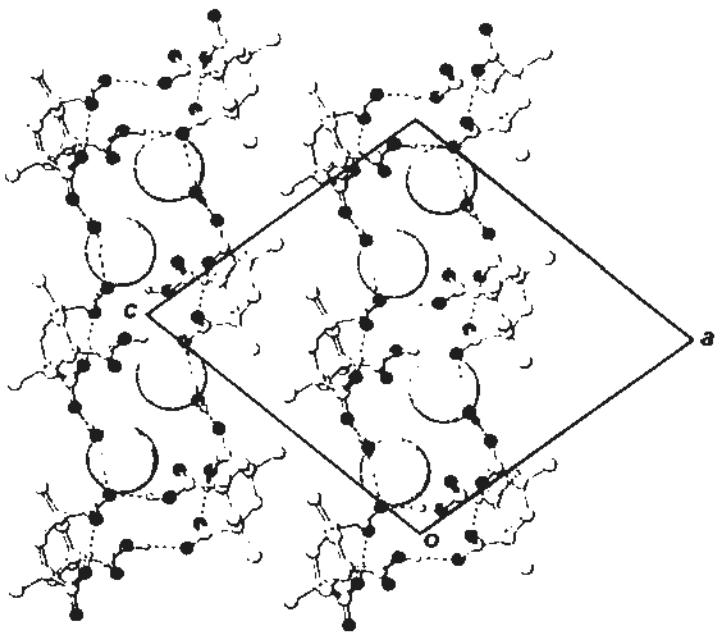

Figure 2.2.2 Projection diagram along the *b* axis showing the packing of double chains and $(CH_3)_4N^+$ ions in the crystal structure of **2.2.1**.

Table 2.2.1 Hydrogen bonds for **2.2.1** [Å and deg.].

D-H...A	d(D-H)	d(H...A)	d(D...A)	∠(DHA)
O(1)-H(1O)...O(3)#1	0.85	1.79	2.641(2)	179.8
O(5)-H(5O)...O(4)	0.85	1.65	2.495(2)	179.9
O(1W)-H(1WA)...O(6)	0.85	2.07	2.915(2)	179.4
O(1W)-H(1WB)...O(3)#2	0.86	2.06	2.914(2)	179.3

Symmetry transformations used to generate equivalent atoms:
#1 -x+1,-y+2,-z+1 #2 x-1/2,-y+3/2,z-1/2

Crystal structure of $[C(NH_2)_3^+] \cdot [C_6H_6(CH_3)_3(COOH)_2(COO^-)]$ (2.2.2)

The fascinating rosette layer structure of $[C(NH_2)_3^+] \cdot [C_6H_6(CH_3)_3(COOH)_2(COO^-)]$ (**2.2.2**) is shown in Figure 2.2.3. In the previous reports of hydrogen-bonded networks exhibiting the rosette motif, the hydrogen carbonate dimer or the nitrate ion is connected with guanidinium, designated as $[(HCO_3)_2\text{–}GM]_2$[49b] or

$(NO_3–GM)_3$ [57], to generate a hexagonal assembly of six molecular components. Detailed hydrogen-bonding geometries are listed in Table 2.2.2.

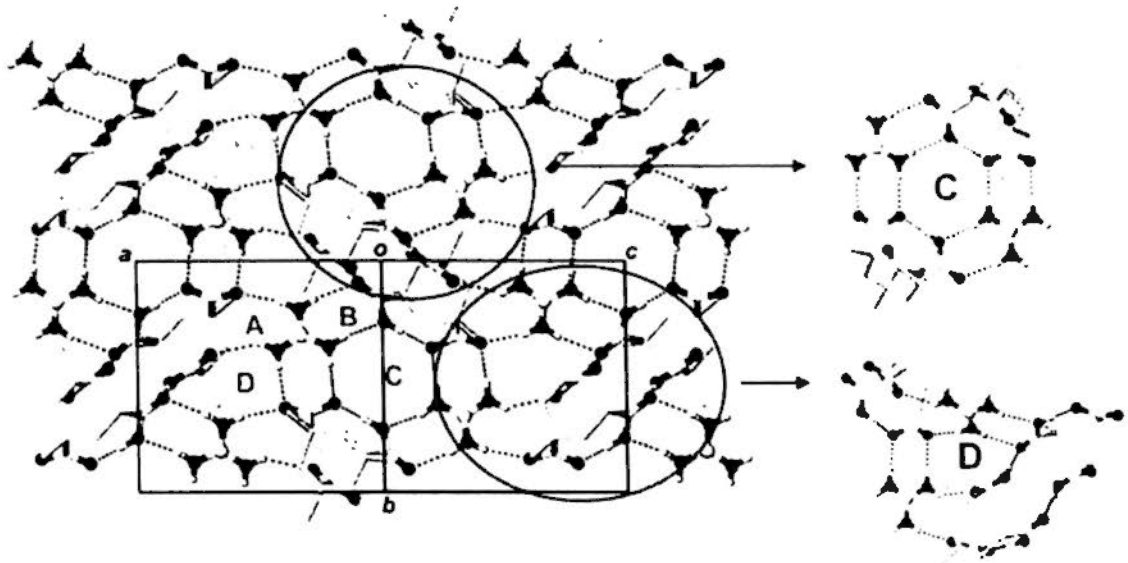

Figure 2.2.3 Projection diagram along the [1 0 1] direction showing two kinds of pseudo rosette motifs (motif [**C**] and [**D**] constructed from four and five molecular moieties, respectively) in the layer structure of complex **2.2.2**. For clarity, hydrogen atoms of methylene and methyl groups are omitted.

In the crystal structure of **2.2.2**, the guanidinium ion is connected with adjacent Kemp's triacid monoanion by a pair of hydrogen bonds to generate a zigzag ribbon showing motif [**A**] and [**B**]. These ribbons are joined together by N–H···O hydrogen bonding between guanidinium and anion, or intermolecular interaction between adjacent anions, to form a rosette motif [**C**] and motif [**D**], respectively.

Intramolecular bonding between one carboxyl group and the carboxylate group of H_2KTA^- mimics that in the $[(HCO_3)_2–GM]_2$ system to generate a rosette motif which is composed of two H_2KTA^- anions (one pointing upward and the other downward) and two guanidiniums. The intramolecular O–H···O distance is about 2.4

Å and the dihedral angle between the carboxyl and carboxylate groups is about 40 °. To our best knowledge, this is a nice reported example to generate of a four-membered rosette motif based on guanidinium and carboxylate in the solid state. The packing diagram of crystal **2.2.2** shows the sinusoid layer structure in Figure 2.2.4.

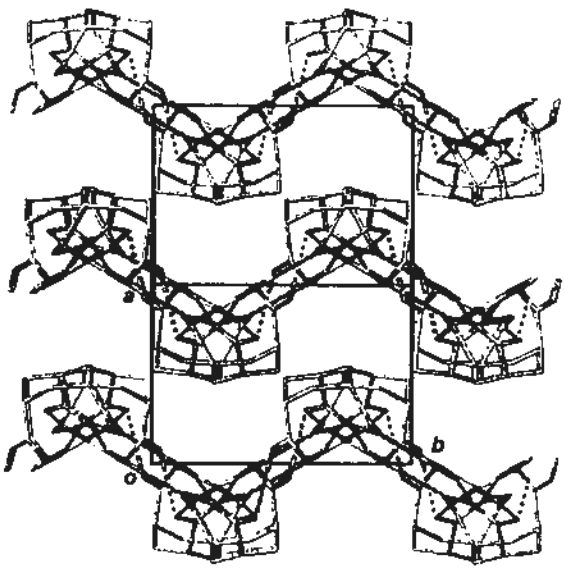

Figure 2.2.4 Sinusoidal layer structure of complex **2.2.2** viewed along the [$\bar{1}$ 0 1] direction. (Hydrogen atom of methylene and methyl groups of H_2KTA^- are omitted for clarity).

Table 2.2.2 Hydrogen bonds for **2.2.2** [Å and deg.].

D-H...A	d(D-H)	d(H...A)	d(D...A)	∠(DHA)
O(4)-H(2)...O(6)#1	0.85	1.90	2.754(2)	180.0
O(5)-H(1)...O(2)	0.85	1.56	2.410(2)	179.9
N(1)-H(1A)...O(1)#2	0.86	2.03	2.890(2)	177.6
N(1)-H(1B)...O(3)#3	0.86	2.26	2.998(2)	143.3
N(1)-H(1B)...O(1)#3	0.86	2.63	3.312(2)	137.6
N(2)-H(2A)...O(6)	0.86	2.15	2.998(2)	170.3
N(2)-H(2B)...O(1)#3	0.86	2.03	2.861(2)	163.3
N(3)-H(3A)...O(5)	0.86	2.07	2.918(2)	166.6
N(3)-H(3B)...O(2)#2	0.86	2.04	2.904(2)	178.5

Symmetry transformations used to generate equivalent atoms:
#1 -x+1,-y+1,-z+1 #2 -x+1,-y+2,-z+1 #3 x-1/2,-y+3/2,z+1

Crystal structure of $3[(C_2H_5)_4N^+] \cdot 20[C(NH_2)_3^+] \cdot 11[C_6H_6(CH_3)_3(COOH)(COO^-)_2] \cdot [C_6H_6(CH_3)_3(COOH)_2(COO^-)] \cdot 17H_2O$ (2.2.3)

The crystal structure of **2.2.3** features a hydrogen-bonded assembly with a centrosymmetric pseudo-octahedral core composed of eight guanidinium ions. There are five guanidinium ions, three H_2KTA^- (two of them are well-ordered and the other is disordered) and ¾ tetraethylammonium cations (N16 is located at a site of symmetry 2 and the other N17 is occupies a $\bar{4}$ site) in the asymmetric unit. In this crystal, the H_2KTA^- can not be distinguished from the eleven $HKTA^{2-}$ anions and total negative charge on the three independent acids is 13.

Three independent guanidinium ions (C38, C40 and C41) are responsible for building faces of the octahedron, and another ion C39 is located inside it (Figure 2.2.5). Water molecules are an additional reinforcement to explore the polyhedral motifs. The center of mass of the three axial carboxyl/carboxylate groups of each H_2KTA^- constitutes a vertex of a distorted octahedron of approximate symmetry $\bar{3}$, with the two central guanidinium ions located close to a pair of opposite faces.

Figure 2.2.6 shows the detail environment of guanidinium ions C39 and C41. Guanidinium C39 is connected with each carboxylate group by two pairwise hydrogen bonds, and bridged water molecule O1w by chelating hydrogen bonds. Guanidinium ion C41 also have two pairwise donor hydrogen bonds connected with each carboxylate group respectively, however, the third two single hydrogen bonds are linked with two different carboxylate groups. Detailed hydrogen-bonding geometries are listed in Table 2.2.3.

(a)

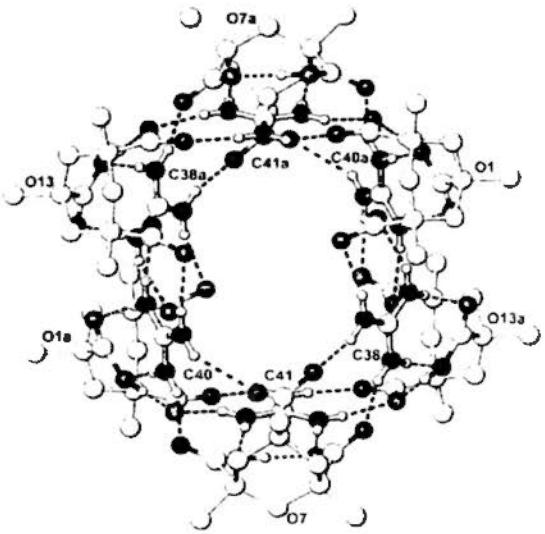

(b)

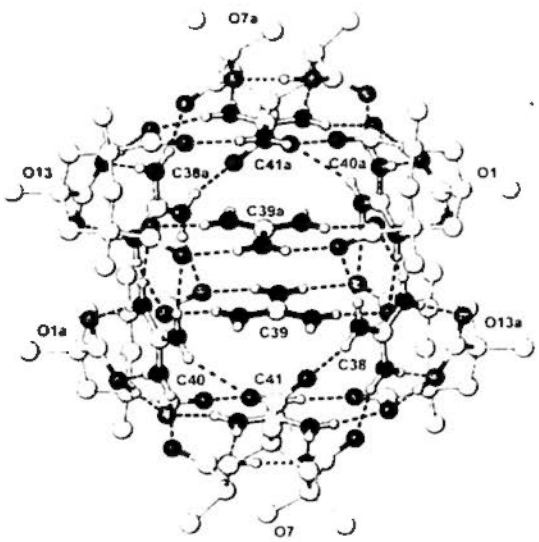

(c)

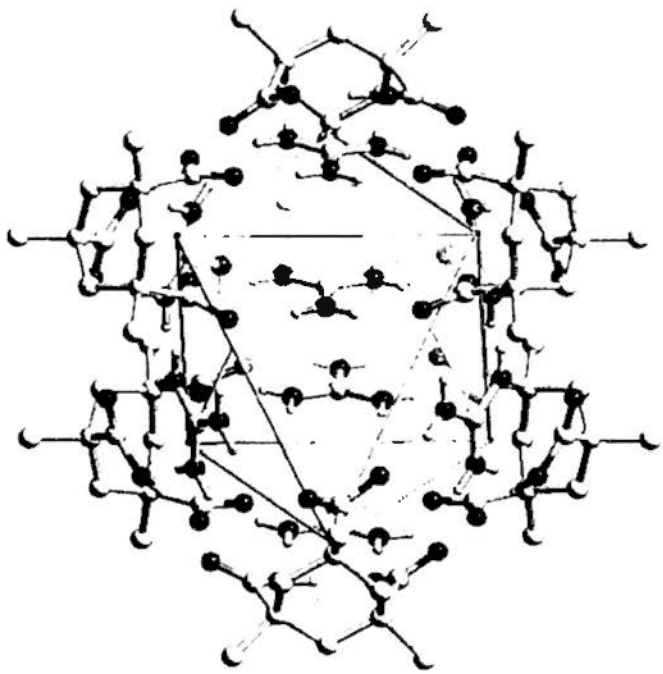

Figure 2.2.5 Hydrogen-bonded centrosymmetric cluster unit composed of six H_2KTA^- and eight guanidinium ions in the crystal structure of **2.2.3**. (a) Six peripheral H_2KTA^- ions arranged around six inner guanidinium ions. (b) Hydrogen bonding involving the remaining two central guanidinium ions C39. (c) Diagram illustrating the geometry of the cluster unit. *Symmetry transformations*: (*a*) $-x, 1-y, 1-z$. For clarity, water molecules are not shown.

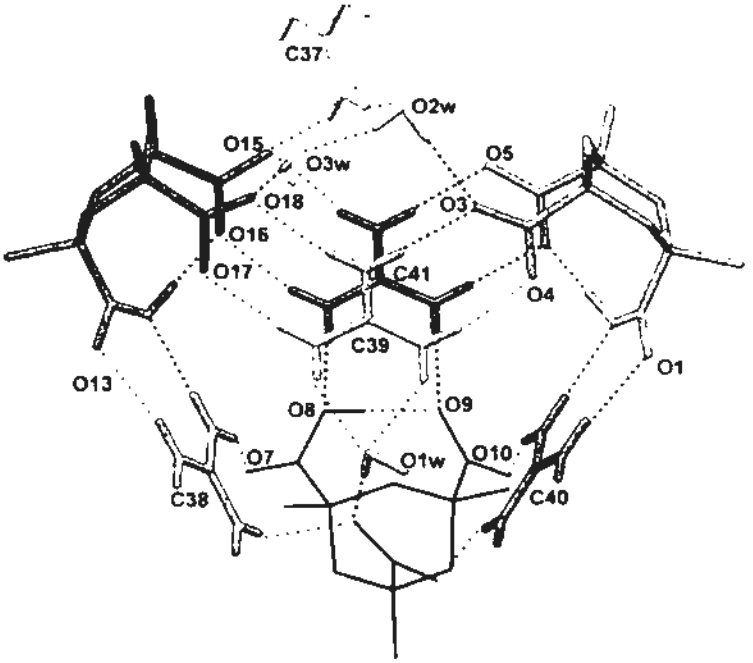

Figure 2.2.6 Hydrogen-bonding environment of guanidinium (C39 and C41) and three independent Kemp's triacid anion with water molecules.

Kemp's triacid anion O1 (for convenience, each anion is denoted by the label of its oxygen atom with the smallest numbering) is hydrogen bonded with guanidinium C38, C39, C40 and C41 by four pairs of hydrogen bonds, and anion O13 is linked with guanidinium C38, C39 and C41 by pairwise hydrogen bonds, with C40 by a single hydrogen bond, and with C37 by a bridging water molecule. In addition, hydrogen bonding between anion O7 and guanidiniums is different from the former two cases. Each guanidinium (C37, C38, C40 and C41) donate its hydrogen atoms to different carboxylate groups of Kemp's triacid anions by forming two single hydrogen bonds between them. Also guanidinium C39 is connected with Kemp's triacid anion by bridging water molecule (Figure 2.2.7).

Between each octahedral motif, guanidinium C37 serves as a linker to join them together. Packing diagram along the *b* axis shows that disordered water

molecules O4w and Et_4N^+ are located in the different voids (Figure 2.2.8). Two independent $(C_2H_5)_4N^+$ cations are accommodated in separate voids.

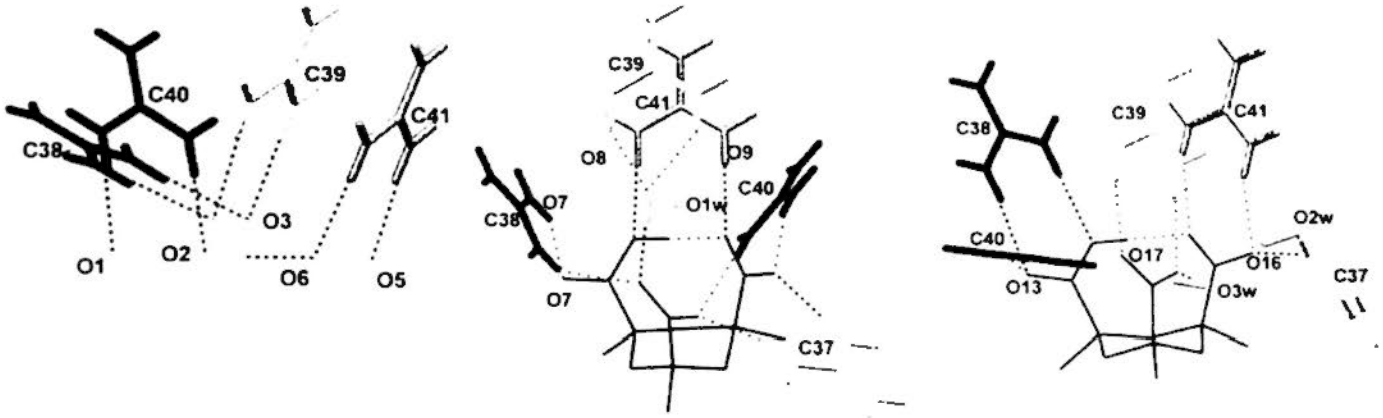

(a) (b) (c)

Figure 2.2.7 Part (a) to (c) comparing the hydrogen-bonding environments of three independent Kemp's triacid anions.

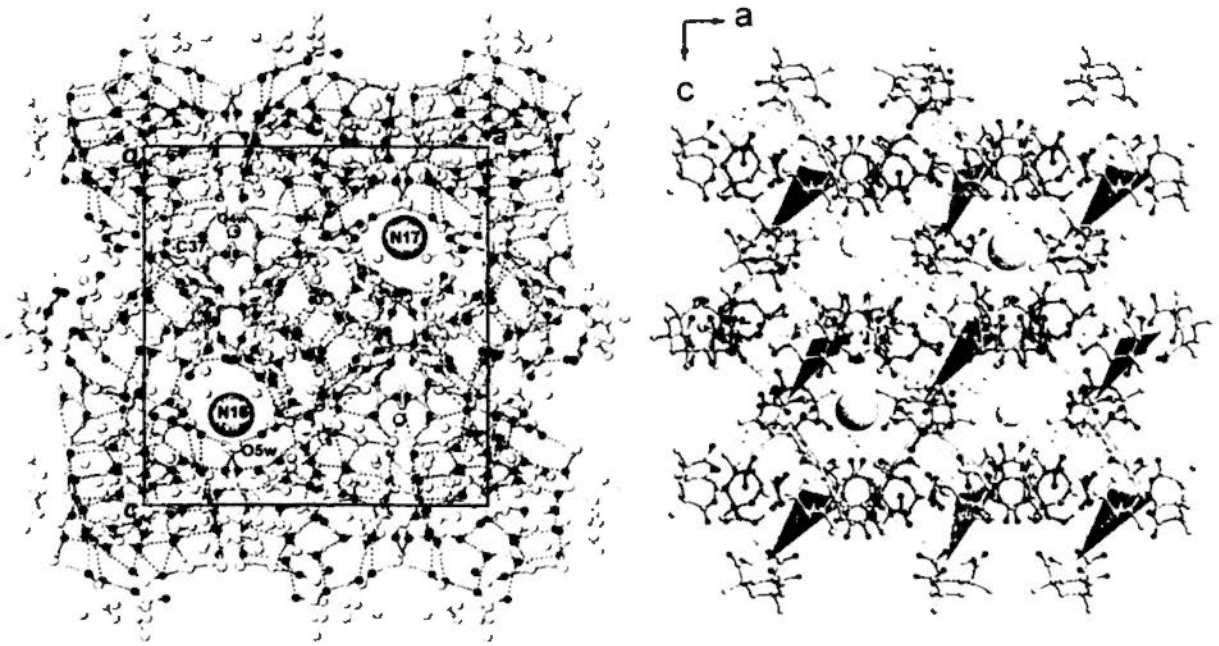

(a) (b)

Figure 2.2.8 (a) Packing diagrams of complex **2.2.3** viewed along the *b* axis. (b) Packing diagram with polyhedral representation of the hydrogen-bonded core units. Et_4N^+ cations (large sphere) are accommodated in separate voids.

Table 2.2.3 Hydrogen bonds for **2.2.3** [Å and deg.].

D-H...A	d(D-H)	d(H...A)	d(D...A)	∠(DHA)
O(2)-H(2O)...O(6)	0.90	1.54	2.435(3)	179.8
O(8)-H(8O)...O(9)	0.90	1.58	2.480(4)	179.9
O(14)-H(14O)...O(16)	0.90	1.58	2.483(6)	179.6
N(1)-H(1C)...O(2W)	0.88	2.13	2.959(4)	156.1
N(1)-H(1D)...O(15)	0.88	2.03	2.851(5)	155.1
N(2)-H(2B)...O(2W)	0.88	2.46	3.203(3)	143.1
N(2)-H(2A)...O(12)#2	0.88	2.07	2.914(3)	159.4
N(3)-H(3D)...O(15)	0.88	2.63	3.305(5)	134.3
N(3)-H(3C)...O(10)#2	0.88	2.01	2.883(4)	173.2
N(4)-H(4A)...O(13)#1	0.88	2.15	3.012(5)	164.5
N(4)-H(4B)...O(4)	0.88	2.08	2.957(4)	172.8
N(5)-H(5C)...O(14)#1	0.88	2.02	2.898(4)	176.3
N(5)-H(5D)...O(7)	0.88	2.03	2.855(3)	155.5
N(6)-H(6A)...O(3)	0.88	2.14	3.015(4)	173.9
N(6)-H(6B)...O(11)	0.88	2.30	3.045(3)	142.7
N(7)-H(7B)...O(3)	0.88	2.02	2.900(3)	174.5
N(7)-H(7A)...O(18)	0.88	2.10	2.97(2)	160.7
N(8)-H(8B)...O(4)	0.88	2.03	2.893(3)	168.1
N(8)-H(8A)...O(1W)#1	0.88	2.19	2.953(4)	145.3
N(9)-H(9B)...O(17)	0.88	2.07	2.928(4)	163.5
N(9)-H(9A)...O(1W)#1	0.88	2.12	2.903(4)	148.0
N(10)-H(10D)...O(12)	0.88	2.06	2.895(3)	158.0
N(10)-H(10E)...O(18)	0.88	2.36	3.213(9)	162.9
N(10)-H(10E)...O(17)	0.88	2.61	3.362(5)	143.8
N(11)-H(11D)...O(1)#1	0.88	1.99	2.863(3)	170.7
N(11)-H(11E)...O(17)	0.88	2.28	3.113(5)	157.3
N(11)-H(11E)...O(13)	0.88	2.44	3.035(4)	125.1
N(12)-H(12E)...O(2)#1	0.88	2.00	2.878(3)	177.0
N(12)-H(12D)...O(10)	0.88	1.99	2.839(3)	162.1
N(13)-H(13C)...O(8)	0.88	2.09	2.965(4)	170.7
N(14)-H(14A)...O(5)#1	0.88	1.99	2.871(5)	174.6
N(14)-H(14B)...O(15)#1	0.88	2.08	2.916(5)	157.9
N(15)-H(15D)...O(6)#1	0.88	2.04	2.912(4)	174.3
N(15)-H(15C)...O(9)	0.88	2.01	2.885(4)	177.1
O(1W)-H(1WA)...O(11)	0.86	1.88	2.743(3)	179.4
O(1W)-H(1WB)...N(10)	0.87	2.36	3.230(4)	178.4
O(2W)-H(2WA)...O(3)	0.85	1.95	2.796(3)	177.7
O(2W)-H(2WB)...O(3W)	0.86	1.93	2.761(3)	164.1
O(3W)-H(3WA)...O(12)	0.86	1.90	2.760(3)	179.4
O(3W)-H(3WB)...O(18)	0.85	1.84	2.70(1)	179.3
O(5W)-H(5WA)...O(13)	0.85	1.60	2.45(1)	179.2
O(5W)-H(5WB)...O(1)#1	0.86	2.06	2.94(1)	179.5

Symmetry transformations used to generate equivalent atoms:
#1 -x,-y+1,-z+1 #2 -y+1/2,x,-z+1/2

Crystal structure of $3[C(NH_2)_3^+] \cdot [C_6H_6(CH_3)_3(COO^-)_3]$ (2.2.4)

The simple salt $3[C(NH_2)_3^+] \cdot [C_6H_6(CH_3)_3(COO^-)_3]$ **(2.2.4)** crystallizes in the trigonal space group *R*3*c*; the guanidinium ion occupies a general position, and the trianion of Kemp's triacid KTA^{3-} is located at a special position of site symmetry 3. In the crystal structure, nine symmetry-related guanidiniums are arranged around one KTA^{3-} to form a total of eighteen donor hydrogen bonds. In turn, the guanidinium ions are arranged around a 3_1 axis, and around each guanidinium there are three KTA^{3-} trianions (Figure 2.2.9 and 2.2.10). Detailed hydrogen-bonding geometries are listed in Table 2.2.4.

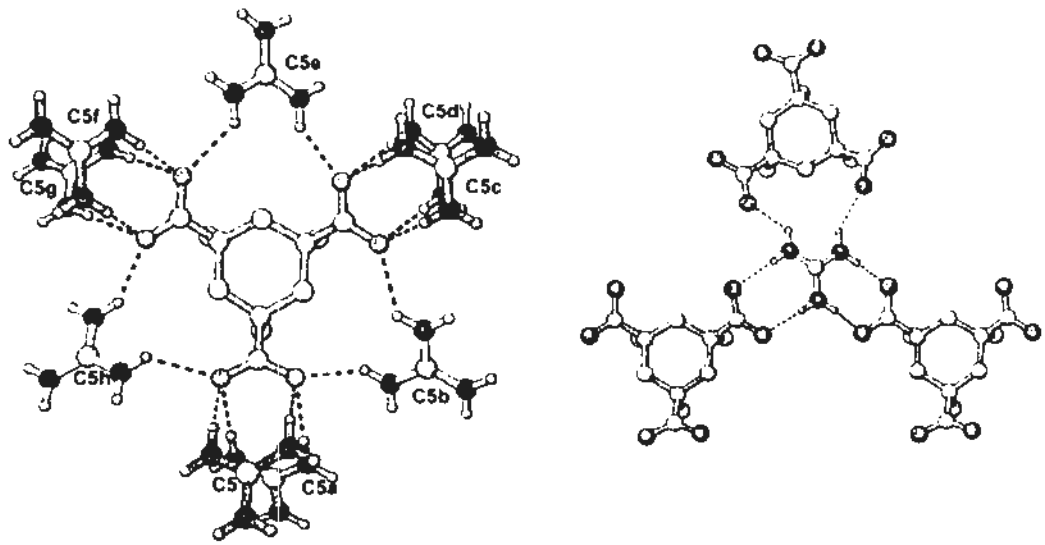

(a) (b)

Figure 2.2.9 (a) Nine guanidiniums arranged around one KTA^{3-} in **2.2.4** viewed along the *c* axis. *Symmetry transformations*: (*a*) 1/3 − *y*, −1/3 + x − *y*, −1/3 + *z*; (*b*) −1/3 + *x*, −2/3 + x − *y*, −1/6 + *z*; (*c*) −2/3 + *y*, −1/3 + *y*, −1/3 + *z*; (*d*) −*x* + *y*, − *x*, *z*; (*e*) −1/3 − *y*, 1/3 − *x*, −2/3 + *z*; (*f*) 1/3 − *x* + *y*, 2/3 − *x*, −1/3 + *z*; (*g*) − *y*, *x* − *y*, *z*; (*h*) 2/3 −*x* + *y*, 1/3 + *y*, −1/6 + *z*; (b) hydrogen-bonding environment of guanidinium ion.

In the crystal packing of **2.2.4**, the KTA^{3-} and guanidinium ions are cross-linked to form a closely knit hydrogen-bonded three dimensional network (Figure 2.2.10).

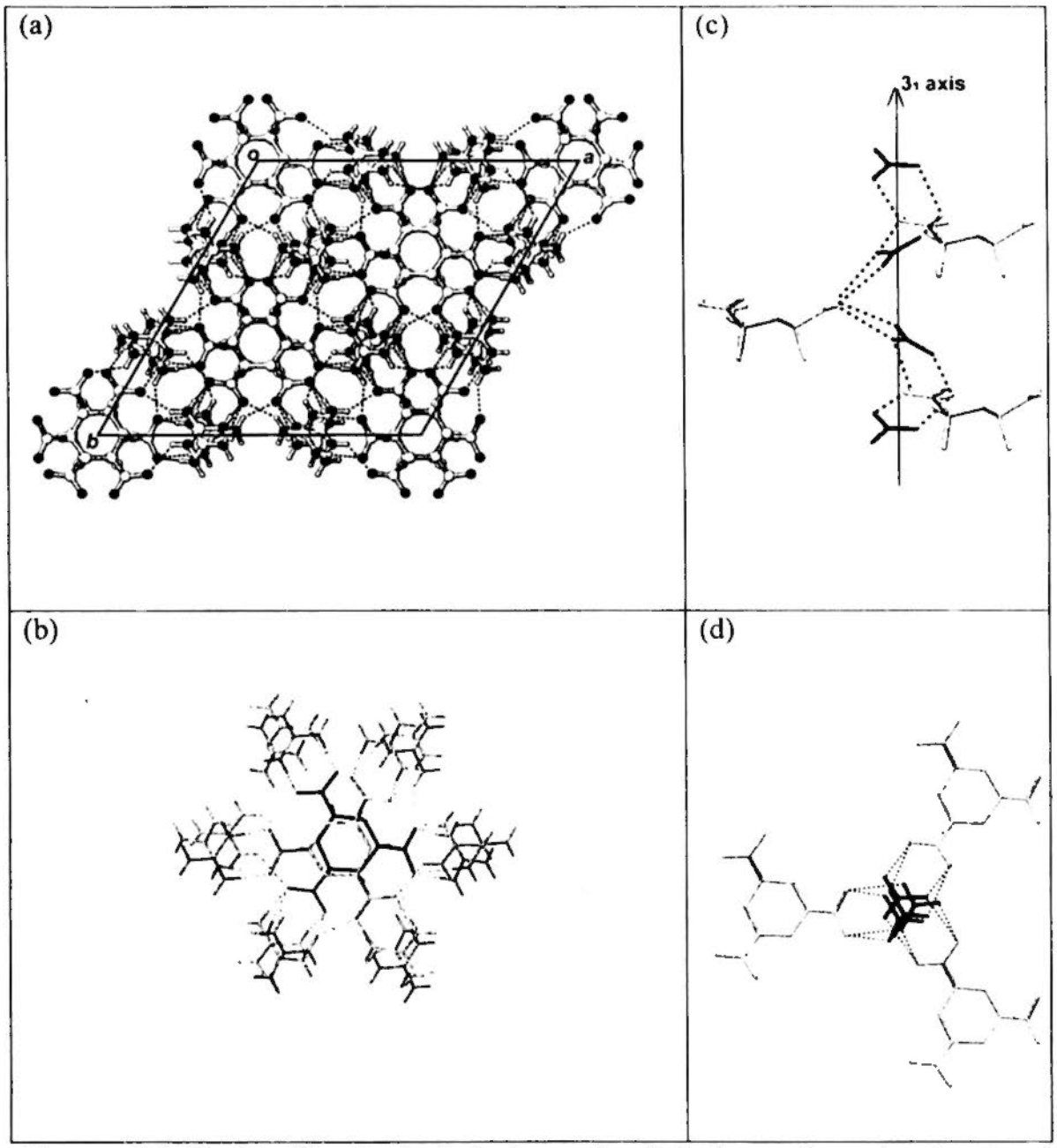

Figure 2.2.10 (a) Closely knit hydrogen-bonded three dimensional network structure of **2.2.4** viewed along the *c* axis; (b) two overlapping but non-connected KTA^{3-} anions each connected with adjacent guanidinium ion viewed almost along the *c* axis and (c) guanidinium ions related by the 3_1 axis are bridged by the

carboxylate groups of adjacent KTA^{3-} anions; (d) the content of part (c) viewed along the *c* axis.

Table 2.2.4 Hydrogen bonds for **2.2.4** [Å and deg.].

D-H...A	d(D-H)	d(H...A)	d(D...A)	∠(DHA)
N(3)-H(3B)...O(1)	0.86	2.16	3.017(2)	177.6
N(3)-H(3A)...O(2)#1	0.86	2.13	2.911(2)	151.4
N(2)-H(2B)...O(1)#1	0.86	1.97	2.808(2)	163.3
N(2)-H(2A)...O(2)#2	0.86	2.12	2.866(2)	145.3
N(1)-H(1B)...O(2)	0.86	2.08	2.928(2)	170.0
N(1)-H(1A) .O(1)#3	0.86	2.48	3.047(2)	124.1

Symmetry transformations used to generate equivalent atoms:
#1 -x+y+2/3,-x+1/3,z+1/3 #2 x+1/3,x-y-1/3,z+1/6 #3 x+y+1/3,y-1/3,z+1/6

Crystal structure of $[(n\text{-}C_3H_7)_4N^+] \cdot 2[C(NH_2)_3^+] \cdot [C_6H_6(CH_3)_3(COO^-)_3]$ (2.2.5)

The tetra-*n*-propylammonium ion serves as a structure-inducing agent in the complex $[(n\text{-}C_3H_7)_4N^+] \cdot 2[C(NH_2)_3^+] \cdot [C_6H_6(CH_3)_3(COO^-)_3]$ (**2.2.5**). Four independent guanidinium cations constitute a tetrahedral central core despite the expected repulsion of their positive charges. This cationic core is consolidated by a pseudo-octahedral arrangement of six independent KTA^{3-} ions, each lying above an edge of the $[C(NH_2)_3^+]_4$ tetrahedron to form four donor hydrogen bonds (Figure 2.2.11). Detailed hydrogen-bonding geometries are listed in Table 2.2.5.

(a)

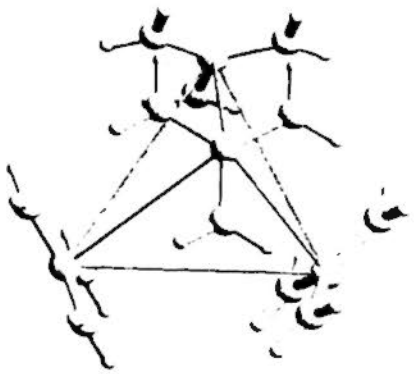

(b) (c)

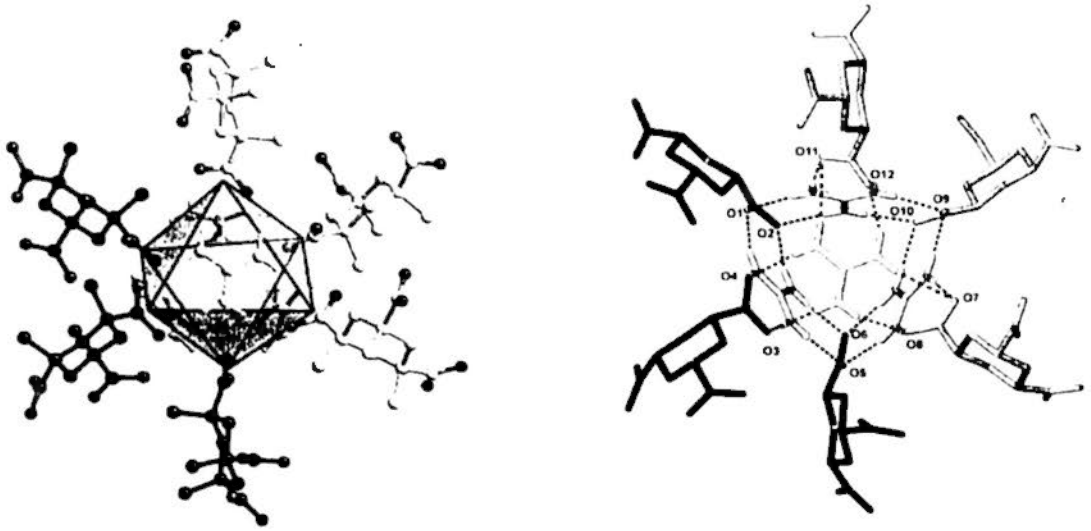

Figure 2.2.11 Structural unit of **2.2.5** composed of a central core of four guanidiniums surrounded by six peripheral KTA^{3-} ions: (a) guanidinium cations constitute a tetrahedral $[C(NH_2)_3^+]_4$ central core with a C atom at each vertex; (b) arrangement of six KTA^{3-} anions around the tetrahedral central core, with the center of mass of a carboxylate group at each vertex of the pseudo-octahedron; and (c) hydrogen-bonding connections between guanidinium and KTA^{3-} ions.

Figure 2.2.12 shows the three-dimensional network structure of **2.2.5** constructed from the assembly of the structural units. The tetra-*n*-propylammonium cations are accommodated in each channel.

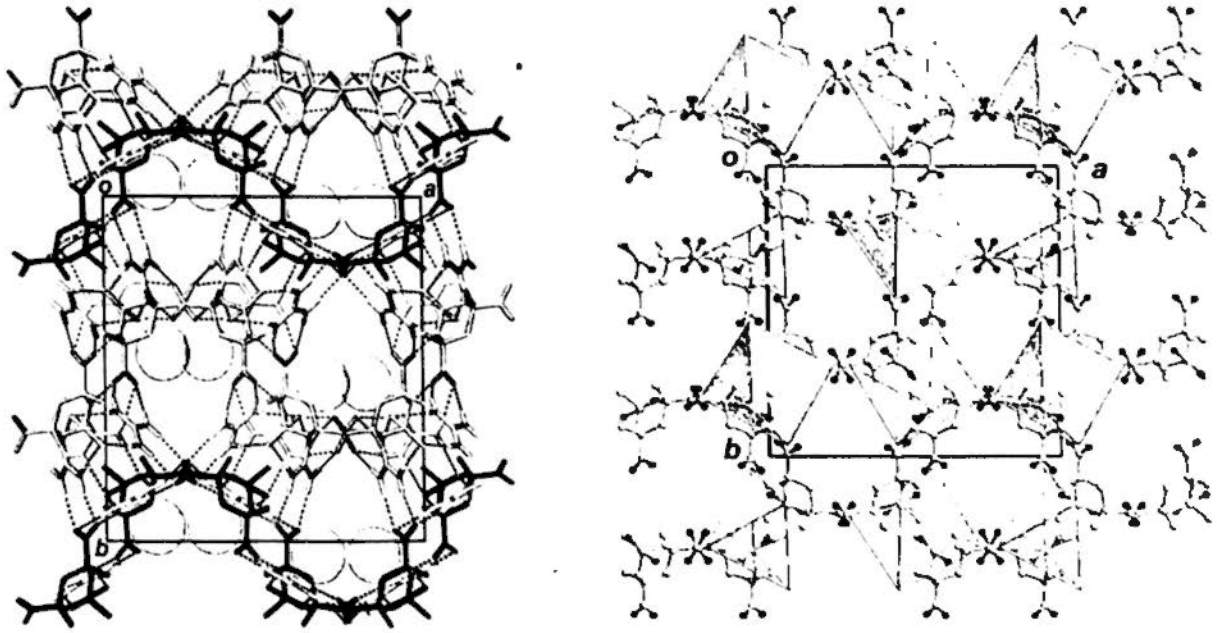

(a) (b)

Figure 2.2.12 (a) Packing diagram of complex **2.2.5** viewed along the *c* axis with each $(n\text{-Pr})_4N^+$ represented by a large sphere. The hydrogen bonds are represented by broken lines. (b) Polyhedral representation with guanidinium and $(n\text{-Pr})_4N^+$ ions omitted for clarity.

Table 2.2.5 Hydrogen bonds for **2.2.5** [Å and deg.].

D-H...A	d(D-H)	d(H...A)	d(D...A)	∠(DHA)
N(1)-H(1C)...O(9)#1	0.86	2.06	2.896(6)	165.5
N(1)-H(1D)...O(12)#2	0.86	2.06	2.876(8)	158.5
N(2)-H(2A)...O(11)#2	0.86	2.07	2.905(7)	163.7
N(2)-H(2B)...O(1)#3	0.86	2.11	2.967(7)	175.4
N(3)-H(3C)...O(10)#1	0.86	2.03	2.868(5)	165.7
N(3)-H(3D)...O(2)#3	0.86	2.09	2.953(5)	178.0
N(4)-H(4A)...O(4)#4	0.86	2.00	2.823(5)	160.2
N(4)-H(4B)...O(1)#3	0.86	1.96	2.803(6)	164.9
N(5)-H(5C)...O(3)#4	0.86	2.07	2.933(5)	177.4
N(5)-H(5D)...O(5)	0.86	1.99	2.843(5)	174.9
N(6)-H(6A)...O(2)#3	0.86	2.05	2.899(5)	168.7
N(6)-H(6B)...O(6)	0.86	2.07	2.925(5)	175.5
N(7)-H(7A)...O(6)	0.86	2.13	2.993(6)	175.8
N(7)-H(7B)...O(10)#1	0.86	2.11	2.967(6)	177.8

N(8)-H(8A)...O(7)	0.86	2.10	2.946(6)	169.9
N(8)-H(8B)...O(9)#1	0.86	2.01	2.870(6)	176.0
N(9)-H(9A)...O(5)	0.86	1.97	2.819(6)	167.7
N(9)-H(9B)...O(8)	0.86	2.02	2.848(7)	161.5
N(10)-H(10D)...O(12)#2	0.86	2.37	3.075(9)	139.1
N(10)-H(10E)...O(4)#4	0.86	1.98	2.838(6)	173.7
N(11)-H(11D)...O(12)#2	0.86	1.97	2.770(8)	155.3
N(11)-H(11E)...O(8)	0.86	2.42	3.125(8)	139.0
N(11)-H(11E)...O(7)	0.86	2.61	3.431(7)	159.7
N(12)-H(12D)...O(3)#4	0.86	2.09	2.941(5)	172.7
N(12)-H(12E)...O(8)	0.86	2.02	2.817(6)	154.4

Symmetry transformations used to generate equivalent atoms:
#1 -x+3/2,y,z+1/2 #2 -x+1,-y+1,z+1/2 #3 -x+1,-y+2,z+1/2 #4 x-1/2,-y+2,z

Crystal structure of $[(CH_3)_4N^+]\cdot 2[C(NH_2)_3^+]\cdot[C_6H_6(CH_3)_3(COO^-)_3]\cdot 2H_2O$ (2.2.6)

In complex **2.2.6**, fully deprotonated Kemp's triacid shows an unusual twist-boat conformation (Figure 2.2.13b). The KTA^{3-} ion and independent bridging water molecules O1w and O2w form a centrosymmetric cyclic hexamer with endocyclic methyl groups (Figure 2.2.13a). These $(KTA^{3-}\cdot 2H_2O)_2$ assemblies are interconnected by two independent guanidinium ions, one (C13) orientated nearly parallel to (0 0 1) and the other (C14) at a slant (Figure 2.2.14a) to form a wide ribbon (Figure 2.2.14b). The double ribbons are further cross-linked by guanidinium C14 and KTA^{3-} ions to from a three-dimensional channel structure Figure 2.2.15. The well-ordered tetramethylammonium cation is located between the wide ribbons. Detailed hydrogen-bonding geometries are listed in Table 2.2.6.

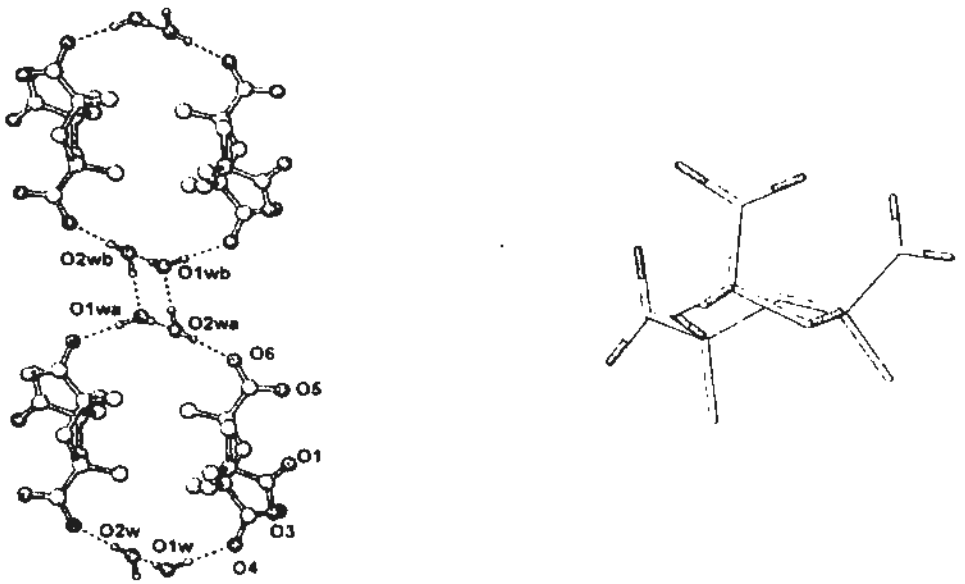

(a) (b)

Figure 2.2.13 (a) Crystal structure of **2.2.6** showing a centrosymmetric cyclic hexamer generated with KTA^{3-} and two water molecules and (b) twist-boat formation of KTA^{3-}. *Symmetry transformations*: (*a*) $1 - x, 1 - y, -z$; (*b*) $x, 1 + y, z$.

Table 2.2.6 Hydrogen bonds for **2.2.6** [Å and deg.].

D-H...A	d(D-H)	d(H...A)	d(D...A)	∠(DHA)
N(1)-H(1C)...O(5)#1	0.86	2.03	2.883(2)	172.9
N(1)-H(1D)...O(3)	0.86	2.34	2.960(2)	129.8
N(2)-H(2B)...O(5)	0.86	2.01	2.778(2)	147.3
N(2)-H(2A)...O(3)#2	0.86	2.13	2.992(2)	178.3
N(3)-H(3C)...O(6)#1	0.86	1.89	2.740(2)	167.3
N(3)-H(3D)...O(4)#2	0.86	1.92	2.740(2)	160.1
N(4)-H(4A)...O(1)	0.86	2.55	3.216(2)	135.4
N(4)-H(4B)...O(2)#2	0.86	1.95	2.765(2)	158.9
N(5)-H(5C)...O(1)	0.86	1.99	2.795(2)	156.4
N(5)-H(5D)...O(3)#3	0.86	2.00	2.819(2)	158.9
N(6)-H(6A)...O(1)#2	0.86	2.05	2.888(2)	164.4
O(1W)-H(1WA)...O(2W)	0.86	1.92	2.780(3)	177.6
O(1W)-H(1WB)...O(4)	0.87	1.87	2.742(2)	178.7
O(2W)-H(2WA)...O(6)#4	0.83	1.94	2.778(2)	177.3
O(2W)-H(2WB)...O(1W)#5	0.95	1.80	2.746(3)	164.7

Symmetry transformations used to generate equivalent atoms:
#1 -x+3/2,y-1/2,z #2 -x+3/2,y+1/2,z #3 x,-y+1,z+1/2 #4 -x+1,-y+1,-z #5 -x+1,-y,-z

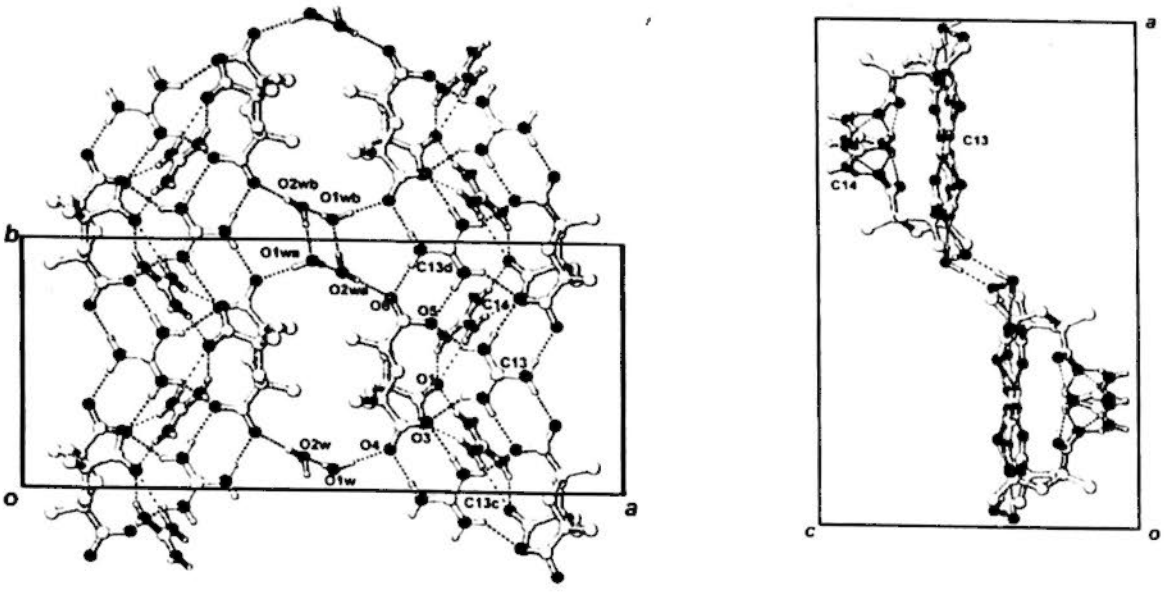

Figure 2.2.14 (a) A wide ribbon in **2.2.6** composed of KTA^{3-}, guanidinium C13, C14 and water molecules viewed along the *c* axis. *Symmetry transformations*: (*a*) 1 − *x*, 1 − *y*, − *z*; (*b*) *x*, 1 + *y*, *z*; (*c*) 1.5 − *x*, − 0.5 + *y* , − *z*; (*d*) 1.5 − *x*, 0.5 + *y*, − *z*. (b) Viewed along the *b* axis.

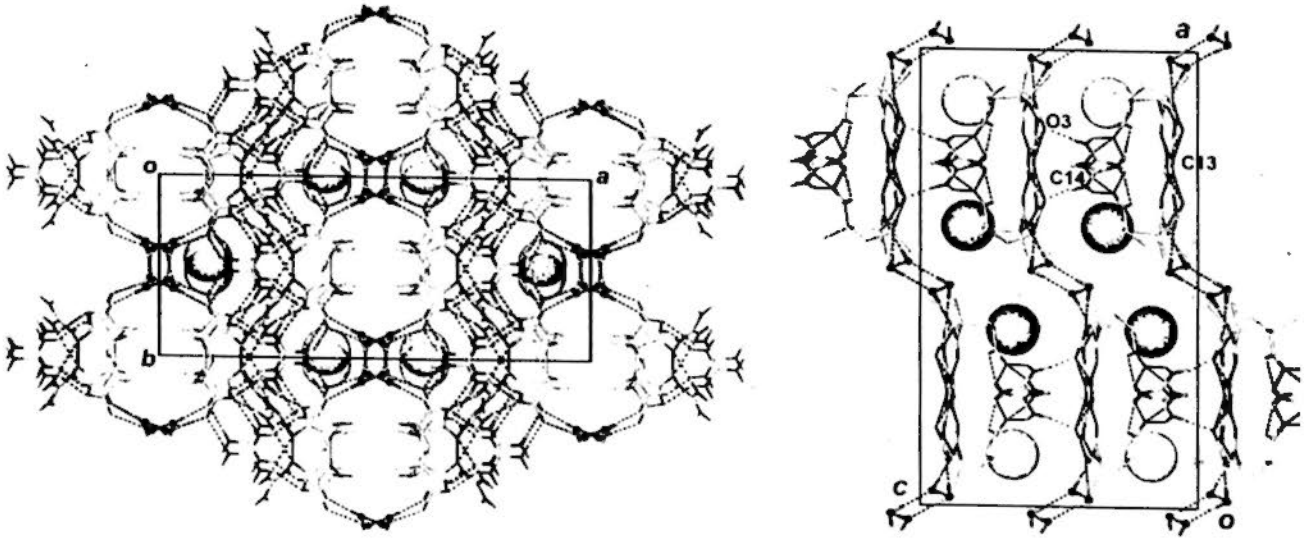

Figure 2.2.15 Packing diagram of complex **2.2.6** (a) viewed along the *c* axis and (b) viewed along the *b* axis.

2.3 Supramolecular hydrogen bonding motifs based on aromatic carboxylic acids

Crystal structure of $3[(n\text{-}C_4H_9)_4N^+]\cdot 2[C(NH_2)_3^+]\cdot 3[1,4\text{-}C_6H_4(COOH)(CO_2^-)]\cdot [1,4\text{-}C_6H_4(CO_2^-)_2]\cdot 2H_2O$ (2.3.1)

In the complex **2.3.1**, there are three tetra-*n*-butylammonium cations, two guanidinium ions, four mix-charged terephthalates (using number *1* to *4* to represent them for convenience) and two water molecules in the asymmetric unit. The 1,4-phenyl-dicarboxylate monoanions *1* and *2* are bridged by water molecules to form motif [**A**] = $R_4^4(22)$ (Figure 2.3.1).

In addition, dianion *4* is joined with guanidinium ions by pairwise hydrogen bonds N4–H···O14 and N5–H···O13 and chelating hydrogen bonds N6a–H···O15 and N4a–H···O15 to form an infinite chain along the *a* axis. Monoanion *3* is hydrogen bonded with adjacent guanidinium ions to form a zigzag chain. Further cross-linkage between these two kinds of chains creates ribbon **I** by forming motif [**B**] = $R_4^4(22)$. Ribbon **I** and repeated motifs [**A**] are further connected together to generate a wavy layer by forming hydrogen-bonding motifs [**C**] and [**D**]. Dihedral angles between phenyl rings in *1* and *2* is about 27 °, and 34 ° in *3* and *4*. The detailed hydrogen-bonding geometries are listed in Table 2.3.1.

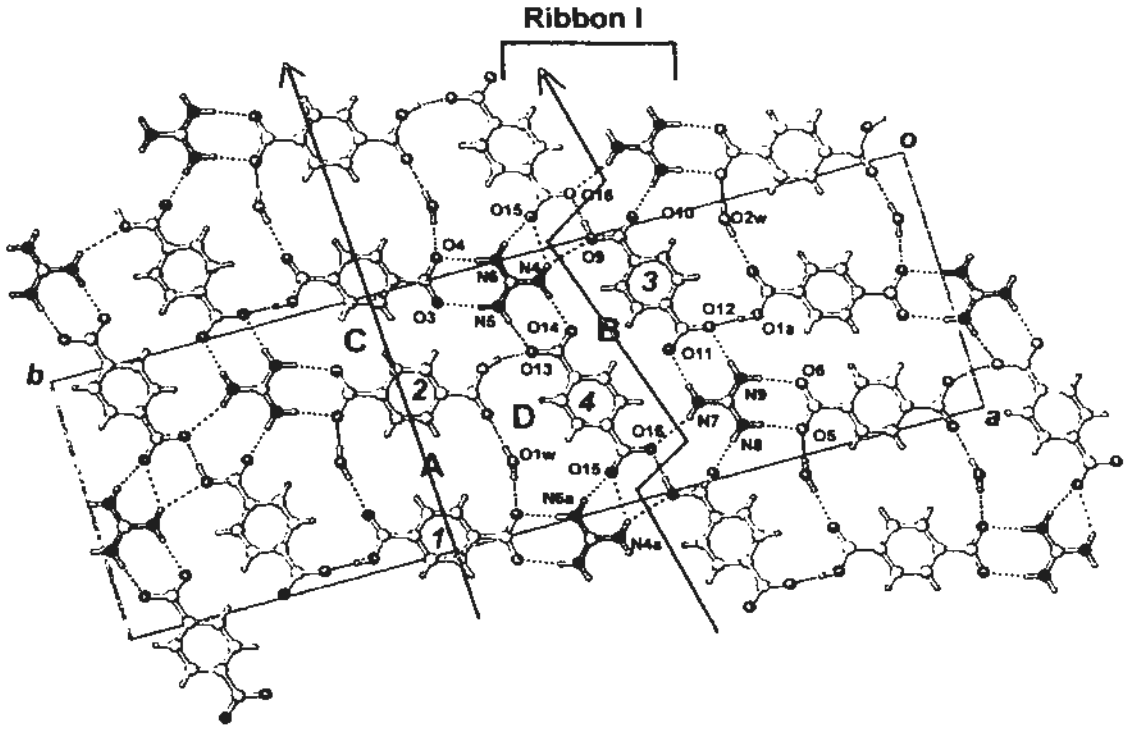

Figure 2.3.1 Projection diagram showing a hydrogen-bonding layer composed of mix-charged terephthalates, guanidinium ions and water molecules in the crystal structure of **2.3.1**. *Symmetry transformations*: (a) 1.5 + *x*, 0.5 + *y*, *z*.

Table 2.3.1 Hydrogen bonds for **2.3.1** [Å and deg.].

D-H...A	d(D-H)	d(H...A)	d(D...A)	∠(DHA)
O(1)-H(1E)...O(12)#1	0.86	1.66	2.525(5)	179.8
O(8)-H(8E)...O(13)#2	0.86	1.67	2.499(5)	161.4
N(4)-H(4A)...O(15)#3	0.86	2.53	3.200(6)	135.2
N(4)-H(4B)...O(14)	0.86	2.06	2.913(6)	175.5
N(5)-H(5B)...O(3)	0.86	2.04	2.892(6)	168.7
N(5)-H(5C)...O(13)	0.86	2.14	2.954(6)	157.9
N(6)-H(6B)...O(4)	0.86	1.95	2.800(6)	169.9
N(6)-H(6C)...O(15)#3	0.86	1.95	2.768(6)	158.9
N(7)-H(7A)...O(16)	0.86	2.52	3.339(6)	158.9
N(7)-H(7B)...O(11)	0.86	2.02	2.878(6)	171.5
N(8)-H(8A)...O(5)	0.86	1.95	2.803(6)	172.3
N(8)-H(8B)...O(10)#4	0.86	1.91	2.771(6)	178.9
N(9)-H(9A)...O(6)	0.86	1.99	2.843(6)	169.0
N(9)-H(9B)...O(12)	0.86	2.08	2.902(6)	160.8
O(1W)-H(1WA)...O(7)#1	0.86	2.16	3.020(7)	178.4
O(1W)-H(1WB)...O(4)#4	0.86	1.97	2.834(7)	178.7
O(2W)-H(2WA)...O(2)#2	0.86	2.15	3.013(6)	178.3
O(2W)-H(2WB)...O(5)#3	0.86	1.88	2.743(7)	178.5

Symmetry transformations used to generate equivalent atoms:
#1 x-1/2,y+1/2,z #2 x+1/2,y-1/2,z #3 x-1,y,z #4 x+1,y,z

The packing diagram of complex **2.3.1** is illustrated in Figure 2.3.2. The well-ordered $(n\text{-}C_4H_9)_4N^+$ ions are sandwiched between nearly planar hydrogen-bonded layers with an interlayer spacing of $c/2$ = 8.25 Å (Figure 2.3.2).

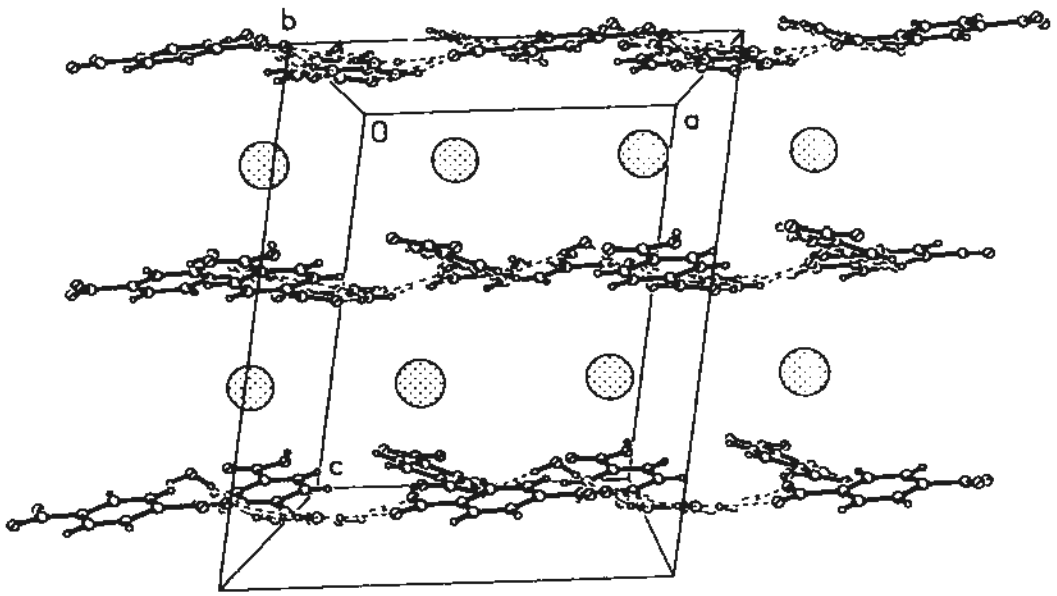

Figure 2.3.2 Layer structure of complex **2.3.1** viewed along the *b* axis with an interlayer spacing of 8.25 Å. The $(n\text{-}C_4H_9)_4N^+$ ion is represented by a large sphere.

Crystal structure of $2[C(NH_2)_3^+] \cdot [2,6\text{-}C_{10}H_4(CO_2^-)_2] \cdot 4H_2O$ (2.3.2)

The asymmetric unit of **2.3.2** is composed of one guanidinium ion, two water molecules and one-half of naphthalene-2,6-dicarboxylate which is located at a center of symmetry. In the crystal structure of **2.3.2**, the centrosymmetric naphthalene-2,6-dicarboxylate dianion (NDC) is hydrogen bonded with two adjacent guanidinium ions by pairwises hydrogen bonds to form a planar NDC–GM trimer (Figure 2.3.3a). Adjacent trimers are cross-bridged by guanidinium-to-carboxylate chelating hydrogen bonds to generate a zigzag band running along the *b* axis. Detailed hydrogen-bonding geometries are listed in Table 2.3.2.

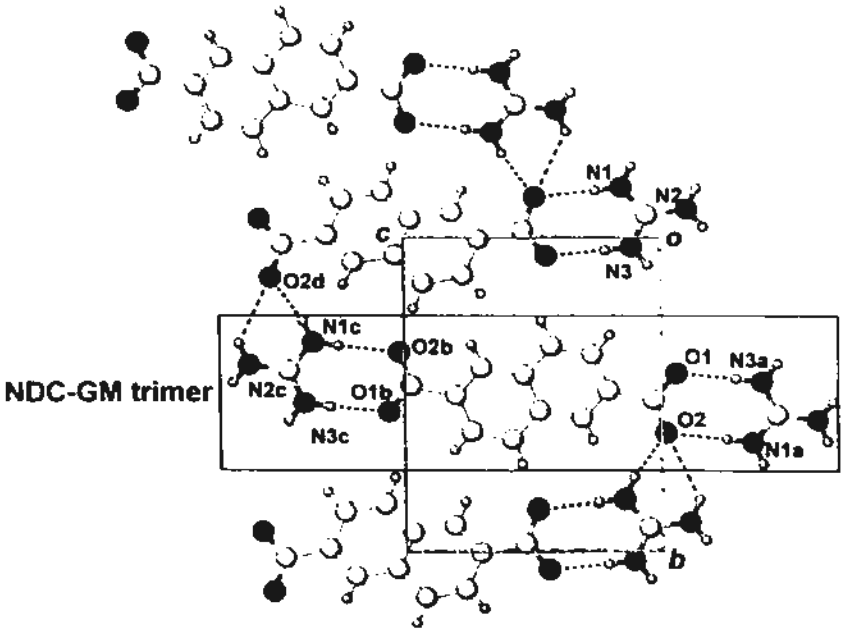

(a)

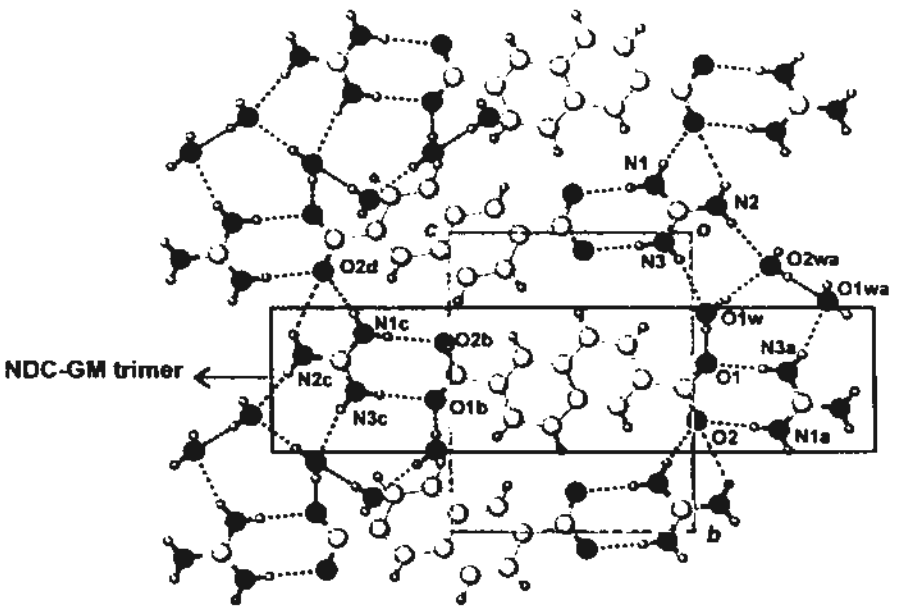

(b)

Figure 2.3.3 Projection along the *a* axis showing hydrogen-bonded layer in **2.3.2** (a) without water molecules; (b) with water molecules. *Symmetry transformations*: (*a*) *x*, 0.5 – *y*, –0.5 + *z*; (*b*) 2 – *x*, 1 – *y*, 1 – *z*; (*c*) 2 – *x*, 0.5 + *y*, 1.5 – *z*; (*d*) 2 – *x*, –0.5 + *y*, 1.5 – *z*.

Table 2.3.2 Hydrogen bonds for **2.3.2** [Å and deg.].

D-H...A	d(D-H)	d(H...A)	d(D...A)	∠(DHA)
N(1)-H(1A)...O(2)#2	0.86	2.03	2.887(2)	173.2
N(1)-H(1B)...O(2)#3	0.86	2.02	2.872(2)	169.2
N(2)-H(2B)...O(2W)#4	0.86	2.21	3.064(2)	175.3
N(3)-H(3A)...O(1)#2	0.86	1.96	2.817(2)	176.6
N(3)-H(3B)...O(1W)	0.86	2.13	2.962(2)	163.0
N(2)-H(2A)...O(2)#3	0.86	2.80	3.464(2)	135.0
O(1W)-H(1WB)...O(2W)#4	0.85	1.94	2.795(2)	178.8
O(2W)-H(2WB)...O(1)#1	0.85	2.21	3.066(2)	179.6

Symmetry transformations used to generate equivalent atoms:
#1 -x+1,-y+1,-z #2 x,-y+1/2,z+1/2 #3 x,y-1,z #4 x,-y+1/2,z-1/2

Similar bands are arranged side by side and cross-linked by water molecules O1w and O2w to create a complicated three-dimensional network (Figure 2.3.4).

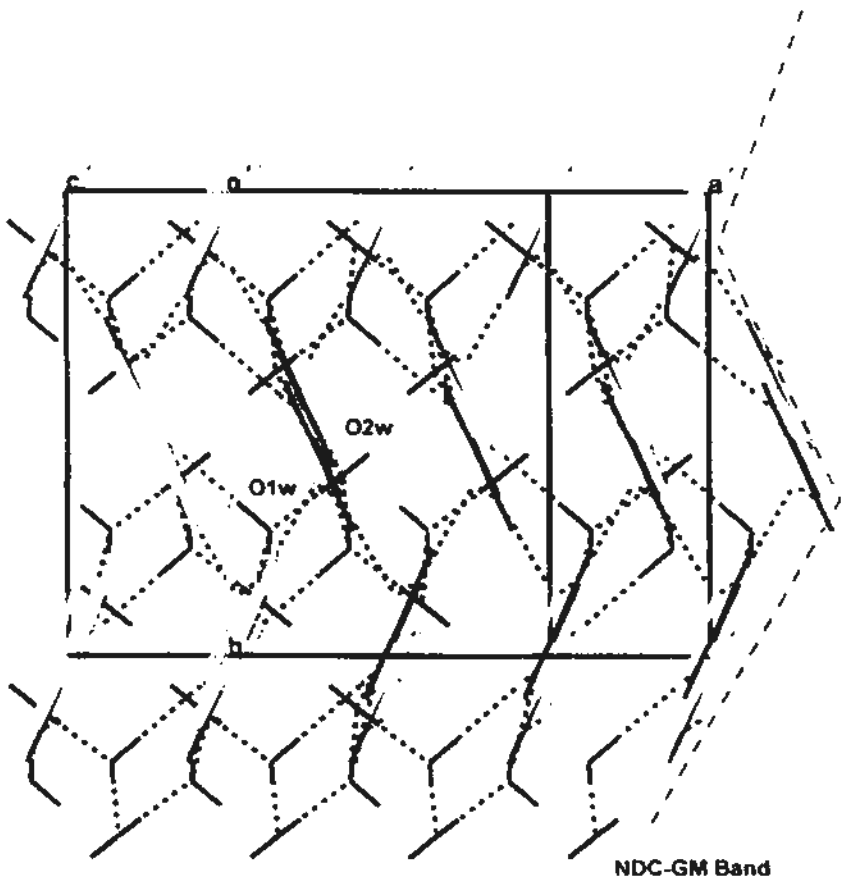

Figure 2.3.4 Packing diagram of complex **2.3.2** viewed almost along the [1 0 3] direction. NDC–GM bands are cross-linked by water molecules O1w and O2w.

Crystal structure of $2[C(NH_2)_3^+] \cdot [(4\text{-}C_6H_4CO_2^-)_2] \cdot 4H_2O$ (2.3.3)

The asymmetric unit of **2.3.3** is composed of one guanidinium ion, one-half of biphenyl dicarboxylate dianion ($BPDC^{2-}$) which is lies at a $\bar{1}$ site, and two water molecules. In the crystal structure, $BPDC^{2-}$ dianion is joined with the guanidiniums at both ends by pairwise hydrogen bonds N1a–H···O1 and N3a–H···O2 to form a planar trimer. Adjacent trimers lying side by side are further join together by chelating N1a–H···O1b and N2a–H···O1b hydrogen bonds to generate a zigzag band running along the *b* axis (Figure 2.3.5). The detailed hydrogen-bonding geometries are listed in Table 2.3.3.

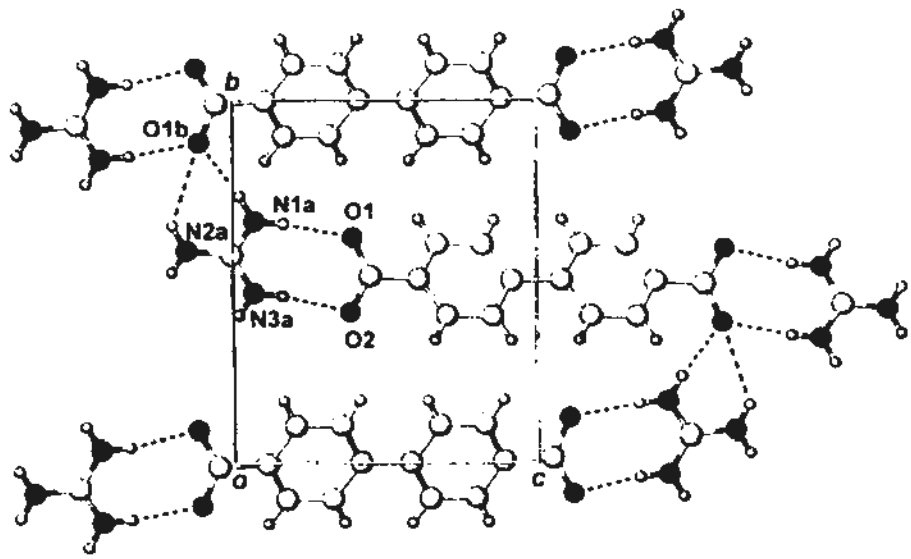

Figure 2.3.5 Projection diagram showing a portion of a zigzag BPDC–GM band in the crystal structure of **2.3.3**. *Symmetry transformations*: (a) $-x$, $1.5 - y$, $-0.5 - z$; (b) $-x$, $1.5 - y$, $0.5 - z$.

Similar to the crystal structure of **2.3.2**, the parallel zigzag BPDC–GM bands are cross-linked by water molecules O1w and O2w to generate a channel structure as viewed along the [1 0 3] direction (Figure 2.3.6).

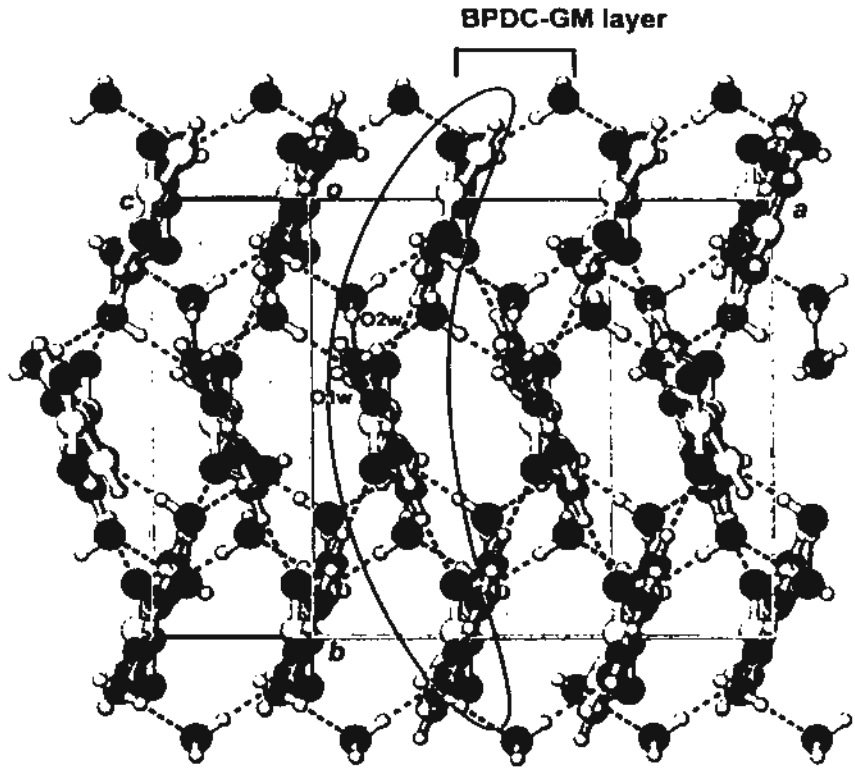

Figure 2.3.6 Packing diagram almost along the [1 0 3] direction showing the hydrogen-bonded framework of **2.3.3**.

Table 2.3.3 Hydrogen bonds for **2.3.3** [Å and deg.]

D-H...A	d(D-H)	d(H...A)	d(D...A)	∠(DHA)
N(1)-H(1A)...O(1)#2	0.86	2.05	2.871(2)	160.2
N(1)-H(1B)...O(1)	0.86	2.02	2.871(2)	173.1
N(2)-H(2A)...O(1W)#3	0.86	2.18	3.035(2)	175.7
N(2)-H(2B)...O(1)	0.86	2.88	3.530(2)	134.0
N(3)-H(3A)...O(2)#2	0.86	2.03	2.888(2)	172.0
N(3)-H(3B)...O(2W)#4	0.86	2.08	2.924(2)	166.7
O(1W)-H(1WA)...O(1)#5	0.82	2.41	2.951(2)	150.0
O(1W)-H(1WB)...O(2W)	0.87	1.90	2.763(2)	169.4
O(2W)-H(2WA)...O(1W)#1	0.87	1.92	2.776(2)	171 0
O(2W)-H(2WB)...O(2)	0.79	1.91	2.706(2)	173.1

Symmetry transformations used to generate equivalent atoms:
#1 x,-y+1/2,z-1/2 #2 x,-y+3/2,z+1/2 #3 x,-y+3/2,z-1/2 #4 x,y+1,z #5 -x,-y+1,-z+1

Crystal structure of $[(CH_3)_4N^+]\cdot 5[C(NH_2)_3^+]\cdot 3[(4\text{-}C_6H_4CO_2^-)_2]\cdot 2.5H_2O$ (2.3.4)

The asymmetric unit of **2.3.4** is composed of a $(CH_3)_4N^+$ cation, five guanidinium ions, three biphenyl dicarboxylate dianions BPDCs (O1, O5 and O9) and water molecules. Figure 2.3.7 shows the orientations of the three independent BPDCs (O1, O5 and O9) in the crystal structure. Each BPDC forms a face-to-face dimer positioned at an inversion center.

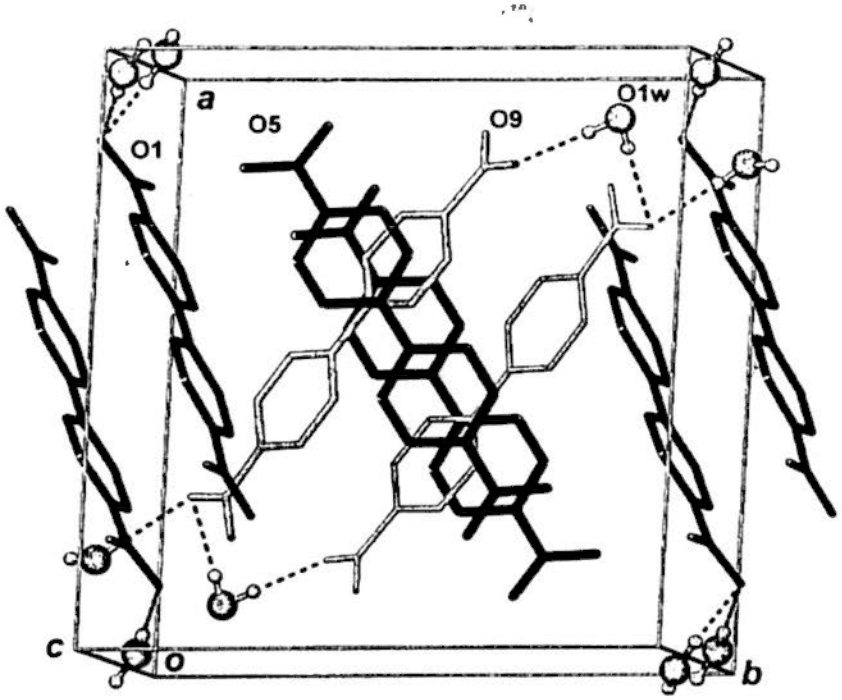

Figure 2.3.7 Orientations of three independent BPDCs that forms face-to-face dimer in **2.3.4**. Guanidinium and tetramethylammonium ions are omitted for clarity.

Figure 2.3.8a shows the hydrogen-bonding environment of BPDC (O1), which is surrounded by seven guanidinium ions (for clarity, BPDC O5 and O9 and tetramethylammonium ions are omitted). Two of them (C43 and C47c) are connected with carboxylate groups by pairwises hydrogen bonds. Three guanidinium ions C44, C46 and C46d are each joined with BPTC through a single hydrogen bond, while C47a, C44b are connected with BPTC by chelating hydrogen bonds. The detailed hydrogen-bonding geometries are listed in Table 2.3.4.

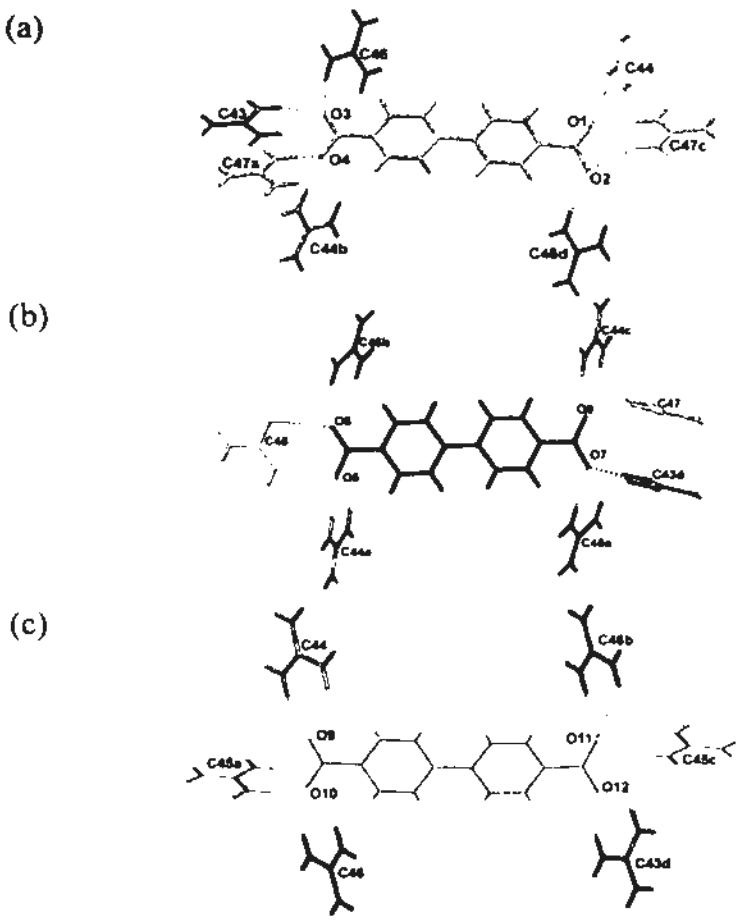

Figure 2.3.8 (a) Hydrogen-bonding environment of BPDC (O1) in **2.3.4**. *Symmetry transformations*: (*a*) $2-x, 1-y, 1-z$; (*b*) $x, y, 1+z$; (*c*) $-1+x, 1+y, z$; (*d*) $1-x, 2-y, 1-z$. (b) Hydrogen-bonding environment of BPDC (O5). *Symmetry transformations*: (*a*) $1-x, 2-y, -z$; (*b*) $1-x, 1-y, 1-z$; (*c*) $x, -1+y, z$; (*d*) $2-x, 1-y, 1-z$; (*e*) $x, y, -1+z$. (c) Hydrogen-bonding environment of BPDC (O9). *Symmetry transformations*: (*a*) $1+x, y, z$; (*b*) $1-x, 1-y, 1-z$; (*c*) $-x, 1-y, 1-z$; (*d*) $1-x, 1-y, 2-z$.

Hydrogen-bonding environment of BPDC (O5) and (O9) are very similar to that of the BPDC (O1) (Figure 2.3.8b and Figure 2.3.8c). However, there are six guanidinium ions around BPDC (O9) instead of seven in BPDC (O1). In all, three BPTCs hydrogen bonded with surrounding guanidinium ions and water molecules construct cage structure as shown in Figure 2.3.9.

Table 2.3.4 Hydrogen bonds for **2.3.4** [Å and deg.]

D-H...A	d(D-H)	d(H...A)	d(D...A)	∠(DHA)
N(10)-H(10A)...O(6)#1	0.86	2.03	2.817(4)	151.5
N(10)-H(10B)...O(11)#1	0.86	2.06	2.893(4)	164.4
N(11)-H(11B)...O(10)	0.86	2.12	2.905(4)	150.6
N(11)-H(11C)...O(2)#2	0.86	2.10	2.932(4)	161.6
N(12)-H(12B)...O(7)#3	0.86	2.22	3.068(4)	168.0
N(12)-H(12C)...O(3)	0.86	2.06	2.833(4)	148.6
N(7)-H(7A)...O(6)	0.86	2.04	2.891(4)	169.3
N(7)-H(7B)...O(11)#4	0.86	2.04	2.879(4)	166.3
N(8)-H(8B)...O(5)	0.86	2.02	2.867(4)	166.8
N(8)-H(8C)...O(1)	0.86	2.01	2.836(4)	160.8
N(9)-H(9B)...O(3W)#1	0.86	2.11	2.889(7)	151.1
N(9)-H(9C)...O(10)#5	0.86	2.21	2.921(4)	139.7
N(1)-H(1A)...O(7)#6	0.86	2.09	2.860(4)	149.1
N(1)-H(1B)...O(12)#7	0.86	2.50	3.172(4)	135.9
N(2)-H(2B)...O(4)	0.86	2.09	2.854(4)	147.7
N(2)-H(2B)...O(3)	0.86	2.63	3.325(4)	138.7
N(2)-H(2C)...O(12)#7	0.86	1.93	2.749(4)	159.4
N(3)-H(3B)...O(3)	0.86	2.08	2.908(4)	162.2
N(3)-H(3C)...O(7)#6	0.86	2.18	2.933(4)	145.7
N(13)-H(13A)...O(1W)#8	0.86	2.43	3.151(4)	141.2
N(13)-H(13B)...O(8)	0.86	2.13	2.900(4)	149.2
N(14)-H(14A)...O(1)#9	0.86	2.34	3.087(4)	145.4
N(14)-H(14A)...O(2)#9	0.86	2.36	3.169(4)	157.4
N(14)-H(14B)...O(2W)#10	0.86	2.04	2.843(4)	155.3
N(15)-H(15A)...O(1)#9	0.86	2.21	2.992(4)	150.5
N(15)-H(15B)...O(1W)#8	0.86	2.12	2.918(5)	154.6
N(4)-H(4A)...O(9)	0.86	2.25	2.996(4)	145.5
N(4)-H(4B)...O(4)#11	0.86	2.12	2.872(4)	146.1
N(5)-H(5B)...O(5)#12	0.86	2.05	2.845(4)	153.0
N(5)-H(5C)...O(4)#11	0.86	2.40	3.088(4)	137.0
N(6)-H(6B)...O(5)#12	0.86	2.37	3.080(4)	140.6
N(6)-H(6C)...O(9)	0.86	2.18	2.948(4)	148.3
O(1W)-H(1WA)...O(12)	0.85	1.98	2.838(4)	179.2
O(1W)-H(1WB)...O(9)#1	0.85	2.29	3.144(4)	178.6
O(2W)-H(2WA)...O(8)#13	0.87	1.87	2.742(4)	179.1
O(2W)-H(2WB)...O(9)	0.86	1.95	2.814(4)	178.5
O(3W)-H(3WA)...O(2)#9	0.85	2.40	3.249(7)	178.5
O(3W)-H(3WB)...O(2)#1	0.85	1.79	2.639(6)	175.7

Symmetry transformations used to generate equivalent atoms:

#1 -x+1,-y+1,-z+1 #2 -x+1,-y+2,-z+1 #3 x,y,z+1 #4 -x,-y+1,-z+1 #5 x-1,y,z
#6 -x+2,-y+1,-z+1 #7 -x+1,-y+1,-z+2 #8 x+1,y,z-1 #9 x+1,y-1,z #10 x,y-1,z
#11 x,y,z-1 #12 -x+1,-y+2,-z #13 x,y+1,z

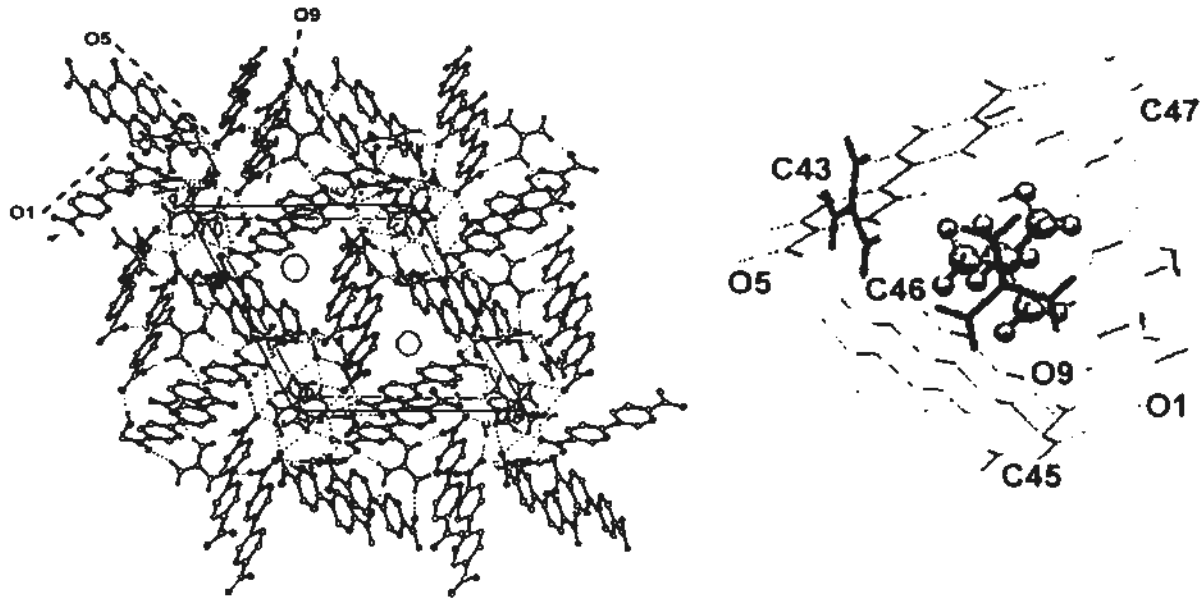

(a) (b)

Figure 2.3.9 (a) Packing diagram showing a portion of cage network in the crystal structure of **2.3.4** viewed along the *a* direction. For clarity, guanidinium ions in the front of cage are omitted. Dotted lines are representing the directions of three independent BPDC molecules. The Me_4N^+ ion is represented by a large sphere. (b) Molecules surrounding Me_4N^+ ion form a cage structure, including three independent BPTCs and four guanidinium ions.

Crystal structure of $4[(n\text{-}C_4H_9)_4N^+] \cdot 2[C(NH_2)_3^+] \cdot 2[C(NH_2)_2{}^+NHCO_2^-] \cdot 3[(4\text{-}C_6H_4CO_2^-)_2] \cdot 8H_2O$ (2.3.5)

Of the two independent biphenyl dicarboxylate dianions in the asymmetric unit, one (represented by O1) occupies a general position and the other O5 is located at an inversion center. The guanidinecarboxylic carbamic acid molecule, which contains intramolecular hydrogen bond, and the guanidinium ion are used to build a centrosymmetric cyclic tetramer to generate a positively charged ribbon exhibiting hydrogen-bonded motif [**A**] = $R_3^2(10)$, [**B**] = $R_2^2(8)$ and [**C**] = $R_4^2(8)$ (Figure 2.3.10). Water molecules O3w and O4w are linked to form a centrosymmetric tetrameric

cluster. Cross-linkage between such two kinds of tetramers and bridging water molecules O1w and O2w generates a guanidinium–guanidinecarboxylic acid–H_2O puckered ribbon.

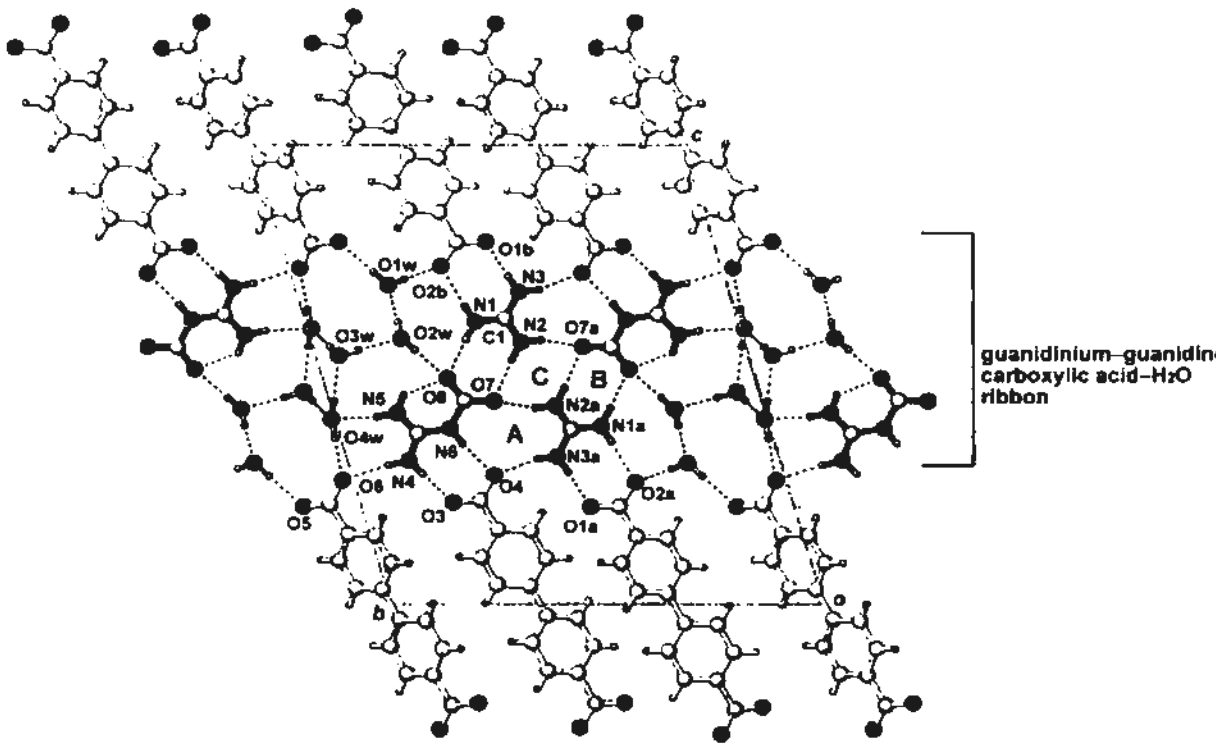

Figure 2.3.10 Projection diagram showing hydrogen-bonding connection between the guanidinium–guanidinecarboxylic acid–H_2O ribbon and biphenyl dicarboxylate anions in the crystal structure of **2.3.5**. *Symmetry transformations*: (a) $-x$, $1-y$, $1-z$; (b) x, y, $1+z$.

Biphenyl dicarboxylate dianions, which are arranged in a linear array along the c axis, cross-link adjacent wide ribbons to generate a wavy layer. The dihedral angle of two phenyl rings in the BPDC (O1) anion occupying a general position is about 20.3 °. Detailed hydrogen-bonding geometries are listed in Table 2.3.5. The well-ordered hydrophobic $(n\text{-Bu})_4N^+$ cations are positioned regularly between adjacent wavy layers with an interlayer spacing of a = 8.26 Å (Figure 2.3.11).

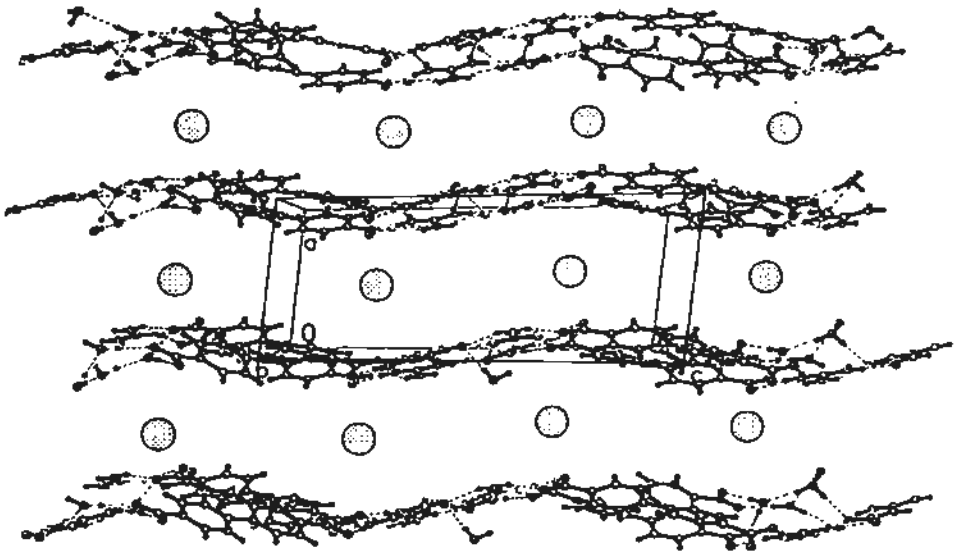

Figure 2.3.11 Crystal structure of complex **2.3.5** viewed along the *b* axis.

Table 2.3.5 Hydrogen bonds for **2.3.5** [Å and deg.].

D-H...A	d(D-H)	d(H...A)	d(D...A)	∠(DHA)
N(6)-H(6B)...O(4)	0.88	1.98	2.856(2)	174.3
N(2)-H(2B)...O(7)#2	0.88	2.03	2.872(3)	160.7
N(2)-H(2A)...O(7)	0.88	1.98	2.857(2)	174.6
N(3)-H(3A)...O(4)#2	0.88	2.05	2.907(2)	165.8
N(3)-H(3B)...O(1)#3	0.88	1.93	2.809(2)	178.0
N(1)-H(1B)...O(2)#3	0.88	2.02	2.872(2)	161.2
N(1)-H(1A)...O(8)	0.88	2.04	2.893(3)	161.8
N(4)-H(4A)...O(6)	0.88	2.05	2.928(3)	173.4
N(4)-H(4B)...O(3)	0.88	1.88	2.755(3)	177.2
N(5)-H(5B)...O(4W)	0.88	1.97	2.831(3)	166.8
N(5)-H(5C)...O(8)	0.88	1.99	2.634(3)	129.0
O(1W)-H(1WB)...O(5)#1	0.85	1.96	2.817(2)	179.7
O(2W)-H(2WA)...O(8)	0.86	2.08	2.950(3)	179.0
O(2W)-H(2WB)...O(1W)	0.87	1.85	2.714(3)	173.5
O(3W)-H(3WA)...O(4W)#1	0.87	1.94	2.801(3)	178.3
O(3W)-H(3WB)...O(2W)	0.87	1.90	2.765(3)	179.4
O(4W)-H(4WA)...O(6)	0.87	1.87	2.733(2)	177.9
O(4W)-H(4WB)...O(3W)	0.85	2.09	2.939(3)	177.7
O(1W)-H(1WA)...O(2)#3	0.85	1.92	2.778(2)	179.7

Symmetry transformations used to generate equivalent atoms:
#1 -x,-y+2,-z+1 #2 -x,-y+1,-z+1 #3 x,y,z+1

Crystal structure of $[(n\text{-}C_3H_7)_4N^+]\cdot[C(NH_2)_3^+]\cdot[1,3\text{-}C_6H_4(CO_2^-)_2]\cdot 3H_2O$ (2.3.6)

The angular benzene-1,3-dicarboxylate and guanidinium ions are linked by N2–H···O1, N3–H···O2 and N1b–H···O4, N3b–H···O3 hydrogen bonds to form a zigzag ribbon along the [$\bar{1}$ 1 0] direction (Figure 2.3:12). Cross-linkage between similar ribbons arranged side by side along the [1 1 0] direction with water molecules (O1w, O2w and O3w) creates a three-dimensional network with open channels. Detailed hydrogen-bonding geometries are listed in Table 2.3.6. Figure 2.3.13 shows the channels viewed in two different directions. Well-ordered tetra-*n*-butylammonium ions are stacked in double columns within each channel.

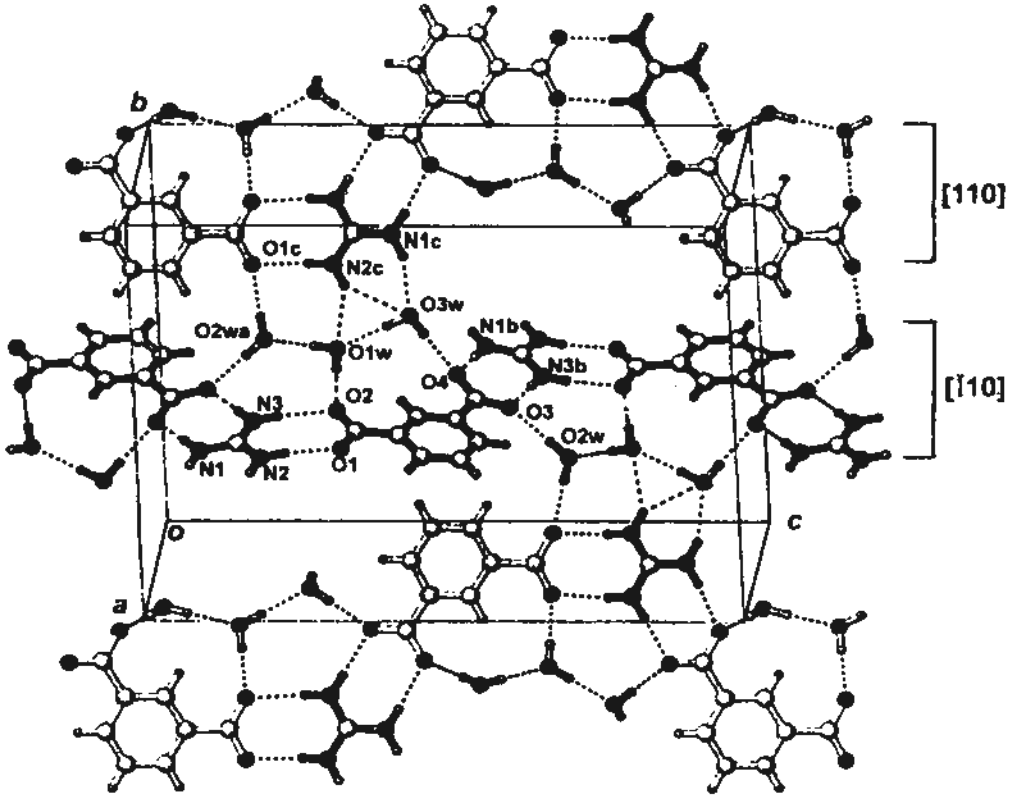

Figure 2.3.12 Perspective diagram showing the cross-linked ribbons along [1 1 0] and [$\bar{1}$ 1 0] directions in **2.3.6**. *Symmetry transformations*: (a) 1.5 – *x*, 1 – *y*, –0.5 – *z*; (b) 1.5 – *x*, 1 – *y*, 0.5 + *z*; (c) 1 – *x*, 0.5 + *y*, 0.5 – *z*.

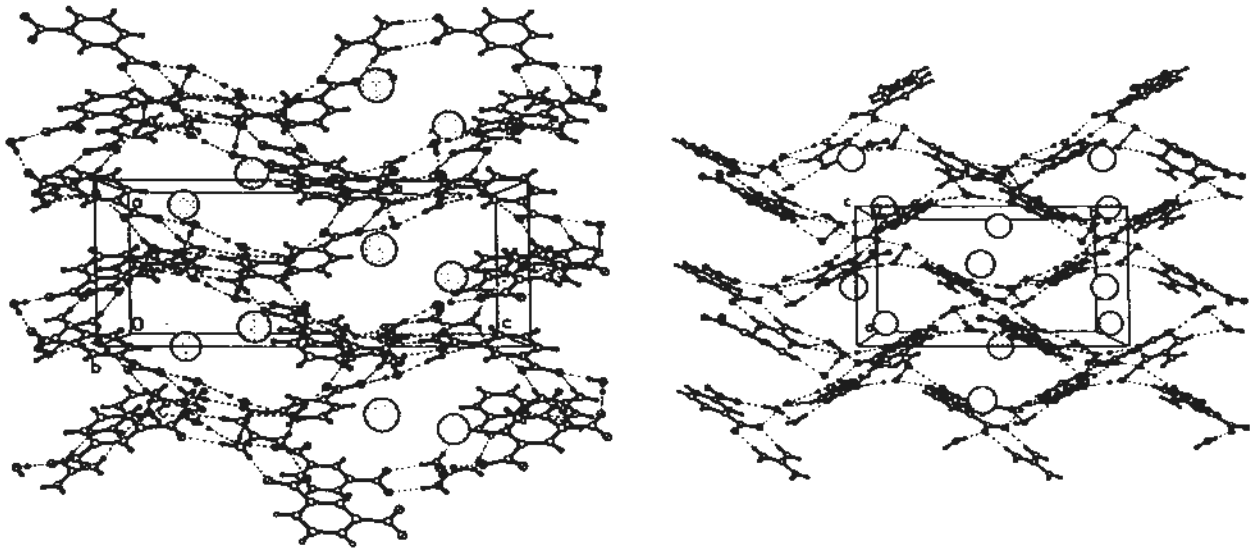

(a) (b)

Figure 2.3.13 Perspective diagrams showing the open channels in the three-dimensional hydrogen-bonded framework of **2.3.6** (a) viewed along the *b* axis, (b) viewed along the *c* axis.

Table 2.3.6 Hydrogen bonds for **2.3.6** [Å and deg.]

D-H...A	d(D-H)	d(H...A)	d(D...A)	∠(DHA)
N(1)-H(1A)...O(4)#1	0.86	1.99	2.849(3)	171.9
N(1)-H(1B)...O(3W)#2	0.86	2.14	2.957(3)	157.9
N(2)-H(2A)...O(1)	0.86	1.93	2.788(3)	173.0
N(2)-H(2B)...O(1W)#2	0.86	2.35	3.082(3)	143.2
N(2)-H(2B)...O(3W)#2	0.86	2.52	3.240(3)	142.1
N(3)-H(3B)...O(2)	0.86	2.03	2.891(3)	173.7
N(3)-H(3C)...O(3)#1	0.86	1.94	2.795(3)	178.4
O(1W)-H(1WA)...O(2)	0.86	1.84	2.695(3)	178.6
O(1W)-H(1WB)...O(2W)#1	0.87	1.91	2.779(3)	178.9
O(2W)-H(2WB)...O(3)	0.86	1.86	2.722(3)	179.4
O(2W)-H(2WA)...O(1)#3	0.85	1.91	2.760(3)	179.3
O(3W)-H(3WA)...O(4)	0.86	1.92	2.784(3)	178.5
O(3W)-H(3WB)...O(1W)	0.87	1.89	2.764(3)	179.0

Symmetry transformations used to generate equivalent atoms:
#1 -x+3/2,-y+1,z-1/2 #2 -x+1,y-1/2,-z+1/2 #3 x+1/2,-y+1/2,-z+1

Crystal structure of $(C_5H_4N^+CH_2COO^-)_2 \cdot 2H_2O$ (2.3.7)

Figure 2.3.14 shows that the zigzag ribbons in **2.3.7** that are composed of water molecules and centrosymmetric *N,N'*-bis(carboxymethyl)-4,4'-bipyridinium betaine. The planar heterocyclic rings with conformational flexible carboxymethyl groups are linked by bridging water molecules O2w to generate a layer zigzag ribbon viewed along the *a* axis. Detailed hydrogen-bonding geometries are listed in Table 2.3.7.

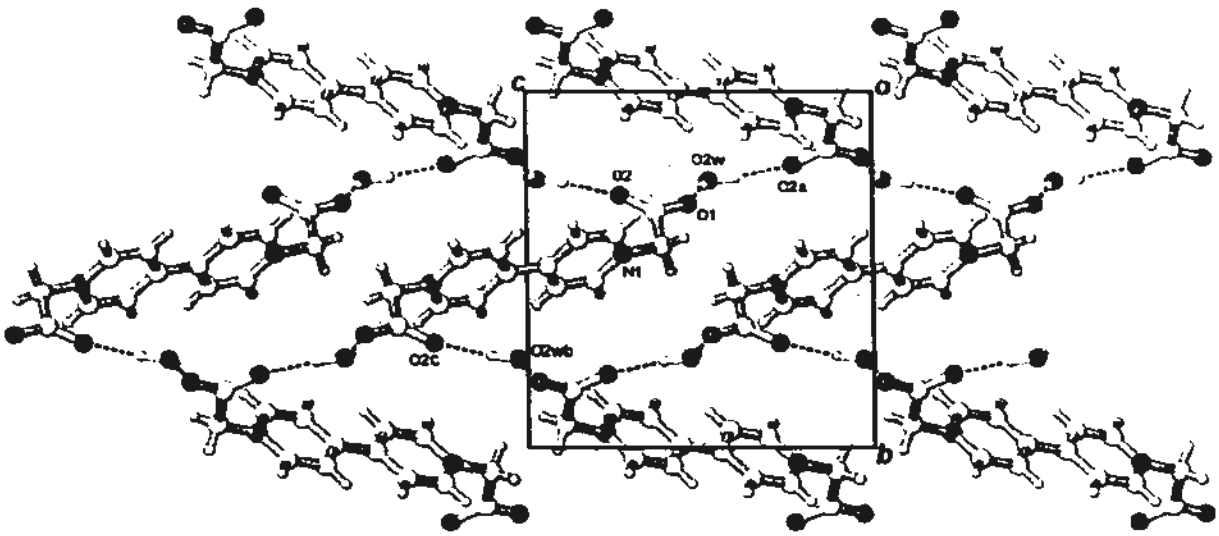

Figure 2.3.14 Projection along the *a* axis showing a layer zigzag betaine ribbon in **2.3.7**. *Symmetry transformations*: (*a*) 0.5 + *x*, 0.5 − *y*, −0.5 + *z*; (*b*) 0.5 − *x*, 0.5 + *y*, 1.5 − *z*; (*c*) − *x*, 1.0 − *y*, 2.0 − *z*.

Table 2.3.7 Hydrogen bonds for **2.3.7** [Å and deg.].

D-H...A	d(D-H)	d(H...A)	d(D...A)	∠(DHA)
O(1W)-H(1WA)...O(2)	0.85	1.97	2.823(2)	171.8
O(1W)-H(1WB)...O(1)#1	0.85	1.95	2.800(2)	174.8
O(2W)-H(2WA)...O(1)	0.85	1.97	2.815(2)	171.5
O(2W)-H(2WB)...O(2)#2	0.85	2.02	2.837(2)	160.1

Symmetry transformations used to generate equivalent atoms:
#1 x+1/2,-y+1/2,z+1/2 #2 x+1/2,-y+1/2,z-1/2

Crystal structure of $[C(NH_2)_3^+] \cdot (C_5H_4N^+CH_2COOH)_2 \cdot CO_3^{2-} \cdot H_2O$ (2.3.8)

In the crystal structure of **2.3.8**, the guanidinium and carbonate ions are interconnected and further bridged by the water molecule to create a non-planar six-membered pseudo-rosette motif (Figure 2.3.15). The water molecule protrudes out of the plane significantly, and the dihedral angle between the guanidinium and bicarbonate is about 26.6 °.

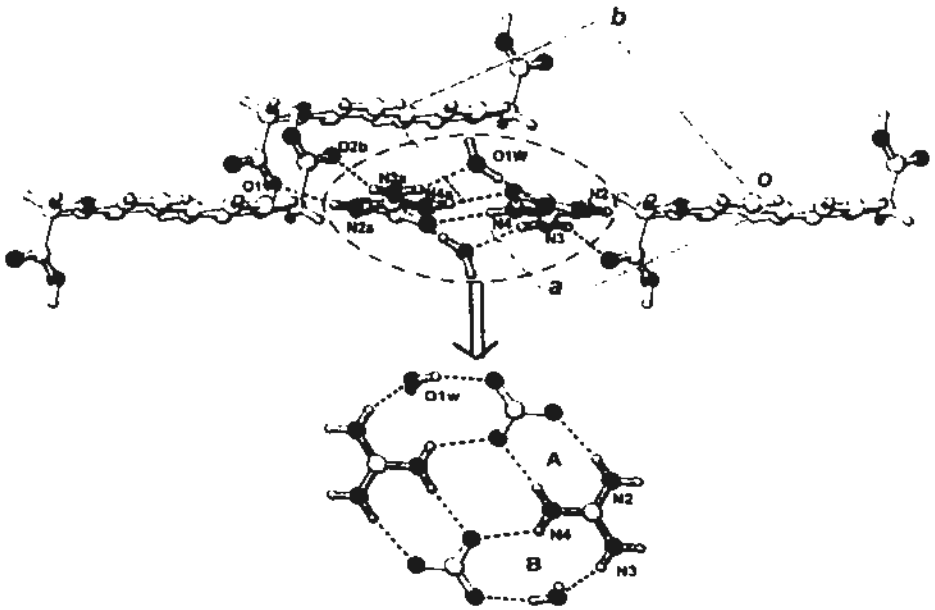

Figure 2.3.15 Projection diagram shows hydrogen-bonding connection between the rosette motif and betaines in the crystal structure of **2.3.8**. *Symmetry transformations*: (a) $-x, 1-y, 2-z$; (b) $-1-x, y, 1-z$.

The guanidinium ion serves as clamp to link with two adjacent betaines whose heterocyclic ring is parallel to the $(1\ \bar{2}\ 0)$ plane by a single hydrogen bond (N3a–H···O2b or N2a–H···O1). Detailed hydrogen-bonding geometries are listed in Table 2.3.8. In addition, water molecule O1w as a member of the pseudo-rosette motif also forms a hydrogen bond with an exocyclic betaine molecule. Totally, there are six betaines around one pseudo-rosette core. Four of them are connected with N2 or N3 atom of guanidinium and the other two are linked with water molecules along

two different directions (Figure 2.3.16a). Packing diagram of **2.3.8** is shown in Figure 2.3.16b. Attempts to introduce R_4N^+ into the system failed, as small void in the crystal is too small to accommodate even the Me_4N^+ ion.

Table 2.3.8 Hydrogen bonds for **2.3.8** [Å and deg.].

D-H...A	d(D-H)	d(H...A)	d(D...A)	<(DHA)
N(2)-H(2A)...O(1)#2	0.86	2.15	2.917(3)	148.8
N(2)-H(2B)...O(5)#3	0.86	2.15	2.961(3)	156.4
N(3)-H(3A)...O(2)#4	0.86	1.99	2.782(3)	152.2
N(3)-H(3B)...O(1W)#5	0.86	2.08	2.859(4)	151.1
N(4)-H(4A)...O(3)#5	0.86	2.34	2.975(3)	130.7
N(4)-H(4A)...O(1W)#5	0.86	2.56	3.225(3)	135.2
N(4)-H(4B)...O(3)#3	0.86	2.07	2.924(3)	172.7
O(1W)-H(1WA)...O(1)#1	0.87	2.00	2.800(3)	151.1
O(1W)-H(1WB)...O(4)	0.87	2.02	2.872(3)	165.7

Symmetry transformations used to generate equivalent atoms:
#1 -x+1,-y,-z+1 #2 x,y+1,z #3 x,y,z+1 #4 -x+1,-y+1,-z+1 #5 -x,-y+1,-z+1

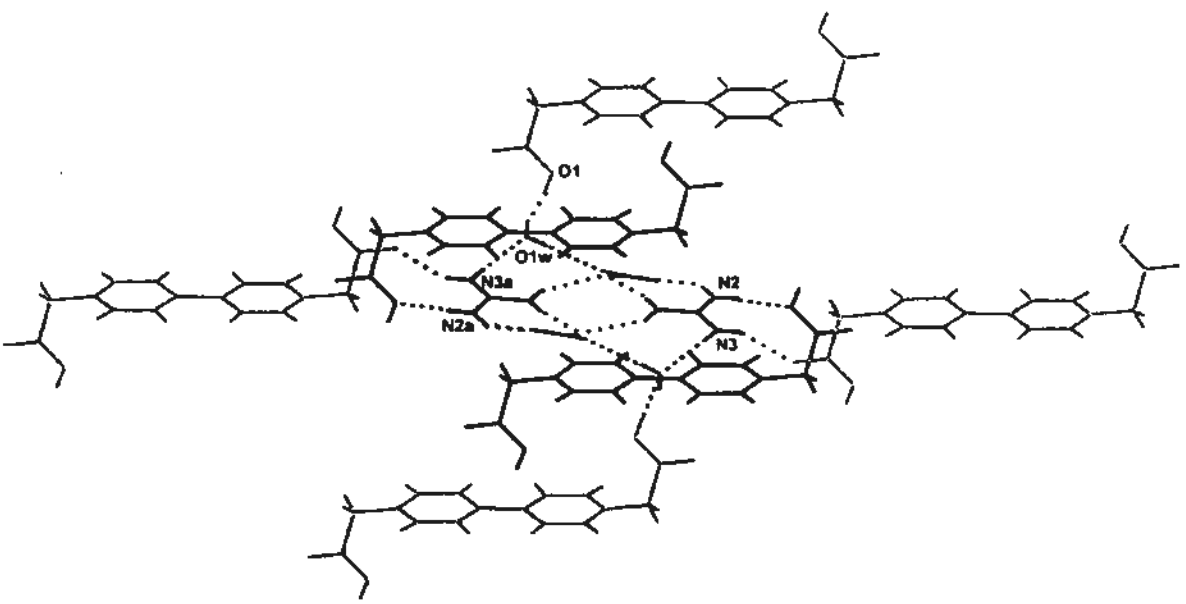

(a)

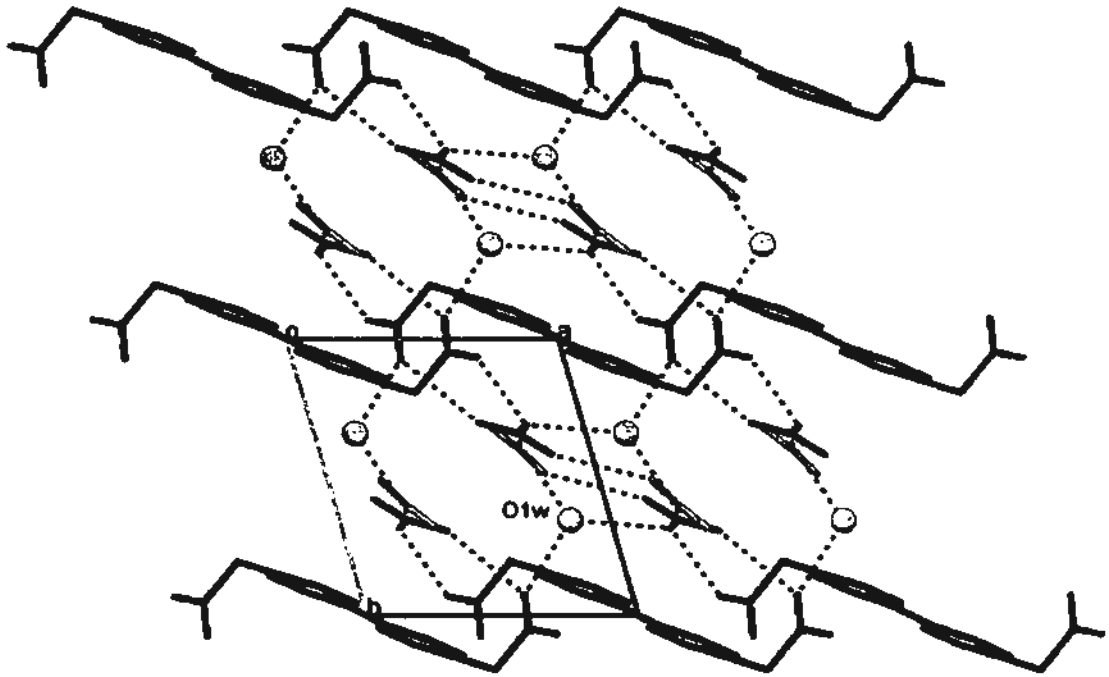

(b)

Figure 2.3.16 (a) Hydrogen-bonding environment of pseudo-rosette motif showing that six betaines are hydrogen-bonded with the pseudo-rosette core. *Symmetry transformations*: (*a*) $-x$, $1 - y$, $2 - z$. (b) Packing diagram of **2.3.8** viewed along the *c* axis. Hydrogen atoms are omitted for clarity, and larger spheres representing water molecules.

2.4 Supramolecular hydrogen bonding motifs based on *N*-heteroaryl acids

2.4.1 Inclusion compounds containing anions of 2-thiobarbituric acid/ trithiocyanuric acid

2-Thiobarbituric acid (H_4TBA) and trithiocyanuric acid (H_3TCA) as cyclic (thio)urea derivatives (Scheme 2.4.1) are selected as the main building blocks to construct (thio)urea/guanidiniums complexes.

Scheme 2.4.1 Structure formulas of (a) 2-thiobarbituric acid (H_4TBA) and (b) trithiocyanuric acid (H_3TCA).

The following complexes have been obtained and structurally characterized:

$[(Et_4N^+)] \cdot [C_4N_2O_2H_3S^-] \cdot H_2O$	**2.4.1**
$[(Et_4N^+)] \cdot [C_4N_2O_2H_3S^-] \cdot 2H_2O$	**2.4.2**
$2[(n\text{-}C_3H_7)_4N^+] \cdot 2[C_4N_2O_2H_3S^-] \cdot 2[CO(NH_2)_2] \cdot 5H_2O$	**2.4.3**
$[(CH_3)_4N^+] \cdot [C_3N_3S_3H_2^-]$	**2.4.4**
$[(n\text{-}C_4H_9)_4N^+] \cdot [C_3N_3S_3H_2^-] \cdot 2H_2O$	**2.4.5**
$2[(CH_3)_4N^+] \cdot [C_3N_3S_3H^{2-}] \cdot 5[CO(NH_2)_2] \cdot H_2O$	**2.4.6**
$[(n\text{-}C_3H_7)_4N^+] \cdot [C_3N_3S_3H_2^-] \cdot [CS(NH_2)_2]$	**2.4.7**
$[(n\text{-}C_3H_7)_4N^+] \cdot [C(NH_2)_3^+] \cdot [C_3N_3S_3H^{2-}]$	**2.4.8**
$[(n\text{-}C_4H_9)_4N^+] \cdot [C(NH_2)_3^+] \cdot [C_3N_3S_3H^{2-}]$	**2.4.9**

Crystal structure of $[(Et_4N^+)] \cdot [C_4N_2O_2H_3S^-] \cdot H_2O$ (2.4.1)

Adjacent 2-thiobarbiturate anions (H_3TBA^-) are connected by pairwise N1–H···O2a and N2a–H···O1 hydrogen bonds around an inversion center to form an infinite $(H_3TBA^-)_\infty$ ribbon along the *b* axis. These ribbons are further consolidated by water molecules O1w and weak sulfur-sulfur interaction (S···S distance is 3.548 Å) to generate a hydrogen-bonded layer (Figure 2.4.1). Detailed hydrogen-bonding geometries are listed in Table 2.4.1.

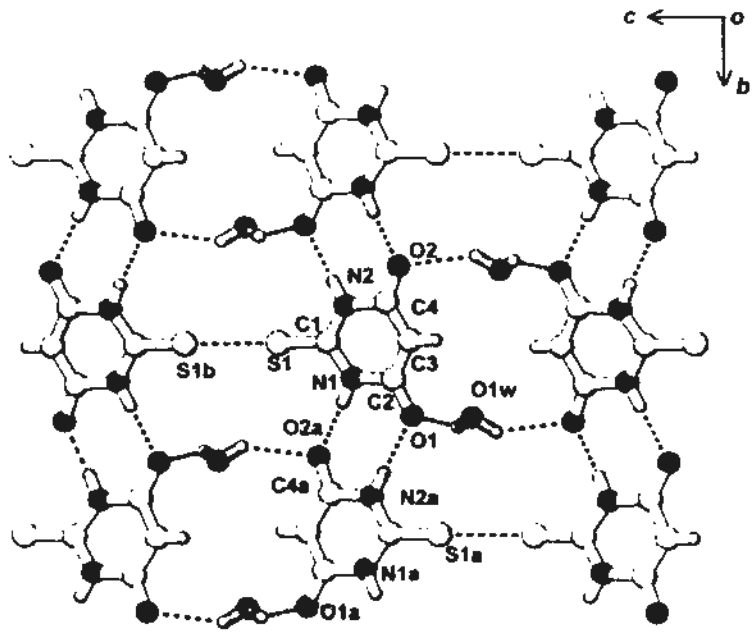

Figure 2.4.1 Projection diagram showing a portion of the $H_3TBA–H_2O$ layer viewed along the *a* axis in the crystal structure of **2.4.1**. *Symmetry transformations*: (a) $0.5 - x, 0.5 + y, 1.5 - z$; (b) $1 - x, 1 - y, 2 - z$.

The packing diagram of **2.4.1** is shown in Figure 2.4.2. The layer is almost planar except for the water molecules that protrude out of the plane. Well-ordered hydrophobic Et_4N^+ cations are positioned regularly between adjacent layers with an interlayer spacing of 7.68 Å.

Table 2.4.1 Hydrogen bonds for **2.4.1** [Å and deg.].

D-H...A	d(D-H)	d(H...A)	d(D...A)	∠(DHA)
N(1)-H(1N)...O(2)#1	0.88	1.94	2.821(2)	176.0
N(2)-H(2N)...O(1)#2	0.83	2.03	2.864(2)	174.0
O(1W)-H(1WB)...O(2)#3	0.86	2.26	3.092(3)	161.5
O(1W)-H(1WA)...O(1)	0.85	2.10	2.957(3)	179.0

Symmetry transformations used to generate equivalent atoms:
#1 -x+1/2,y+1/2,-z+3/2 #2 -x+1/2,y-1/2,-z+3/2 #3 -x,-y+1,-z+1

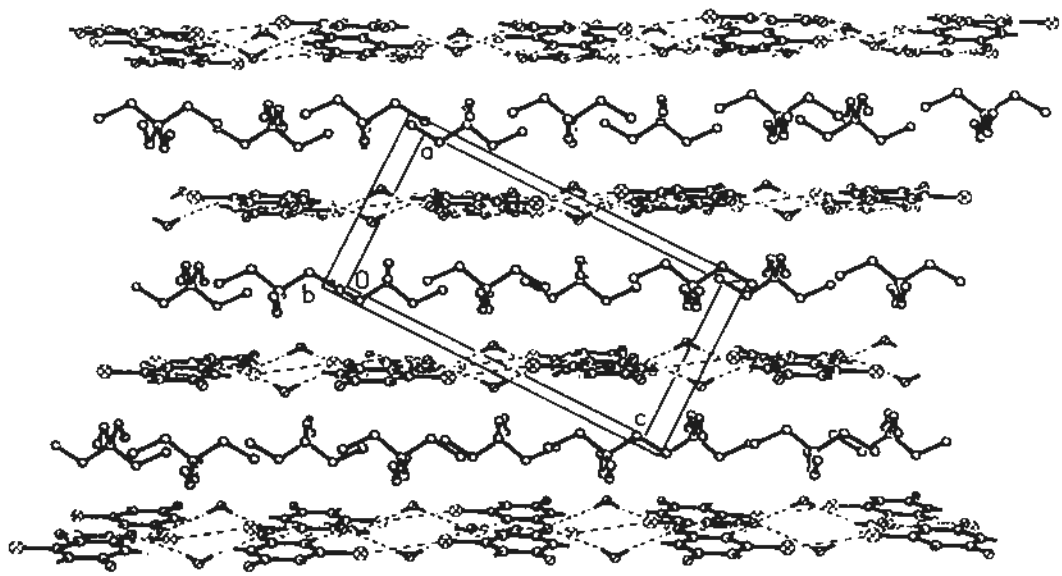

Figure 2.4.2 Layer structure of complex **2.4.1** viewed along the *b* axis.

Crystal structure of $[(Et_4N^+)] \cdot [C_4N_2O_2H_3S^-] \cdot 2H_2O$ (2.4.2)

The structural formula of **2.4.2** differs from that of **2.4.1** in regard to the number of co-crystallized water molecules. In this structure, the continuous 2-thiobarbiturate anionic chain found in **2.4.1** is interrupted by water molecules, and planar centrosymmetric H_3TBA^- dimers are present (Figure 2.4.3). These dimers are linked by water molecules O2w and O2wb arranged around an adjacent inversion center to generate a $H_3TBA–H_2O$ ribbon along the *c* axis. In addition, the other independent water molecule O1w is responsible for bridging adjacent

$(H_3TBA–H_2O)_\infty$ ribbons to form an almost planar layer, except for the water molecules that protrude out of the plane.

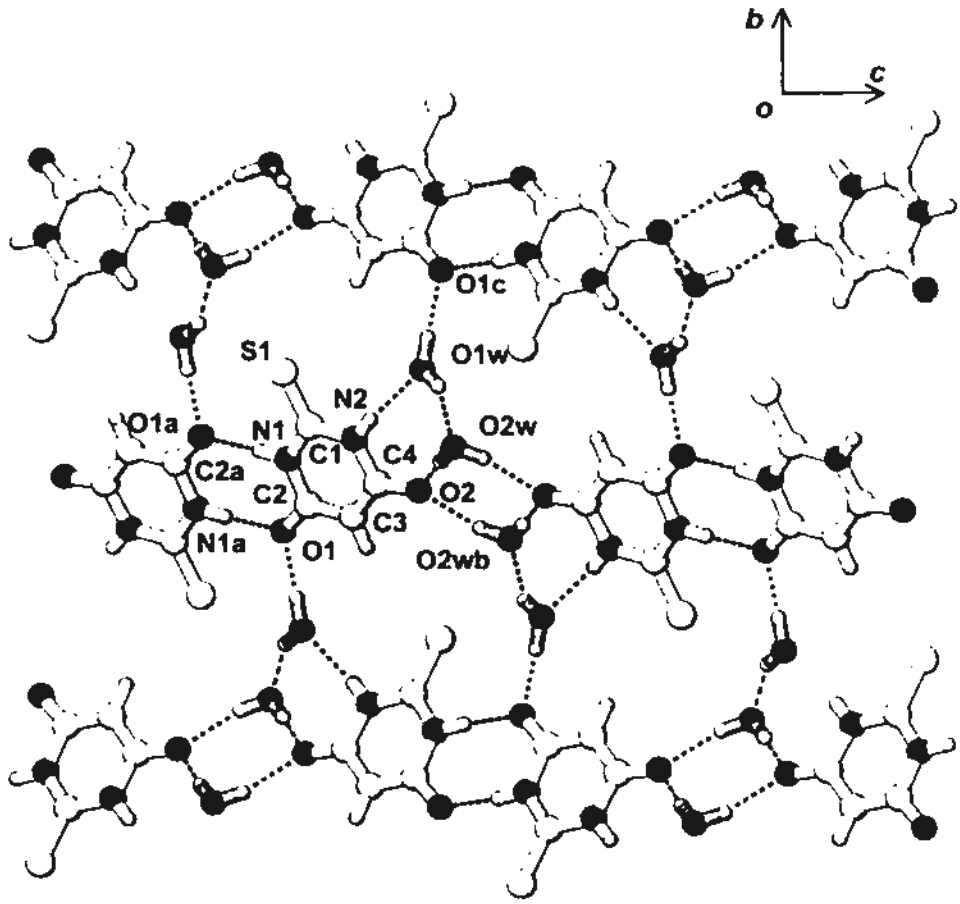

Figure 2.4.3 Projection diagram showing a portion of the $H_3TBA–H_2O$ layer viewed along the *a* axis in the crystal structure of **2.4.2**. *Symmetry transformations*: (a) $-x, 1-y, 1-z$; (b) $1-x, 1-y, 2-z$; (c) $0.5-x, 0.5+y, 1.5-z$.

Figure 2.4.4 shows the layer structure of complex **2.4.2** with an interlayer spacing of about 7.09 Å. Disordered hydrophobic Et_4N^+ cations are positioned regularly between adjacent layers. Detailed hydrogen-bonding geometries are listed in Table 2.4.2.

Table 2.4.2 Hydrogen bonds for **2.4.2** [Å and deg.].

D-H...A	d(D-H)	d(H...A)	d(D...A)	∠(DHA)
N(1)-H(1N)...O(1)#1	0.98	1.82	2.804(3)	174.0
N(2)-H(2N)...O(1W)	0.72	2.15	2.857(3)	168.0
O(1W)-H(1WA)...O(2W)	0.85	1.96	2.808(3)	179.9
O(2W)-H(2WB)...O(2)	0.85	1.92	2.772(3)	179.8
O(1W)-H(1WB)...O(1)#2	0.85	1.92	2.765(2)	179.9
O(2W)-H(2WA)...O(2)#3	0.85	1.98	2.828(3)	179.9

Symmetry transformations used to generate equivalent atoms:
#1 -x,-y+1,-z+1 #2 -x+1/2,y+1/2,-z+3/2 #3 -x+1,-y+1,-z+2

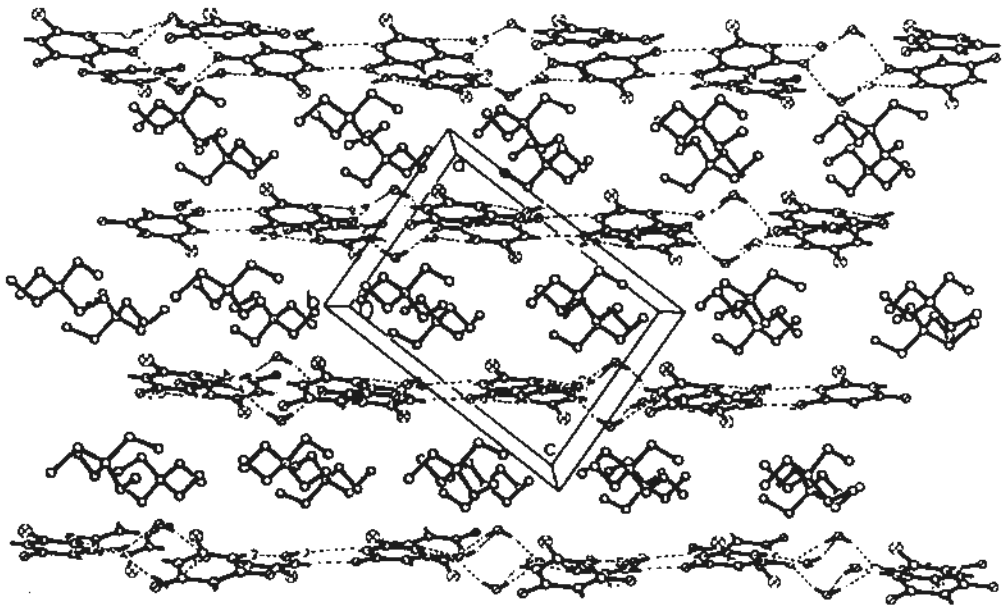

Figure 2.4.4 Projection diagram showing the crystal structure of **2.4.2** viewed along the *b* axis.

Crystal structure of $2[(n\text{-}C_3H_7)_4N^+]\cdot 2[C_4N_2O_2H_3S^-]\cdot 2[CO(NH_2)_2]\cdot 5H_2O$ (2.4.3)

There are two independent H_3TBA^- anions, two ureas, two tetra-*n*-propylammonium cations and five water molecules in the asymmetric unit of complex **2.4.3**. Figure 2.4.5 shows that two crossed series of ribbons along the [1 1 0] and [1 $\bar{1}$ 0] directions are interconnected into a three-dimensional framework

containing open channels. Well-ordered $(n\text{-}C_3H_7)_4N^+$ cations are accommodated in double columns within each channel.

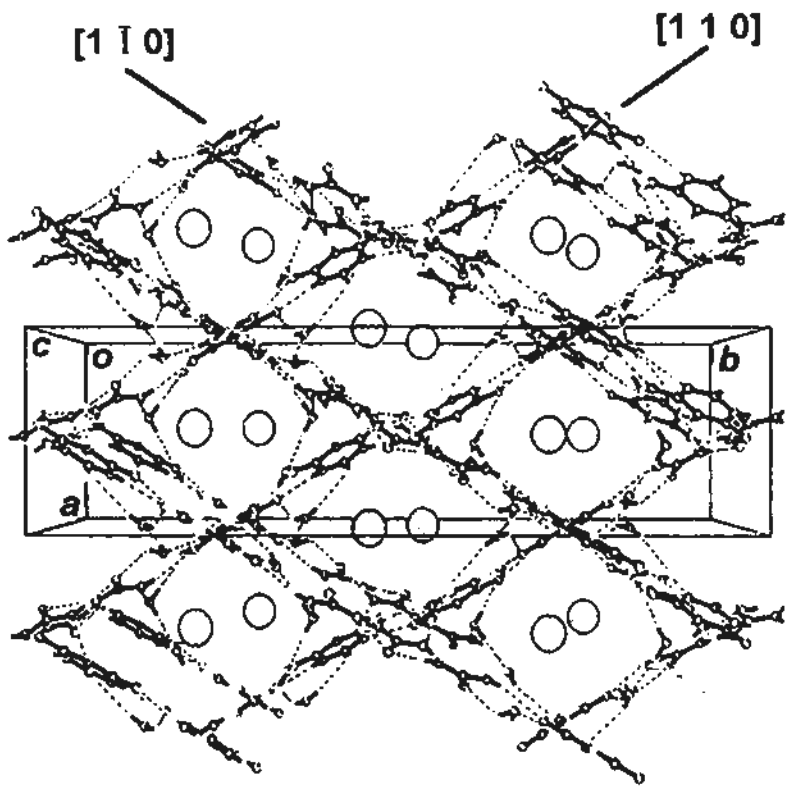

Figure 2.4.5 Channel structure of **2.4.3** view along the *c* axis.

Figure 2.4.6 shows a portion of the crystal structure along the *a* axis. The independent H_3TBA^- anions form a hydrogen-bonded dimer, and two centrosymmetrically-related dimers constitute a linear tetramer. In like manner, the independent urea molecules O5 and O6 generate a cyclic tetramer centered at an adjacent $\bar{1}$ site. These two kinds of tetramers are alternately linked with the acid of bridging water molecule O1w to generate identical infinite ribbons directed along the [1 1 0] and [1 $\bar{1}$ 0] directions.

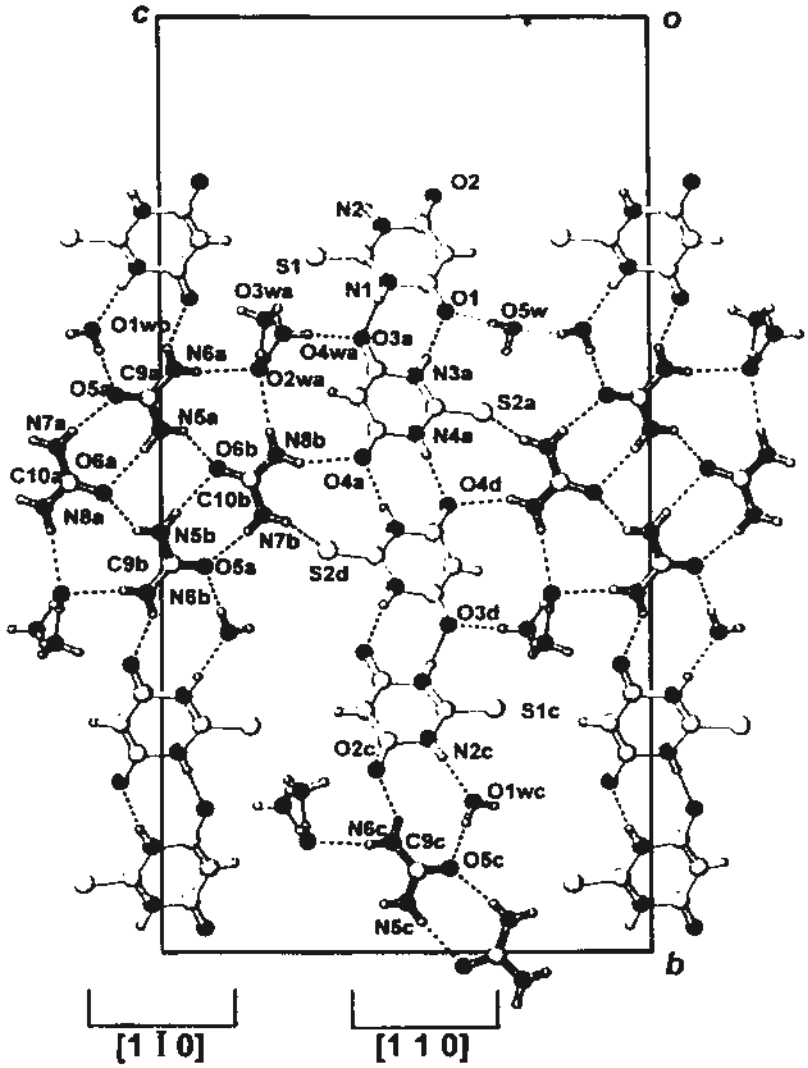

Figure 2.4.6 Projection view of the crystal structure of complex **2.4.3** viewed along the *a* axis. *Symmetry transformations*: (a) $-1 + x$, $0.5 - y$, $0.5 + z$; (b) $-x$, $0.5 + y$, $1.5 + z$; (c) $-1 - x$, $1 - y$, $1 - z$; (d) $-x$, $0.5 + y$, $0.5 - z$.

Between junctions of adjacent ribbons, cross-linkage occurs through urea to H_3TBA^- donor hydrogen bonding and bridging water to give rise to a three-dimensional channel structure. Detailed hydrogen-bonding geometries are listed in Table 2.4.3.

Table 2.4.3 Hydrogen bonds for **2.4.3** [Å and deg.].

D-H...A	d(D-H)	d(H...A)	d(D...A)	∠(DHA)
N(1)-H(1N)...O(3)#1	0.85	1.96	2.810(2)	174.0
N(2)-H(2N)...O(1W)	0.86	1.96	2.819(2)	174.9
N(3)-H(3N)...O(1)#2	0.84	2.08	2.910(2)	170.0
N(4)-H(4N)...O(4)#3	0.85	1.96	2.810(2)	174.0
N(5)-H(5A)...O(6)	0.86	2.12	2.980(3)	175.1
N(5)-H(5B)...O(6)#4	0.86	2.20	2.913(2)	139.8
N(6)-H(6A)...O(2)	0.86	2.34	3.087(2)	145.9
N(6)-H(6B)...O(2W)	0.86	2.22	3.066(2)	166.8
N(7)-H(7A)...O(5)	0.86	2.20	3.056(3)	173.7
N(7)-H(7B)...S(2)#5	0.86	2.73	3.448(2)	142.3
N(8)-H(8A)...O(2W)#4	0.86	2.29	3.149(3)	173.7
N(8)-H(8B)...O(4)#4	0.86	2.20	2.960(2)	147.6
O(1W)-H(1WA)...O(5W)#6	0.85	1.96	2.812(2)	173.9
O(1W)-H(1WB)...O(5)	0.85	1.92	2.771(2)	177.5
O(2W)-H(2WA)...O(4W)	0.85	1.99	2.848(2)	179.8
O(2W)-H(2WB)...O(3W)	0.85	1.99	2.840(2)	179.9
O(3W)-H(3WA)...S(1)#7	0.88	2.63	3.472(2)	158.6
O(3W)-H(3WB)...O(2)	0.88	1.85	2.728(2)	170.9
O(4W)-H(4WA)...S(1)#2	0.85	3.02	3.644(2)	132.5
O(4W)-H(4WB)...O(3)	0.85	1.85	2.696(2)	175.3
O(5W)-H(5WA)...O(1)	0.88	1.91	2.788(2)	152.7
O(5W)-H(5WB)...S(2)#1	0.85	2.61	3.437(2)	166.6

Symmetry transformations used to generate equivalent atoms:
#1 x-1,-y+1/2,z+1/2 #2 x+1,-y+1/2,z-1/2 #3 -x+1,-y,-z #4 -x+1,-y,-z+1 #5 x,y,z+1
#6 x,-y+1/2,z+1/2 #7 x,-y+1/2,z-1/2

Crystal structure of $[(CH_3)_4N^+] \cdot [C_3N_3S_3H_2^-]$ (2.4.4)

In the crystal structure of **2.4.4**, the trithiocyanurate anions (H_2TCA^-) form almost centrosymmetric planar dimers by pairwise hydrogen bonds. Each dimer is further connected with its four neighbors by single hydrogen bonds of the type N1b–H···N2a with large torsion angle C1b–N1b···N2a–C2a = 52.4° to generate a pleated sheet possessing the rosette motif (Figure 2.4.7). Detailed hydrogen-bonding geometries are listed in Table 2.4.4.

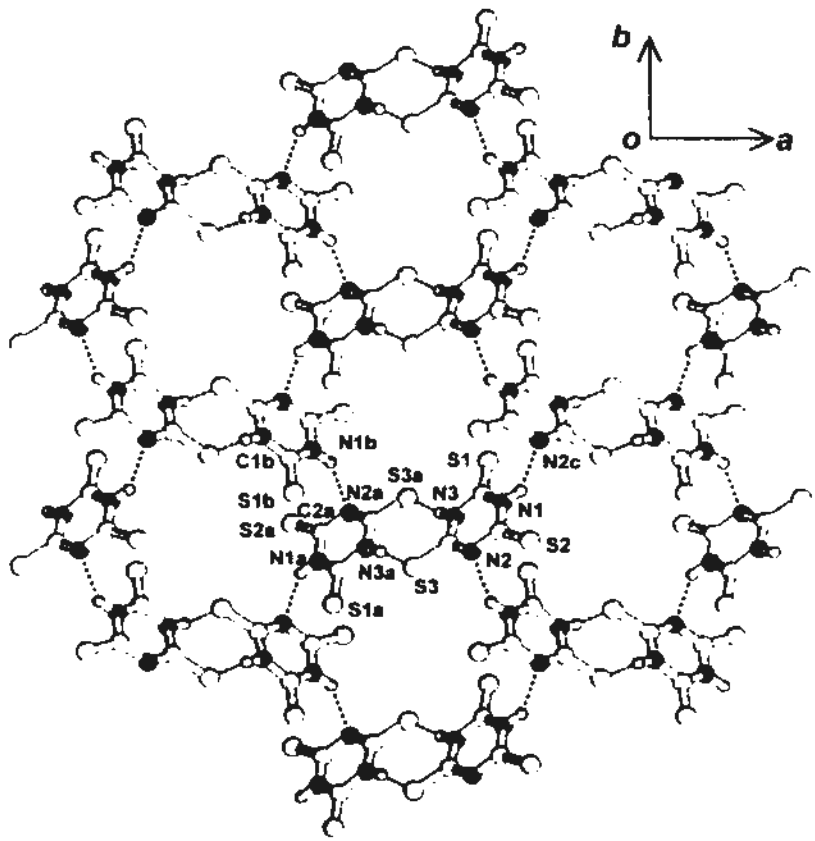

Figure 2.4.7 Rosette-like layer built of trithiocyanurate ions in the crystal structure of **2.4.4** viewed along the *c* axis. *Symmetry transformations*: (a) $1 - x, 1 - y, - z$; (b) $-0.5 + x, 1.5 - y, - z$; (c) $1.5 - x, 0.5 + y, z$.

Table 2.4.4 Hydrogen bonds for **2.4.4** [Å and deg.].

D-H...A	d(D-H)	d(H...A)	d(D...A)	∠(DHA)
N(3)-H(3N)...S(3)#1	0.85	2.49	3.334(2)	170.6
N(1)-H(1N)...N(2)#2	0.86	2.22	2.968(2)	146.1

Symmetry transformations used to generate equivalent atoms:
#1 -x+1,-y+1,-z #2 -x+3/2,y+1/2,z

Figure 2.4.8 shows that the pleated sheet structure viewed along the *b* axis. The well-ordered $(CH_3)_4N^+$ cations are accommodated between the layers.

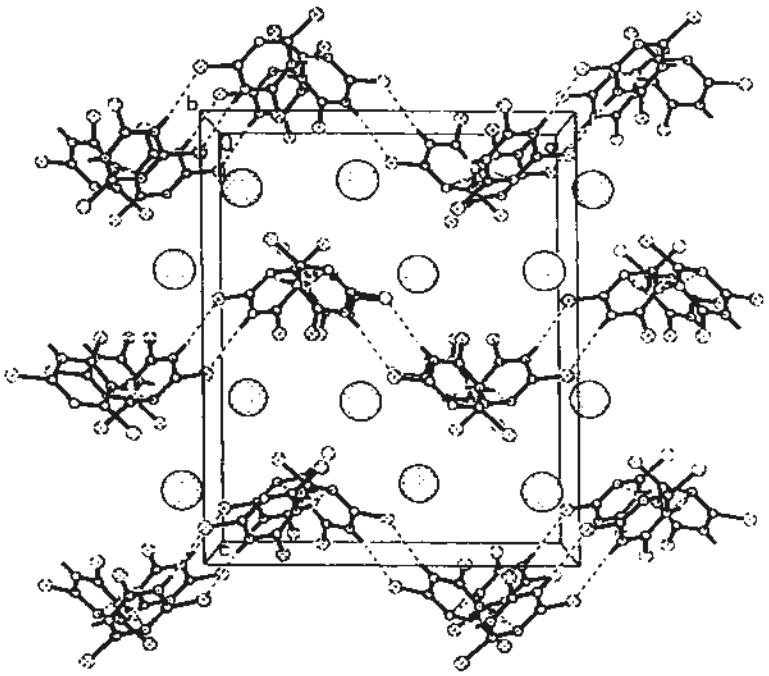

Figure 2.4.8 Crystal structure of complex **2.4.4** viewed along the *b* axis.

Crystal structure of $[(n\text{-}C_4H_9)_4N^+] \cdot [C_3N_3S_3H_2^-] \cdot 2H_2O$ (2.4.5)

When the larger tetra-*n*-butylammonium ion is used to form a trithiocyanurate salt, two water molecules are introduced into the system, yielding a stepped hydrogen-bonded layer structure (Figure 2.4.9). The well-ordered $(n\text{-}C_4H_9)_4N^+$ cations are accommodated between the layers.

In this crystal structure, H_2TCA^- dimers located at successive inversion centers along the *b* axis are joined together by pairs of N–H···S hydrogen bonds to form a zigzag chain. The independent water molecules O1w and O2w located close to an inversion center generate a centrosymmetric zigzag $(H_2O)_4$ link to bridge adjacent zigzag H_2TCA^- ribbons to form a stepped layer structure. The tetra-*n*-butylammonium cation located in the interlayer region has one alkyl leg extending into a layer void (Figure 2.4.10). Detailed hydrogen-bonding geometries are listed in Table 2.4.5.

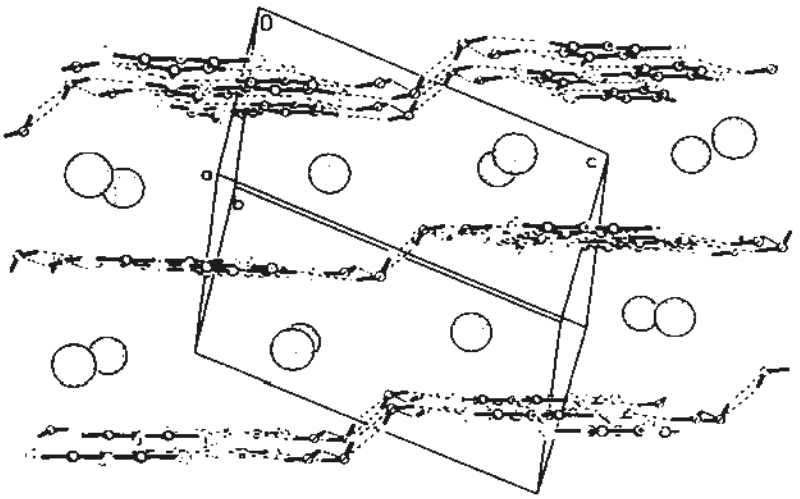

Figure 2.4.9 Layer structure of **2.4.5** with interlayer spacing about 7.36 Å viewed along the [$\bar{1}$ 1 0] direction. Well-ordered tetra-*n*-butylammonium cations are accommodated between the layers.

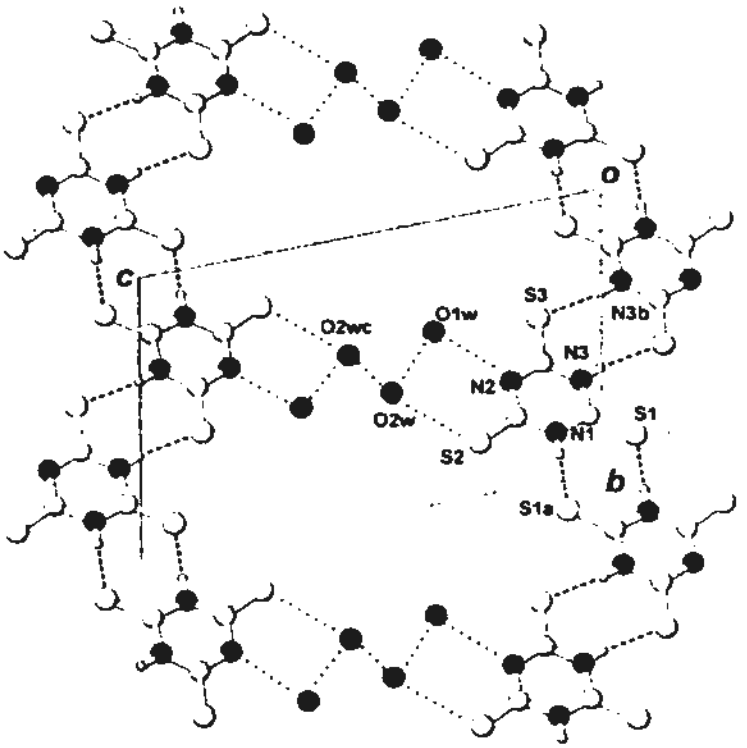

Figure 2.4.10 Projection view of the crystal structure of complex **2.4.5** viewed along the *a* axis. (Note: hydrogen atoms of water molecules are omitted, and the hydrogen atom lying between O2w and O2wc is necessarily disordered). *Symmetry transformations*: (a) $1-x, 2-y, -z$; (b) $2-x, 1-y, -z$; (c) $1-x, 1-y, 1-z$.

Table 2.4.5 Hydrogen bonds for **2.4.5** [Å and deg.].

D-H...A	d(D-H)	d(H...A)	d(D...A)	∠(DHA)
N(3)-H(3N)...S(3)#1	0.86	2.49	3.344(3)	169.9
N(1)-H(1N)...S(1)#2	0.86	2.47	3.319(3)	167.4
O(1W)-H(1WB)...O(2W)	0.87	1.98	2.85(1)	179.5
O(1W)-H(1WA)...N(2)	0.85	2.58	3.083(6)	119.5
O(1W)-H(1WA)...S(3)	0.85	2.69	3.531(5)	179.5
O(2W)-H(2WA)...S(2)	0.85	2.54	3.390(5)	179.3
O(2W)-H(2WB)...O(2W)#3	0.85	1.89	2.75(1)	179.4

Symmetry transformations used to generate equivalent atoms:
#1 -x+2,-y+1,-z #2 -x+1,-y+2,-z #3 -x+1,-y+1,-z+1

Crystal structure of $2[(CH_3)_4N^+] \cdot [C_3N_3S_3H^{2-}] \cdot 5[CO(NH_2)_2] \cdot H_2O$ (2.4.6)

Employing a molar ratio of $[(CH_3)_4N^+]:[C_3N_3S_3H^{2-}] = 2:1$ in the synthesis of complex **2.4.6** leads to formation of the trithiocyanurate dianions $HTCA^{2-}$. Two of the five independent urea molecules in the asymmetric unit, O1 and O4, are used to construct the layer shown in Figure 2.4.11.

As illustrated in Figure 2.4.11, urea molecule O4 is connected with $HTCA^{2-}$ by pairwise hydrogen bonds to form a dimer. Successive dimers related by the *b* translation generate an approximately planar zigzag ribbon. Adjacent anti-parallel ribbons are cross-linked by weak sulfur-sulfur interaction and hydrogen bonds between each pair of inversion-related urea molecules to create a thick ribbon along the *b* axis. These kind of thick ribbons are further connected by centrosymmetric urea O1 dimers to form an almost planar layer orientated close to the ($\bar{2}$ 0 2) plane, which serves as one wall (HTCA–urea) of a box-like cage structure (Figure 2.4.12).

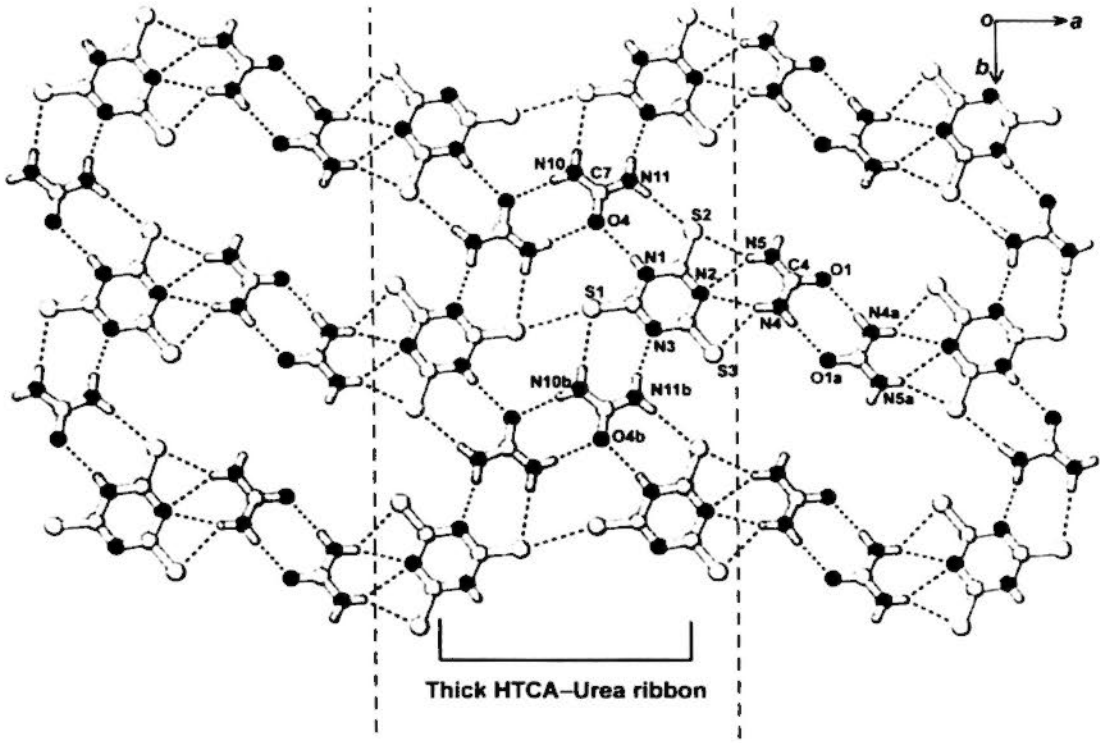

Figure 2.4.11 One wall of the cage structure of crystal **2.4.6** viewed along the *c* axis. *Symmetry transformations*: (a) $-x, -y, -z$; (b) $x, 1+y, z$.

The other three independent urea molecules, namely O2, O3 and O5, are involved in forming a urea ribbon net between the walls. Detailed hydrogen-bonding geometries are listed in Table 2.4.6.

A perspective drawing of the crystal structure of **2.4.6** is illustrated in Figure 2.4.12a. It can be seen that the urea net, which is composed of urea molecules O2, O3 and O5 linked in the head-to-tail fashion, cross-linked the HTCA–urea walls to form a three-dimensional framework. One of the two independent tetramethylammonium cation N15 is enclosed in a box-like cage, and the other one

N14 is stacked in a channel which is bounded by opposite HTCA–urea walls and urea nets.

The detail bonding mode of the urea net is shown in the Figure 2.4.12b. Urea O5a and O5b are connected in the head-to-tail fashion to generate an infinite ribbon along the *b* axis. In addition, urea O2 and O3 also linked in the head-to-tail way to form a dimer, which is further connected with O5a by chelating hydrogen bonds to generate a urea net. Water molecules O1w bridges urea O2 and O1, the latter being a component of the HTCA–urea wall.

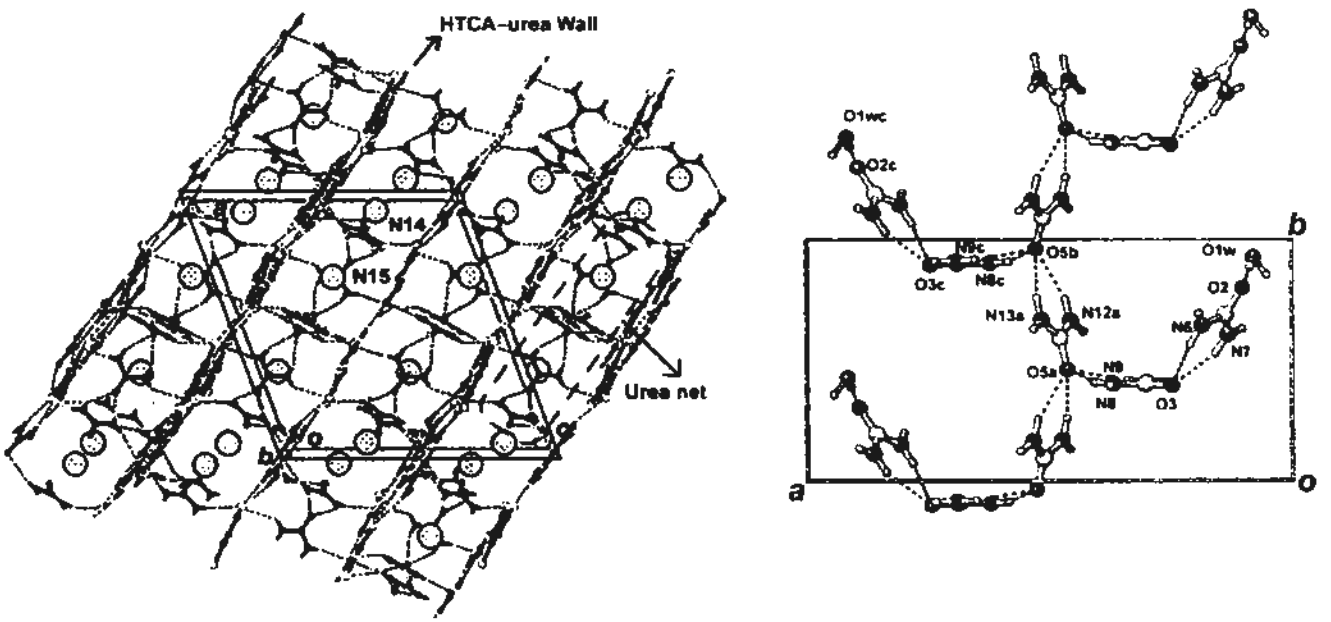

(a) (b)

Figure 2.4.12 (a) Perspective view of cage structure of **2.4.6** viewed along the *b* axis. (b) urea net connected in the head-to-tail mode between the walls viewed along the *c* axis. *Symmetry transformations*: (*a*) x, $1.5 - y$, $0.5 + z$; (*b*) $1 - x$, $2 - y$, $1 - z$; (*c*) $1 - x$, $0.5 + y$, $1.5 - z$.

Table 2.4.6 Hydrogen bonds for **2.4.6** [Å and deg.].

D-H...A	d(D-H)	d(H...A)	d(D...A)	∠(DHA)
N(1)-H(1N)...O(4)	0.85	2.17	3.023(2)	176
N(4)-H(4A)...O(1)#1	0.86	2.14	2.990(3)	169.8
N(4)-H(4B)...N(2)	0.86	2.42	3.252(3)	162
N(4)-H(4B)...S(3)	0.86	2.77	3.447(2)	137.2
N(5)-H(5A)...O(1W)#2	0.86	2.04	2.903(3)	175.4
N(5)-H(5B)...S(2)	0.86	2.64	3.417(2)	150.2
N(5)-H(5B)...N(2)	0.86	2.72	3.479(3)	148.2
N(6)-H(6A)...S(3)#3	0.86	2.62	3.469(3)	171.6
N(6)-H(6B)...O(3)	0.86	2.49	3.213(4)	142.5
N(7)-H(7A)...O(1)#4	0.86	2.50	3.336(3)	163.4
N(7)-H(7B)...O(3)	0.86	2.08	2.899(3)	158.6
N(8)-H(8A)...O(4)	0.86	2.22	3.040(3)	158.6
N(8)-H(8B)...O(5)#5	0.86	2.31	3.100(3)	153.5
N(9)-H(9A)...N(2)#6	0.86	2.56	3.222(3)	134.5
N(9)-H(9B)...O(5)#5	0.86	2.32	3.106(3)	152.5
N(10)-H(10A)...O(4)#7	0.86	2.22	3.074(2)	175.4
N(10)-H(10B)...S(1)#3	0.86	2.67	3.532(2)	177.9
N(11)-H(11A)...S(2)	0.86	2.57	3.412(2)	165
N(11)-H(11B)...N(3)#3	0.86	2.17	3.016(3)	166
N(12)-H(12B)...O(5)#8	0.86	2.24	3.055(3)	157.1
N(12)-H(12A)...N(3)#3	0.86	2.66	3.461(3)	155.2
N(13)-H(13A)...O(4)#9	0.86	2.16	3.015(3)	174.2
N(13)-H(13B)...O(5)#8	0.86	2.41	3.185(3)	149.6
O(1W)-H(1WA)...O(2)	0.86	1.95	2.811(3)	179.1
O(1W)-H(1WB)...O(1)#4	0.86	1.93	2.794(3)	179.2

Symmetry transformations used to generate equivalent atoms:
#1 -x,-y,-z #2 x,-y+3/2,z-1/2 #3 x,y+1,z #4 -x,y+1/2,-z+1/2 #5 x,-y+3/2,z+1/2
#6 x,-y+1/2,z+1/2 #7 -x+1,-y+1,-z+1 #8 -x+1,y-1/2,-z+1/2 #9 -x+1,y+1/2,-z+1/2

Crystal structure of $[(n\text{-}C_3H_7)_4N^+] \cdot [C_3N_3S_3H_2^-] \cdot [CS(NH_2)_2]$ (2.4.7)

In the crystal structure of **2.4.7**, centrosymmetrically-related trithiocyanurate dimer and thiourea dimer are connected to form an infinite kinked $(H_2TCA^-)_2$ – $(thiourea)_2$ ribbon (Figure 2.4.13). The ribbons are further cross-linked to generate a wavy layer exhibiting two different ten-membered voids [**A**] and [**B**]. Motif [**A**] is composed of four H_2TCA^- and six thiourea molecules, while [**B**] is built of six H_2TCA^- and four thiourea molecules.

(a)

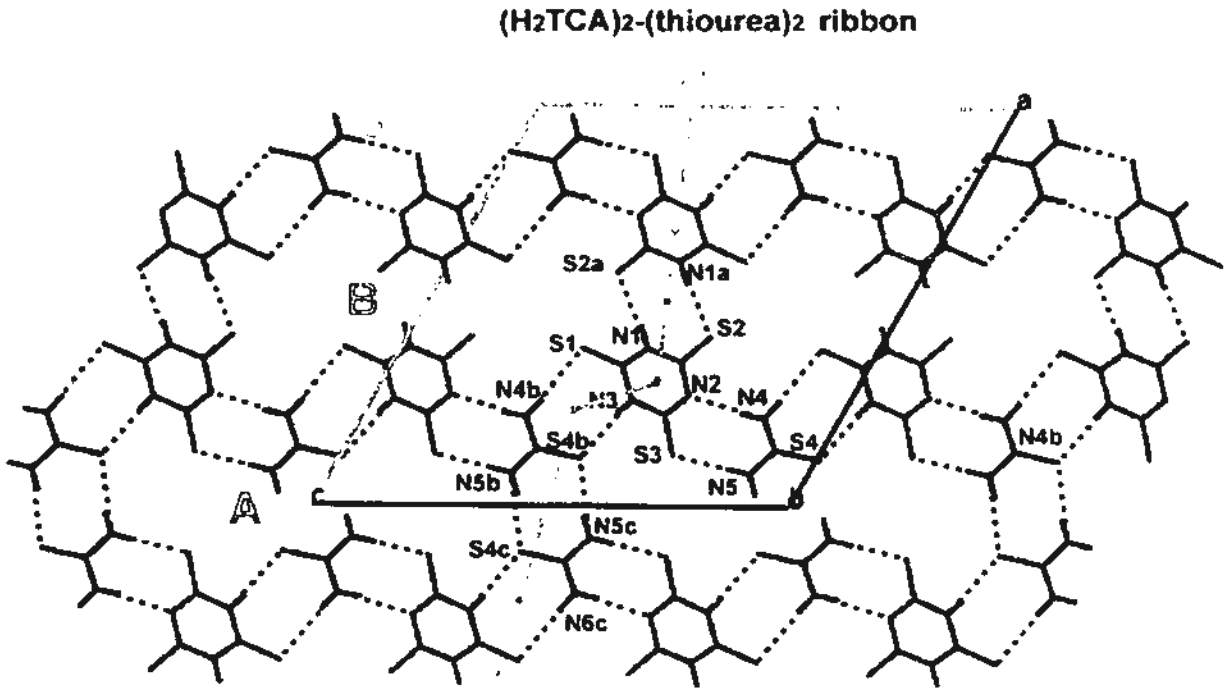

(b)

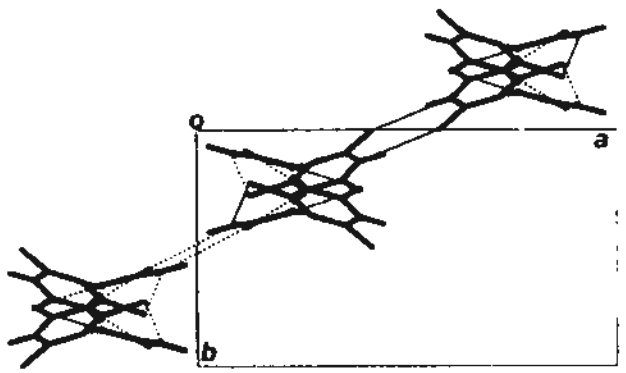

Figure 2.4.13 (a) Projection diagram showing a hydrogen-bonded layer in **2.4.7** viewed along the *b* axis; this layer is composed of different ten-membered void [**A**] and [**B**]. (b) The layer is orientated parallel to the ($\bar{2}\,\bar{2}$ 0) plane, as viewed along the *c* axis. *Symmetry transformations*: (*a*) 1 – *x*, – *y*, 1 – *z*; (*b*) *x*, 0.5 – *y*, 0.5 + *z*; (*c*) – *x*, –*y*, – *z*.

Two equivalent layers with different orientations are cross-linked to form a three-dimensional open channel structure, as shown in Figure 2.4.14. Well-ordered $(n\text{-}C_3H_7)_4N^+$ cations are accommodated in each channel. Detailed hydrogen-bonding geometries are listed in Table 2.4.7.

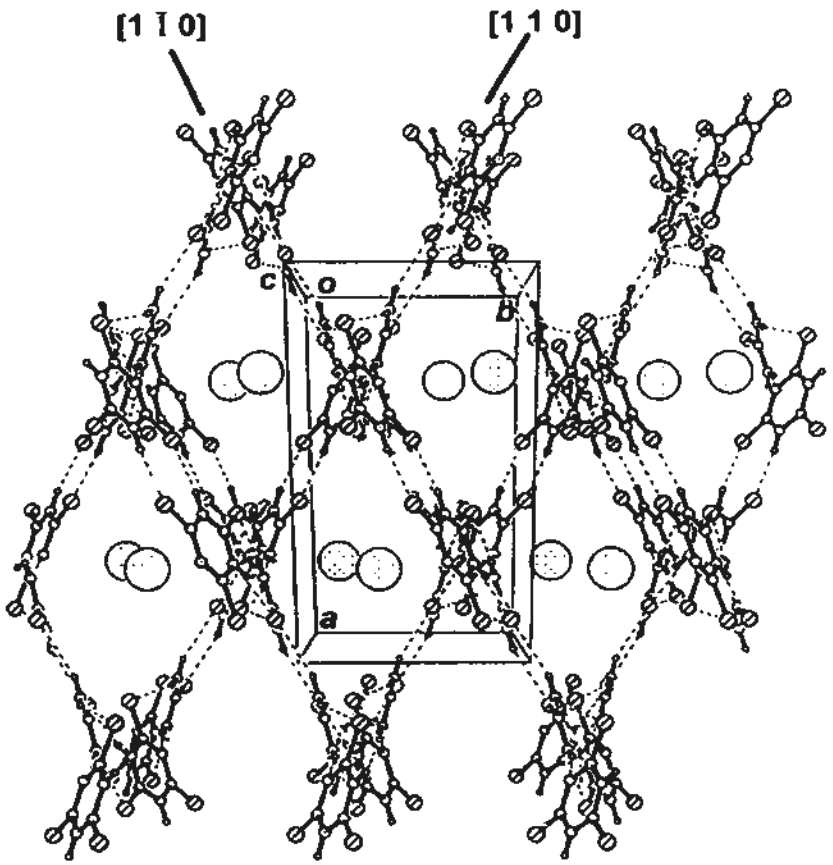

Figure 2.4.14 Channel structure of complex **2.4.7** viewed along the *c* axis.

Table 2.4.7 Hydrogen bonds for **2.4.7** [Å and deg.].

D-H...A	d(D-H)	d(H...A)	d(D...A)	∠(DHA)
N(1)-H(1N)...S(2)#1	0.92	2.44	3.350(2)	169.0
N(3)-H(3N)...S(4)#2	0.85	2.46	3.297(2)	169.0
N(4)-H(4A)...N(2)	0.86	2.10	2.937(3)	165.6
N(4)-H(4B)...S(1)#3	0.86	2.62	3.475(2)	170.9
N(5)-H(5D)...S(3)	0.86	2.58	3.367(2)	151.8
N(5)-H(5E)...S(4)#4	0.86	2.64	3.466(2)	160.3

Symmetry transformations used to generate equivalent atoms:
#1 -x+1,-y,-z+1 #2 x,-y+1/2,z+1/2 #3 x,-y+1/2,z-1/2 #4 -x,-y,-z

Crystal structure of $[(n\text{-}C_3H_7)_4N^+] \cdot [C(NH_2)_3^+] \cdot [C_3N_3S_3H^{2-}]$ (2.4.8)

The $HTCA^{2-}$ and guanidinium ions (GM) are connected alternately to generate a zigzag ribbon along the *c* axis. A pair of anti-parallel ribbons is further cross-linked to form a double HTCA–GM ribbon. Between the double ribbons, interaction between each pair of inversion-related $HTCA^{2-}$ by hydrogen bonds of the types N3b–H···S1 and N3–H···S1b creates a wavy layer (Figure 2.4.15).

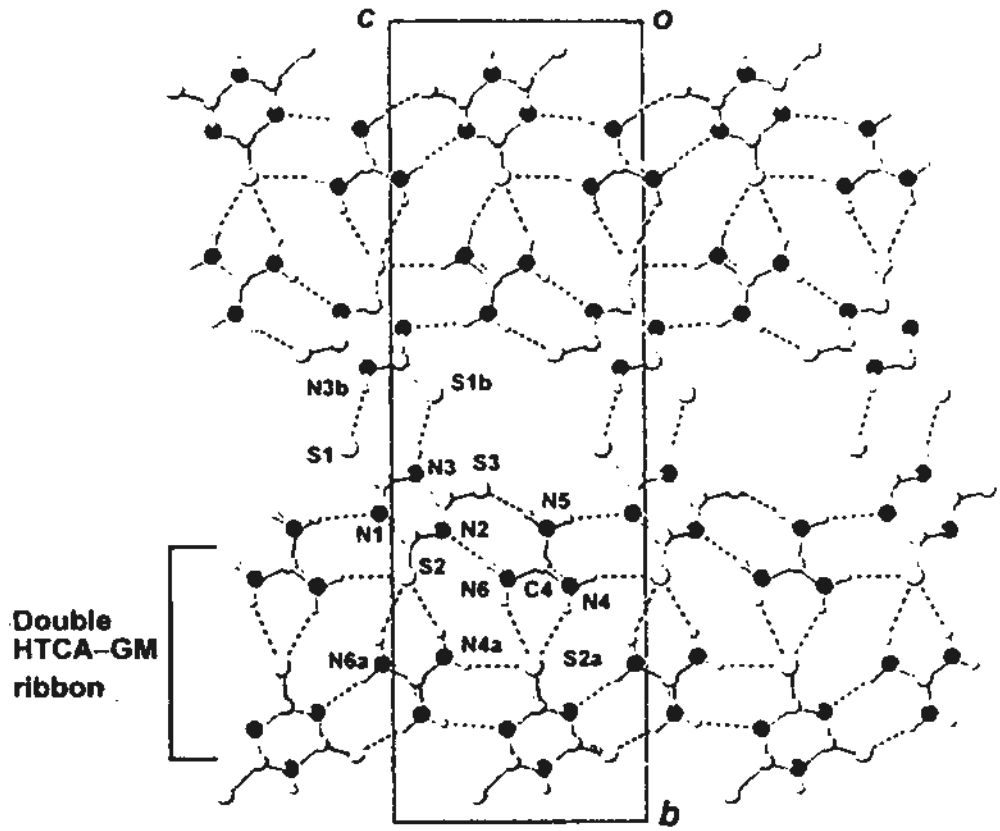

Figure 2.4.15 Crystal structure of **2.4.8** shows a layer composed of double HTCA–GM ribbons viewed along the *a* axis. *Symmetry transformations*: (a) x, 1.5 – y, –0.5 + z; (b) 1 – x, 1 – y, 2– z.

Figure 2.4.16 shows a perspective view of the crystal structure of **2.4.8** along the *c* axis. The distance separating the mean planes of adjacent HTCA–GM wavy layers is a = 8.93 Å, and between them there is a layer composed of stacked columns

of ordered tetrahedral $(n\text{-}C_3H_7)_4N^+$ cations. Detailed hydrogen-bonding geometries are listed in Table 2.4.8.

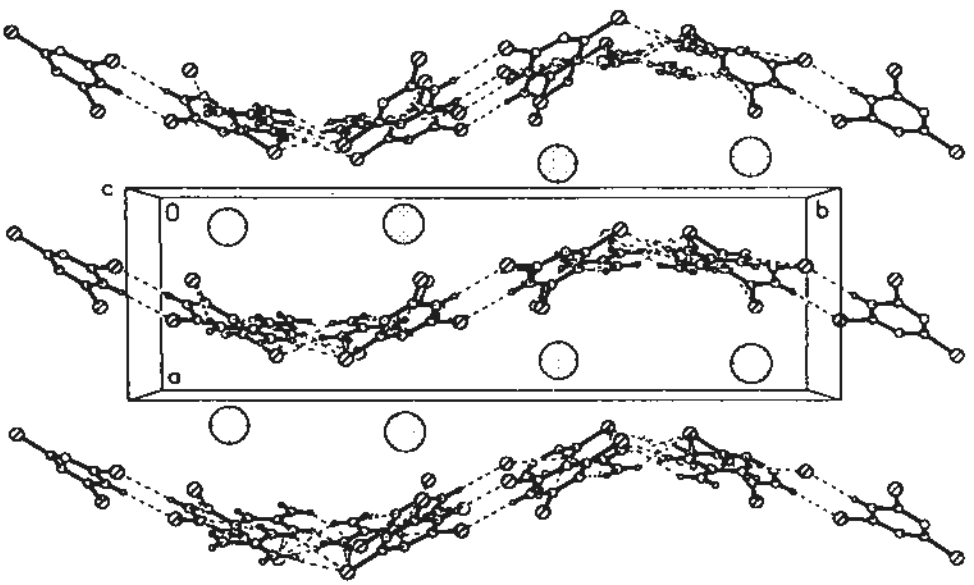

Figure 2.4.16 Crystal structure of **2.4.8** showing the packing of wavy layers viewed along the *c* axis. Well-ordered tetra-*n*-propylammonium cations are accommodated between the layers.

Table 2.4.8 Hydrogen bonds for **2.4.8** [Å and deg.].

D-H...A	d(D-H)	d(H...A)	d(D...A)	∠(DHA)
N(3)-H(3N)...S(1)#1	0.86	2.57	3.422(2)	171.8
N(4)-H(4A)...S(2)#2	0.86	2.49	3.295(3)	157.3
N(4)-H(4B)...S(2)#3	0.86	2.51	3.306(3)	154.5
N(5)-H(5A)...N(1)#2	0.86	2.26	3.088(3)	161.4
N(5)-H(5A)...S(1)#2	0.86	2.86	3.514(2)	134.6
N(5)-H(5B)...S(3)	0.86	2.55	3.335(3)	152.1
N(6)-H(6A)...N(2)	0.86	2.09	2.918(3)	160.1
N(6)-H(6B)...S(2)#3	0.86	2.90	3.608(2)	141.5

Symmetry transformations used to generate equivalent atoms:
#1 -x+1,-y+1,-z+2 #2 x, y, z-1 #3 x,-y+3/2,z-1/2

Crystal structure of $[(n\text{-}C_4H_9)_4N^+] \cdot [C(NH_2)_3^+] \cdot [C_3N_3S_3H^{2-}]$ (2.4.9)

In the crystal structure of **2.4.9**, the $HTCA^{2-}$ and guanidinium ions are interconnected to form a wavy layer exhibiting a ten-membered ring motif (Figure 2.4.17a). As illustrated in Figure 2.4.18a, each guanidinium is connected with three adjacent $HTCA^{2-}$ by pairwise and chelating hydrogen bonds. The trithiocyanurate dianions S2 and S3b are parallel to each other, while S1a is inclined to them at a dihedral angle of about 68.2 °. In turn, the $HTCA^{2-}$ dianions is joined with three neighboring guanidiniums by acceptor hydrogen bonds (Figure 2.4.18b).

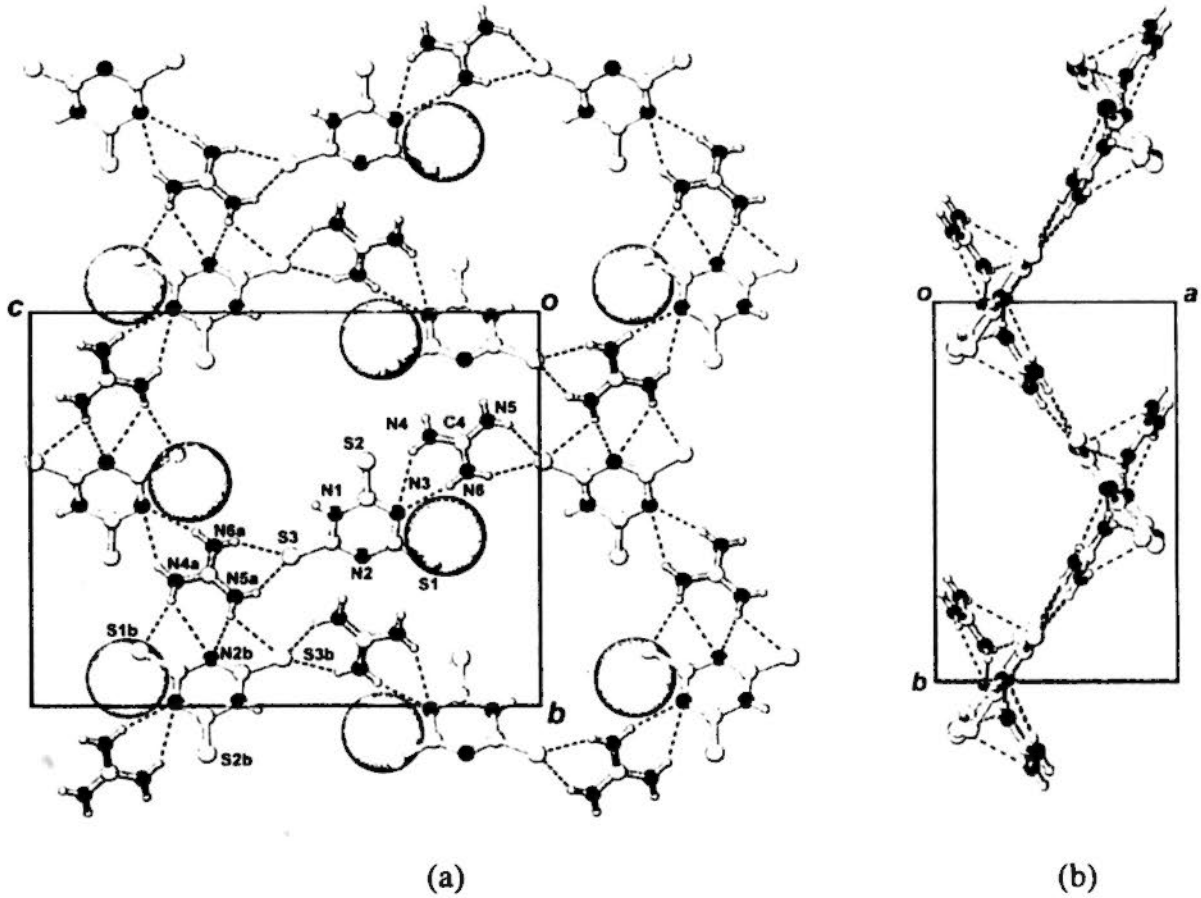

(a) (b)

Figure 2.4.17 (a) Ten-membered ring motif in **2.4.9** composed of five guanidiniums and five $HTCA^{2-}$ molecules; (b) Project diagram showing the pleated sheet structure viewed along the *c* axis. *Symmetry transformations*: (*a*) $1.5 - x, 1 - y, 0.5 + z$; (*b*) $-0.5 + x, 1.5 - y, 1 - z$.

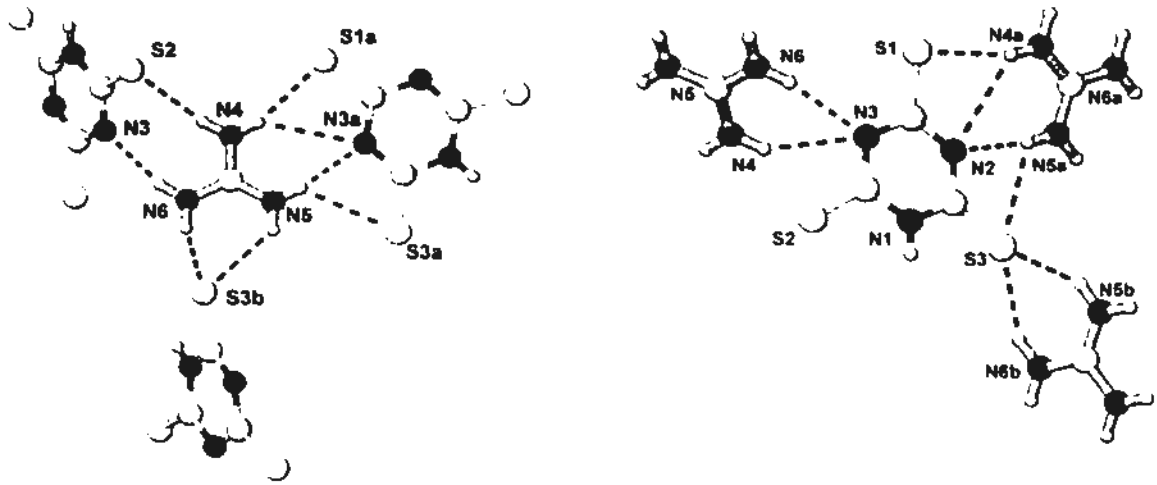

(a) (b)

Figure 2.4.18 (a) Hydrogen-bonding environment of guanidinium. *Symmetry transformations*: (*a*) 1.5 – *x*, 1.0 – *y*, –0.5 + *z*; (*b*) 2 – *x*, -0.5 + *y*, 0.5 – *z*; (b) hydrogen-bonding environment of $HTCA^{2-}$. *Symmetry transformations*: (*a*) 2 – *x*, 0.5 + *y*, 0.5 – *z*; (*b*) 1.5 – *x*, 1.0 – *y*, 0.5 + *z*.

Compound **2.4.9** can be contrasted with the thiourea complex **2.4.7**, which has unequal numbers of two components in each ten-membered void. The $HTCA^{2-}$–guanidinium layer is a pleated sheet structure as seen along the *c* direction. Detailed hydrogen-bonding geometries are listed in Table 2.4.9.

Further cross-linkage between adjacent pleated sheet ribbons generates three-dimensional channel (Figure 2.4.19). Well-ordered $(n\text{-}C_4H_9)_4N^+$ cations are accommodated in each channel.

Table 2.4.9 Hydrogen bonds for **2.4.9** [Å and deg.].

D-H...A	d(D-H)	d(H...A)	d(D...A)	∠(DHA)
N(4)-H(4A)...S(1)#1	0.86	2.52	3.351(5)	163.0
N(4)-H(4B)...N(3)	0.86	2.65	3.387(6)	144.9
N(5)-H(5D)...N(2)#1	0.86	2.22	3.070(6)	170.2
N(5)-H(5D)...S(3)#1	0.86	2.89	3.472(4)	127.0
N(6)-H(6A)...S(3)#2	0.86	2.69	3.471(4)	152.0
N(6)-H(6B)...N(3)	0.86	2.25	3.087(5)	163.3

Symmetry transformations used to generate equivalent atoms:
#1 -x+2,y-1/2,-z+1/2 #2 -x+3/2,-y+1,z-1/2

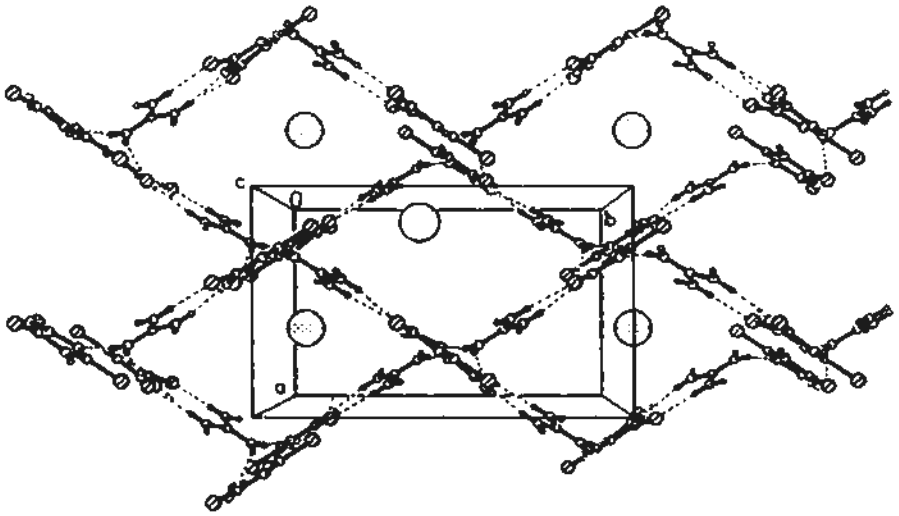

Figure 2.4.19 The packing diagram shows that the channel structure of **2.4.9**.

2.4.2 Inclusion compounds containing anions of 5-nitrobarbituric acid

The crystal structure of 5-nitrobarbituric acid was first reported in 1963.[89] The acid forms salt complexes with alkali, alkaline and rare-earth metals.[90] A search of the Cambridge Structural Database (Version 5.28) using the term nitrobarbituric/nitrobarbiturate and dilituric acid only yielded 7 hits for five compounds. These are 5-nitrobarbituric acid (NBARBA),[89] 5-nitrobarbituric acid trihydrate (NBARBT, NBARBT01, NBARBT02),[91] ammonium 5-nitrobarbiturate (DAKFAW),[92] hexa-aqua-magnesium bis(5-nitrobarbiturate) dihydrate (NOGLAW),[93] and hexa-aqua-calcium bis(5-nitrobarbiturate) dihydrate

(NOGLEA).[93] Since barbiturate derivatives possess a cyclic urea skeleton, in the solid state 5-nitrobarbiturate has the tendency to form a dimer using its oxygen and nitrogen atoms at different positions relative to the nitro group. To facilitate subsequent discussion, three kinds of possible dimers of nitrobarbiturate are designated as type **A**, **B** and **C**, as illustrated in Scheme 2.4.2. Among these, type **A** (*para*-to-*para*) appears in neat 5-nitrobarbituric acid, type **B** (*ortho*-to-*ortho*) is found in hexa-aqua-calcium bis(5-nitrobarbiturate) dihydrate, and both type **A** and type **B** occur in ammonium 5-nitrobarbiturate and 5-nitrobarbituric acid trihydrate. To our best knowledge there is as yet no report on inclusion compounds containing 5-nitrobarbituric acid as a host component.

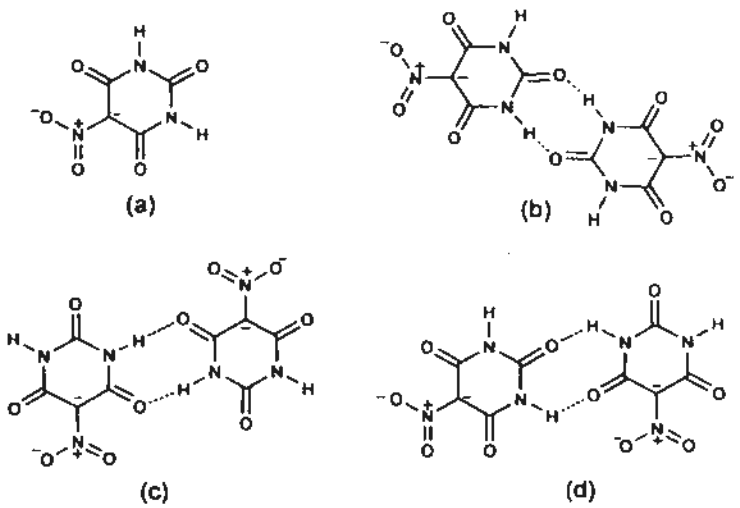

Scheme 2.4.2 (a) Structural formula of the monoanion of 5-nitrobarbituric acid. (b) Type **A** (*para*-to-*para*), (c) Type **B** (*ortho*-to-*ortho*), and (d) Type **C** (*para*-to-*ortho*) dimer linkage; the designation of *para* or *ortho* refers to the carbonyl group that is involved in intermolecular hydrogen bonding, whose position is relative to that of the nitro group.

Crystal structure of $[(CH_3)_4N^+] \cdot [(C_4H_2N_3O_5)^-]$ (2.4.10)

The crystal lattice is built from wavy layers each composed of zigzag ribbons running parallel to the *c* axis (Figure 2.4.20). Inversion-related 5-nitrobarbiturate ions form a type **A** dimer (Scheme 2.4.2) via a pair of N2–H···O4a = 2.959 (2) Å hydrogen bonds in the *para*-to-*para* fashion. Such dimers use nitrogen atom N3 and oxygen atom O5 (*ortho* with respect to the nitro group) to connect with adjacent dimers to form a hydrogen-bonded zigzag chain along the *c* axis. In this zigzag chain, each 5-nitrobarbiturate ion uses a pair of cyclic hydrogen bonds to form a type **A** dimer and a single hydrogen bond to connect adjacent dimers together in an alternating single-double hydrogen-bonding connection mode. These chains lie side by side and are linked by N3c–H···O5 = 2.974(2) Å hydrogen bonds to give a wavy layer. It is worthy of note that the nitro group is almost co-planar with the heterocyclic ring, and it does not participate in intermolecular interaction except for weak C–H···O hydrogen bonding.

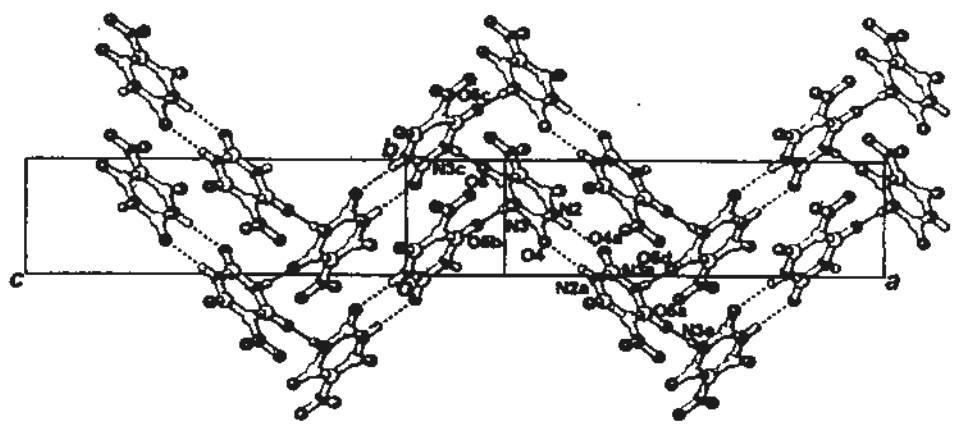

Figure 2.4.20 Double zigzag ribbon of complex **2.4.10**, viewed almost along the [1 0 1] direction. *Symmetry transformations*: (a) 1.5 – *x*, 0.5 – *y*, 1 – *z*; (b) 1.5 – *x*, –0.5 + *y*, 1.5 – *z*; (c) 1.5 – *x*, 0.5 + *y*, 1.5 – *z*; (d) *x*, 1 – *y*, –0.5 + *z*; (e) *x*, – *y*, –0.5 + *z*.

In addition, π–π interaction also serves as an associating driving force for formation of the layer structure, as the nearest inter-planar separation between dimers is about 3.4 Å. The closest distance between two off-set heterocycles is about 4.3 Å, and the dihedral angle between two connected dimers is about 77 °, as shown in Scheme 2.4.3a. For clarity, differently connected dimers are represented by different rectangles.

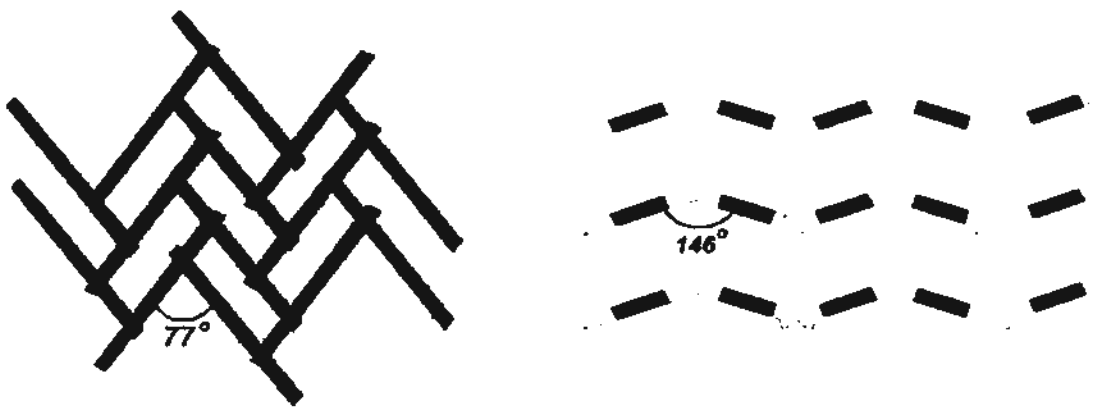

(a) Complex **1** (b) Complex **2**

Scheme 2.4.3 Different dimer connection modes and angles in the different complexes.

The well-ordered, tetramethylammonium cations are stacked between the wavy layers and interact with the nitro groups by weak C–H···O interactions ranging from 3.2 to 3.5 Å (Figure 2.4.21). Detailed hydrogen-bonding geometries are listed in Table 2.4.10.

Figure 2.4.21 Perspective of the crystal structure of complex **2.4.10**, viewed along the *b* axis.

Table 2.4.10 Hydrogen bonds for **2.4.10** [Å and deg.].

D-H...A	d(D-H)	d(H...A)	d(D...A)	∠(DHA)
N(2)-H(2N)...O(4)#1	0.83	2.13	2.959(2)	176.0
N(3)-H(3N)...O(5)#2	0.86	2.12	2.974(2)	175.2

Symmetry transformations used to generate equivalent atoms:
#1 -x+3/2,-y+1/2,-z+1 #2 -x+3/2,y-1/2,-z+3/2

Crystal structure of $[(n\text{-}C_3H_7)_4N^+] \cdot [(C_4H_2N_3O_5)^-] \cdot H_2O$ (2.4.11)

Figure 2.4.22 shows one layer in the crystal structure of complex **2.4.11**. The nitrobarbiturates are inter-linked to form a tetramer, in which two different connection modes are present: one is type **B** *ortho*-to-*ortho*, and the other is type **C** *para*-to-*ortho* (see Scheme 2.4.2). Two nitrobarbiturates related by an inversion center are connected together by a pair of N3–H···O5a hydrogen bonds in the type **B** *ortho*-to-*ortho* mode. The dimer is consolidated by water molecules O1w and O1wa and further connected with terminal nitrobarbiturates by N2–H···O9 and N6–H···O3

hydrogen bonds in the *para*-to-*ortho* fashion to form a tetramer. Such tetramers are inter-connected by bridging water molecule O2w to generate puckered layers with large voids that match the (1 0 0) plane. The dihedral angle between two connected tetramers is about 146° (Scheme 2.4.3b), which is larger than that found in complex **2.4.10**. Detailed hydrogen-bonding geometries are listed in Table 2.4.11.

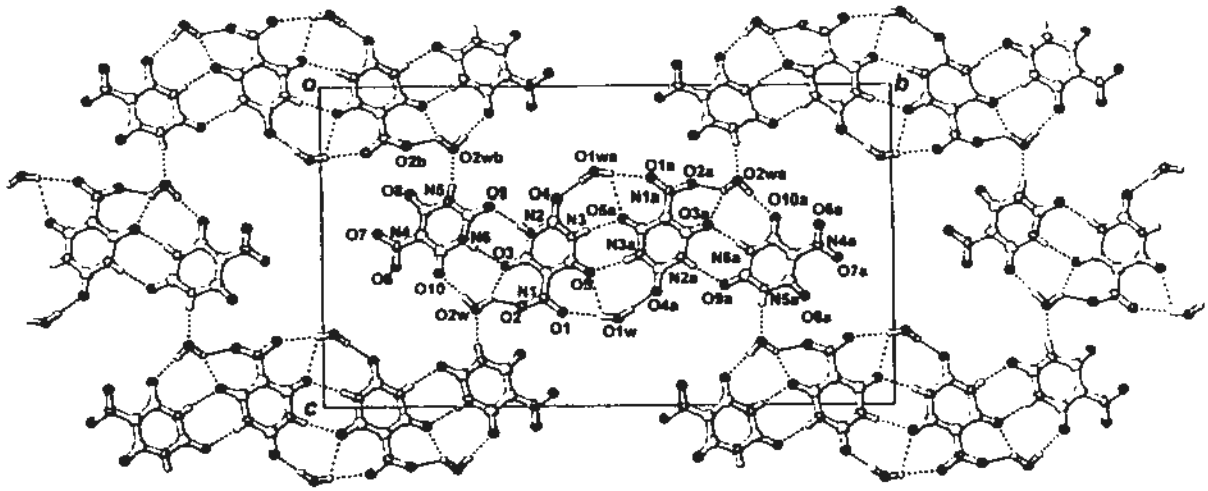

Figure 2.4.22 Projection of the crystal structure of complex **2.4.11** viewed along the *a* axis. *Symmetry transformations*: (a) $-x, 1-y, 1-z$; (b) $x, 0.5-y, -0.5+z$.

The interlayer distance is about 7.3 Å in this crystal lattice (Figure 2.4.23). The tetra-*n*-propylammonium cations are sandwiched between each layer, with one alkyl leg pointing toward the center of a void.

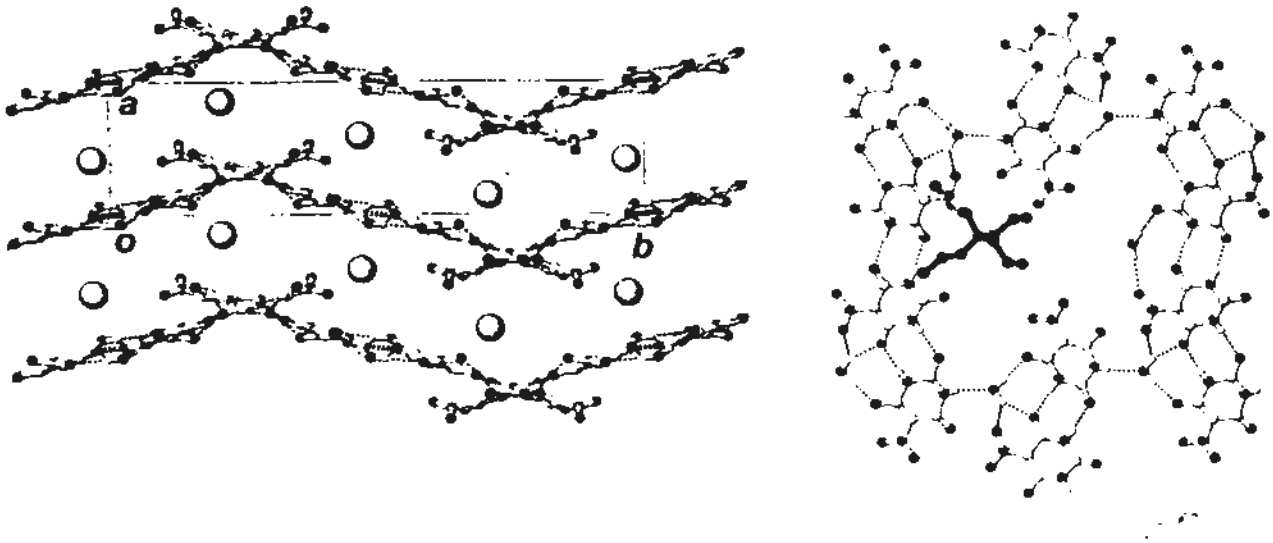

(a) (b)

Figure 2.4.23 (a) Layer structure of complex **2.4.11** viewed along the *c* axis, with large spheres representing the ordered $(n\text{-}Pr_4)N^+$ cations that are accommodated between sinusoidal layers. (b) Terminal methyl group deviating from the main plane points to the center of the void, as viewed along the *a* axis.

Table 2.4.11 Hydrogen bonds for **2.4.11** [Å and deg.].

D-H...A	d(D-H)	d(H...A)	d(D...A)	∠(DHA)
N(2)-H(2N)...O(9)	0.77	2.14	2.911(3)	173
N(3)-H(3N)...O(5)#1	0.84	2.08	2.908(3)	166
N(5)-H(5N)...O(2W)#2	0.78	2.10	2.861(3)	167
N(6)-H(6N)...O(3)	0.78	2.09	2.866(3)	173
O(1W)-H(1WA)...O(4)#1	0.87	1.92	2.789(4)	179.8
O(1W)-H(1WB)...O(1)	0.84	2.20	3.045(3)	178.3
O(1W)-H(1WB)...O(5)	0.84	2.50	2.928(4)	112.0
O(2W)-H(2WA)...O(3)	0.96	2.06	2.937(2)	151.9
O(2W)-H(2WA)...O(2)	0.96	2.47	3.223(3)	134.9
O(2W)-H(2WB)...O(10)	0.86	1.90	2.766(2)	178.5

Symmetry transformations used to generate equivalent atoms:
#1 -x,-y+1,-z+1 #2 x,-y+1/2,z-1/2

Crystal structure of $2[(CH_3)_4N^+] \cdot 2[(C_4H_2N_3O_5)^-] \cdot (NH_2)_2CS$ (2.4.12)

Two channels of different sizes exist in the crystal structure of inclusion complex **2.4.12**. As shown in Figure 2.4.24, two independent 5-nitrobarbiturate anions are linked in the *para*-to-*para* fashion by N6–H···O4 and N2–H···O9 hydrogen bonds to form a dimer, and successive dimers related by the *a* translation associate in the *ortho*-to-*ortho* fashion to generate an approximately planar zigzag ribbon. The deviation of its molecular components from co-planarity is shown by the torsion angles C6a–N5a···O5–C4 = −14.54, C4–N3···O8a–C6a = −21.95, C3–N2···O9–C7 = 6.07, and C7–N6···O4–C3 = −3.22 °. Detailed hydrogen-bonding geometries are listed in Table 2.4.12.

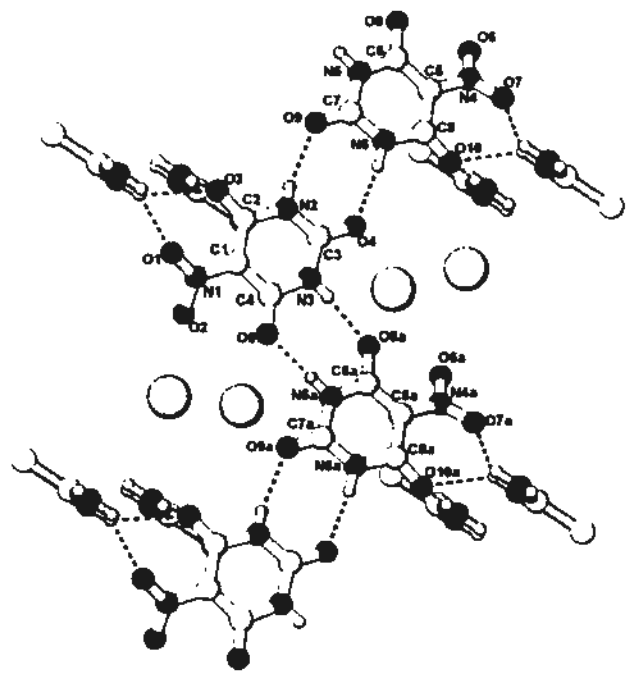

Figure 2.4.24 Zigzag ribbon formed by 5-nitrobarbiturate ions and the hydrogen-bonded scheme in the thiourea–anion host lattice of complex **2.4.12**, viewed along the *b* axis. The large spheres represent $(CH_3)_4N^+$ ions. *Symmetry transformations*:(a) $1+x, y, z$.

Adjacent ribbons are bridged by thiourea molecules to form two distinct channels (Figure 2.4.25). It is observed that two *syn* hydrogens of thiourea are connected with two parallel 5-nitrobarbiturate ribbons by N7–H···O3 = 2.977(3) and N8–H···O10c = 2.920(3) Å hydrogen bonds to form the larger channel, and the inter-ribbon spacing is about 7.3 Å. In contrast, two *anti* hydrogens of thiourea are connected with oxygen atoms of the nitro group by N7–H···O1a = 2.968(3), N7–H···O3a = 3.196(3), N8–H···O7b = 3.107(3) and N8–H···O10b = 3.130(3) Å hydrogen bonds, yielding a smaller channel with an inter-ribbon spacing of 3.6 Å. In the latter case, π–π interaction exists between closely spaced ribbons, which reinforces the role of thiourea acting as a clamp. Interestingly, the sulfur atom of the thiourea molecule has no obvious interaction with adjacent molecules, which is a rare phenomenon among the inclusion compounds of thiourea. The closest distance between two sulfur atoms in the crystal structure is about 6.3 Å. The tetramethylammonium cation occupied the larger channels in double columns.

Table 2.4.12 Hydrogen bonds for **2.4.12** [Å and deg.].

D-H...A	d(D-H)	d(H...A)	d(D...A)	∠(DHA)
N(2)-H(2N)...O(9)#1	0.76	2.21	2.950(3)	165
N(3)-H(3N)...O(8)#2	0.81	2.05	2.854(3)	170
N(5)-H(5N)...O(5)#3	0.87	1.95	2.808(3)	171
N(6)-H(6N)...O(4)#1	0.87	2.07	2.917(3)	166
N(7)-H(7A)...O(1)#4	0.86	2.2	2.968(3)	148.4
N(7)-H(7A)...O(3)#4	0.86	2.49	3.197(3)	140.3
N(7)-H(7B)...O(3)#1	0.86	2.12	2.977(3)	175.6
N(8)-H(8A)...O(10)#5	0.86	2.48	3.130(3)	132.6
N(8)-H(8A)...O(7)#5	0.86	2.53	3.107(3)	125.3
N(8)-H(8B)...O(10)#6	0.86	2.06	2.920(3)	176.4

Symmetry transformations used to generate equivalent atoms:
#1 x,y,z #2 x+1,y,z #3 x-1,y,z #4 -x+1,-y+1,-z #5 x,y,z-1 #6 -x+1,-y+2,-z+1

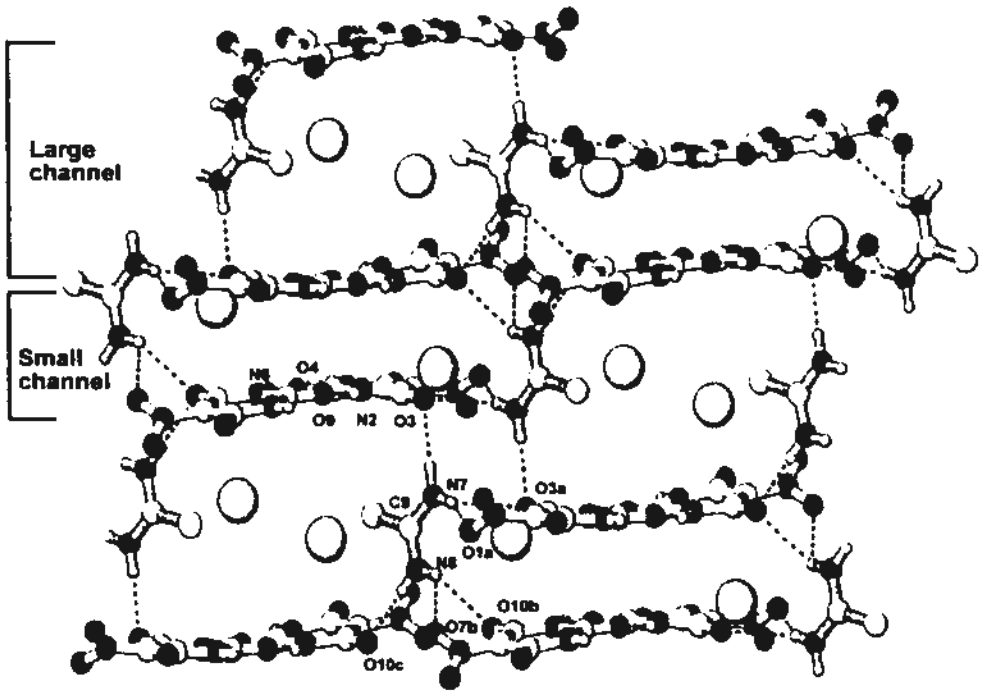

Figure 2.4.25 Perspective view of the crystal structure of complex **2.4.12** viewed along the *a* axis. *Symmetry transformations*: (a) $1 - x, 1 - y, - z$; (b) $x, y, -1 + z$; (c) $1 - x, 2 - y, 1 - z$.

A search of the Cambridge Structural Database (Version 5.28) using the term thiourea (drawing) yielded 206 hits excluding organometallic complexes, of which 54 structures make use of the *syn* hydrogens of thiourea in donor hydrogen bonding. It is noted that only 3 crystal structures utilize thiourea as a strut or clamp to connect two ribbons or layers together. These are 4,4'-bipyridine-*N,N'*-dioxide thiourea clathrate (CSD Refcode: BAFVEJ),[94] *S*-methylthiouronium tetracyanoquinodimethanide (COFRIY10)[95] and bis(*S*-methylthiouronium)tris(7,7,8,8-tetracyano-*p*-quino dimethane) dihydrate (KOBSOJ).[96] In addition, among the 206 hits of thiourea crystal structures (excluding sulfur-substituted thiourea), there is only one example in which the sulfur atom has no interaction with neighboring molecules or the intermolecular interaction

is extremely weak, namely bis(8-quinolyl-oxy)-ethoxy-ethyl)ether (QUETHU).[197] In the vast majority of cases the sulfur atom of thiourea is involved in acceptor hydrogen bonding in the crystalline state.

Crystal structure of $2[(C_2H_5)_4N^+] \cdot [(C_4HN_3O_5)^{2-}] \cdot 2(NH_2)_2CS \cdot H_2O$ (2.4.13)

The structure of complex **2.4.13** can be considered as a combination of two major structural components designated as type **I** and type **II**, which are interlinked by N–H···O and N–H···N hydrogen bonds (Figure 2.4.26).

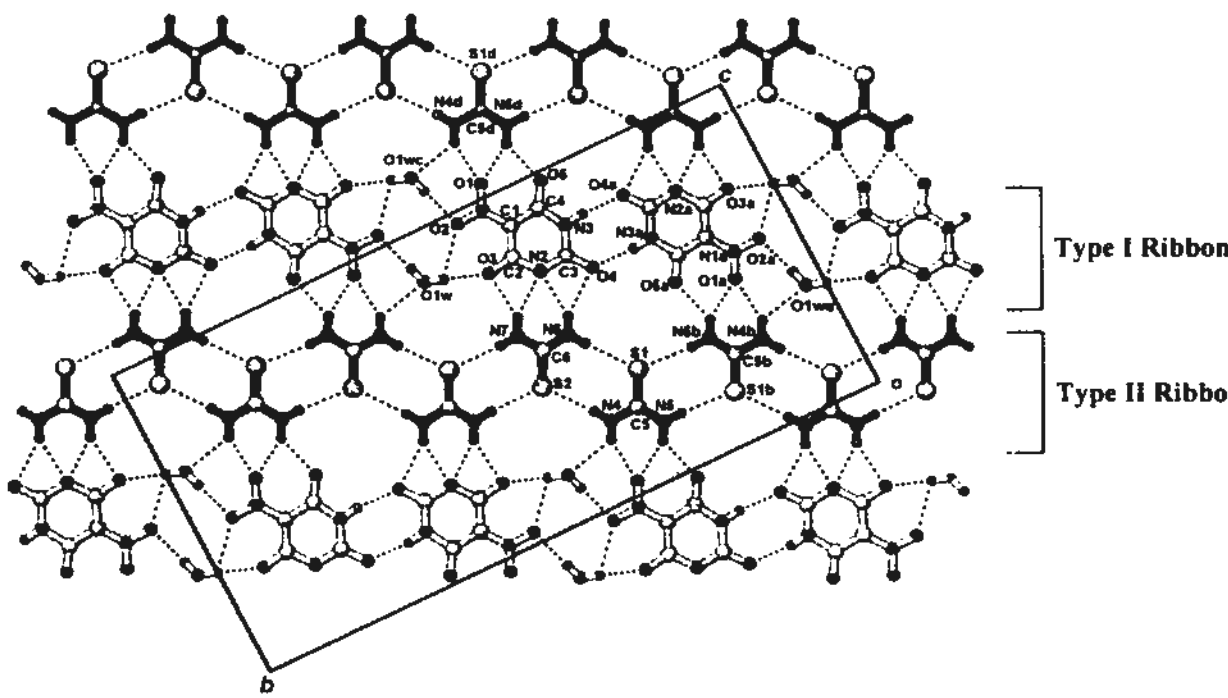

Figure 2.4.26 Projection of the crystal structure of complex **2.4.13** viewed along the *a* axis. *Symmetry transformations*: (a) x, 0.5 – y, 1.5 + z; (b) x, 0.5 – y, 0.5 – z; (c) 1 – x, 1 – y, 2 – z; (d) x, y, 1 + z; (e) 1 – x, –0.5 + y, –0.5 + z.

The type **I** component is a 5-nitrobarbiturate–water ribbon. Centrosymmetric 5-nitrobarbiturate dianions are connected to each other by a pair of O4–H···N3a hydrogen bonds to form a dimer in the *para*-to-*para* fashion. Adjacent dimers are

further bridged by a pair of inversion-related water molecules O1w and O1wc with multiple hydrogen bonds to form an infinite ribbon along the [0 1 1] direction.

The type **II** component consists of thiourea molecules that are alternately linked together in the shoulder-to-shoulder fashion to form an almost planar ribbon extending parallel to the type **I** ribbon. The relevant torsion angles in each thiourea ribbon are: C6–N6···S1–C5 = 8.6, C5–N4···S2–C6 = –24.0, and C5–N5···S1b–C5b = –0.3 °. Detailed hydrogen-bonding geometries are listed in Table 2.4.13.

With these two kinds of ribbons arranged side by side, atoms O1, O5, O3, O4 and N2 of the 5-nitrobarbiturate–water ribbon are cross-linked with atoms N4, N5, N6 and N7 belonging to the thiourea ribbons to yield a slightly puckered layer normal to [1 0 0]. The interlayer distance is about 7.4 Å and the tetraethylammonium cations are located at $x \approx ¼$ and ¾ (Figure 2.4.27).

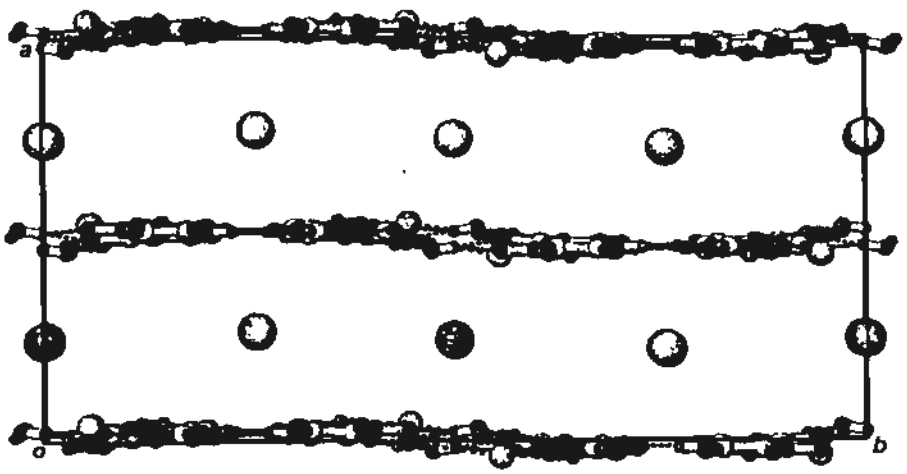

Figure 2.4.27 Packing diagram of complex **2.4.13** projected along the *c* axis with large sphere representing the hydrophobic Et_4N^+ cations positioned at $x = ¼$ and ¾.

Table 2.4.13 Hydrogen bonds for **2.4.13** [Å and deg.].

D-H...A	d(D-H)	d(H...A)	d(D...A)	∠(DHA)
N(3)-H(3N)...O(4)#2	0.89	1.98	2.862(4)	170.0
N(4)-H(4A)...O(1)#3	0.86	2.22	2.978(4)	146.1
N(4)-H(4A)...O(1W)#4	0.86	2.52	3.145(4)	130.0
N(5)-H(5A)...O(1)#3	0.86	2.15	2.921(4)	149.4
N(5)-H(5A)...O(5)#3	0.86	2.25	2.927(3)	136.0
N(5)-H(5B)...S(1)#5	0.86	2.52	3.378(3)	172.6
N(7)-H(7B)...S(2)#4	0.86	2.52	3.376(3)	175.2
O(1W)-H(1WA)...O(2)#1	0.84	2.16	3.002(4)	179.2
O(1W)-H(1WA)...O(1)#1	0.84	2.58	3.178(5)	128.9
N(4)-H(4B)...S(2)	0.86	2.51	3.351(3)	167.7
N(6)-H(6)...N(2)	0.86	2.34	3.113(4)	149.4
N(6)-H(6)...O(4)	0.86	2.42	3.212(4)	153.5
N(6)-H(6B)...S(1)	0.86	2.59	3.391(3)	156.0
N(7)-H(7)...O(3)	0.86	2.32	3.053(4)	143.8
N(7)-H(7)...N(2)	0.86	2.31	3.092(4)	150.7
O(1W)-H(1WB)...O(3)	0.86	2.01	2.875(4)	179.8
O(1W)-H(1WB)...O(2)	0.86	2.58	2.993(4)	110.7

Symmetry transformations used to generate equivalent atoms:
#1 -x+1,-y+1,-z+2 #2 x,-y+1/2,-z+3/2 #3 x,y,z-1 #4 -x+1,-y+1,-z+1
#5 x,-y+1/2,-z+1/2

Crystal structure of $[(n\text{-}C_3H_7)_4N^+] \cdot [(C_4H_2N_3O_5)^-] \cdot (NH_2)_2CS \cdot 2H_2O$ (2.4.14)

No dimer of nitrobarbiturate occurs in complex **2.4.14**. As shown in Figure 2.4.28, two adjacent nitrobarbiturate ions are separated from each other by bridging thiourea C5 (designated by its central carbon atom for convenience in description) and water molecules O1w and O2w to form a nitrobarbiturate–thiourea–$(H_2O)_2$ tetramer motif. Detailed hydrogen-bonding geometries are listed in Table 2.4.14.

Adjacent tetramers are linked by multiple hydrogen bonds to form infinite chains along the [1 1 0] and [1 $\bar{1}$ 0] directions and that are further cross-linked to constitute the three-dimensional channel-type host network shown in Figure 2.4.29. The open-channel system extends parallel to the *c* axis, and well-ordered tetra-*n*-propylammonium cations are accommodated as a double column within each channel.

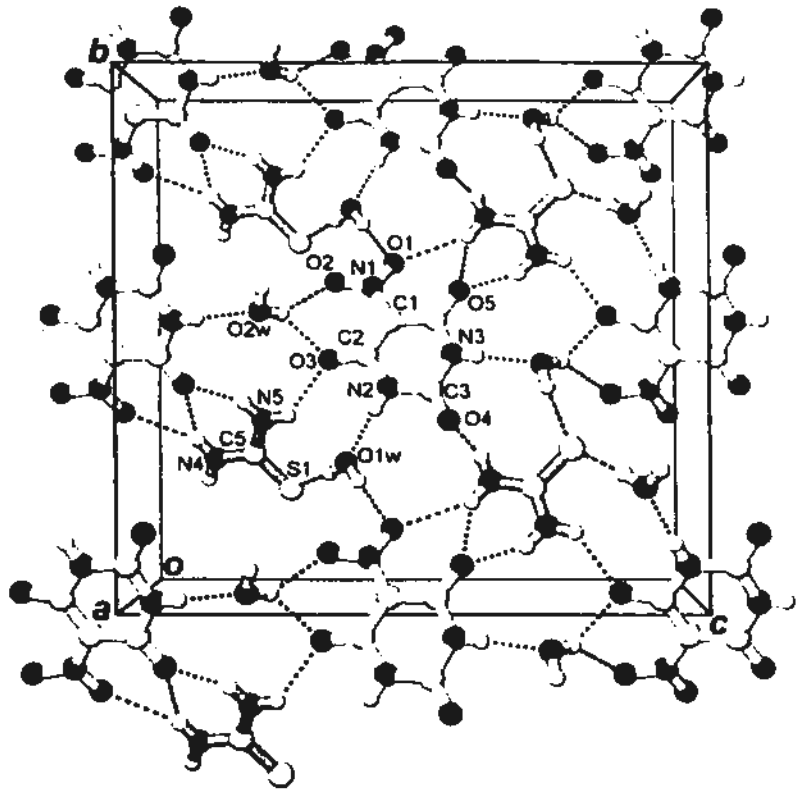

Figure 2.4.28 Perspective view of complex **2.4.14** along the *a* axis, showing the hydrogen-bonding environment of a 5-nitrobarbiturate species.

Table 2.4.14 Hydrogen bonds for **2.4.14** [Å and deg.].

D-H...A	d(D-H)	d(H...A)	d(D...A)	∠(DHA)
N(2)-H(2N)...O(1W)	0.82	1.99	2.807(2)	175.0
N(3)-H(3N)...O(2W)	0.79	2.03	2.813(2)	177.0
N(4)-H(4A)...O(5)#1	0.86	2.08	2.838(2)	147.2
N(4)-H(4A)...O(1)#1	0.86	2.63	3.372(2)	145.4
N(4)-H(4B)...O(4)#2	0.86	1.99	2.800(2)	156.1
N(5)-H(5A)...O(5)#1	0.86	2.00	2.779(2)	150.6
N(5)-H(5B)...O(3)	0.86	2.28	2.942(2)	134.4
O(1W)-H(1WA)...O(1)#3	0.85	2.07	2.917(2)	174.5
O(1W)-H(1WB)...S(1)	0.85	2.41	3.247(2)	165.2
O(2W)-H(2WA)...O(3)#4	0.85	2.19	2.879(2)	137.9
O(2W)-H(2WA)...O(2)#4	0.85	2.35	3.106(3)	148.3
O(2W)-H(2WB)...S(1)#5	0.85	2.59	3.424(2)	166.7

Symmetry transformations used to generate equivalent atoms:
#1 x,-y+1,z-1/2 #2 x-1/2,-y+1/2,z-1/2 #3 x+1/2,y-1/2,z
#4 x,-y+1,z+1/2 #5 x+1/2,-y+1/2,z+1/2

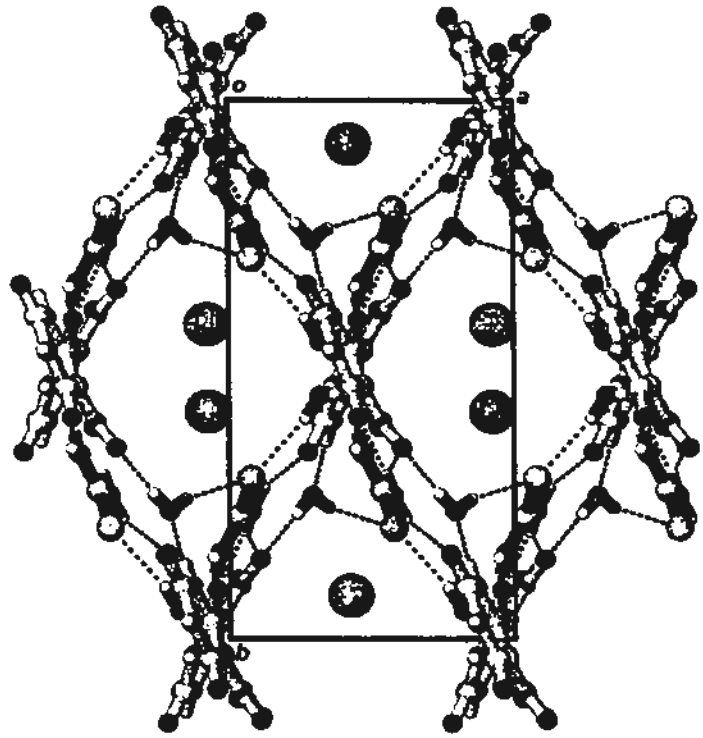

Figure 2.4.29 Projection view of the crystal structure of complex **2.4.14** along the *c* axis.

Crystal structure of $2[(n\text{-}C_4H_9)_4N^+] \cdot 2[(C_4H_2N_3O_5)^-] \cdot (NH_2)_2CS \cdot H_2O$ (2.4.15)

In the host layer of complex **2.4.15**, the two independent 5-nitrobarbiturate ions each forms a cyclic hydrogen-bonded centrosymmetric dimer in the *para*-to-*para* fashion (Figure 2.4.30). The two kinds of dimers are alternately interlinked by hydrogen bonds in the *ortho*-to-*ortho* fashion to form a zigzag ribbon along the [0 1 $\bar{1}$] direction, which is similar to the zigzag chain found in complex **2.4.12**. The torsion angles along the zigzag ribbon (C7–N6···O9c–C7c = 8.7, C2–N2···O8–C6 = –25.9 and C6–N5···O3–C2 = –20.3, C4–N3···O5a–C4a = 17.0 °) indicate that the layer has a slightly twisted configuration. In addition, the ribbons are cross-linked by thiourea S1 and water molecule O1w to form a puckered layer with quatrefoil-like channels parallel to the *a* axis. Detailed hydrogen-bonding geometries are listed in Table 2.4.15.

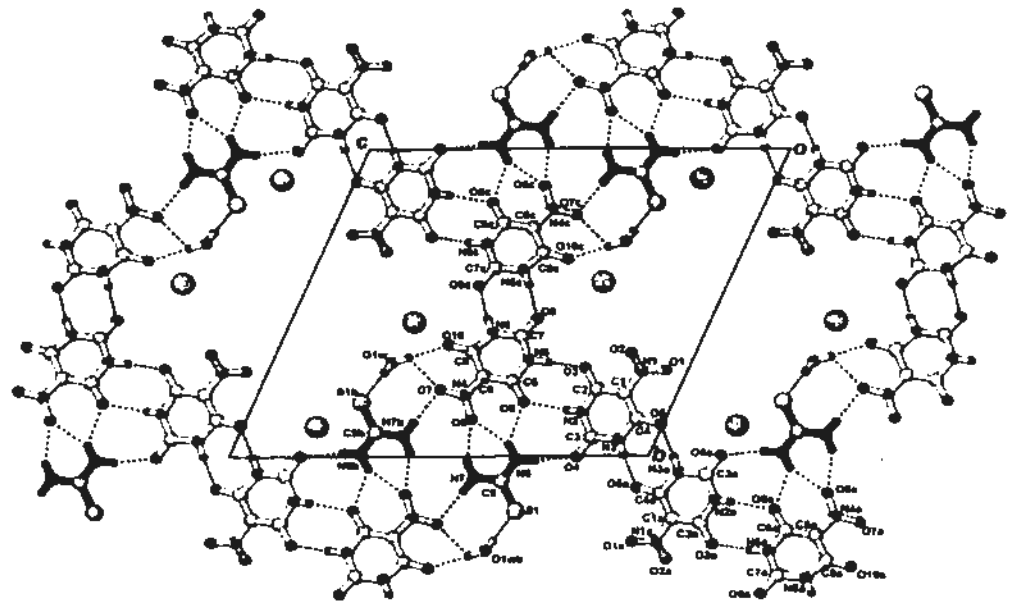

Figure 2.4.30 Projection of the crystal structure of complex **2.4.15** viewed along the *a* axis. *Symmetry transformations*: (a) $2 - x, -y, 2 - z$; (b) $2 - x, -y, 1 - z$; c $1 - x, 1 - y, 1 - z$.

Table 2.4.15 Hydrogen bonds for **2.4.15** [Å and deg.].

D-H...A	d(D-H)	d(H...A)	d(D...A)	∠(DHA)
N(2)-H(2N)...O(8)	0.75	2.15	2.864(4)	168
N(3)-H(3N)...O(5)#1	0.85	2.06	2.862(3)	157
N(5)-H(5N)...O(3)	0.79	2.08	2.856(3)	170
N(6)-H(6N)...O(9)#2	0.73	2.19	2.910(4)	168
N(7)-H(7A)...O(6)	0.86	2.22	2.997(3)	149.7
N(7)-H(7B)...O(7)#3	0.86	2.30	3.100(3)	155.7
N(8)-H(8A)...O(6)	0.86	2.21	2.987(3)	150.1
N(8)-H(8A)...O(8)	0.86	2.28	2.952(3)	135.0
N(8)-H(8B)...O(4)	0.86	2.08	2.928(3)	166.6
O(1W)-H(1WA)...O(10)	0.85	2.05	2.901(4)	177.3
O(1W)-H(1WA)...O(7)	0.85	2.64	3.058(4)	111.6
O(1W)-H(1WB)...S(1)#3	0.83	2.46	3.291(3)	177.5

Symmetry transformations used to generate equivalent atoms:
#1 -x+2,-y,-z+2 #2 -x+1,-y+1,-z+1 #3 -x+2,-y,-z+1

A projection of the crystal structure is illustrated in Figure 2.4.31. The $(n\text{-}C_4H_9)_4N^+$ ions are sandwiched between adjacent 5-nitrobarbiturate–thiourea anionic layers with an interlayer separation 7.5 Å. One alkyl chain of the cation extends into

the central void of a quatrefoil-like channel to stabilize the wavy layer structure (Figure 2.4.31).

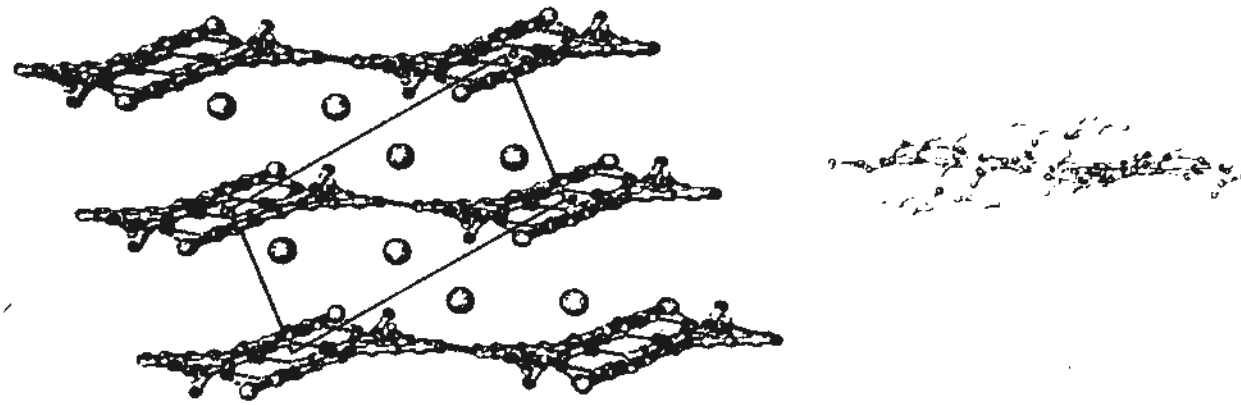

(a) (b)

Figure 2.4.31 (a) Projection of the crystal structure of complex **2.4.15** viewed along the *c* axis showing the layer-type host framework. (b) Terminal methyl group deviating from the main plane points into the center of the void, as viewed along the [$\bar{1}$ 1 0] direction.

In subsequent studies, we used urea to replace thiourea as a building block to construct the nitrobarbiturate–urea inclusion compounds **2.4.16**, **2.4.17** and **2.4.18**, which exhibit three connection modes designated as type **D**, type **E** and type **F** in the respective crystal structures (Scheme 2.4 4).

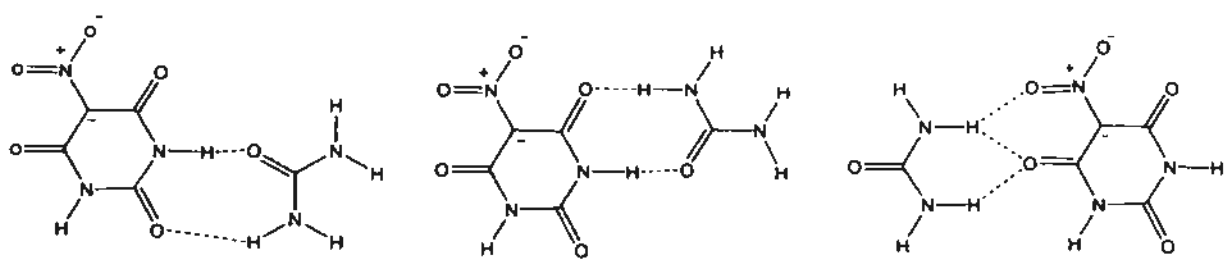

Type **D** Type **E** Type **F**

Scheme 2.4.4 The nitrobarbiturate–urea connection modes found in hydrogen-bonded complexes: Type **D** (*para* shoulder-to-shoulder), Type **E** (*ortho* shoulder-to-shoulder) and Type **F** (head-to-tail).

Crystal structure of $[(C_2H_5)_4N^+] \cdot [(C_4H_2N_3O_5)^-] \cdot 2(NH_2)_2CO \cdot 2H_2O$ (2.4.16)

In this crystal structure, there is no intermolecular interaction between 5-nitrobarbiturate ions. Figure 2.4.32 shows a portion of a hydrogen-bonded layer viewed along the *a* axis.

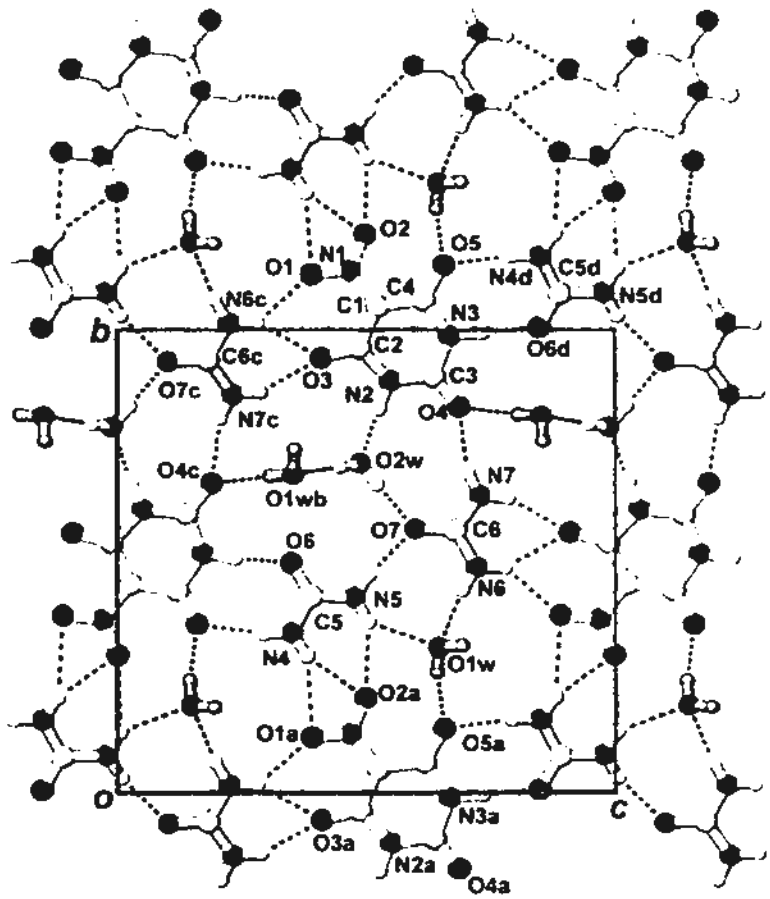

Figure 2.4.32 Projection view of the crystal structure of complex **2.4.16** viewed along the *a* axis. *Symmetry transformations*: (a) $x, -1+y, z$; (b) $2+x, 1+y, 1+z$; (c) $x, 1.5-y, -0.5+z$; (d) $x, 1.5-y, 0.5+z$.

Water molecules play an important role in stabilization of the layer structure. The 5-nitrobarbiturate, urea C6, and O2w molecules are inter-linked by N2–H···O2w, O2w–H···O7 and N7–H···O4 hydrogen bonds to form a trimer. Successive nitrobarbiturate–urea–water trimers are further bridged by urea C5 and water molecule O1w to form a ribbon running parallel to the *b* axis. The ribbons are cross-linked via three distinguishable modes with urea molecules. Urea C6c is connected with 5-nitrobarbiturate in type **F** mode (head-to-tail) by N7c–H···O3, N6c–H···O1 and N6c–H···O3 hydrogen bonds; urea C5d is linked with 5-nitrobarbiturate O1 in a typical ortho shoulder-to-shoulder mode (type **E**) by N4d–H···O5 and N3–H···O6d hydrogen bonds, and urea C5 donates its two *anti*-hydrogen atoms to the nitro group of the nitrobarbiturate ion to form triple hydrogen bonds. Detailed hydrogen-bonding geometries are listed in Table 2.4.16.

In addition, water molecule O1w and its symmetry equivalents are alternatively connected to two layers by O1w–H···O5a, N5–H···O1w, N6–H···O1w (in the same layer) and O1wb–H···O4c, O2w–H···O1wb (in the other layer) hydrogen bonds to generate a double-layer structure (Figure 2.4.33). The thickness of the double layer is about 3.4 Å (distance **I**), and the separation between adjacent double layers is about 6.8 Å (distance **II**). The former distance indicates that π–π interaction exists within a double layer.

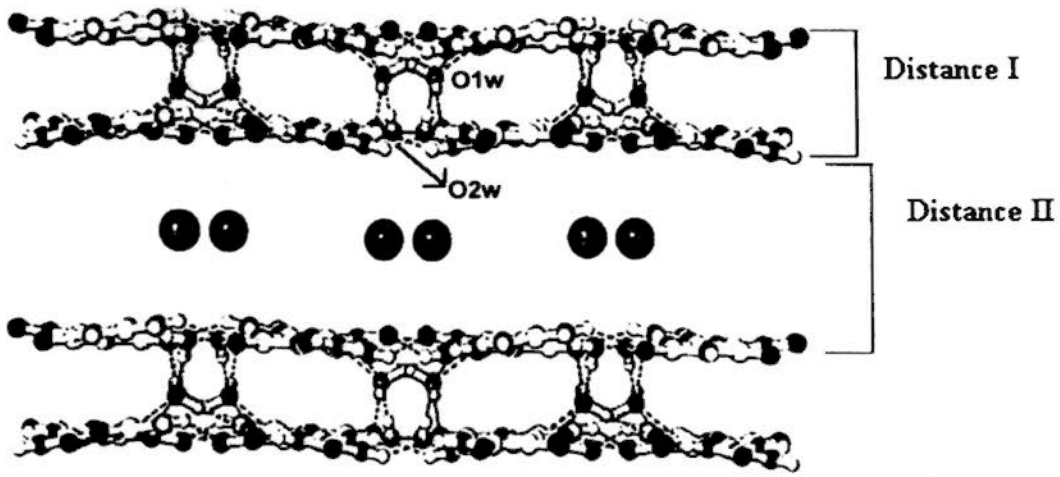

Figure 2.4.33 Perspective view of the crystal structure of complex **2.4.16** viewed along the *b* axis.

Table 2.4.16 Hydrogen bonds for **2.4.16** [Å and deg.].

D-H...A	d(D-H)	d(H...A)	d(D...A)	∠(DHA)
N(2)-H(2N)...O(2W)	0.96	1.83	2.789(3)	177.0
N(3)-H(3N)...O(6)#1	0.99	1.79	2.762(2)	170.0
N(4)-H(4A)...O(5)#2	0.86	2.09	2.938(2)	167.9
N(4)-H(4B)...O(2)#3	0.86	2.40	3.167(3)	148.2
N(4)-H(4B)...O(1)#3	0.86	2.64	3.401(3)	147.5
N(5)-H(5A)...O(7)	0.86	2.09	2.931(3)	166.8
N(5)-H(5B)...O(1W)	0.86	2.47	3.159(3)	138.0
N(5)-H(5B)...O(2)#3	0.86	2.48	3.222(3)	145.5
N(6)-H(6A)...O(1W)	0.86	2.38	3.156(3)	150.5
N(6)-H(6B)...O(1)#1	0.86	2.26	2.965(2)	139.1
N(6)-H(6B)...O(3)#1	0.86	2.29	3.060(2)	149.0
N(7)-H(7A)...O(4)	0.86	2.20	2.965(3)	148.1
N(7)-H(7B)...O(3)#1	0.86	2.17	2.967(2)	154.5
O(1W)-H(1WA)...O(4)#4	0.79	2.17	2.961(2)	170.5
O(1W)-H(1WB)...O(5)#3	0.88	1.95	2.822(2)	170.3
O(1W)-H(1WB)...O(2)#3	0.86	2.53	3.060(2)	119.8
O(2W)-H(2WA)...O(1W)#5	0.86	2.05	2.907(3)	179.7
O(2W)-H(2WB)...O(7)	0.87	1.86	2.732(2)	179.2

Symmetry transformations used to generate equivalent atoms:
#1 x,-y+3/2,z+1/2 #2 x,-y+3/2,z-1/2 #3 x,y-1,z #4 -x+2,y-1/2,-z+3/2
#5 -x+2,-y+1,-z+1

It is notable that in this structure the two independent water molecules play different roles. O2w is responsible for connecting adjacent molecules, which lie

almost in the same plane, while O1w is responsible for bridging two adjacent layers to generate the double-layer inclusion complex.

Crystal structure of $[(n\text{-}C_3H_7)_4N^+] \cdot [(C_4H_2N_3O_5)^-] \cdot 2(NH_2)_2CO$ (2.4.17)

Complex **2.4.17** exhibits a three-dimensional structure with channels extending parallel to the [1 0 0], [1 0 1] and [0 1 1] directions. Figure 2.4.34 shows the structure viewed along the [1 0 0] direction. The channel framework is built of symmetry-related ribbons which run parallel to the [0 1 1] and [0 $\bar{1}$ 1] directions, respectively.

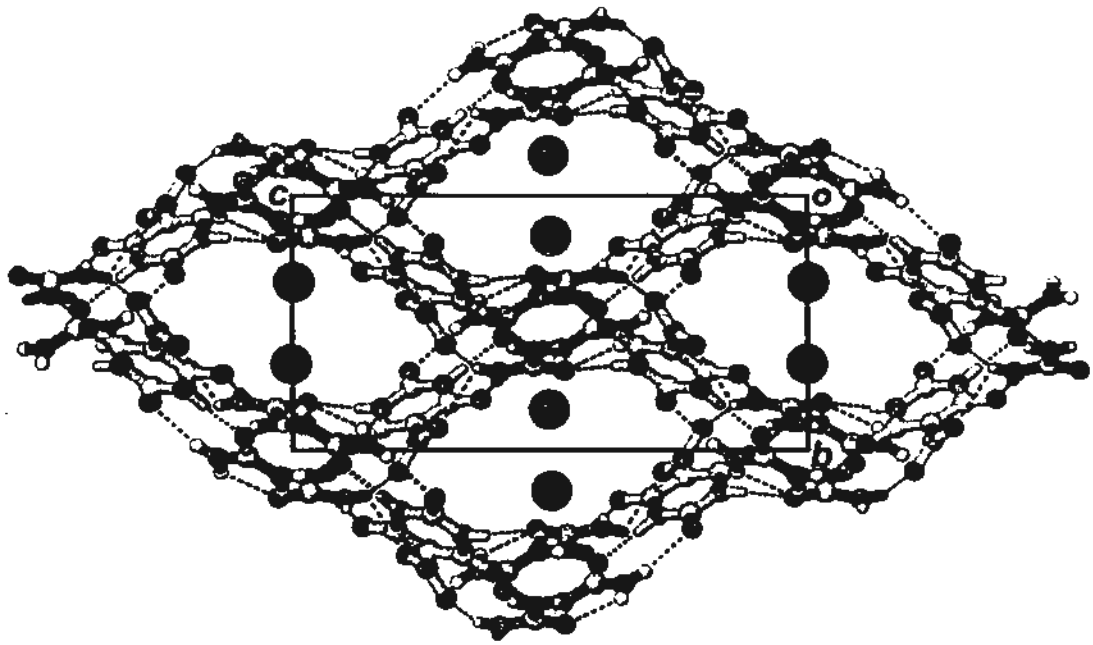

Figure 2.4.34 Projection view of the crystal structure of complex **2.4.17** viewed along the *a* axis.

The ribbon is built of a tetramer and a dimer of urea. Centrosymmetric pairs of nitrobarbiturates and urea molecules are connected to form a tetramer by N6a–H···O3d, N6a–H···O2d, N7a–H···O2d, N6a–H···O3 and N2–H···O7 hydrogen bonds (Figure 2.4.35) involving type **E** and **F** connection modes (Scheme 2.4.4). Detailed hydrogen-bonding geometries are listed in Table 2.4.17.

These tetramers are further connected by dimeric urea units in type **D** fashion (*para* shoulder-to-shoulder) through N3–H···O6 and N4–H···O4 hydrogen bonds to generate ribbons along the [0 1 1] or [0 $\bar{1}$ 1] direction. These equivalent ribbons are alternately linked together by N5c–H···O7b and N4c–H···O7b hydrogen bonds (in head-to-tail fashion) and N7b–H···O5c to generate a three-dimensional channel system. The dihedral angle between adjacent planar ribbons which run along the [0 1 1] or [0 $\bar{1}$ 1] direction is about 78°. Well-ordered tetra-*n*-propylammonium cations are accommodated as a double column within each channel, as illustrated in Figure 2.4.34.

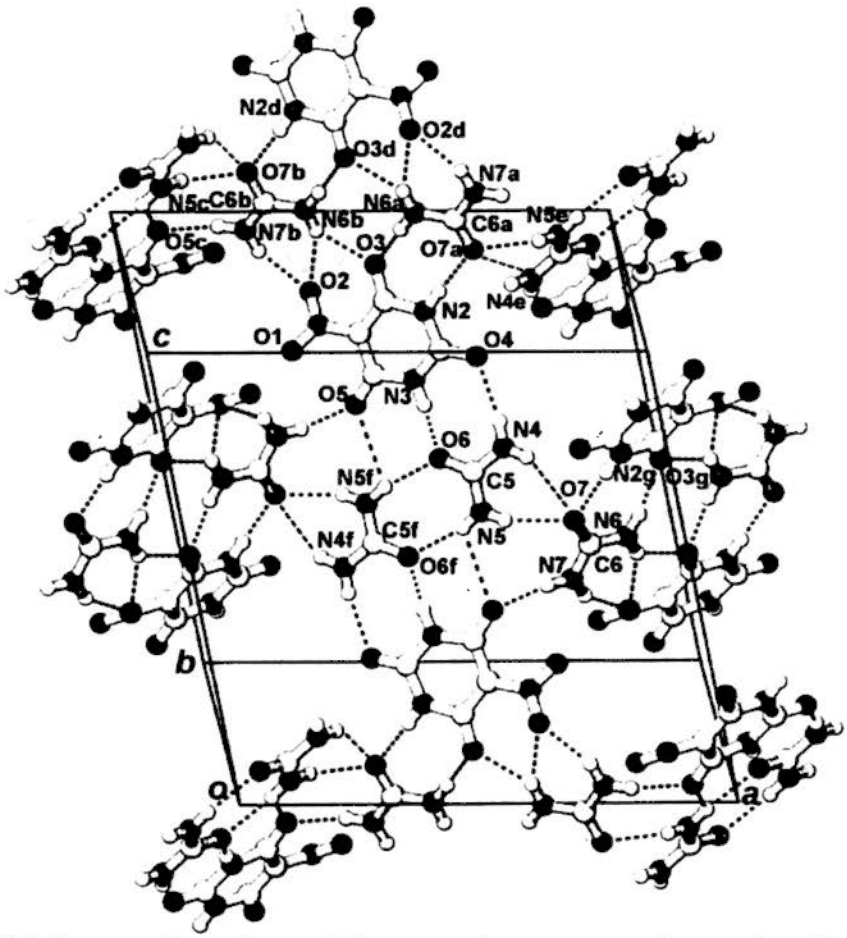

Figure 2.4.35 Perspective view of the crystal structure of complex **2.4.17** viewed almost along [0 1 $\bar{1}$] direction. *Symmetry transformations*: (a) 1.5 – *x*, 0.5 + *y*, 1.5 – *z*; (b) –0.5 + *x*, 1.5 – *y*, 1 + *z*; (c) 0.5 – *x*, 0.5 + *y*, 1.5 – *z*; (d) 1 – *x*, 2 – *y*,

2 – *z*; (e) 1.5 – *x*, 0.5 + *y*, 1.5 – *z*; (f) 1 – *x*, 1 – *y*, 1 – *z*; (g) 1.5 – *x*, –0.5 + *y*, 1.5 – *z*.

Table 2.4.17 Hydrogen bonds for **2.4.17** [Å and deg.].

D-H...A	d(D-H)	d(H...A)	d(D...A)	∠(DHA)
N(2)-H(2N)...O(7)#1	0.87(2)	2.00	2.865(2)	175.2
N(3)-H(3N)...O(6)	0.91(2)	1.83	2.740(2)	174.0
N(4)-H(4A)...O(4)	0.86	2.30	3.139(2)	166.3
N(4)-H(4B)...O(7)	0.86	2.63	3.324(2)	139.0
N(5)-H(5A)...O(6)#2	0.86	2.17	3.011(3)	166.4
N(5)-H(5B)...O(7)	0.86	2.22	3.009(2)	152.5
N(6)-H(6AA)...O(3)#3	0.86	1.98	2.827(2)	169.8
N(6)-H(6BA)...O(3)#4	0.86	2.23	2.927(2)	137.6
N(6)-H(6BA)...O(2)#4	0.86	2.31	3.078(2)	148.5
N(7)-H(7A)...O(5)#2	0.86	2.08	2.924(2)	168.2

Symmetry transformations used to generate equivalent atoms:
#1 -x+3/2,y+1/2,-z+3/2 #2 -x+1,-y+1,-z+1 #3 -x+3/2,y-1/2,-z+3/2
#4 x+1/2,-y+3/2,z-1/2

Crystal structure of $[(n\text{-}C_4H_9)_4N^+] \cdot [(C_4H_2N_3O_5)^-] \cdot (NH_2)_2CO \cdot 2H_2O$ (2.4.18)

As shown in Figure 2.4.36, the 5-nitrobarbiturate ions are directly linked to independent water molecules O1w and O2w by donor N3–H···O1w and acceptor O2w–H···O5 hydrogen bonds, respectively. Detailed hydrogen-bonding geometries are listed in Table 2.4.18.

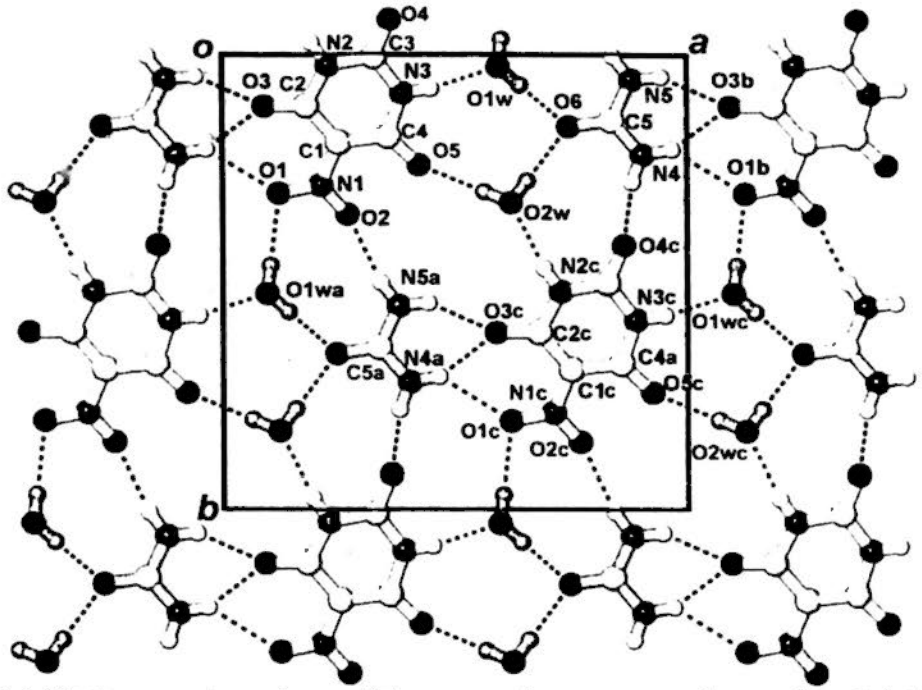

Figure 2.4.36 Perspective view of the crystal structure of complex **2.4.18** viewed along the *c* axis. *Symmetry transformations*: (a) $-0.5 + x$, $0.5 + y$, z; (b) $1 + x$, y, z; (c) $0.5 + x$, $0.5 + y$, z.

In addition, each water molecule donates one hydrogen atom to an adjacent urea molecule C5 in forming two fairly strong hydrogen bonds: O1w–H···O6 = 2.787(3) and O2w–H···O6 = 2.982(3) Å. The resulting nitrobarbiturate–$(H_2O)_2$–urea tetramers are aligned parallel to the *a* axis, and head-to-tail linkage between the nitrobarbiturate and urea moieties (type **F**) yields an infinite chain running in the *a* direction.

The equivalent chains are cross-linked to generate a layer normal to the *c* axis. The well-ordered tetra-*n*-butylammonium cations are alternately arranged and sandwiched between adjacent layers at z = ¼ and ¾, as shown in Figure 2.4.37.

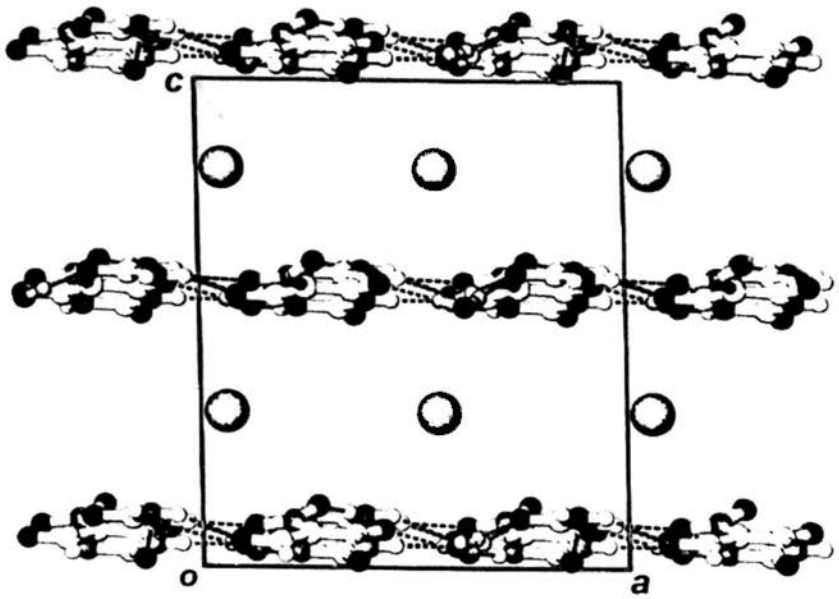

Figure 2.4.37 Perspective view of the crystal structure of complex **2.4.18** viewed along the *b* axis.

Table 2.4.18 Hydrogen bonds for **2.4.18** [Å and deg.].

D-H...A	d(D-H)	d(H...A)	d(D...A)	∠(DHA)
N(2)-H(2N)...O(2W)#1	0.85	2.12	2.952(3)	168(3)
N(3)-H(3N)...O(1W)	0.84	2.02	2.854(3)	170(2)
N(4)-H(4A)...O(4)#2	0.86	2.20	2.977(3)	150.1
N(4)-H(4B)...O(3)#3	0.86	2.17	2.940(3)	149.7
N(4)-H(4B)...O(1)#3	0.86	2.43	3.120(3)	137.2
N(5)-H(5A)...O(2)#4	0.86	2.24	3.093(3)	169.6
N(5)-H(5B)...O(3)#3	0.86	2.28	3.031(3)	145.3
O(1W)-H(1WA)...O(6)	0.97	1.82	2.787(3)	169.6
O(1W)-H(1WB)...O(1)#4	0.78	2.28	3.028(3)	161.9
O(2W)-H(2WA)...O(5)	0.73	2.25	2.970(3)	171.8
O(2W)-H(2WB)...O(6)	0.94	2.05	2.982(3)	169.1

Symmetry transformations used to generate equivalent atoms:
#1 x-1/2,y-1/2,z #2 x+1/2,y+1/2,z #3 x+1,y,z #4 x+1/2,y-1/2,z

2.4.3 Inclusion compounds containing anions of imidazole-4,5-dicarboxylic acid

Crystal structure of $3[(C_2H_5)_4N^+] \cdot (H^+)[C_3HN_2^-(CO_2^-)(CO_2H)]_2 \cdot 8H_2O$ (2.4.19)

In the crystal structure of **2.4.19**, there are two independent tetraethylammonium ions, a 1*H*-imidazole-4,5-carboxylate (H_2imdc^{2-}) dimer bridged by a proton at an inversion sites and four independent water molecules. In each 1*H*-imidazole-4,5-carboxylate dianion, intramolecular hydrogen bonding occurs between O2 and O3 atoms by sharing common hydrogen atom H1. Two centrosymmetrically-related 1*H*-imidazole-4,5-carboxylates (H_2imdc^2) are joined together by a pair of weak hydrogen bonds (C3–H···O1a and C3a–H···O1) bridging proton H2N to form a dimer (Figure 2.4.38).

Adjacent $[H(H_2Imdc)_2]^{3-}$ dimers related by a two-fold axis are bridged by a pair of type O2w molecules to give a zigzag ribbon aligned in the [4 0 4] direction. The remaining three water molecules O1w, O3w and O4w are arranged around a center of symmetry to form a hydrogen-bonded hexagonal cluster. Linkage between the zigzag ribbons and water clusters by hydrogen bonds of the type O4w–H···O3, O1wb–H···O1d and O3w–H···O2w generates a corrugated layer normal to the *b* axis. Detailed hydrogen-bonding geometries are listed in Table 2.4.19. In the crystal lattice of **2.4.19**, well-ordered tetraethylammonium cations N3 (designated by their central nitrogen atoms for convenience in description) located at a special position of symmetry 2 and the other tetraethylammonium cation N4 located at a general position are sandwiched between the wavy layers with an interlayer spacing of $b/2$ = 7.27 Å (Figure 2.4.39).

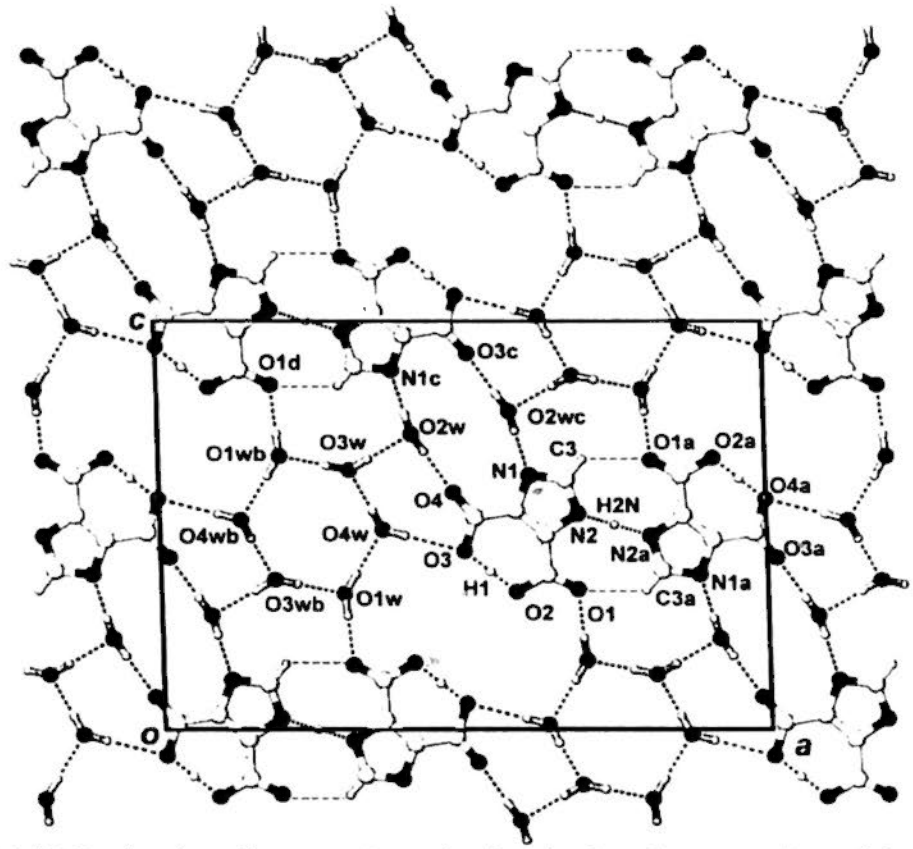

Figure 2.4.38 Projection diagram along the *b* axis showing a portion of the layer at *y* = ¼ in the crystal structure of **2.4.19**. *Symmetry transformations*: (a) 1.5 – *x*, 0.5 – *y*, 1 – *z*; (b) 0.5 – *x*, 0.5 – *y*, 1 – *z*; (c) 1 – *x*, *y*, 1.5 – *z*; (d) –0.5 + *x*, 0.5 – *y*, 0.5 – *z*.

Table 2.4.19 Hydrogen bonds for **2.4.19** [Å and deg.].

D-H...A	d(D-H)	d(H...A)	d(D...A)	∠(DHA)
O(2)-H(1)...O(3)	0.98	1.44	2.419(3)	176
O(1W)-H(1WA)...O(4W)	0.85	1.90	2.758(3)	179.9
O(1W)-H(1WB)...O(1)#2	0.86	1.89	2.764(3)	178.5
O(2W)-H(2WA)...N(1)#3	0.85	1.96	2.823(3)	179.1
O(2W)-H(2WB)...O(4)	0.85	2.00	2.863(3)	179.0
O(3W)-H(3WA)...O(2W)	0.84	1.95	2.798(4)	179.2
O(3W)-H(3WB)...O(1W)#4	0.89	1.84	2.743(4)	178.8
O(4W)-H(4WB)...O(3W)	0.84	1.88	2.725(4)	178.1
O(4W)-H(4WA)...O(3)	0.85	2.28	3.134(3)	179.2
O(4W)-H(4WA)...O(4)	0.85	2.46	3.031(3)	124.4
C(3)-H(3)...O(1)#5	0.93	2.51	3.157(3)	126.4

Symmetry transformations used to generate equivalent atoms:
#1 -x+2,y,-z+3/2 #2 -x+1,y,-z+1/2 #3 -x+1,y,-z+3/2 #4 -x+1/2,-y+1/2,-z+1
#5 -x+3/2,-y+1/2,-z+1

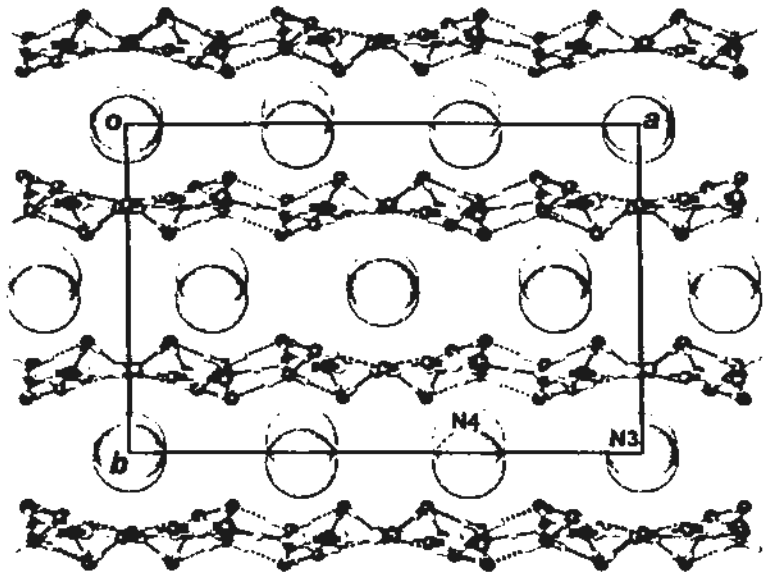

Figure 2.4.39 Layer structure of **2.4.19** viewed along the *c* axis, with large spheres representing the ordered Et_4N^+ cations that are accommodated between layers.

Crystal structure of $2[(C_2H_5)_4N^+]\cdot[C_3HN_2^-(CO_2^-)(CO_2H)]\cdot 2[(NH_2)_2CS]$ (2.4.20)

The 1*H*-imidazole-4,5-carboxylate ion contains an intramolecular hydrogen bond between its carboxylate groups. Independent thiourea molecules C6d and C7 are connected to each other in the shoulder-to-shoulder fashion to form a dimer. Each thiourea moiety attached to an imino N atom of one 1*H*-imidazole-4,5-dicarboxylate and to a carboxylate group of another by pairwise hydrogen bonds to form a tetramer. Cross-linkage between tetramers related by the *b* glide generates motif [**A**]. In addition, further linkage of dimers related by the *a* translation, generates motif [**B**] = $R_4^4(14)$ (Figure 2.4.40). Detailed hydrogen-bonding geometries are listed in Table 2.4.20.

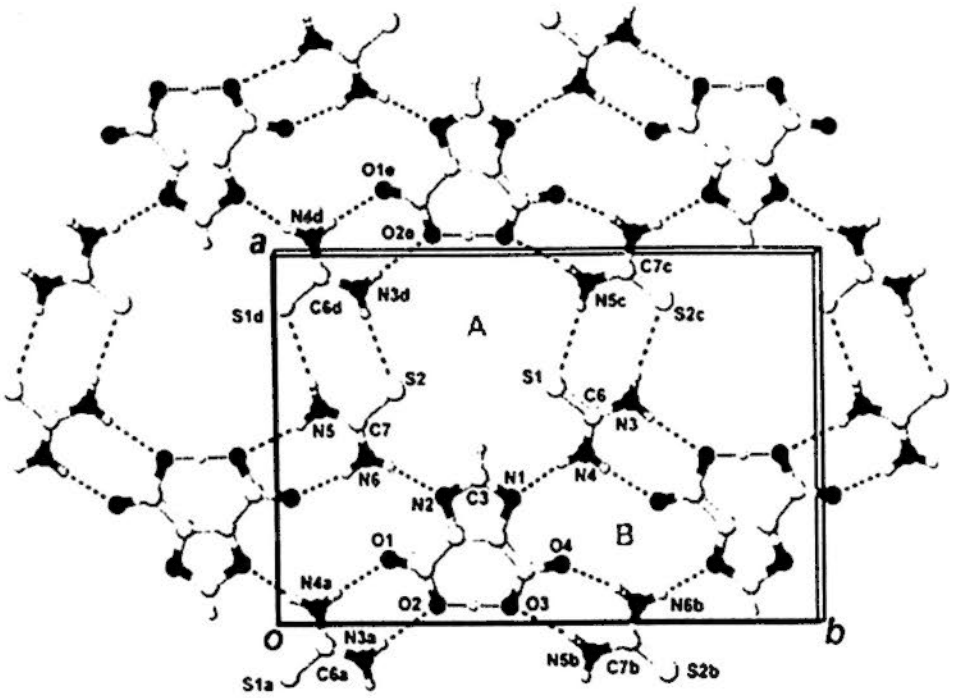

Figure 2.4.40 Projection diagram along the *c* axis showing a portion of the layers at $y = ¾$ in the crystal structure of **2.4.20**. *Symmetry transformations*: (a) $0.5 - x, -0.5 + y, 1.5 - z$; (b) $0.5 - x, 0.5 + y, 1.5 - z$; (c) $1.5 - x, 0.5 + y, 1.5 - z$; (d) $1.5 - x, -0.5 + y, 1.5 - z$; (e) $1.0 + x, y, z$.

Table 2.4.20 Hydrogen bonds for **2.4.20** [Å and deg.].

D-H...A	d(D-H)	d(H...A)	d(D...A)	∠(DHA)
O(2)-H(1)...O(3)	1.21	1.22	2.430(3)	180.0
N(3)-H(3A)...O(2)#1	0.88	2.21	3.033(3)	155.3
N(3)-H(3B)...S(2)#2	0.88	2.57	3.415(2)	162.3
N(4)-H(4A)...O(1)#1	0.88	2.04	2.875(3)	158.4
N(4)-H(4B)...N(1)	0.88	2.05	2.888(3)	159.6
N(5)-H(5A)...O(3)#3	0.88	2.36	3.214(3)	163.7
N(5)-H(5A)...O(4)#3	0.88	2.48	3.215(3)	141.0
N(5)-H(5B)...S(1)#4	0.88	2.62	3.441(2)	155.6
N(6)-H(6A)...O(4)#3	0.88	2.03	2.873(3)	161.0
N(6)-H(6B)...N(2)	0.88	2.00	2.863(3)	164.8

Symmetry transformations used to generate equivalent atoms:
#1 -x+1/2,y+1/2,-z+3/2 #2 -x+3/2,y+1/2,-z+3/2 #3 -x+1/2,y-1/2,-z+3/2 #4 -x+3/2,y-1/2,-z+3/2

In the packing diagram (Figure 2.4.41), well-ordered tetraethylammonium cations located at z = ½ and 1 are sandwiched between almost planar layers with an interlayer spacing of $c/2$ = 7.57 Å.

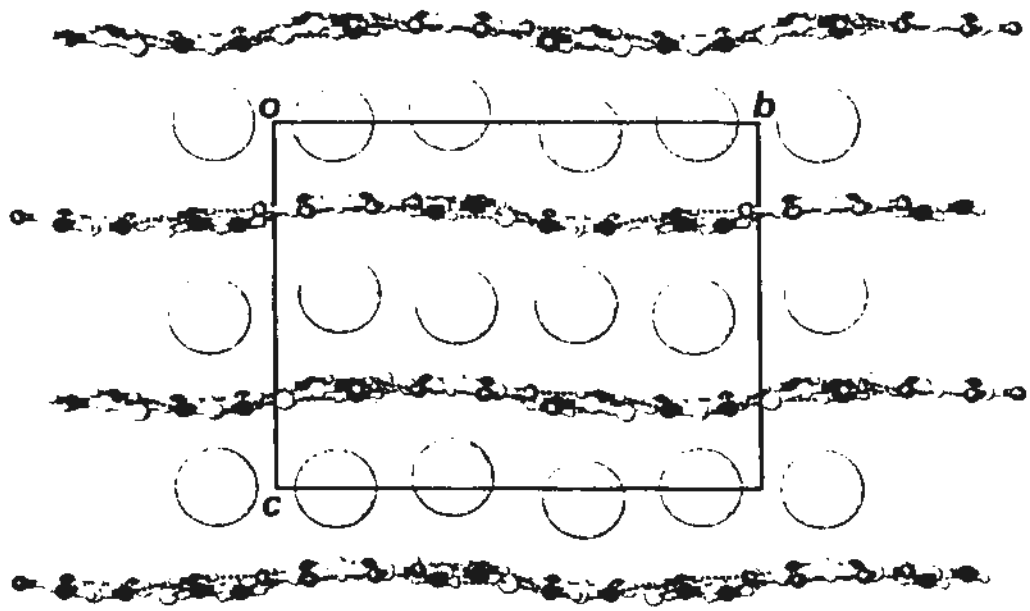

Figure 2.4.41 Packing diagram of **2.4.20** projected along the *a* axis, with large sphere representing the well-ordered hydrophobic Et_4N^+ cations positioned regularly between adjacent layers with an interlayer spacing of $c/2$ = 7.57 Å.

Crystal structure of $[(n\text{-}C_4H_9)_4N^+] \cdot [C_3HN_2H(CO_2^-)(CO_2H)] \cdot [(NH_2)_2CS]\cdot 2H_2O$ (2.4.21)

In the crystal structure of **2.4.21**, distinctive bond lengths between C5–O3 and C5–O4 of 1*H*-imidazole-4,5-dicarboxylate shows that the carboxyl H atom is attached to the O3 atom. 1*H*-imidazole-4,5-dicarboxylate is cross-linked with adjacent thioureas to form a zigzag $(H_3imdc\text{–thiourea})_\infty$ ribbon along the *c* axis in two ways. Thiourea C6 is connected with the imino group and carboxyl group by N3–H···N1 and N4–H···O4 hydrogen bonds to form motif [**A**] = $R_2^2(9)$, whereas

motif [**B**] = $R_2^2(9)$ is generated by hydrogen bonding interaction in a shoulder-to-shoulder fashion between 1*H*-imidazole-4,5-dicarboxylate and thiourea C6a (Figure 2.4.42). Furthermore, these ribbons lie side by side and are cross-linked by a pair of water molecules, which bridge two adjacent 1*H*-imidazole-4,5-dicarboxylates (motif [**C**] = $R_5^5(14)$) and thiourea molecules C6b to create a planar layer by forming motif [**D**] = $R_7^5(16)$. Detailed hydrogen-bonding geometries are listed in Table 2.4.21.

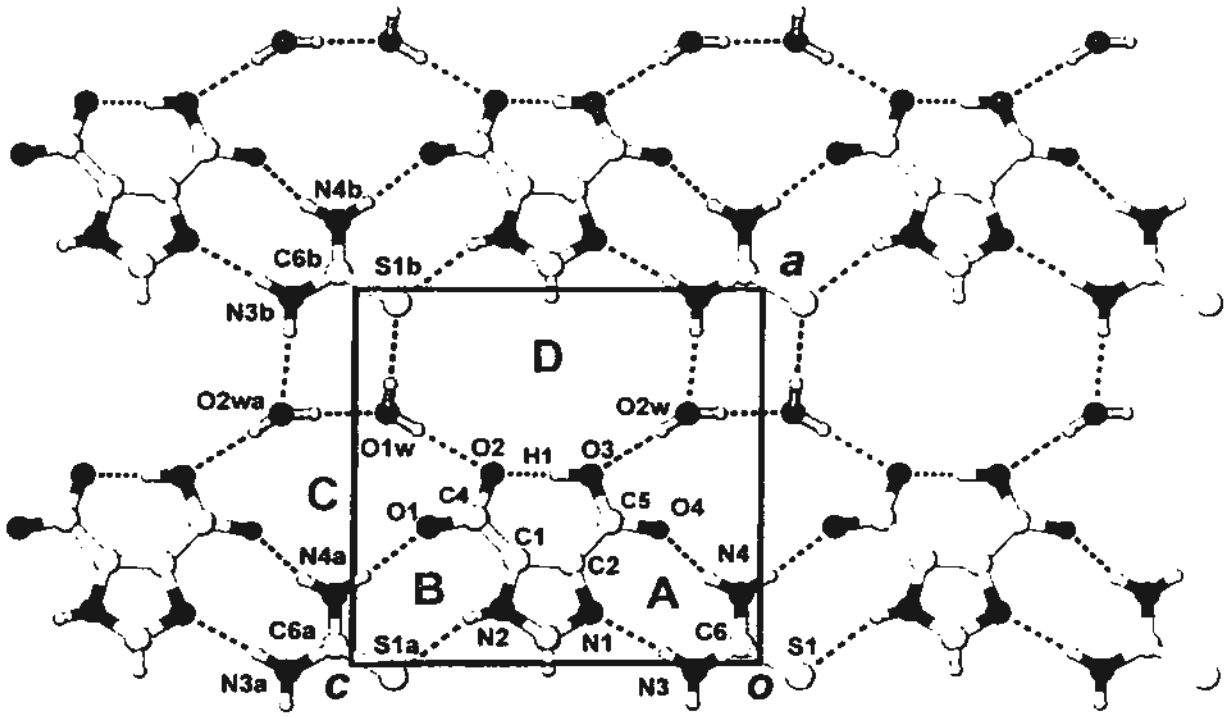

Figure 2.4.42 Projection diagram viewed along the *b* axis showing the layer structure in the crystal of **2.4.21**. *Symmetry transformations*: (a) *x*, *y*, 1 + *z*; (b) 1 + *x*, *y*, 1 + *z*.

Table 2.4.21 Hydrogen bonds for **2.4.21** [Å and deg.].

D-H...A	d(D-H)	d(H...A)	d(D...A)	∠(DHA)
O(3)-H(1)...O(2)	0.85	1.60	2.448(4)	180.0
N(4)-H(2C)...O(4)	0.86	2.05	2.868(4)	157.7
N(4)-H(2D)...O(1)#1	0.86	2.04	2.875(4)	164.3
N(3)-H(3C)...N(1)	0.86	2.15	3.007(4)	174.8
N(3)-H(3D)...O(2W)#2	0.86	2.13	2.969(4)	166.1
N(2)-H(2N)...S(1)#3	0.84	2.46	3.249(4)	157
O(1W)-H(1WA)...S(1)#4	0.86	2.41	3.276(4)	178.7
O(1W)-H(1WB)...O(2)	0.86	2.14	3.002(5)	178.7
O(1W)-H(1WB)...O(1)	0.86	2.57	3.136(4)	123.7
O(2W)-H(2WB)...O(3)	0.86	2.36	3.217(4)	178.7
O(2W)-H(2WA)...O(1W)#1	0.86	1.93	2.788(7)	179.2

Symmetry transformations used to generate equivalent atoms:
#1 x,y,z-1 #2 x-1,y,z #3 x,y,z+1 #4 x+1,y,z+1

Large hydrophobic n-Bu_4N^+ cations are positioned regularly between adjacent layers with an interlayer spacing of $b/2$ = 8.00 Å (Figure 2.4.43).

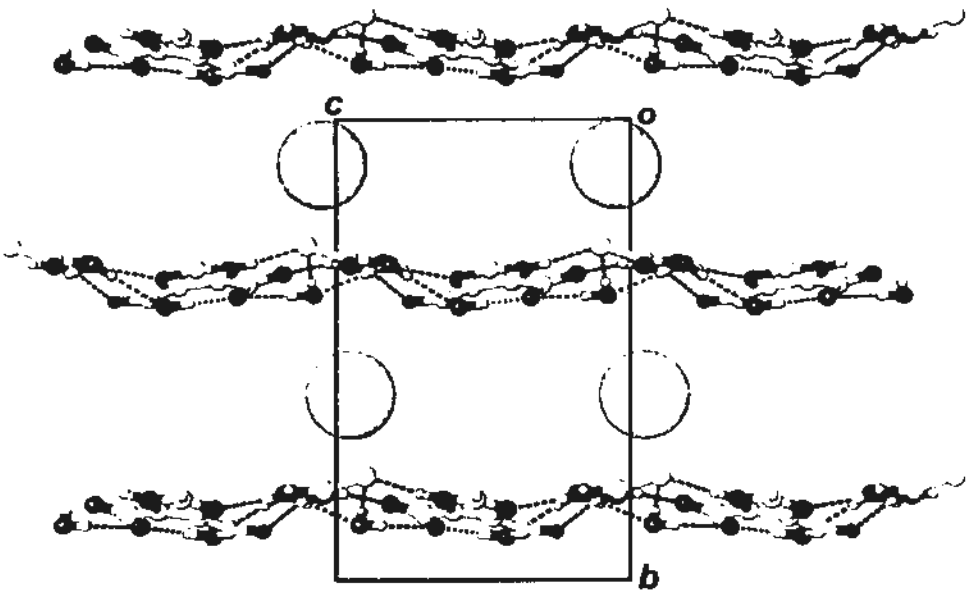

Figure 2.4.43 Packing diagram of **2.4.21** projected along the a axis, with large sphere representing the well-ordered hydrophobic n-Bu_4N^+ cations positioned regularly between adjacent layers with an interlayer spacing of $b/2$ = 8.00 Å.

Crystal structure of $[(n\text{-}C_3H_7)_4N^+]\cdot[C_3HN_2^-(CO_2^-)(CO_2H)]\cdot[C(NH_2)_3^+]\cdot H_2O$ (2.4.22)

Similar to complex **2.4.20**, in **2.4.22** both imino nitrogen atoms of the 1*H*-imidazole-4,5-dicarboxylate molecule are fully deprotonated and behave as hydrogen-bond acceptors, and two carboxylate groups form intramolecular hydrogen bond through a common hydrogen atom H2. The guanidinium cation is connected with deprotonated imino and carboxyl groups to form a $(H_2imdc\text{–}GM)_\infty$ ribbon along the *a* axis (Figure 2.4.44).

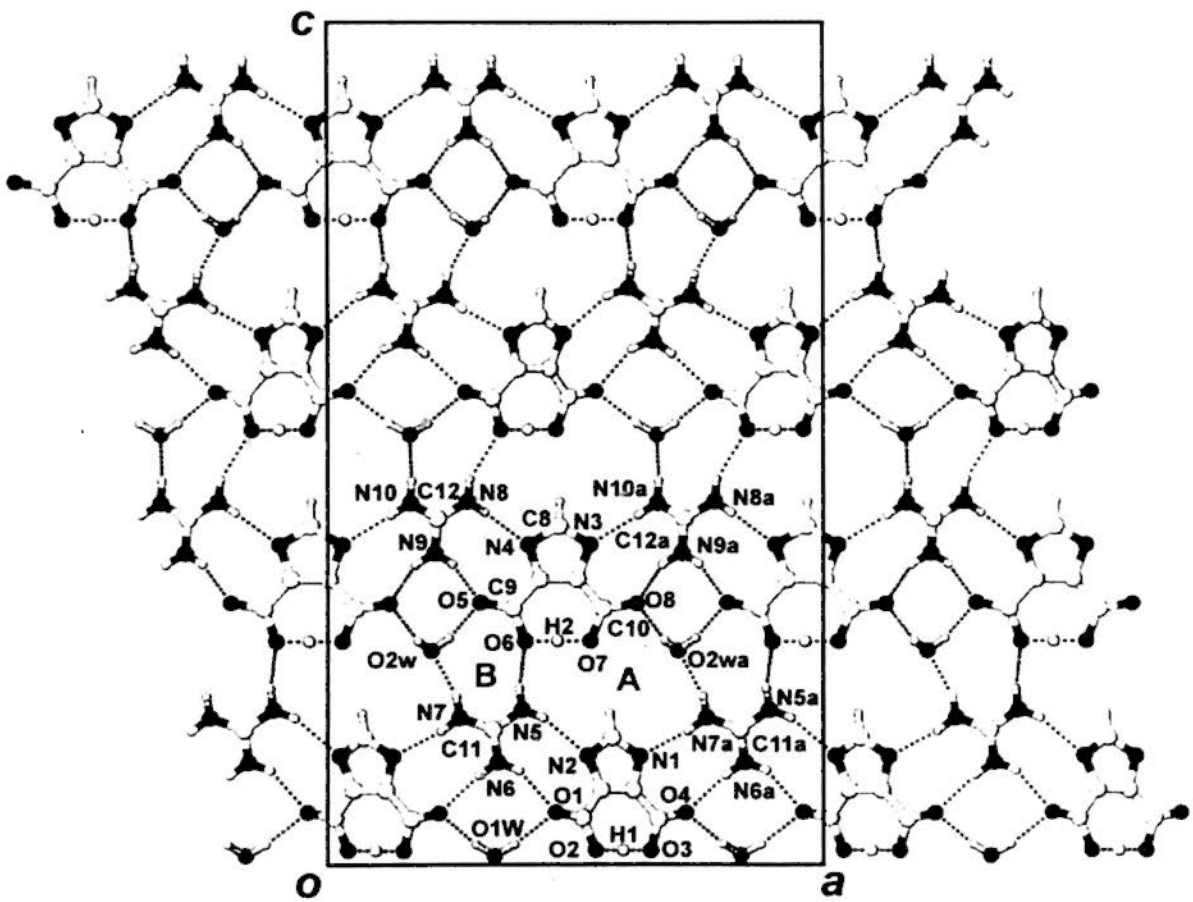

Figure 2.4.44 Projection diagram along the *b* axis showing a portion of the layers at $y = 1/2$ in **2.4.22**. *Symmetry transformations*: (a) $0.5 + x$, $1.0 - y$, z.

A water molecule bridging two carboxyl groups of imidazole-4,5-carboxylate reinforces the hydrogen bonded ribbon. These parallel ribbons are further cross-linked to generate a wide wavy layer through N5–H···O6, N7–H···O2w and N7a–H···O2wa hydrogen bonds by forming motif **[A]** and **[B]**. Detailed hydrogen-bonding geometries are listed in Table 2.4.22.

The wavy layer structure is shown in Figure 2.4.45, and the well-ordered hydrophobic $(n\text{-}Pr_4)N^+$ cations are positioned regularly between adjacent layers with an interlayer spacing of b = 8.22 Å.

Table 2.4.22 Hydrogen bonds for **2.4.22** [Å and deg.].

D-H...A	d(D-H)	d(H...A)	d(D...A)	∠(DHA)
O(2)-H(1)...O(3)	0.86	1.58	2.435(3)	175.1
O(6)-H(2)...O(7)	0.86	1.57	2.418(3)	168.8
N(5)-H(5A)...N(2)	0.86	2.15	2.956(4)	155.1
N(5)-H(5B)...O(6)	0.86	2.27	3.086(4)	159.2
N(6)-H(6A)...O(1)	0.86	2.11	2.899(4)	152.0
N(6)-H(6B)...O(4)#1	0.86	2.04	2.879(4)	166.6
N(7)-H(7A)...O(2W)	0.86	1.96	2.785(4)	159.3
N(7)-H(7B)...N(1)#1	0.86	2.00	2.849(4)	167.2
N(8)-H(8A)...O(3)#2	0.86	2.16	2.947(4)	152.3
N(8)-H(8B)...N(4)	0.86	2.11	2.963(4)	169.3
N(9)-H(9B)...O(8)#1	0.86	2.09	2.869(4)	150.7
N(9)-H(9A)...O(5)	0.86	1.95	2.776(4)	160.0
N(10)-H(10B)...N(3)#1	0.86	2.10	2.931(4)	162.8
N(10)-H(10A)...O(1W)#3	0.86	2.07	2.890(4)	158.9
O(1W)-H(1WA)...O(1)	0.85	2.01	2.846(3)	168.4
O(1W)-H(1WB)...O(4)#1	0.85	1.93	2.771(3)	172.1
O(2W)-H(2WA)...O(5)	0.85	1.86	2.692(4)	167.5
O(2W)-H(2WB)...O(8)#1	0.85	2.07	2.892(4)	161.1

Symmetry transformations used to generate equivalent atoms:
#1 x-1/2,-y+1,z #2 -x+1,-y+1,z+1/2 #3 -x+1/2,y,z+1/2

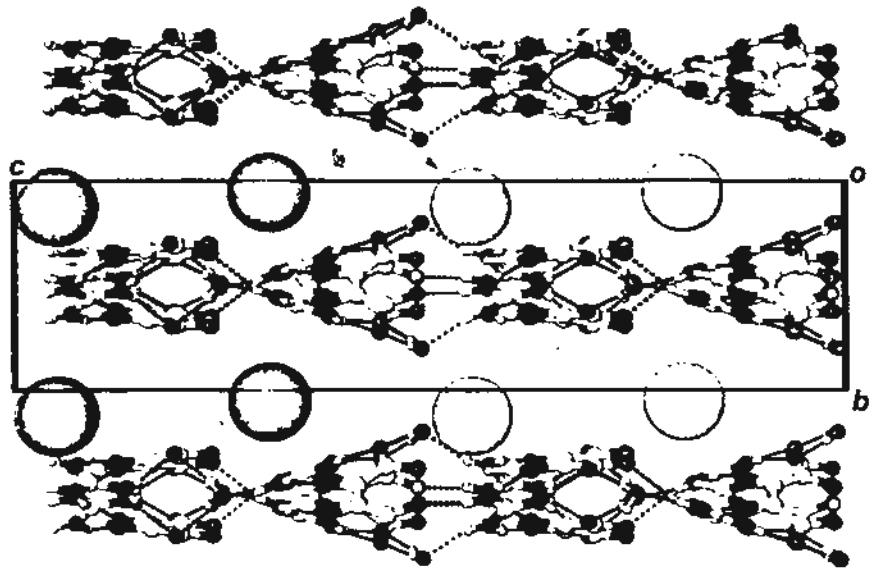

Figure 2.4.45 Packing diagram of **2.4.22** projected along the *a* axis, with large sphere representing the well-ordered hydrophobic $(n\text{-}Pr_4)N^+$ cations positioned regularly between adjacent layers with an interlayer spacing of b = 8.22 Å.

Chapter 3. Summary and Discussion

3.1 Strategies in designing new supramolecular rosette motifs

In Chapter 2.1, we aimed at designing self-assembled rosette motifs from various molecular components with different hydrogen-bonding capabilities.

Historically, molecules possessing C_3 symmetry are usually selected as major components in building classical hydrogen-bonded rosette motifs in the solid state. Matching of equal numbers of hydrogen-bond donor and acceptor sites leads to the formation of hexagonal ring modules exhibiting the rosette motif. This design principle can be applied and extended in the construction of even more complex rosette motifs by relaxing the requirement of exact C_3 symmetry and/or the addition of extra components.

The guanidinium ion (GM) is a hydrogen-bond donor and the carbonate anion is a hydrogen-bond acceptor, both possessing *D3h* symmetry. The sheet structure of orthoboric acid is the archetypal example of a single-component hydrogen-bonded rosette layer,[153] in which the C_{3h} boric acid molecule functions as both hydrogen-bond donor and acceptor. In aqueous solution at pH = 8~10 boric acid easily undergoes condensation to give a polyborate if the boron concentration is higher than about 0.025 mol/L. Therefore, it is very essential to keep the trigonal planar form of boric acid in order to build rosette motifs according to the geometrical requirement.

Based on the above consideration, the molecular building blocks employed in our construction of anionic host lattices are the C_3-symmetric species guanidinium (GM), boric acid (BA) and carbonate (CB), as well as the less

symmetric dianions 1,2-dithiosquarate (DTS) and 1,1'-biphenyl-2,2',6,6'-tetracarboxylate (BPTC), as displayed in Scheme 3.1.1

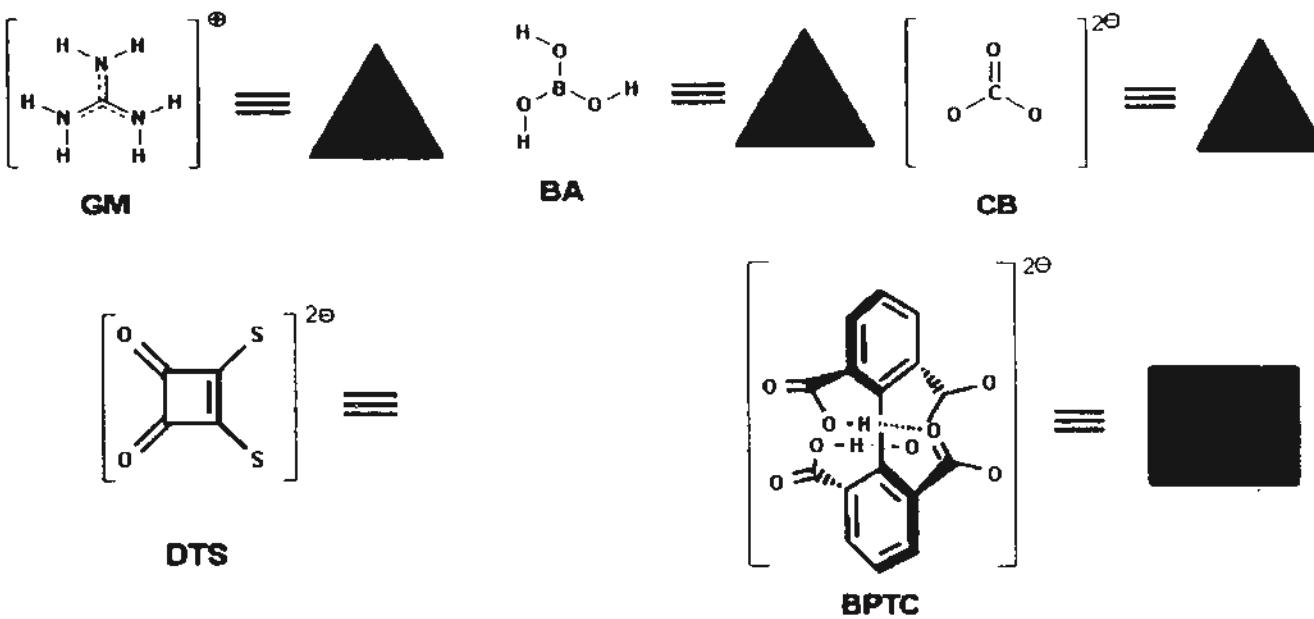

Scheme 3.1.1 Molecular building blocks employed in the construction of rosette motifs and their graphical representation.

In Chapter 2.1.1, boric acid in crystals **2.1.3** and **2.1.4** maintains its C_{3h} symmetry, while in the crystal structure of **2.1.1** and **2.1.2**, the condensed species tetraborate $H_4B_4O_9^{2-}$ and pentaborate $H_4B_5O_{10}^-$ are present, respectively. In complex **2.1.2**, the pentaborate anions are associated into dimers, and no rosette motif is generated. In the crystal structure of **2.1.1**, although the tetraborate anion does not conform to C_3 symmetry, skew pseudo-rosette double layers are still generated by pairing of N_{GM}–H···O_{BA} hydrogen bonds. It is worthy to note that three pairs of hydrogen bonds around each tetraborate are angled at about 120° to each other. During the synthetic studies of **2.1.1**, attempts to introduce various tetraalkylammonium cations into the system were unsuccessful. This is indicative of

the robustness of the hydrogen-bonding framework formed by the tetraborate and guanidinium ions.

In complex **2.1.3** and **2.1.4**, three kinds of connection modes are used as potential supramolecular synthons to create a rosette motif (Scheme 3.1.2).

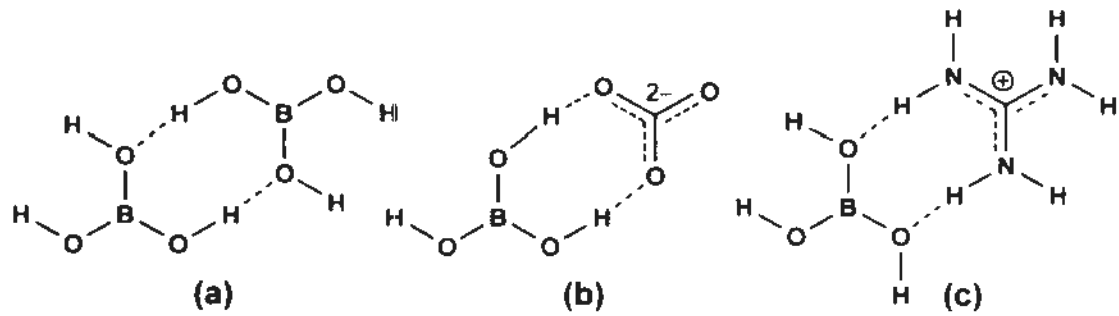

Scheme 3.1.2 Supramolecular synthons based on boric acid present in complex **2.1.3** and **2.1.4**: (a) boric acid dimer; (b) boric acid forming donor hydrogen bonds to the carbonate ion; (c) boric acid as a hydrogen-bond acceptor to the guanidinium ion.

These supramolecular synthons also proved to be effective in constructing the rosette structure in $[(n\text{-}C_3H_7)_4N^+] \cdot [C(NH_2)_3^+] \cdot 2B(OH)_3 \cdot CO_3^{2-}$ (**2.1.4**). The boric acid dimer severs as both hydrogen-bond donor and acceptor to generate a three-component, slightly wavy guanidinium–boric acid–carbonate (1:2:1) layer, which is composed of two distinguishable rosette motifs [**A**] and [**B**] and stays intact without further stabilization by any interlayer linker (Figure 2.1.8). This is accounted for by the presence of the boric acid molecule which, by virtue of its pronounced tendency for in-plane bonding, restraints the carbonate ion from engagement in extensive out-of-plane interaction with other hydrogen-bond donor sites. In previously reported rosette layer structures $4[(C_2H_5)_4N^+] \cdot 8[C(NH_2)_3^+] \cdot 3CO_3^{2-} \cdot 3(C_2O_4)^{2-} \cdot 2H_2O$ (**a**)[69] and $[(C_2H_5)_4N^+] \cdot 7[C(NH_2)_3^+] \cdot 3CO_3^{2-} \cdot$

$[C_3N_2H_2(COO^-)_2]$ (**b**)[70] , interlayer support is a requisite. In the crystal structure of $[(C_2H_5)_4N^+] \cdot 7[C(NH_2)_3^+] \cdot 3CO_3^{2-} \cdot [C_3N_2H_2(COO)_2]$, there is an entirely different kind of wavy guanidinium–carbonate–1*H*-imidazole-4,5-dicarboxylate (4:1:1) layer that functions as a lamina between the essentially planar guanidinium–carbonate (1:1) rosette layers to reinforce the whole structure (Scheme 1.3.7).

In Chapter 2.1.2 and 2.1.3, we also extended the conventional topological design of supramolecular rosette layer structures by relaxing the requirement of exact or near C_3 symmetry of the molecular building blocks. In this instance, 1,2-dithiosquaric acid and non-planar 1,1'-biphenyl-2,2',6,6'-tetracarboxylic acid proved to be suitable starting materials for the construction of distorted hydrogen-bonded rosette layers with suitable C_3 related counterpart.

Our initial attempts to generate rosette motifs based on the squarate ion were unfruitful. The squarate mono anion prefers to form a dimer, and the squarate dianion has a tendency to form hydrogen-bonding interactions along two or four directions (some examples done by our group are shown in Scheme 1.3.8). In addition, its non-benzenoid aromatic character also precludes it from masquerading as a C_3-mimic that forms hydrogen bonds to three neighboring donors.

Against this background, 1,2-dithiosquarate $C_4O_2S_2^{2-}$ (DTS) was selected as a building block instead of the squarate dianion to explore the possibility of forming a rosette motif. In the crystals structure of **2.1.6** to **2.1.9**, different molar equivalents of thioureas and/or different sizes of tetraalkylammonium cations were explored. Due to disordered oxygen and sulfur atoms in complex **2.1.6**, the directional characteristics of hydrogen bonds around DTS cannot be clearly specified. The structural analysis of complex **2.1.7** and **2.1.8** showed that the dithio analog is better adapted to acceptor hydrogen bonding in three principal directions owing to the

weakness of the (guanidinium)N–H···S hydrogen bond compared to N–H···O. This is an important factor in the designed construction of a hexagonal rosette structure. Further investigation revealed that there are three thioureas around a DTS in complex **2.1.7**, and two thioureas plus one water molecules around a DTS in complex **2.1.8**. However, due to the formation of shoulder-to-shoulder dimeric thiourea in the two crystals, there is no resulting rosette motif.

For generation of a rosette network, the guanidinium cation is selected to prevent formation of the dimer. In the crystal structure of **2.1.9**, dithiosquarate is amenable to forming acceptor hydrogen bonds with GM in three directions that mimic the requirement of approximate C_3-symmetry As a result, its two carbonyl oxygen atoms each serves as a bifurcated acceptor in two separate directions (type **I**, Scheme 3.1.3), whereas the sulfido terminals pair up to form a pair of acceptor hydrogen bonds along the third direction (type **II**).

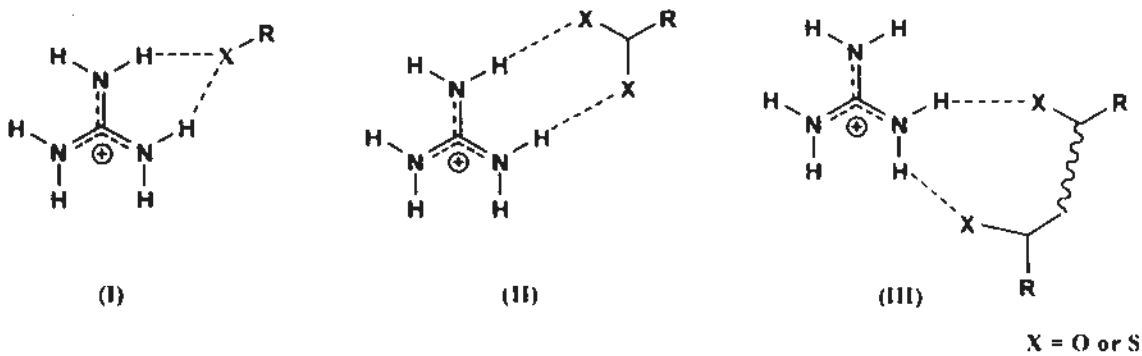

Scheme 3.1.3 Three types of hydrogen-bonding modes in quasi-rosette motifs constructed with non C_3-symmetric dianions. Guanidinium ion forms donor hydrogen-bonds with oxygen or sulfur atoms in three linkage modes that involve geminal hydrogen bonds (**I**), a pair of parallel hydrogen bonds (**II**), or two inclined hydrogen bonds (**III**).

A comparison of the geometric parameters of [(*n*-$C_4H_9)_4N^+$] · [$C(NH_2)_3^+$] · [$C_4O_2S_2^{2-}$] **2.1.9** with related structures composed of squarate and guanidinium/urea/thiourea shows that the C–N(guanididnium)···(sulfido)S–C torsion angle of type **II** hydrogen bonds between the thiosquarate sulfur atom and GM in this case is considerably larger than that involving the squarate oxygen atom (Table 3.1.1). This agrees with the previous finding that, in general, hydrogen bonds to sulfur not only are weaker than those to oxygen but also show a marked preference for a more "perpendicular" direction of approach to the donor atom.[198]

Table 3.1.1 Comparison of torsion angles* in related crystal structures containing a squarate ion connected to a guanidinium ion or urea or thiourea species by a pair of hydrogen bonds.

CSD entry code	Compound Name	Torsion angles(°)	Reference
present work	(tetra-*n*-butylammonium) 1,2-dithiosquarate (guanidinium)	58.74, 52.31	70
XAHQIG	bis(tetraethylammonium) squarate bis(thiourea) dihydrate	-8.06, -11.75	73a
XAHQEC	bis(tetraethylammonium) squarate hexakis(thiourea)	-17.88, -13.20	73a
XAHQAY	bis(tetraethylammonium) squarate tetrakis(thiourea) dihydrate	-17.54, -20.79	73a
WOWMOK	bis(tetra-*n*-propylammonium) squarate urea clathrate dihydrate	1.09, 4.18	73b
RAVWAM	guanidinium hydrogen squarate	-6.23, -17.30	99
QIRKAD	squaric acid urea monohydrate	13.13,14.55	100

* Torsion angles C–N···O(S)–C are given for type **II** hydrogen bonds (see Scheme 3.1.3) involving the squarate ion and one guanidinium/urea/thiourea molecule.

The non-planar 1,1'-biphenyl-2,2',6,6'-tetracarboxylate dianion (BPTC) replaces the planar dithiosquarate dianion as a building block to construct a supramolecular rosette layer in Section 2.1.3. In complexes **2.1.11** to **2.1.14**, an intramolecular hydrogen bond occurs in BPTC, resulting in a dihedral angle between its two phenyl rings in the range of 83 to 90 °.

In BPTC–thiourea complex **2.1.11**, there are six-membered rosette motifs composed of two dimeric thioureas and two BPTCs. However, these rosette motifs are not continuous. Two similar rosette layers are created in complex **2.1.13** and **2.1.14** with tetraalkylammonium cations of relative larger sizes. The result shows that the carbonyl group of non-planar 1,1'-biphenyl-2,2',6,6'-tetracarboxylate dianion BPTC has no strong directional preference as a hydrogen-bond acceptor, and hence it is conducive to formation of the rosette motif. The directional characteristics of the hydrogen-bonding interaction between guanidinium and BPTC in $[(C_2H_5)_4N^+] \cdot [C(NH_2)_3^+] \cdot [(C_6H_3)_2(COOH)_2(COO^-)_2]$ **2.1.13** and $[(n\text{-}C_3H_7)_4N^+] \cdot [C(NH_2)_3^+] \cdot [(C_6H_3)_2(COOH)_2(COO^-)_2]$ **2.1.14** are shown in Scheme 3.1.4. Both type **II** and **III** hydrogen-bonding modes (Scheme 3.1.3) are present, but the rosette motif in **2.1.13** is more planar than that in **2.1.14**. In complex **2.1.13**, the dihedral angle between three guanidinium cations in the same rosette motif ranges from 26 ° to 40 °. In complex **2.1.14**, two guanidinium cations are orientated parallel to each other, whereas the third one makes a large dihedral angle of about 75 ° with the former two to generate a pleated sheet structure (Scheme 3.1.4).

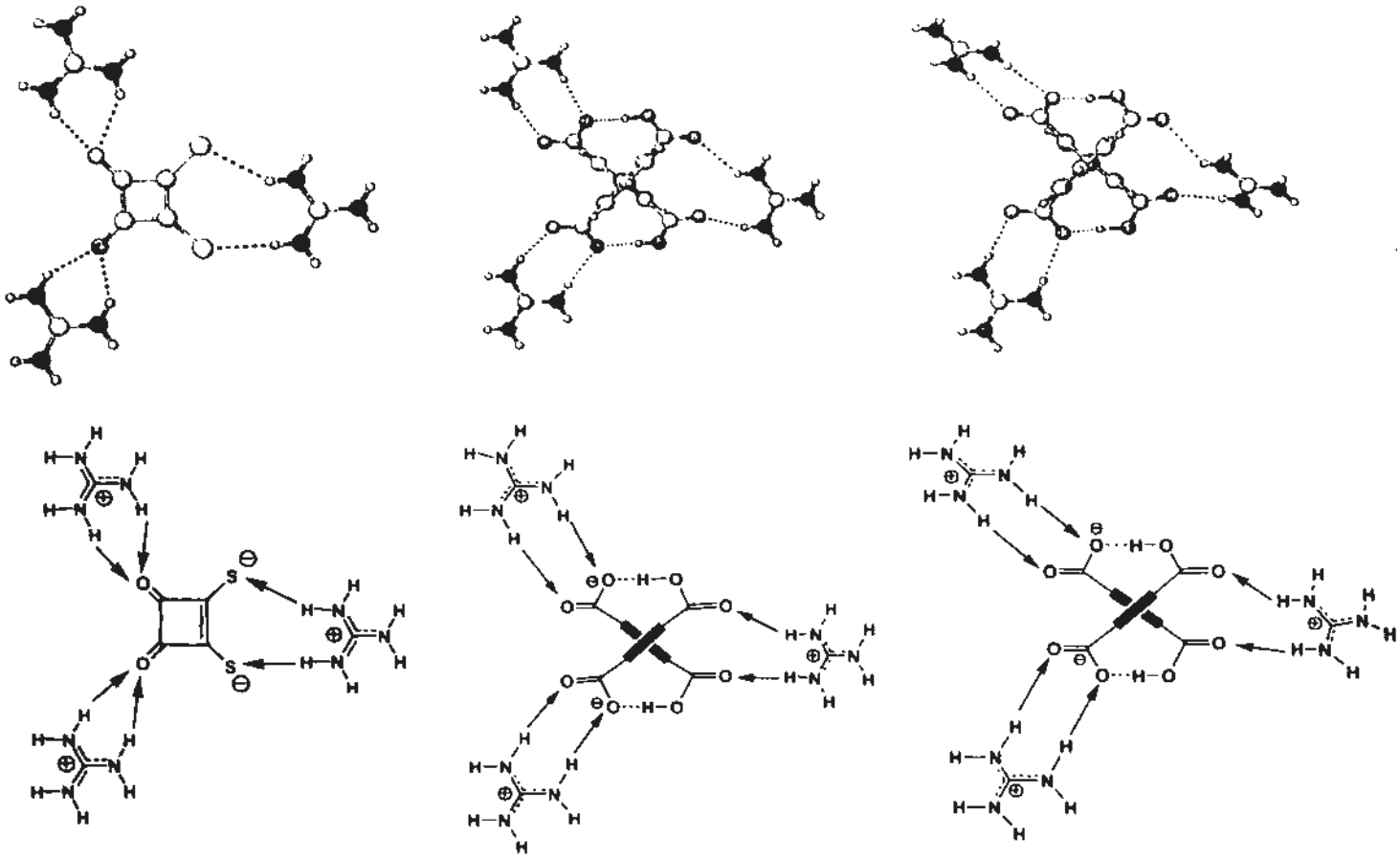

(a) (b) (c)

Scheme 3.1.4 Three principal hydrogen-bonding directions around a non-C_3-symmetric dianion in a distorted rosette layer. The surrounding guanidinium cations in complex **2.1.9** (a) and **2.1.13** (b) are almost co-planar, but one of the three guanidinium cations in complex **2.1.14** (c) is inclined to the other two by about 75 °.

Diagrammatic representation of different rosette motifs and their graph-set notations is shown in Scheme 3.1.5. Scheme 3.1.5b is a representation of the centrosymmetric $R_6^4(12)$ assembly around rosette [**A**] (Figure 2.1.8), which may be designated as [$\mathbf{GM_2 \cdot CB_2 \cdot BA_2}$], while the $R_6^5(12)$ assembly around rosette [**B**] having mirror symmetry can be represented as [$\mathbf{GM_1 \cdot CB_1 \cdot BA_4}$], as shown in Scheme 3.1.5c.

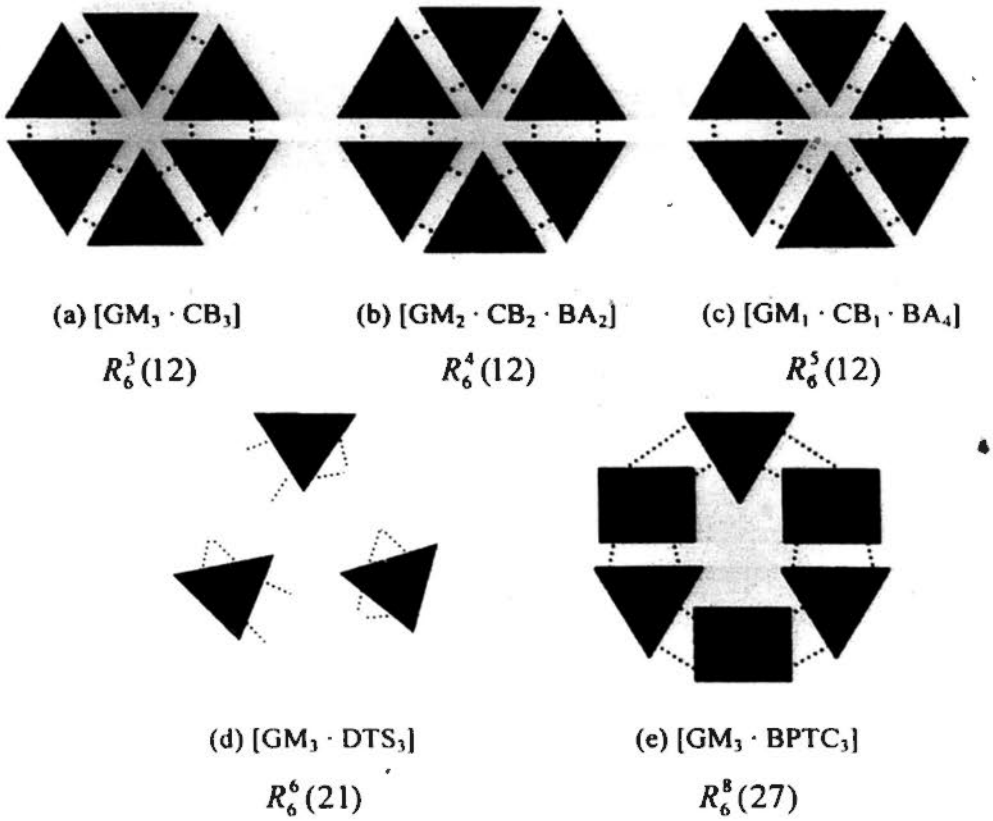

Scheme 3.1.5 Diagrammatic representation of different rosette motifs and their graph-set notations: (a) two-component rosette built of C_3-symmetric components; (b) and (c) three-component rosette built of C_3-symmetric components; (d) and (e) rosette involving non C_3-symmetric components.

In comparing the rosette motifs in the present series of inclusion complexes with that in the reference compounds $4[(C_2H_5)_4N^+]\cdot 8[C(NH_2)_3^+]\cdot 3(CO_3)^{2-}\cdot 3(C_2O_4)^{2-}\cdot 2H_2O$ (**a**)[69] and $[(C_2H_5)_4N^+]\cdot 7[C(NH_2)_3^+]\cdot 3CO_3^{2-}\cdot [C_3N_2H_2(COO^-)_2]$ (**b**),[70] it is noted that there is considerable variation in size and shape. The shape changes from regular to irregular, and the sizes are modified significantly. For the purpose of comparison, the size of a rosette is defined by the three sides of a triangle whose vertices are the guanidinium carbon atoms. The sizes of individual rosettes in the complexes are: (7.29 × 8.41 × 9.74 Å) in **2.1.1**; rosette motif **A** (6.79 × 6.94 × 7.06

Å) and **B** (6.61 × 6.89 × 6.89 Å) in **2.1.4**; (9.26 × 9.48 × 9.58 Å) in **2.1.9**; rosette motif **A** (10.15 × 11.09 × 11.76 Å) and **B** (10.15 × 10.97 × 11.64 Å) in **2.1.13**; (10.24 × 10.24 × 10.67 Å) in **2.1.14**; (6.25 × 6.59 × 7.08 Å) in (**a**) and **A** (7.12 × 7.13 × 7.38 Å) and **B** (6.89 × 6.95 × 7.03 Å) in (**b**) (Scheme 1.3.6). The rosette units composed of non C_3-symmetric molecular components are obviously larger than that in guanidinium–carbonate (1:1).

The structural characteristics of rosette layers therein, in comparison with some representative examples from the literature, are displayed in Table 3.1.2.

Table 3.1.2 Structural characteristics of hydrogen-bonded rosette networks.

Chemical formula		Composition of rosette layer	No. of hydrogen bonds between building units
H_3BO_3		boric acid	double
$C_6H_3(COOH)_3$		trimesic acid	double
$C_6H_3(COOH)_3$		trimesic acid	double
$C_3N_3(NH_2)_3 \cdot (NH)_3(CO)_3$		melamine–cyanuric acid (1:1)	triple
$C_3N_3(NH_2)_3 \cdot (NH)_3(CS)_3$		melamine–trithiocyanuric acid (1:1)	triple
$[C(NH_2)_3^+] \cdot NO_3^-$		guanidinium–nitrate (1:1)	double
$[C(NH_2)_3^+] \cdot RSO_3^-$		guanidinium–sulfonate (1:1)	double
$[(cyclo\text{-}C_6H_{11})_2NH_2^+]_3 \cdot [1,3,5\text{-}C_3H_3(COO^-)_3] \cdot x$MeOH**		dicyclohexylammonium–trimesate (3:1)†	double#
$2\{(C_2H_5)_4N^+] \cdot [C(NH_2)_3^+] \cdot [1,3,5\text{-}C_3H_3(COO^-)_3] \cdot 6H_2O$		guanidinium–trimesate (1:1)	double
$4[(C_2H_5)_4N^+] \cdot [C(NH_2)_3^+] \cdot 3CO_3^{2-} \cdot 3(C_2O_4)^{2-} \cdot 2H_2O$		guanidinium–carbonate (1:1)	double
$[(C_2H_5)_4N^+] \cdot [C(NH_2)_3^+]_7 \cdot 3CO_3^{2-} \cdot [C_3N_2H_2(COO^-)_2]$		guanidinium–carbonate (1:1)	double
$[(n\text{-}C_3H_7)_4N^+] \cdot [C(NH_2)_3^+] \cdot CO_3^{2-} \cdot 2B(OH)_3$	**2.1.4**	guanidinium–boric acid–carbonate (1:2:1)	double
$[(n\text{-}C_4H_9)_4N^+] \cdot [C(NH_2)_3^+] \cdot [C_4O_2S_2^{2-}]$	**2.1.9**	guanidinium–dithiosquarate (1:1)	double and bifurcated
$[(C_2H_5)_4N^+] \cdot [C(NH_2)_3^+] \cdot [(C_6H_3)_2(COOH)_2(COO^-)_2]$	**2.1.13**	guanidinium–diphenyltetracarboxylate dianion (1:1)	double
$[(n\text{-}C_3H_7)_4N^+] \cdot [C(NH_2)_3^+] \cdot [(C_6H_3)_2(COOH)_2(COO^-)_2]$	**2.1.14**	guanidinium–diphenyltetracarboxylate dianion (1:1)	double

Chemical formula		Net charge of rosette layer	Configuration of rosette layer	Reference
H_3BO_3		neutral	planar	53
$C_6H_3(COOH)_3$		neutral	interpenetrated pleated sheet	46
$C_6H_3(COOH)_3$		neutral	non-planar	54
$C_3N_3(NH_2)_3 \cdot (NH)_3(CO)_3$		neutral	planar	55
$C_3N_3(NH_2)_3 \cdot (NH)_3(CS)_3$		neutral	planar	56
$[C(NH_2)_3^+] \cdot NO_3^-$		neutral	planar	57
$[C(NH_2)_3^+] \cdot RSO_3^-$		neutral	planar/corrugated*	58
$[(cyclo\text{-}C_6H_{11})_2NH_2^+]_3 \cdot [1,3,5\text{-}C_3H_3(COO^-)_3] \cdot x$MeOH**		neutral	wavy	59
$2[(C_2H_5)_4N^+] \cdot [C(NH_2)_3^+] \cdot [1,3,5\text{-}C_3H_3(COO^-)_3] \cdot 6H_2O$		anionic	planar§	69
$4[(C_2H_5)_4N^+] \cdot [C(NH_2)_3^+] \cdot 3CO_3^{2-} \cdot 3(C_2O_4)^{2-} \cdot 2H_2O$		anionic	wavy	69
$[(C_2H_5)_4N^+] \cdot [C(NH_2)_3^+]_7 \cdot 3CO_3^{2-} \cdot [C_3N_2H_2(COO^-)_2]$		anionic	nearly planar	70
$[(n\text{-}C_3H_7)_4N^+] \cdot [C(NH_2)_3^+] \cdot CO_3^{2} \cdot 2B(OH)_3$	**2.1.4**	anionic	wavy	70
$[(n\text{-}C_4H_9)_4N^+] \cdot [C(NH_2)_3^+] \cdot [C_4O_2S_2^{2-}]$	**2.1.9**	anionic	wavy	70
$[(C_2H_5)_4N^+] \cdot [C(NH_2)_3^+] \cdot [(C_6H_3)_2(COOH)_2(COO^-)_2]$	**2.1.13**	anionic	nearly planar	70
$[(n\text{-}C_3H_7)_4N^+] \cdot [C(NH_2)_3^+] \cdot [(C_6H_3)_2(COOH)_2(COO^-)_2]$	**2.1.14**	anionic	pleated sheet	70

* The rosette layer is constructed from the cross-linkage of zigzag guanidinium-sulfonate ribbons, and the inter-ribbon dihedral angle θ_R changes according to the nature of the *R* group, ranging from 171° for small *R* (methyl) to 146° for large *R* (2-naphthyl); a planar rosette type has $\theta_R = 180°$.

** Three MeOH molecules are hydrogen-bonded to the grid outside the cavity and there appear to be several disordered MeOH molecules within the honeycomb.

† Adjacent trimesate ions, considered as building units, are doubly bridged by a pair of ammonium ions in a $R_4^2(8)$ motif

‡ Mediated by a pair of ammonium spacers.

§ A cyclohexane-like $(H_2O)_6$ cluster occupies the central cavity of each rosette.

The present work has demonstrated several effective strategies toward the designed construction of hydrogen-bonded anionic rosette layers. Because thiourea easily forms a dimer in the crystal structure, it is not a good building block for the rosette structure. Incorporation of boric acid into the guanidinium-carbonate system generates an unprecedented tertiary rosette layer guanidinium–boric acid–carbonate (1:2:1) that features two distinct motifs.

Inherent three-fold molecular symmetry used to be regarded as a sacrosanct requirement for molecular building blocks in the construction of two-dimensional hydrogen-bonded network structures bearing the rosette motif. The synthesis of complexes **2.1.9**, **2.1.13** and **2.1.14** showed that this condition can be relaxed to a considerable extent. Deliberate use of the dithiosquarate dianion in **2.1.9** as a substitute for a C_3-symmetric species has proved that construction of a rosette layer is still feasible, although conspicuous deviation from perfect coupling between hydrogen-bond donor and acceptor has to be tolerated. An alternative reduction in symmetry of the acceptor component, employing the non-planar dianionic form of 1,1'-biphenyl-2,2',6,6'-tetracarboxylic acid, also succeeded in generating similar distorted rosette layers, as observed in **2.1.13** and **2.1.14**. The present findings nicely illustrate the general validity of isostructural exchange between equivalent building blocks in supramolecular self-assembly,[101] and as such provide a promising guiding principle in the crystal engineering of new rosette systems from simple molecular components.

3.2 Hydrogen-bonded molecular complexes based on Kemp's triacid

Kemp's triacid is a cyclohexane derivative and accordingly its six-membered ring can take the chair, boat, twist-boat and twist conformations. The distance between the carbon atoms of the pair of carboxyl/carboxylate groups of mono-deprotonated Kemp's triacid in the solid state are in the range of 3.0 Å to 3.6 Å[102] which is very closely to that between the dimer of hydrogen carbonate (bicarbonate). We have previously reported a hydrogen-bonded, anionic two-dimensional rosette ribbon assembled with guanidinium and bicarbonate ions.[49b] The O–H···O hydrogen bonding distance in the hydrogen carbonate is about 2.4 Å. Due to the conformational flexibility and non-planar character related to changeable number of deprotonated hydrogen atoms, Kemp's triacid (including its mono- or di- anionic form) is expected to serve as a non-planar analog of the bicarbonate dimer by forming intramolecular interactions between a pair of carboxyl/carboxylate groups (Scheme 3.2.1).

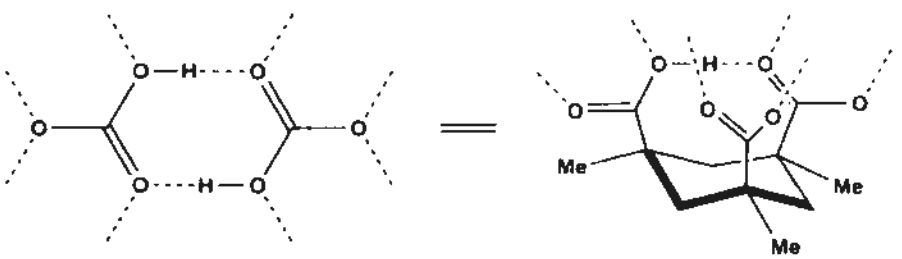

Scheme 3.2.1 Similarity between planar cyclic dimer of hydrogen carbonate and intramolecular hydrogen bonding motif of an anionic form of Kemp's triacid.

The mono- or dianion of Kemp's triacid is known to form five to seven acceptor hydrogen bonds (mostly six hydrogen bonds)[103,104] as a hub for

supramolecular assembly, and hence it would be of interest to see if the C_3 symmetric tricarboxylate form of Kemp' triacid can better this record. In Section 2.2, six new crystal structures based on mono-, di-, or tri- deprotonated forms of Kemp's triacid as main building blocks are described.

Deprotonated forms of Kemp's triacid takes the stable chair conformation in complex **2.2.1** to **2.2.5**. In crystals containing the monoanion H_2KTA^-, the distance between carbon atoms of carboxyl/carboxylate groups are in the range of 3.1 to 3.7 Å. In the KTA^{3-} complexes, all three carboxylate groups occupy the equatorial positions of the chair-like cyclohexane skeleton due to electrostatic repulsion, and the corresponding C···C distances reaches 4.9 Å. In complex **2.2.6**, KTA^{3-} adopts a twist-boat conformation which results in unequal distances between the carboxylate groups in a large range of 3.4 to 5.0 Å (Table 3.2.1).

Table 3.2.1 Number of hydrogen bonds, dihedral angle and distance information of carboxyl/carboxylate groups in complexes **2.2.1**~**2.2.6**.

Entry	**2.2.1**	**2.2.2**	**2.2.3**	**2.2.4**	**2.2.5**	**2.2.6**
Conformation of cyclohexane ring	chair	chair	chair	chair	chair	twist-boat
Degree of deprotonation	mono-	mono-	mixed mono/di	tri-	tri-	tri-
Max. No. of H-bonds*	4	8	9 or 10	12	18	11
Distance (Å) between carbon atoms of carboxyl/carboxylate groups	3.1 3.6 3.4	3.1 3.4 3.7	3.0~3.7	4.9~5.0	4.9	3.4 4.4 5.0

*Max. No. of hydrogen bonds around a deprotonated Kemp's triacid (exclude intramolecular hydrogen bonding.

The four-membered rosette motif $(GM{-}Acid)_2$ in complex **2.2.2** is comparable in size to the six-membered rosette motif $(GM{-}CO_3^{2-})_2$.[70] The distance between the central carbon atoms of guanidinium ions in each rosette motif is 8.4

and 8.1 Å, respectively. This is a good example of mimicing a known supramolecular synthon with a designed assembly of molecular components.

The crystal structure of **2.2.3** features a hydrogen-bonded assembly with a centrosymmetric pseudo-octahedron composed of the carboxylate groups of six peripheral H_2KTA^- ions surrounding an inner core of eight guanidinium ions.

The trianion of Kemp's triacid forms a record number of eighteen hydrogen bonds with convergent N–H donor sites from nine guanidinium molecules in complex **2.2.4** with near 3*m* symmetry.

Four independent guanidinium cations constitute a tetrahedral centron, which is similar to our reported work,[70] that is consolidated by a pseudo-octahedral arrangement of six independent KTA^{3-} ions in complex **2.2.5**. However, the size of this tetrahedral guanidinium core is slightly changed compared with the reported one.[70] The distances between each carbon atom of guanidinium are about 4.3 to 4.7 Å, while those in the reported example lie in the range of 4.1 to 4.8 Å. The result indicates that this highly charged positive hub is an unexpectedly robust building motif which can be formed in different systems.

Intramolecular hydrogen bonds are present in both complex **2.2.1** and **2.2.2**. In each system, intermolecular interactions between adjacent Kemp's triacids are also formed in these two complexes, but the dihedral angles of three carboxyl/carboxylate groups are significantly different. The former one has dihedral angles in the larger range of 21 to 74 °, and the later ones are in a relative small range of 30 to 43 °. The result highlights the unexpected flexibilities of carboxyl/carboxylate groups of Kemp's triacid in designed systems in the solid state.

In summary, we have investigated a series of crystal structures based on deprotonated Kemp's triacid ions and that the results obtained include separated

ribbons (complex **2.2.1**) and four-membered rosette motif (complex **2.2.2**) structures. In complex **2.2.4**, a record of number of hydrogen bonds around Kemp's triacid is generated. Guanidinium octahedral and tetrahedral cores stabilized by peripheral carboxylate groups are found in complex **2.2.3** and **2.2.5**, respectively. In complex **2.2.6**, KTA^{3-} has a twist-boat cyclohexane conformation instead of the common chair conformation which occurs in complex **2.2.1**~ **2.2.5**.

3.3 Supramolecular hydrogen bonding motifs based on the aromatic carboxylic acid

In Chapter 2.3, five kinds of linear or angular carboxylic acids are used to form complexes with the guanidinium ions. Scheme 3.3.1 shows the structural characteristics of the five acids. In the first three linear molecules (a) to (c) as building blocks, the hydrogen-bonding environment of mono-protonated (a) in **2.3.1** does not lead to an expected linear crystal structure. In **2.3.2** and **2.3.3**, naphthalene-2,6-dicarboxylate dianion (NDC) and biphenyl dicarboxylate dianion ($BPDC^{2}$) are joined with the guanidiniums by pairwise hydrogen bonds in each crystal structure to form a relative planar trimer, and further connection by chelating guanidinium–to–carboxylate chelating hydrogen bonds generates a zigzag band. Water molecules play an important role in connecting such bands together to yield similar layer structures in the two systems.

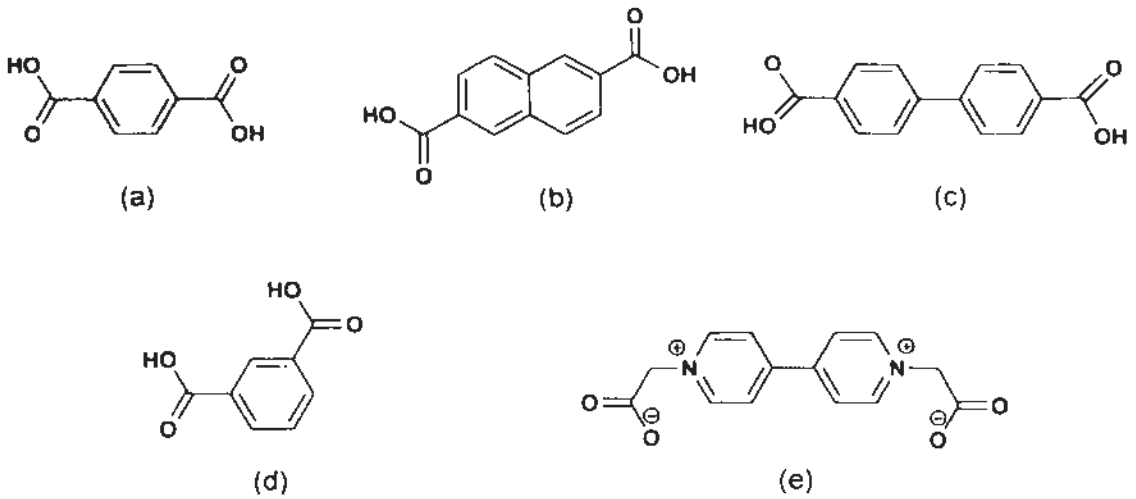

	Rigid	Linear	Angular	Non-planar	Rotation of two phenyl rings	Distance between two carboxylate/carboxyl (Å)
a	√	√				5.8
b	√	√				8.0
c	√	√			√	10.2
d	√		√			5.0
e			√	√	√	11.2

Scheme 3.3.1 Structural characteristics of the five bicarboxylate/bicarboxylic acid studied in the thesis.

All the crystal structures (**2.3.1~2.3.8**) involved in type **A** hydrogen bonding mode with graph-set $R_2^2(8)$, that is carboxylate connected with guanidinium by pairwise hydrogen bonds. In addition, chelating hydrogen bonding $R_2^1(6)$ designated as type **B**, is also present in **2.3.1**, **2.3.2** and **2.3.4**. Table 3.3.1 shows torsion angles between the guanidinium ion and carboxylate and relative hydrogen bonded types of eight carboxylate complexes.

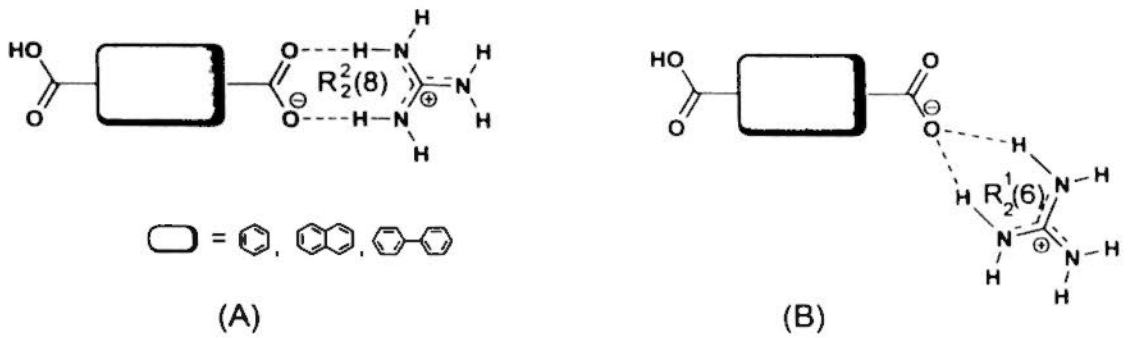

Scheme 3.3.2 Main hydrogen bonding modes (type **A** and **B**) between carboxylate and guanidinium ion.

Table 3.3.1 Torsion angles between the guanidinium (GM) and carboxylate and relative hydrogen bonded types of eight carboxylate complexes.

	Torsion angles between GM and carboxylate *	Hydrogen bonding type between GM and carboxylate
2.3.1	5.24/13.73, 9.38/16.93 10.73/19.42, 13.24/34.67	A+B
2.3.2	5.24/13.73	A+B
2.3.3	12.42/34.86	A
2.3.4	18.02/42.50, 0.97/15.50	A+B
2.3.5	19.51/29.50, 24.88/3.80	A
2.3.6	2.86/9.68	A
2.3.7	NA**	A
2.3.8	NA**	A

* Only for pairs of hydrogen bond, ** no pairwise hydrogen bonds between GM and carboxylate.

In the crystal structure of **2.3.8**, the rosette motif $(GM–CO_3–H_2O)_2$ is present as a linkage mode (Scheme 3.3.3a). Interestingly, **2.3.5** has an isostructural unit in which a carboxylate oxygen atom replace the water molecules, and the carbonate is replaced by a fragment of the guanidinecarboxylate (Scheme 3.3.3b). The two

rosette motifs with different graph-sets are [**A**] = $R_2^2(8)$, [**B**] = $R_3^3(10)$ in **2.3.8** and [**A**] = $R_2^2(8)$, [**C**] = $R_3^2(10)$ in **2.3.5**, respectively.

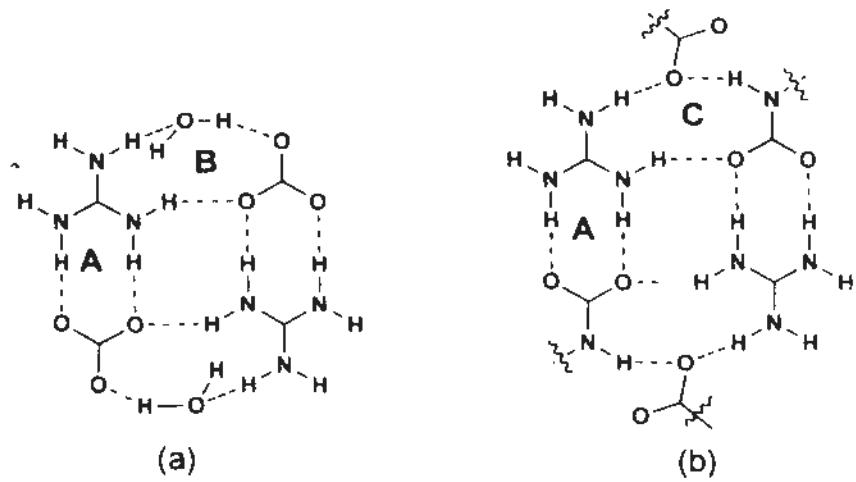

Scheme 3.3.3 Isostructural rosette motif (a) in **2.3.8** and (b) in **2.3.5**.

As a structure building unit, *N,N'*-bis(carboxymethyl)-4,4'-bipyridinium betaine behaves totally differently from phenyl carboxylate, as its positively charged heterocyclic ring and torsional carboxymethyl group result in a three dimensional structure in **2.3.8**.

3.4 Supramolecular hydrogen bonding motifs based on *N*-heteroaryl acid

3.4.1 Discussion about inclusion compounds containing anions of 2-thiobarbituric acid/trithiocyanuric acid

In a series of nine compounds **2.4.1**–**2.4.9**, dimers of 2-thiobarbiturate (TBA) or trithiocyanurate (TCA) are present in seven crystal structures. Most dimers are almost planar, and the values of their torsion angles are tabulate in Table 3.4.1.

Table 3.4.1 Characteristic of nine crystal structures of **2.4.1** to **2.4.9**.

Entry	Types of TBA or TCA	Torsion angle (°) between dimer/tetramer of TBA or TCA	Max. No. of H-bonds around TBA or TCA	Charge of TBA/TCA
2.4.1	Ribbon	18.36, 8.86	7	-1
2.4.2	Dimer	6.08	5	-1
2.4.3	Tetramer	13.22, 21.26/6.95	7	-1
2.4.4	Dimer	6.55	4	-1
2.4.5	Ribbon	10.38/7.49	6	-1
2.4.6	Separated	–	9	-2
2.4.7	Dimer/ Separated	18.28, 20.20	6	-1
2.4.8	Dimer/ Separated	0.77	8	-2
2.4.9	Separated	–	8	-2

In the urea/thiourea/guanidinium inclusion compounds, pairwise hydrogen bonding interaction between the TBA/TCA and neighbors is the dominating feature. Scheme 3.4.1 shows the four main hydrogen-bonding modes of the heterocyclic ring. In 2-thiobarbiturate complexes, dimers of thiobarbiturate are formed in all three crystal structures through N–H···O rather than N–H···S hydrogen bonding. Therefore, linear ribbons of thiobarbiturate are found in the crystal structures of **2.4.1** and **2.4.3**.

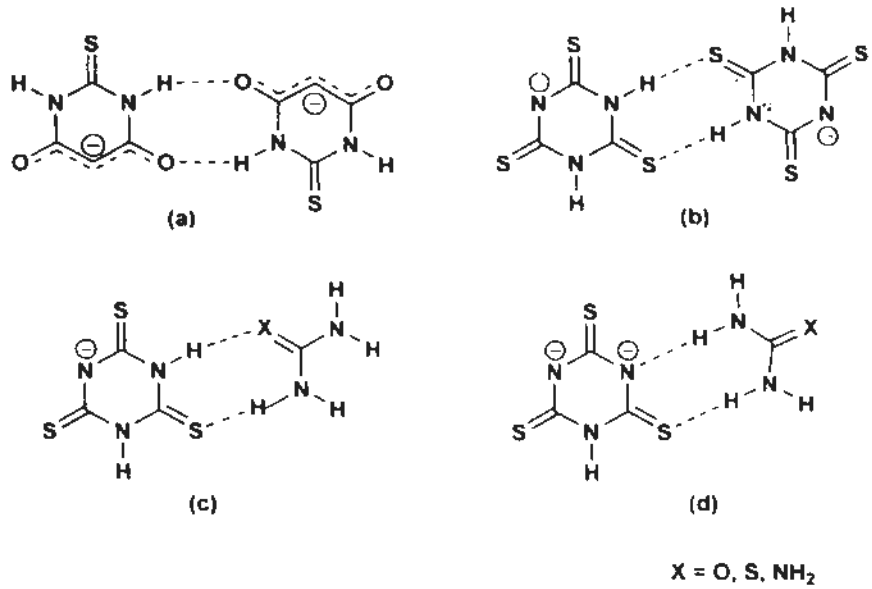

Scheme 3.4.1 Main hydrogen-bonding connection modes present in the 2-thiobarbiturate and trithiocyanurate crystal structures.

For trithiocyanuric acid (H_3TCA), the possible hydrogen bonding directions are increased and the acceptor hydrogen bonding capability of each group is averaged. In trithiocyanurate complexes, trithiocyanurate dimers are formed along one or two dimensions in **2.4.4**, **2.4.5**, **2.4.7** and **2.4.8**. Hydrogen bonding interactions of each trithiocayanurate are mostly along three directions, except for one case in **2.4.8**.

3.4.2 Discussion about inclusion compounds containing anions of 5-nitrobarbituric acid

In Chapter 2.4.2, the connection mode, distortion of the 5-nitro group, deprotonation number of 5-nitrobarbituric acid are discussed in the following parts:

(a). Connection mode of 5-nitrobarbiturate

The 5-nitrobarbiturate dimer occurs in the two ammonium salts and in three of the four thiourea–anion complexes, but is absent in all three urea complexes. 5-Nitrobarbiturate is formally a cyclic urea, and therefore it has a tendency to form

three types of dimers due to different matching modes between the donor-acceptor functional groups (Scheme 2.4.2).

Only the type **A** dimer occurs in complex **2.4.10**. The connection mode and dihedral angle (about 77 °) between consecutive dimers are represented by the rectangle in Scheme 2.4.3a. In complex **2.4.11**, type **B** and type **C** dimers are used to connect each other to form a wavy layer, and the dihedral angle between dimers is about 146 ° (Scheme 2.4.3b).

The different values of dihedral angles indicate that the smaller-size tetramethylammonium guest favors the formation of a sharply folded zigzag ribbon (Complex **2.4.10**). With an increase in cationic size, the ribbon tends to flatten in order to better accommodate the guest species. In the same way, the tetramer formed by type **A** and type **B** dimers in complex **2.4.15** is almost planar due to the presence of the bulky tetra-*n*-butylammonium cation in the system.

The difference between urea and thiourea in generating complexes **2.4.12–18** arises from their relative capability in hydrogen bonding. Normally, a N–H···S hydrogen bond is much weaker than a N–H···O hydrogen bond.[98] The possibility of forming a nitrobarbiturate dimer is closely related to the competition between urea and thiourea for interaction with nitrobarbiturate. In the nitrobarbiturate–urea crystal system, the two components are about equally good as hydrogen-bond formers, and their competition disfavors intermolecular connection between two nitrobarbiturates. However, in the nitrobarbiturate–thiourea system, the N–H···O hydrogen bonds formed between nitrobarbiturate molecules are stronger than N–H···S hydrogen bonds formed between nitrobarbiturate and thiourea. As a consequence, the dimer of nitrobarbiturate occurs more readily in the thiourea system than in the urea system.

(b). Distortion of the 5-nitro group in different complexes

The nitro group is an effective hydrogen-bond acceptor in view of its electronic properties and the directionality of its oxygen lone pair electrons, which can be modulated by interaction with hydrogen-atom donating groups. Table 3.4.2 shows the dihedral angles between the heterocyclic ring and nitro group in complex **2.4.10** to **2.4.18**. In complex **2.4.10**, **2.4.11** and **2.4.15**, there is at least one nitro group that has no involvement in hydrogen bonding or interacts extremely weakly with its neighboring atoms. The dihedral angle between non-bonding nitro group and heterocyclic ring is about 3.4 ° in complex **2.4.10**, 39.0 ° in complex **2.4.11**, and 23.4 ° in complex **2.4.15**.

Table 3.4.2 Selected dihedral angles (°) and bond distances (Å) of nitro groups in complex **2.4.10 to 2.4.18.**

2.1.X (X=10 –18)	**10**	**11**	**12**	**13**	**14**	**15**	**16**	**17**	**18**
Dihedral angle between nitro group O1–N1–O2 and heterocyclic ring	3.44	25.41	29.31	5.02	19.69	47.15	9.79	29.23	13.87
Dihedral angle between nitro group O6–N4–O7 and heterocyclic ring		39.04	29.09			23.38			
N1–O1	1.23	1.23	1.24	1.20	1.23	1.23	1.22	1.22	1.23
N1–O2	1.22	1.24	1.23	1.22	1.22	1.22	1.23	1.25	1.24
C1–N1	1.41	1.42	1.41	1.39	1.41	1.41	1.40	1.41	1.42
N4–O6		1.23	1.23			1.21			
N4–O7		1.23	1.23			1.22			
C5–N4		1.44	1.41			1.43			
N1–O1 + N1–O2	2.45	2.47	2.47	2.42	2.45	2.45	2.45	2.47	2.47
N4–O6 + N4–O7		2.46	2.46			2.43			

In the other complexes, hydrogen-atom donating groups such as the water and (thio)urea molecule modulate the orientation of the nitro group, resulting in dihedral angles in the range of 5 to 29 °. In addition, the sum of the N1–O1 and

N1–O2 distance also varies in different crystal structures, indicating that π-electron delocalization of the nitro group changes with respect to orientation. In complex **2.4.12**, both independent nitro groups have similar dihedral angles of about 29 °, allowing the thiourea molecule to act as a strut or clamp to connect two nitrobarbiturate ribbons.

(c). Deprotonation of 5-nitrobarbituric acid under different conditions

5-Nitrobarbituric acid is a fairly strong acid that exists in a tri-keto structure. In the present of a base, deprotonation occurs at the C5 atom that carries the nitro group.[105] It is also possible to form a dianion by detaching a second hydrogen atom from one of the two exocyclic –NH groups. Notably, the bulky and hydrophobic tetra-alkylammonium ion plays a dual and complementary role in the formation of the present series of nine complexes. It serves as a template for the self-assembly of the anionic host lattice and, abetted by the presence of (thio)urea as an additional component, provides a suitably alkaline aqueous medium to convert 5-nitrobarbituric acid into its monoanion or dianion.

In complex **2.4.13**, nitrobarbiturate takes the form of a dianion, whereas in the other eight complexes it exists as a monoanion. As expected, the measured dihedral angles and bond distances of the nitro group in **2.4.13** are different from those in the other eight complexes. In particular, the C1–N1 bond distance of **2.4.13** is significantly shorter, which is indicative of its distinctive double-bond character.

In complex **2.4.13**, the nitrobarbiturate dianions mutually associate to form dimers, so that the presence of an additional hydrogen-bond donor is needed to stabilize the crystal structure. In this case, water molecules serve to connect the dimers to form a ribbon along the [0 1 $\bar{1}$] direction. The typical zigzag thiourea infinite chain occurs in this structure due to the large amount of thioureas used in the

synthesis. The maximum number of hydrogen bonds is formed between the deprotonated nitrogen atoms of the nitrobarbiturate dianion and thiourea molecules in accordance with optimal side-by-side arrangement of the two kinds of ribbons.

(d). Versatile roles of (thio)urea in the 5-nitrobarbiturate inclusion systems

The series of inclusion compounds **2.4.12–2.4.15** exhibit thiourea–nitrobarbiturate host lattices that are distinctly different from one another, depending on their stoichiometric ratio in the presence of the tetra-alkylammonium cation and co-crystallized water molecules. Thiourea acts as a strut or clamp in complex **2.4.12**, when a small amount of thiourea is used together with a small tetra-alkylammonium ion (molar ratio 5-nitrobarbiturate:thiourea = 2:1). The conventional shoulder-to-shoulder thiourea connection mode occurs in the structure of **2.4.14**, which is consistent with the addition of an excess amount of thiourea (5-nitrobarbiturate:thiourea = 1:2) in the synthesis. In complex **2.4.14**, the molar ratio of nitrobarbiturate to thiourea is 1:1, and both thiourea and 5-nitrobarbiturate are effectively prevented from forming a dimer or a ribbon. In complex **2.4.15**, when a small amount of thiourea is added into the system (5-nitrobarbiturate:thiourea = 2:1), all thioureas molecules are separated from one another. The 5-nitrobarbiturates are interconnected to form a tetramer, and thiourea acts as a linker to connect the tetramers together with reinforcement by the water molecules. In contrast, in the urea–anion complexes, urea competes with nitrobarbiturate in hydrogen bonding, resulting in three main types of connection modes as shown in Scheme 2.4.4. The data on molar ratio and types of connection modes in all complexes are tabulated in Table 3.4.3.

Table 3.4.3 Molar ratio of each component and connection modes of complex **2.4.10** to **2.4.18**.

Complex	Molar ratio (NBA*:(thio) urea: R_4N^+)	Type of NBA dimer	Type of urea or thiourea	No. of H-bonds formed by nitro group	Max. No. of H-bonds around each NBA
2.4.10	1:0:1	A	-	none	4
2.4.11	1:0:1	B + C	-	none/2 **	4/7
2.4.12	1:0.5:1	A + B	F	1	9
2.4.13	1:2:2	A	F	4	12
2.4.14	1:1:1	no dimer	F	3	10
2.4.15	1:0.5:1	A + B	F	none/4 **	5/10
2.4.16	1:2:1	no dimer	E + F	4	12
2.4.17	1:2:1	no dimer	D + E + F	2	9
2.4.18	1:1:1	no dimer	F	3	9

* NBA is an abbreviation of 5-nitrobarbiturate.

** There are two 5-nitrobarbiturates in each complex. Nitro group of one 5-nitrobarbiturate has no interaction in each complex, while 2 or 4 hydrogen-bonds formed by nitro group in the other 5-nitrobarbiturate.

(e). Tetra-alkylammonium ions as templates

Based on the crystal structures of nine complexes, we can draw some preliminary conclusion at this stage on the template effect. The large tetra-alkylammonium ions favor the formation of layer-type structures, and the smallest Me_4N^+ ion leads to a channel structure. However, using a middle-size tetra-alkylammonium ion, a balance between the two kinds of structures can be achieved by varying the molar ratio of the reactants and the reaction conditions. For complex **2.4.14** and **2.4.17**, the channel structure is present, while **2.4.11**, **2.4.13** and **2.4.16** all adopt a layer structure.

Comparing complex **2.4.10** and **2.4.11**, a smaller tetra-alkylammonium cation results in a smaller dihedral angle between linked dimeric units. In complex **2.4.12**, the small tetramethylammonium cation can be placed between two parallel zigzag ribbons. At the same time, the co-planar property of the nitrobarbiturate is changed in order to match the reach of the thiourea molecule, which uses its *syn* or *anti* hydrogens to connect with the oxygen atoms of nitrobarbiturate. In complex

2.4.15, the tetra-*n*-butylammonium cation is large, and hence an almost planar layer is generated.

5-Nitrobarbituric acid, from which one or two protons can be readily detached, is a versatile ingredient for supramolecular assembly through hydrogen bonding. Dimers of the monoanion have been found to be inter-connected in three distinct hydrogen-bonded connection modes (*para*-to-*para*, *ortho*-to-*ortho* and *para*-to-*ortho*), whereas that of the dianion can associate in the *para*-to-*para* fashion. A variety of hydrogen-bonded host networks constructed with these anions, in the presence of neutral components such as urea, thiourea and/or water molecules, are generated by the use of different-sized tetra-alkylammonium ions as templates. A properly selected combination of reactant molar ratio and specific tetra-alkylammonium ion yields complex **2.4.12**, which exhibits a most unusual crystal structure.

3.4.3 Discussion about inclusion compounds containing anions of imidazole-4,5-dicarboxylic acid

In Chapter 2.4.3, 1*H*-imidazole-4,5-dicarboxylic acid is used as a building block. Dimerization in the crystal structures of imidazole-4,5-dicarboxylic acid derivatives has been systematic studied.[106] It is easy to form a strong centrosymmetric hydrogen-bonded dimer exhibiting motif type [**A**] = $R_2^2(10)$ or type [**B**] = $R_2^2(8)$, as shown in Scheme 3.4.2. In the crystal structure of **2.4.19**, a pair of imidazole-4,5-dicarboxylate anions is connected by triple hydrogen bonds in type **B** fashion to form a centrosymmetric dimer. In contrast, no dimer of imidazole-4,5-dicarboxylate is found in **2.4.20**~**2.4.22**.

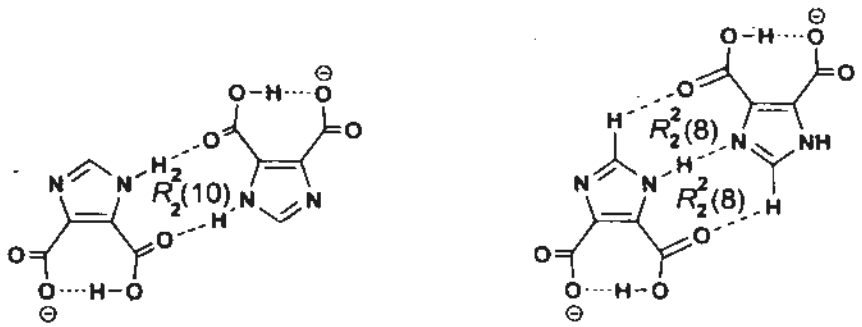

Scheme 3.4.2 Hydrogen-bonding connection modes reported between two adjacent imidazole-4,5-dicarboxylate derivatives.

Hydrogen-bonding connection modes and graph-set notations between imidazole-4,5-dicarboxylate and adjacent molecules studied in the thesis are given in Scheme 3.4.3. In the crystal structure containing the imidazole-4,5-dicarboxylate anion **2.4.21** and imidazole-4,5-dicarboxylate dianion **2.4.22**, both take type **D** and **E** or **F** connection modes with the same graph-set $R_2^2(9)$. In complex **2.4.20**, the type **C** connection mode occurs.

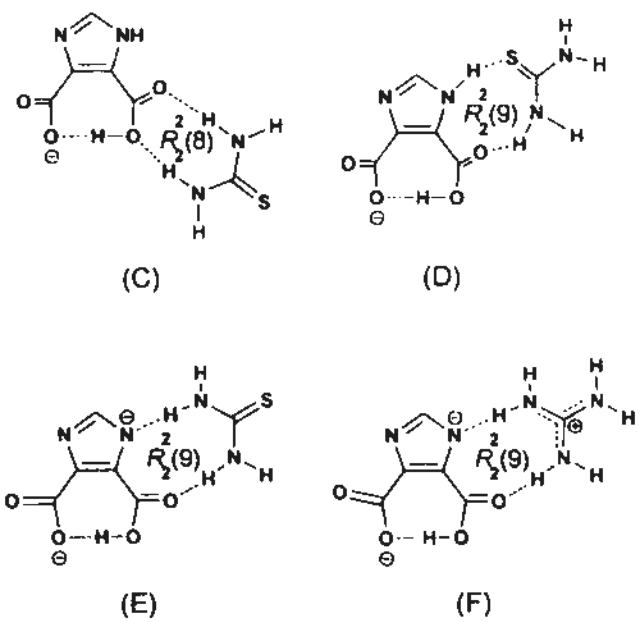

Scheme 3.4.3 Hydrogen-bonding connection modes and graph-set notations between imidazole-4,5-dicarboxylate and adjacent molecules studied in the thesis.

Details of the connection modes and related imidazole-4,5-dicarboxylate hydrogen bonding properties are listed in Table 3.4.4. In **2.4.19**, **2.4.20** and **2.4.22**, imidazole-4,5-dicarboxylate is used as a hydrogen-bond acceptor build block, while in **2.4.21** it severs as a hydrogen-bond donor as well as an acceptor.

1*H*-imidazole-4,5-carboxylate exhibits a strong tendency in generating layer type structures due to its rigidity, which is dependent on intramolecular hydrogen bonding and its effectiveness as a hydrogen-bond donor as well as acceptor, although tetraalkylammonium templates of different sizes are involved.

Table 3.4.4 Hydrogen bonds information of 1*H*-imidazole-4,5-carboxylate (Imdc) and connection modes in complex **2.4.19** to **2.4.22**.

Entry	Charge of Imdc	No. of Acceptor	No.of Donor	Max. Number of H-bond around Imdc	Graph-set between Imdc and neighboring molecules	Hydrogen bonding Type
2.4.19	1.5	4	0	4	$R_2^1(8)$	B
2.4.20	2	6	0	6	$R_2^1(8)$	C
2.4.21	1	5	1	6	$R_1^2(9)$	D and E
2.4.22	2	6	0	7	$R_2^1(9)$	F

3.5 Conclusions

In the present thesis, a rich variety of hydrogen-bonding patterns and topologies are described in the previous sections. Some supramolecular synthons involved in the construction of the host networks are particularly notable.

The linkage modes of some dimeric molecular species are listed in Scheme 3.5.1. Most of them are connected by pairwise hydrogen bonds with graph-set

$R_2^2(8)$, expect hydrogen bonding between dimeric squarate monoanion with $R_2^2(10)$ and head-to-tail dimeric urea with $R_2^1(6)$.

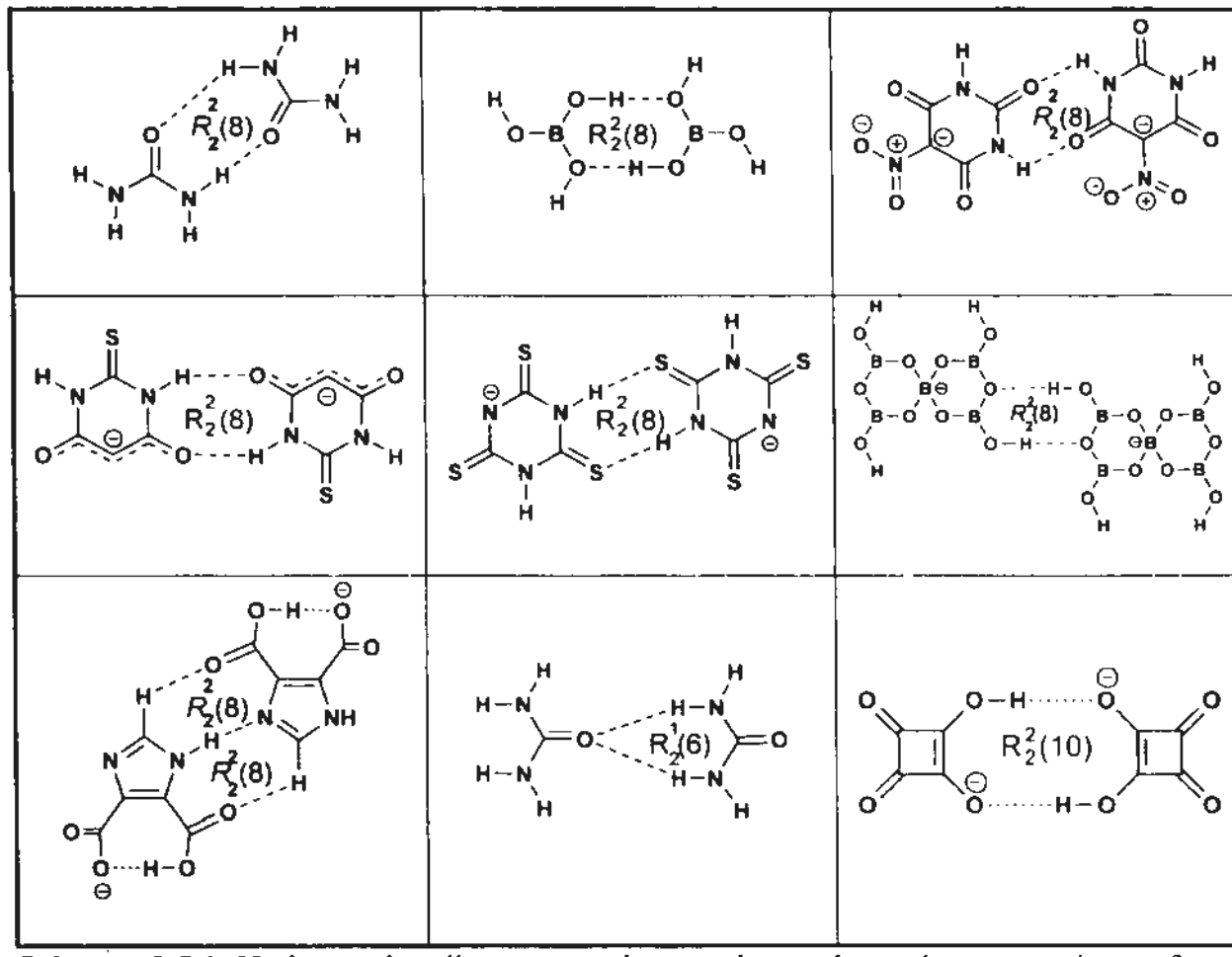

Scheme 3.5.1 Hydrogen-bonding connection modes and graph-set notations of dimeric building blocks.

Various supramolecular synthons involving urea/thiourea/guanidinium ions are summarized in Scheme 3.5.2. There are two main kinds of supramolecular synthons: (a) pairwise hydrogen bonds, and (b) chelating hydrogen bond with graph-set $R_2^2(8)$ or $R_2^2(9)$ and $R_2^1(6)$, respectively.

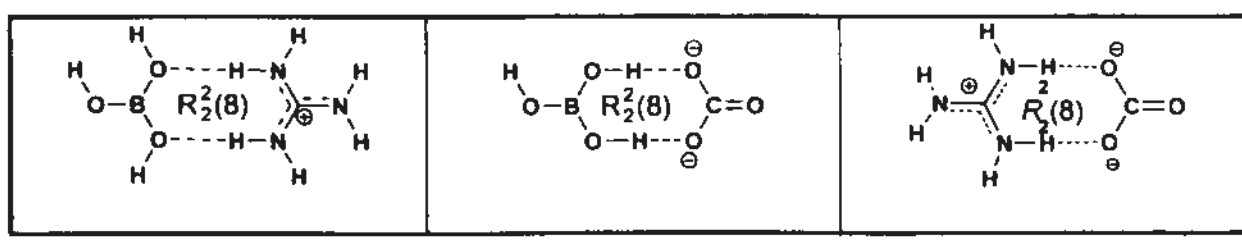

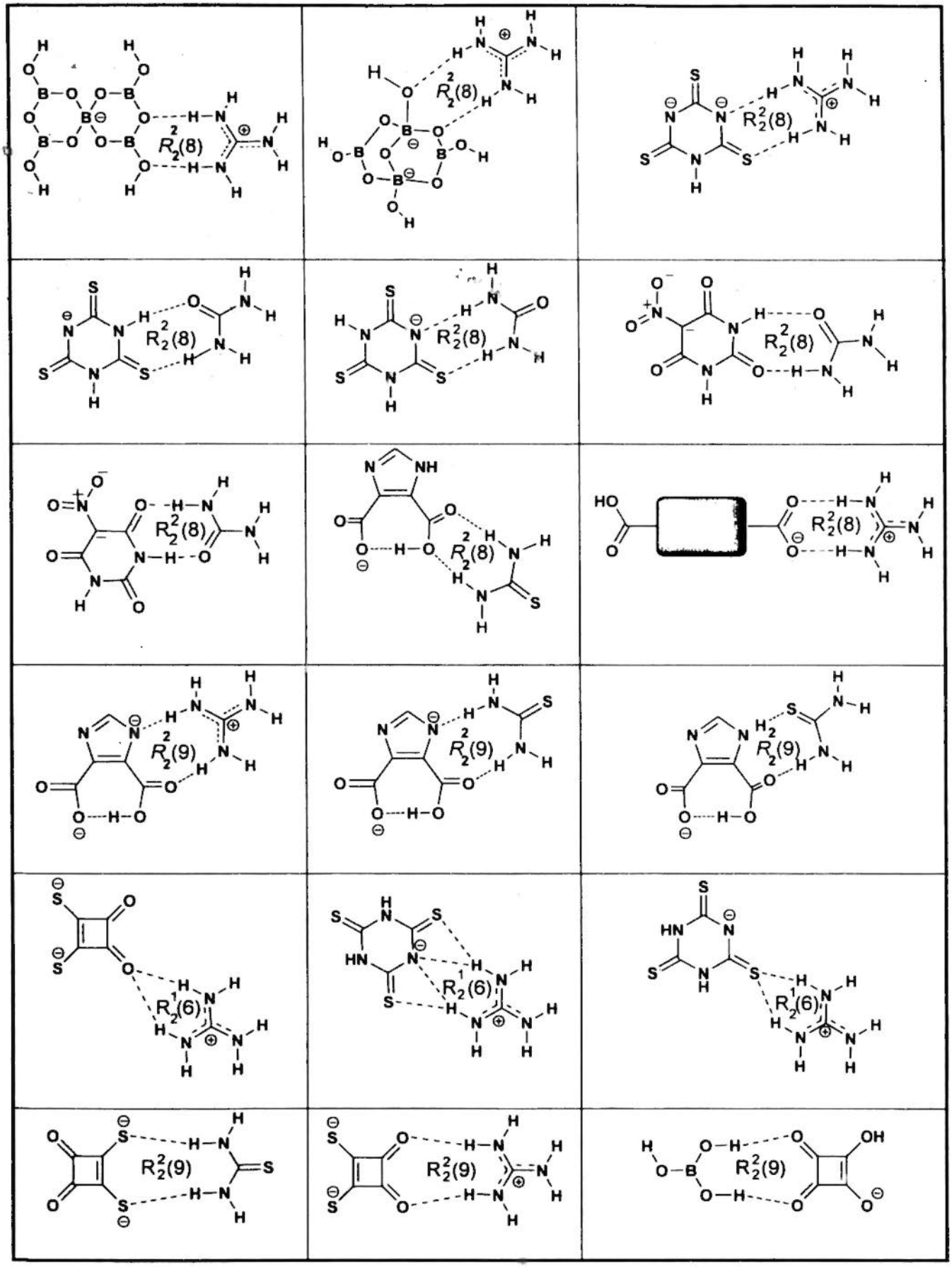
R22(8)
R22(8)
R22(8)
R22(8)
R22(8)
R22(8)
R22(8)
R22(8)
R22(8)
R22(9)
R22(9)
R22(9)
R21(6)
R21(6)
R21(6)
R22(9)
R22(9)
R22(9)

Scheme 3.5.2 Hydrogen-bonding connection modes and graph-set notations between urea/thiourea/guanidinium and main building blocks.

In addition, flexible building blocks, such as those containing solvated water molecules, also play an important role in crystal engineering. The cooperativity of water hydrogen bonding in **2.1.10**, **2.4.19**, **2.4.21** and **2.4.22** facilitates the construction and stabilization of hydrogen-bonded networks, leading to the interplay of flexible (water cluster) and rigid (urea, carboxylate, etc.) supramolecular synthons in crystal engineering. Some examples are shown below (Scheme 3.5.3).

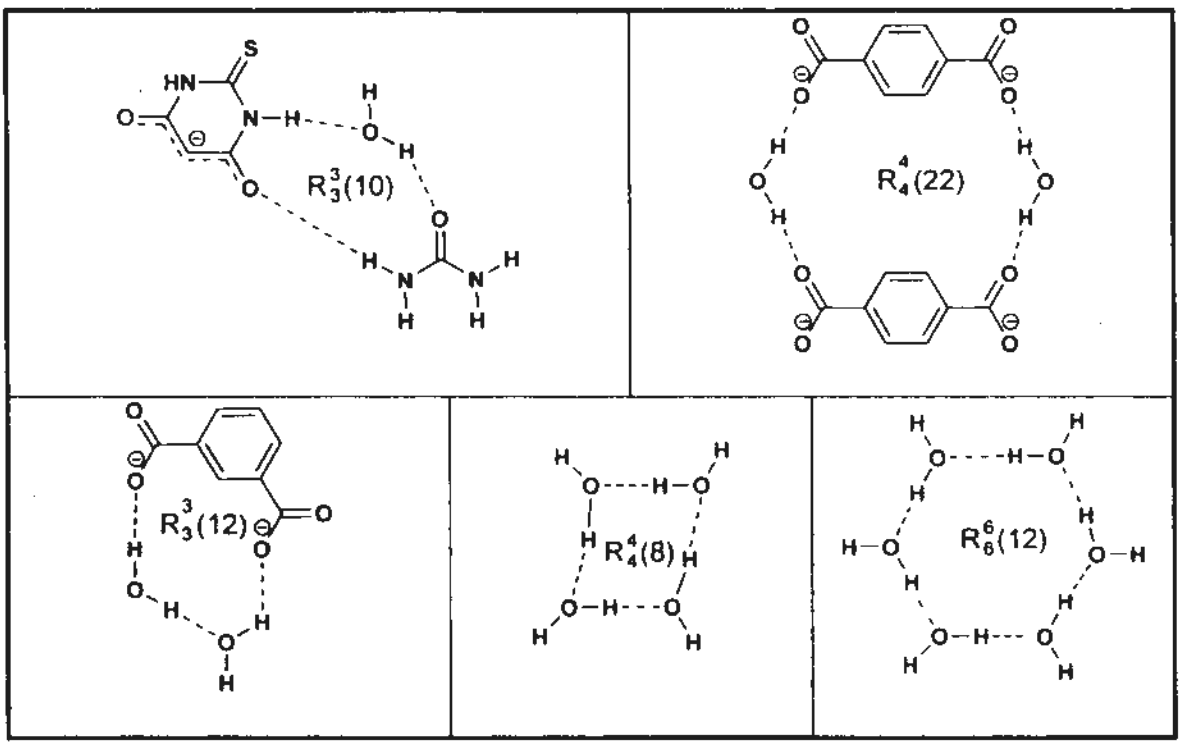

Scheme 3.5.3 Hydrogen-bonding connections and graph-set notations between main building blocks and water molecules.

Maddox's famous statement made in an editorial in Nature in 1988 is still valid today: "*One of the continuing scandals in the physical sciences is that it remains in general impossible to predict the structure of even the simplest crystalline solids from a knowledge of their chemical composition.*" Therefore, a

better understanding of the patterns of non-bonded interactions will definitely continue to be pursued by workers in the field of crystal design and prediction.

Chapter 4. Experimental

4.1 Preparation

4.1.1 Materials and physical measurements

Commercially available thiourea, urea, guanidinium carbonate (commonly known as guanidine carbonate), Kemp's triacid (*cis*,*cis*-1,3,5-trimethylcyclohexane-1,3,5-tricarboxylic acid), squaric acid, naphthalene-2,6-dicarboxylic acid, 1,4-biphenyl dicarboxylic acid, terephthalic acid, isophthalic acid, 2-thiobarbituric acid, trithiocyanuric acid, 5-nitrobarbituric acid, imidazole-4,5-dicarboxylic acid, aqueous tetramethylammonium hydroxide, tetraethylammonium hydroxide, tetra-*n*-propylammonium hydroxide and tetra-*n*-butylammonium hydroxide were used as received without further purification.

IR spectra were recorded with KBr pellets on a Nicolet Impact 420 FT-IR spectrometer in the region of 4000-400 cm^{-1}. Melting points (uncorrected) were measured on a IA9100 Electrothermal Digital Melting Point Apparatus.

Sodium dithiosquarate,[107] 1,1'-biphenyl-2,2',6,6'-tetracarboxylic acid[108] and *N*,*N*'-bis(carboxymethyl)-4,4'-bipyridinium[109] were prepared according to literature methods.

4.1.2 Preparation of complexes

For **2.1.1** and **2.1.2**, boric acid and guanidinium carbonate were mixed in an aqueous solution in molar ratio of 2:1 (**2.1.1**) and in MeOH/H_2O solution (v:v = 1:4) in a molar ratio of 1:1 (**2.1.2**). The solution was stirred for about 5 minutes and slight heated to about 303 K for about 15 minuets and then filtered. The colorless filtrate was subjected to slow evaporation at room temperature in a desiccator

charged with anhydrous silica gel, which yielded colorless crystals in the form of large blocks after a few weeks.

For **2.1.3**, a molar equivalent of tetraethylammonium hydroxide is added into an aqueous solution of boric acid. CO_2 was bubbled through the solution for about 15 minutes and then filtered. The colorless filtrate was subjected to slow evaporation at room temperature in a desiccator charged with anhydrous silica gel.

For **2.1.4**, guanidinium carbonate (24 mg, 0.2 mmol) and tetra-*n*-propylammonium hydroxide were mixed in a molar ratio of 1:1, and a minimum quantity of water was added to dissolve the solid. After CO_2 was bubbled through the solution for about 30 minutes, two molar equivalents of boric acid in an aqueous solution (24 mg, 0.4 mmol) were slowly added. The solution was stirred for about 15 minutes and then filtered. Colorless block-like crystals of **2.1.4** were deposited in nearly quantitative yield over a period of several weeks. M.p. 178.0–179.6 °C. IR (KBr): 3345, 2975, 2884, 2471, 1922, 1694, 1626, 1596, 1493, 1488, 1460, 1385, 1183, 1148, 1032, 1006, 969, 876, 836, 758, 707, 665, 570, 517 cm^{-1}.

For **2.1.5**, squaric acid was neutralized with a molar equivalent of tetra-*n*-butylammonium hydroxide. Then, the 1:1 (molar ratio) boric acid aqueous solution was added. The solution is evaporated at room temperature in a desiccator charged with anhydrous silica gel to obtain colorless crystals.

For **2.1.6** to **2.1.8**, the corresponding tetraalkylammonium hydroxide aqueous bases were added in 1:1(molar ratio) in **2.1.6**, and 1:2 in **2.1.7** and **2.1.8**. Then, different molar equivalents of thiourea were added for each experiment: two, four and six molar equivalents, respectively. M.p.129.1–131.0 °C (**2.1.6**), 92.3–94.8 °C (**2.1.7**), and 131.1–132.5 °C (**2.1.8**).

For **2.1.9**, aqueous tetra-*n*-butylammonium hydroxide (0.2 mmol) was added to sodium dithiosquarate (38 mg, 0.2 mmol) and guanidinium carbonate (24 mg, 0.2 mmol) and stirred for about 15 minutes and then filtered. The yellow filtrate was subjected to slow evaporation at room temperature in a desiccator charged with anhydrous silica gel. Deposition of **2.1.9** as yellow rectangular prisms occurred in nearly quantitative yield over a period of several weeks. M.p. 148.5–149.2 °C. IR (KBr): 3362, 3135, 2959, 2937, 2874, 1705, 1646, 1631, 1555, 1483, 1336, 1324, 1201, 1151, 941, 923, 739, 630, 523 cm^{-1}.

For **2.1.10**, 1,1'-biphenyl-2,2',6,6'-tetracarboxylic acid was neutralized with one molar equivalent tetramethylammonium hydroxide solution and then filtered. M.p. 266.9–269.3 °C.

For **2.1.11** and **2.1.12**, 1,1'-biphenyl-2,2',6,6'-tetracarboxylic acid was neutralized with two or one molar equivalent of the corresponding base in **2.1.11** or **2.1.12**, respectively. Two molar equivalents of thiourea was added for **2.1.11** and one molar equivalent of guanidinium was added for **2.1.12**. About 5 ml of deionized water was added to fully dissolve the solid, and the solution was stirred for about 5 minutes then filtered. The filtrate was subjected to slow evaporation at room temperature in a desiccator charged with anhydrous silica gel. M.p. 283.9–287.2 °C (**2.1.11**) and M.p. 242.1–244.3 °C (**2.1.12**)

For the synthesis of **2.1.13**, 1,1'-biphenyl-2,2',6,6'-tetracarboxylic acid (33 mg, 0.1 mmol) was neutralized with two molar equivalents of aqueous tetraethylammonium hydroxide (0.2 mmol). Next, guanidinium carbonate (12 mg, 0.1 mmol) was added and the solution was stirred for about 15 minutes and then filtered. The colorless filtrate was subjected to slow evaporation at room temperature in a desiccator charged with anhydrous silica gel. Deposition of **2.1.13** in the form of

colorless blocks occurred in nearly quantitative yield over a period of several weeks. M.p. 257.2–259.8 °C. IR (KBr): 3430, 2993, 2610, 1730, 1715, 1698, 1613, 1579, 1463, 1435, 1388, 1236, 1176, 1150, 1034, 1000, 883, 821, 779, 697, 669, 654, 577 cm^{-1}.

For the synthesis of **2.1.14**, 1,1'-biphenyl-2,2',6,6'-tetracarboxylic acid (33 mg, 0.1 mmol) was neutralized with two molar equivalents of aqueous tetra-*n*-propylammonium hydroxide (0.2 mmol). Next, guanidinium carbonate (12 mg, 0.1 mmol) was added and the solution was stirred for about 15 minutes and then filtered. The colorless filtrate was subjected to slow evaporation at room temperature in a desiccator charged with anhydrous silica gel. Compound **2.1.14** was obtained as colorless block-like crystals in nearly quantitative yield over a period of several weeks. M.p. 317.9–320.1 °C. IR (KBr): 3359, 3168, 2975, 2885, 1688, 1607, 1557, 1473, 1435, 1385, 1336, 1270, 1141, 988, 837, 820, 790, 764, 693, 625, 578, 556, 526 cm^{-1}.

For **2.2.1** and **2.2.2**, tetramethylammonium hydroxide solution or guanidinium carbonate was added into an aqueous solution of Kemp's triacid in 1:1 molar ratio. Increasing the molar ratio of guanidinium carbonate to three molar equivalents resulted in the formation of **2.2.4**. For **2.2.5** and **2.2.6**, Kemp's triacid was deprotonated by one molar equivalent of the corresponding aqueous base. Guanidinium carbonate was added in two molar equivalents in **2.2.5** and **2.2.6**. For **2.2.3**, an aqueous solution of Kemp's triacid was neutralized by one half-equivalent of tetraethylammonium hydroxide, and then one molar equivalent guanidinium carbonate was added. An additional 2 ml of EtOH was introduced. The colorless solution was subjected to slow evaporation at room temperature in a desiccator charged with anhydrous silica gel. M.p. 247.5–248.1 °C. IR (KBr): 3393, 3071,

3018, 2959, 2929, 1681, 1562, 1557, 1470, 1450, 1421, 1403, 1375, 1355, 1328, 1227, 1301, 1206, 1010, 993, 975, 956, 948, 890, 863, 834, 775, 640, 598, 542 cm^{-1} (**2.2.1**); M.p. 257.5–258.2 °C. IR (KBr): 3391, 3066, 2991, 2980, 1720, 1687, 1662, 1546, 1470, 1444, 1422, 1402, 1358, 1336, 1309, 1208, 1171, 1091, 1002, 978, 902, 888, 865, 832, 788, 704, 637, 564 cm^{-1} (**2.2.2**); M.p. 222.6–234.2 °C. IR (KBr): 3400, 3057, 2980, 2838, 1689, 1664, 1545, 1487, 1471, 1442, 1403, 1357, 1336, 1309, 1220, 1209, 1184, 1173, 1094, 1047, 1002, 888, 866, 830 ,791, 666, 625, 564 cm^{-1}(**2.2.3**); M.p. 278.5–279.2 °C. IR (KBr): 3384, 3051, 2953, 1680, 1544, 1488, 1470, 1402, 1358, 1338, 1309, 1232, 1208, 1157, 1106, 1047, 1007, 982, 956, 948, 904, 887, 829, 800, 791, 780, 673, 564 cm^{-1} (**2.2.4**); M.p. 280.8–283.5 °C. IR (KBr): 3360, 3153, 2972, 2940, 1661, 1628, 1508, 1472, 1459, 1394, 1383, 1331, 1174, 1101, 1037, 1107, 1037, 1007, 982, 970, 922, 885, 933, 757, 703, 663, 555 cm^{-1} (**2.2.5**); M.p. 238.5–239.9 °C. IR (KBr): 3378, 3058, 2980, 2954, 1688, 1668, 1546, 1487, 1470, 1439, 1403, 1358, 1309, 1220, 1208, 1158, 1093, 1007, 1047, 979, 956, 948, 885, 830, 802, 755, 701, 622, 563 cm^{-1} (**2.2.6**).

Adducts **2.3.2** and **2.3.3** were prepared by mixing an aqueous solution of naphthalene-2,6-dicarboxylic acid or 1,4-biphenyl dicarboxylic acid, respectively, with guanidinium carbonate in a 2:1 molar ratio. **2.3.1**, and **2.3.4** to **2.3.6** were prepared by mixing terephthalic acid, 1,4-biphenyl dicarboxylic acid or isophthalic acid with guanidinium carbonate in the corresponding tetraalkylammonium hydroxide solution in a molar ratio of 1:2:2 in **2.3.1**, in 1:2:1 in **2.3.4**, 1:1:2 in **2.3.5** and 1:1:1 in **2.3.6**. An additional molar quantity of 1:1 guanidine carboxylic acid : guanidinium carbonate was also added into the reaction mixture to obtain **2.3.5**. The solution was subjected to slow evaporation of solvent at ambient temperature in a

desiccator charged with drierite. Diffraction-quality crystals were obtained in nearly quantitative yield over a period of several weeks. M.p. 235.3–236.1 °C (**2.3.1**), 243.1–245.0 °C (**2.3.2**), 207.7–208.6 °C (**2.3.3**), 222.6–224.0 °C (**2.3.4**), 215.6–218.2 °C (**2.3.5**) and 278.2–281.0 °C (**2.3.6**).

Crystal **2.3.7** was obtained by crystallization from aqueous solution of *N,N'*-di(carboxymethyl)-4,4'-bipyridinium. The crystal decomposed at 120 °C. For **2.3.8**, guanidinium carbonate was added to the aqueous solution of *N,N'*-di(carboxymethyl)-4,4'-bipyridinium, then CO_2 was bubbled through the solution for about 30 minutes and filter. The filtrate was subjected to slow evaporation at room temperature in a desiccator charged with anhydrous silica gel to obtain block crystals over a period of several weeks.

Diffraction quality crystals of complexes **2.4.1**~**2.4.3** were prepared by crystallizing the two or three components: 2-thiobarbituric acid and tetraethylammonium hydroxide solution from EtOH/H_2O (v:v = 1:1) for **2.4.1** and from water for **2.4.2**, 2-thiobarbituric acid, urea and tetra-*n*-propylammonium hydroxide aqueous solution in molar ratio 1:1:1 for **2.4.3**. Trithiocyanuric acid was crystallized from an aqueous solution of the corresponding base to obtain crystals **2.4.4** and **2.4.5**. For **2.4.6**~**2.4.8**, trithiocyanuric acid was neutralized with one molar equivalent of aqueous tetraalkylammonium hydroxide solution in **2.4.7**~**2.4.9**, and two molar equivalents in **2.4.6**. Then five equivalents of urea was added for **2.4.6**. One molar equivalent of thiourea or guanidinium carbonate was added for **2.4.7** and **2.4.8**/**2.4.9**, respectively. M.p. 248.6–249.2 °C (**2.4.1**), 256.9–258.3 °C (**2.4.2**), 209.3–212.2 °C (**2.4.3**), 189.8–190.2 °C (**2.4.4**), 205.6–207.5 °C (**2.4.5**),

233.2–236.0 °C (**2.4.6**), 208.5–210 °C (**2.4.7**), 229.0–229.5 °C (**2.4.8**), and 233.6–236.7 °C (**2.4.9**).

For **2.4.10**, 5-nitrobarbituric acid (52 mg, 0.3 mmol) was neutralized with one molar equivalent of aqueous tetramethylammonium hydroxide (0.3 mmol). The solution was stirred for about 5 minutes and then filtered. The yellow filtrate was subjected to slow evaporation at room temperature in a desiccator charged with anhydrous silica gel. Deposition of yellow block-like crystals of **2.4.10** occurred in nearly quantitative yield over a period of several weeks. Decomposition temp. *ca.* 310 °C. IR (KBr): 3389, 3175, 3019, 2836, 1721, 1651, 1488, 1448, 1432, 1385, 1283, 1254, 1068, 957, 948, 854, 792, 756, 693, 616, 529 cm^{-1}.

For **2.4.11**, 5-nitrobarbituric acid (52 mg, 0.3 mmol) was neutralized with one molar equivalent of aqueous tetra-*n*-propylammonium hydroxide (0.3 mmol). A minimum quantity of water was used to dissolve the solid, and the solution was stirred for about 15 minutes and then filtered. Yellow block-like crystals of **2.4.11** were deposited in nearly quantitative yield over a period of several weeks. M.p. 238–239.5 °C. IR (KBr): 3412, 3141, 3027, 2995, 2972, 2961, 2928, 2870, 1727, 1651, 1487, 1449, 1432, 1386, 1294, 1146, 1060, 1031, 1011, 971, 853, 829, 792, 756, 767, 694, 616, 530 cm^{-1}.

For **2.4.12**, 5-nitrobarbituric acid (52 mg, 0.3 mmol) was neutralized with one molar equivalent of aqueous tetramethylammonium hydroxide (0.3 mmol). A minimum quantity of water was used to dissolve the solid, and thiourea (11 mg, 0.15 mmol) was added to the solution, which was then stirred for about 15 minutes and filtered. The yellow filtrate was subjected to slow evaporation at room temperature in a desiccator charged with anhydrous silica gel. Yellow block-like crystals of **2.4.12** were deposited in nearly quantitative yield over a period of several weeks.

The crystals decompose at about 260 °C. IR (KBr): 3392, 3173, 3019, 2835, 1723, 1651, 1487, 1443, 1434, 1385, 1289, 1254, 1067, 947, 853, 792, 756, 615, 529, 462 cm^{-1}.

For **2.4.13**, 5-nitrobarbituric acid (52 mg, 0.3 mmol) was neutralized with two molar equivalents of aqueous tetraethylammonium hydroxide (0.6 mmol). A minimum quantity of water was used to dissolve the solid, and thiourea (46 mg, 0.6 mmol) was added to the solution in a 1:2 molar ratio for acid: thiourea. The solution was then stirred for about 15 minutes and filtered. The yellow filtrate was subjected to slow evaporation at room temperature in a desiccator charged with anhydrous silica gel. Yellow block-like crystals of **2.4.13** were deposited in nearly quantitative yield over a period of several weeks. M.p. 121–122.5 °C. IR (KBr): 3349, 3270, 3172, 3007, 2838, 1723, 1656, 1609, 1484, 1449, 1387, 1292, 1173, 1147, 1076, 1000, 853, 792, 756, 733, 694, 616, 531 cm^{-1}.

For **2.4.14**, the above procedure was repeated with 5-nitrobarbituric acid (52 mg, 0.3 mmol), aqueous tetra-*n*-propylammonium hydroxide (0.3 mmol) and thiourea (23 mg, 0.3 mmol) to obtain yellow block-like crystals of **2.4.14** in nearly quantitative yield. M.p. 101.5–102.5 °C. IR (KBr): 3515, 3445, 3326, 3284, 3167, 3028, 2994, 2972, 2930, 2871, 1724, 1660, 1651, 1621, 1487, 1449, 1385, 1293, 1256, 1147, 1087, 1032, 1009, 971, 909, 853, 793, 767, 757, 745, 727, 694, 616, 531 cm^{-1}.

For **2.4.15**, the previous procedure was repeated with 5-nitrobarbituric acid (52 mg, 0.3 mmol), tetra-*n*-butylammonium hydroxide (0.3 mmol) and thiourea (11 mg, 0.15 mmol) to obtain yellow block-like crystals of **2.4.15** in nearly quantitative

yield. M.p. 111–113.0 °C. IR (KBr): 3348, 3148, 2962, 2875, 1723, 1651, 1486, 1449, 1385, 1292, 1147, 1008, 880, 792, 756, 744, 694, 616, 530 cm^{-1}.

For **2.4.16**, 5-nitrobarbituric acid (52 mg, 0.3 mmol) was neutralized with one molar equivalent of aqueous tetraethylammonium hydroxide (0.3 mmol). A minimum quantity of water was used to dissolve the solid, and urea (36 mg, 0.6 mmol) was added to the solution. The solution was then stirred for about 15 minutes and filtered. The yellow filtrate was subjected to slow evaporation at room temperature in a desiccator charged with anhydrous silica gel. Yellow block-like crystals of **2.4.16** were deposited in nearly quantitative yield over a period of several weeks. M.p. 102–103.5 °C. IR (KBr): 3437, 3369, 3174, 2981, 1695, 1645, 1633, 1568, 1489, 1442, 1392, 1369, 1174, 1055, 1001, 785, 704, 611, 518 cm^{-1}.

For **2.4.17**, the previous procedure was repeated with 5-nitrobarbituric acid (52 mg, 0.3 mmol), tetra-*n*-propylammonium hydroxide (0.3 mmol), and urea (36 mg, 0.6 mmol) to yield yellow block-like crystals of **2.4.17**. M.p. 198–200.5 °C. IR (KBr): 3393, 3167, 3028, 2978, 2879, 2839, 1730, 1652, 1628, 1481, 1448, 1432, 1389, 1230, 1183, 1147, 1028, 968, 854, 792, 757, 694, 616, 562, 529 cm^{-1}.

For **2.4.18**, the above procedure was repeated with 5-nitrobarbituric acid (52 mg, 0.3 mmol), tetra-*n*-butylammonium hydroxide (0.3 mmol), and urea (18 mg, 0.3 mmol) to obtain yellow block-like crystals of **2.4.18**. M.p.168–170.0 °C. IR (KBr): 3451, 3408, 3184, 2963, 2876, 2840, 1762, 1723, 1689, 1651, 1634, 1487, 1435, 1385, 1290, 1242, 1172, 1144, 1057, 1028, 1009, 879, 831, 793, 758, 693, 683, 615, 546, 531, 513 cm^{-1}.

For **2.4.19** to **2.4.22**, 1*H*-imidazole-4,5-dicarboxylic acid was neutralized with two or one molar equivalent of aqueous tetraalkylammonium hydroxide in

2.4.19/2.4.20 and **2.4.21/2.4.22**, respectively. Next, thiourea was added in molar ratio 1:2 and 1:1 in **2.4.20** and **2.4.21**, respectively, and the solution was stirred for about 5 minutes then filtered. For **2.4.22**, one molar equivalent of guanidinium carbonate was added. The solutions were subjected to slow evaporation of solvent at ambient temperature in a desiccator charged with drierite. Diffraction-quality crystals were obtained in nearly quantitative yield over a period of several weeks. M.p.177.2–177.3 °C (**2.4.19**), 182.7–183.3 °C (**2.4.20**), 188.7–189.6 °C (**2.4.21**), 193.1–195.8 °C (**2.4.22**).

4.2 X-ray crystallography

Intensity data of compound were collected on a Bruker SMART 1000 CCD system with Mo *Kα* radiation (λ = 0.71073 Å) or on a BrukerAXS Kappa APEX II CCD diffractometer with Cu *Kα* radiation (λ = 1.54178 Å) from a sealed-tube generator. Data collection and reduction were performed using SMART and SAINT software,[110] and empirical absorption corrections were applied.[111] All the structures were solved by direct methods and refined by full-matrix least squares on F^2 using the SHELXTL program package.[112]

Oxford Cryostream 700 Plus® system was used for low-temperature data collection. Reflection data for complex **2.1.7**, **2.2.3**, **2.3.5** and **2.4.20** were collected at 173 K, and those for other complexes were collected at 293 K.

Crystal data are tabulated in **Appendix II**. Final atomic coordinates, thermal parameters, bond lengths and bond angles, along with their estimated standard deviations are present in **Appendix III**, of which an electronic version is available.

References

1. Powell, H. M. *J. Chem. Soc.* **1948**, 61.
2. Mandelcorn, L. Ed. *Non-stoichiometric compounds*, Academic Press: New York, **1964**.
3. Takemoto, K.; Sonoda, N. in *Inclusion Compounds*, Ed. Atwood, J. I.; Davies, J. E. D.; MacNicol, D. D. Academic Press: London, **1985**, vol. 2, pp. 47.
4. For examples: (a) Carruthers, C.; Ronson, T. K.; Sumby, C. J.; Westcott, A.; Harding, L. P.; Prior, T. J.; Riskallah, P.; Hardie, M. J. *Chem. Eur. J.* **2008**, *14*, 10286. (b) Dong, C. Q; Shao, L. W.; Guo, J. C.; Ren, J. C. *Chem. Phys. Chem.* **2008**, *9*, 2245. (c) Gadde, S.; Batchelor, E. K.; Weiss, J. P.; Ling, Y. H.; Kaifer, A. E. *J. Am. Chem. Soc.* **2008**, *130*, 17114. (d) Braga, D.; Desiraju, G. R.; Miller, J. S.; Orpen, A. G.; Price, S. L. *CrystEngComm.* **2002**, *4*, 500. (e) Braga, D.; Grepioni, F. *Acc. Chem. Res.* **2000**, *33*, 601. (f) Vögtle, F. *Comprehensive Supramolecular Chemistry*, Pergamon Press: Oxford, **1996**, vol. 2. (g) Gokel, G. W. *Comprehensive Supramolecular Chemistry*, Pergamon Press: Oxford, **1996**, vol. 1. (h) Nassimbeni, L. R. *Acc. Chem. Res.* **2003**, *36*, 631. (i) Hamilton, A. D. *Tetrahedron* **1995**, *51*, 343. (j) Gellman, S. H. *Chem. Rev.* **1997**, *97*, 1231.
5. For examples: (a) Felicitas, S.; Daniel, E; Cokoja, M.; Maurits, W. E. van den B.; Oleg, I. L.; Gustaaf, V. T.; Bernadeta, W.; Gerd, B.; Hans-Heinrich, L.; Bruno, C; Fischer, R. A. *J. Am. Chem. Soc.* **2008**, *130*, 6119. (b) Schwarz, P.; Siebel, E.; Fischer, R. D.; Apperley, D. C.; Davies, N. A.; Harris, R. K. *Angew. Chem. Int. Ed.* **1995**, *34*, 1197. (c) Li, H.; Eddaoudi, M.; O'Keeffe, M.; Yaghi, O. M. *Nature* **1999**, *402*, 276.

6. For examples: (a) Brown, M. E.; Hollingsworth, M. D. *Nature* **1995**, *376*, 323. (b) Małuszyńska, H.; Czarnecki, P. *Z. Kristallogr.* **2006**, *221*, 218. (c) Hollingsworth, M. D.; Peterson, M. L.; Pate, K. L.; Dinkelmeyer, B. D.; Brown, M. E. *J. Am. Chem. Soc.* **2002**, *124*, 2094.

7. For examples: (a) Ramamurthy, V.; Eaton, D. F. *Chem. Mater.* **1994**, *6*, 1128. (b) Rashid, A. N.; Kirschbaum, K.; Shoemaker, R. K. *J. Mol. Struct.* **2006**, *785*, 1. (c) Harris, K. D. M.; Jupp, P. E. *Chem. Phys. Lett.* **1997**, *274*, 525. (d) Hulliger, J.; Rogin, P.; Quintel, A.; Rechsteiner, P.; Konig, O.; Wubbenhorst, M. *Adv. Mater.* **1997**, *9*, 677.

8. Pramanik, A.; Bhuyan, M.; Das. G. *J. Photochem. Photobiol.* **2008**, *197*, 149.

9. Binkowski, C.; Hapiot, F.; Lequart, V.; Martin, P.; Monflier, E. *Org. Biomol. Chem.* **2005**, *3*, 1129.

10. Süss, H. I.; Hulliger, J. Microporous Mesoporous *Mater.* **2005**, *78*, 23.

11. Chae, H. K.; Siberio-Perez, D. Y.; Kim, J.; Go, Y. B.; Eddaoudi, M.; Matzger, J.; O'Keeffe, M.; Yaghi, O. M. *Nature* **2004**, *427*, 523.

12. Müller, M.; Lebedev, O. L.; Fischer, R. A. *J. Mater. Chem.* **2008**, *18*, 5274.

13. Haneda, T.; Kawano, M.; Kojima, T.; Fujita, M. *Angew. Chem. Int. Ed.* **2007**, *46*, 6643.

14. Holman, K. T.; Pivovar, A. M.; Ward, M. D. *Science* **2001**, *294*, 1907.

15. Horner, M. J.; Holman, K. T.; Ward, M. D. *J. Am. Chem. Soc.* **2007**, *129*, 14640.

16. For examples: (a) Holman, K. T.; Pivovar, A. M.; Swift, J. A.; Ward, M. D. *Acc. Chem. Res.* **2001**, *34*, 107. (b) Holman, K. T.; Martin, S. M.; Parker, D. P.; Ward, M. D. *J. Am. Chem. Soc.* **2001**, *123*, 4421.

17. (a) Mark, H.; Weissenberg, K. *Z. Phys.* **1923**, *16*, 1. (b) Hendricks, S. B. *J. Am. Chem. Soc.* **1928**, *50*, 2455. (c) Wyckoff, R. *Z. Phys.* **1930**, *75*, 529. (d) Wyckoff, R. *Z. Kristallogr.* **1932**, *81*, 102. (e) Wyckoff, R. Z.; Corey, R. B. *Z. Kristallogr.* **1934**, *891*, 462.

18. (a) Schlenk, W. *Liebigs Ann. Chem.* **1949**, *565*, 204. (b) Schlenk, W. *Angew. Chem.* **1950**, *62*, 299.

19. For examples: (a) Lee, S.-O.; Kariuki, B. M.; Harris, K. D. M. *New J. Chem.* **2005**, 1266. (b) Harris, K. D. M. in *Encyclopaedia of Supramolecular Chemistry*, Ed. Atwood J. L.; Steed, J. W.; Dekker, M. New York, **2004**, vol. 2, pp. 1538. (c) Lee, S.-O.; Kariuki, B. M.; Richardson, A. L.; Harris, K. D. M. *J. Am. Chem. Soc.* **2001**, *123*, 12684. (d) Harris, K. D. M. *Chem. Soc. Rev.* **1997**, *26*, 279. (e) Hollingsworth, M. D.; Brown, M. E.; Hillier, A. C.; Santarsiero, B. D.; Chaney, J. D. *Science* **1996**, *273*, 1355. (f) Hollingsworth, M. D.; Harris, K. D. M. in *Comprehensive Supramolecular Chemistry*, Ed. MacNicol, D. D.; Toda, F.; Bishop, R. Pergamon Press: Oxford, **1996**, vol. 6, pp. 177. (g) Lee, S.-O.; Kariuki, B. M.; Harris, K. D. M. *Angew. Chem. Int. Ed.* **2002**, *41*, 2181. (h) Hollingsworth, M. D.; Santarsiero, B. D.; Harris, K. D. M. *Angew. Chem. Int. Ed.* **1994**, *33*, 649. (i) Park, K.-M.; Iwamoto, T. *J. Chem. Soc., Chem. Commun.* **1992**, 72. (j) Hough, E.; Nicholson, D. G. *J. Chem. Soc., Dalton Trans.* **1978**, 15. (k) Schiessler, R. W.; Flitter, D. *J. Am. Chem. Soc.* **1950**, *74*, 1720.

20. For representative reviews: (a) Schneider, H.-J.; Yatsimirsky, A. K. *Chem. Soc. Rev.* **2008**, 263. (b) Blondeau, P.; Segura, M.; Pérez-Fernández, R.; Mendoza, J. de, *Chem. Soc. Rev.* **2007**, 198. (c) Miyata, M.; Tohnai, N.; Hisaki, I. *Acc. Chem. Res.* **2007**, *40*, 694. (d) Wan, Y.; Yang, H.; Zhao, D. *Acc. Chem. Res.*

2006, *39*, 423. (e) Nishikiori, S.-i.; Yoshikawa, H.; Sano, Y.; Iwamoto, T. *Acc. Chem. Res.* **2005**, *38*, 227. (f) Nassimbeni, L. R. *Acc. Chem. Res.* **2003**, *36*, 631. (g) Seidel, S. R.; Stang, P. J. *Acc. Chem. Res.* **2002**, *35*, 972. (h) Hawthorne, M. F.; Zheng, Z. *Acc. Chem. Res.* **1997**, *30*, 267. (i) Cram, D. J.; Cram, J. M. *Acc. Chem. Res.* **1978**, *11*, 8.

21. For representative reviews: (a) Radhakrishnan, T. P. *Acc. Chem. Res.* **2008**, *41*, 367. (b) Plass, K. E.; Grzesiak, A. L.; Matzger, A. J. *Acc. Chem. Res.* **2007**, *40*, 287. (c) Dalgarno, S. J.; Thallapally, P. K.; Barbour, L. J.; Atwood, J. L. *Chem. Soc. Rev.* **2007**, 236. (d) Chen, X.-M.; Tong, M.-L. *Acc. Chem. Res.* **2007**, *40*, 162. (e) Glaser, R. *Acc. Chem. Res.* **2007**, *40*, 9. (f) Dalgarno, S. J.; Thallapally, P. K.; Barbour, L. J.; Atwood, J. L. *Chem. Soc. Rev.* **2007**, 236. (g) Metrangolo, P.; Neukirch, H.; Pilati, T.; Resnati, G. *Acc. Chem. Res.* **2005**, *38*, 386. (h) Kellam, B.; Bank, P. A. De; Shakesheff, K. M. *Chem. Soc. Rev.* **2003**, 327. (i) Evans, O. R.; Lin, W. *Acc. Chem. Res.* **2002**, *35*, 511. (j) Desiraju, G. R. *Acc. Chem. Res.* **2002**, *35*, 565. (k) Desiraju, G. R. *Angew. Chem. Int. Ed.* **2007**, *46*, 8342. (l) Braga, D.; Grepioni, F. *Acc. Chem. Res.* **2000**, *33*, 601. (m) Moulton, B.; Zaworotko, M. J. *Chem. Rev.* **2001**, *101*, 1629.

22. (a) Ward, M. D. *Curr. Opin. Colloid Interface Sci.* **1997**, *2*, 51. (b) Ward, M. D. *Chem. Rev.* **2001**, *101*, 1697.

23. Mak, T. C. W.; Li, Q. in *Advances in Molecular Structure and Research*, Ed. Hargittai, M.; Hargittai, I. JAI Press: Stamford, Connecticut, **1998**, vol. 4, pp. 151.

24. (a) Steiner, T. *Angew. Chem. Int. Ed.* **2002**, *41*, 48. (b) Prins, L. J.; Reinhoudt, D. N.; Timmerman, P. *Angew. Chem. Int. Ed.* **2001**, *40*, 2382. (c) Beer, P. D.; Gale, P. A. *Angew. Chem. Int. Ed.* **2001**, *40*, 486.

25. (a) Mak, T. C. W.; Yip, W. -H.; Li, Q. *J. Am. Chem. Soc.* **1995**, *117*, 11995. (b) Li, Q.; Mak, T. C. W. *Supramol. Chem.* **1996**, *8*, 73.

26. Li, Q.; Xue, F.; Mak, T. C. W. *Inorg. Chem.* **1999**, *38*, 4142.

27. (a) Lam, C.-K.; Mak, T. C. W. *Chem. Commun.* **2001**, 1568. (b) Lam, C.-K.; Mak, T. C. W. *Angew. Chem. Int. Ed.* **2001**, *40*, 3453.

28. Lam, C.-K.; Cheng, M.-F.; Li, C.-L.; Zhang, J.-P.; Chen, X.-M.; Li, W.-K.; Mak, T. C. W. *Chem. Commun.* **2004**, 448.

29. Lam, C.-K.; Chan, T.-L.; Mak, T. C. W. *CrystEngComm.* **2004**, 290.

30. For examples: (a) Pajzderska, A.; Wasicki, J.; Maluszynska, H.; Czarnecki, P.; Toupet, L.; Collet, E. *J. Chem. Phys.* **2008**, *129*, 104501. (b) Parsonage, N. G.; Pemberton, R. C. *Trans. Faraday Soc.* **1967**, *63*, 311. (c) Chatani, Y.; Taki, Y.; Tadokoro, H. *Acta Crystallogr., Sect. B.* **1977**, *33*, 309. (d) Chatani, Y.; Anraku, H.; Taki, Y. *Mol. Cryst. Liq. Cryst.* **1978**, *48*, 219. (e) Fukao, K. *J. Chem. Phys.* **1990**, *92*, 6867. (f) Lynden-Bell, R. M. *Mol. Phys.* **1993**, *79*, 313. (g) Yeo, L.; Kariuki, B. M.; Serrano-Gonza´lez, H.; Harris, K. D. M. *J. Phys. Chem. B* **1997**, *101*, 9926. (h) Le Lann, H.; Odin, C.; Toudic, B.; Ameline, J. C.; Gallier, J.; Guillaume, F.; Breczewski, T. *Phys. Rev. B* **2000**, *62*, 5442.

31. For examples: (a) Casal, H. L.; Cameron, D. G.; Kelusky, E. C. *J. Chem. Phys.* **1984**, *80*, 1407. (b) Harris, K. D. M.; Jonsen, P. *Chem. Phys. Lett.* **1989**, *154*, 593. (c) El Baghdadi, A.; Dufourc, E. J.; Guillaume, F. *J. Phys. Chem.* **1996**, *100*, 1746. (d) Guillaume, F.; Sourisseau, C.; Dianoux, A.-J. *J. Chim. Phys. (Paris)* **1991**, *88*, 1721. (e) Smart, S. P.; Guillaume, F.; Harris, K. D. M.; Dianoux, A.-J. *J. Phys.: Condens. Matter* **1994**, *6*, 2169. (f) Girard, P.; Aliev, A. E.; Guillaume, F.; Harris, K. D. M.; Hollingsworth, M. D.; Dianoux, A.-J.; Jonsen, P. *J. Chem. Phys.* **1998**, *109*, 4078.

32. For examples: (a) Rubio-Pena, L.; Breczewski, T.; Bocanegra, E. H.; Madariaga, G. *Ferroelectrics* **2003**, *290*, 177. (b) Rubio-Pena, L.; Breczewski, T.; Bocanegra, E. H. *Ferroelectrics* **2002**, *269*, 171.

33. Steed, J. W.; Atwood, J. L. *Supramolecular Chemistry*, Wiley: Chichester, U.K., **2000**, Chapter 1.

34. (a) Jeffrey, G. A.; Saenger, W. *Hydrogen Bonding in Biological Structures*, Springer-Verlag, Berlin, Heidelberg, New York, **1991**. (b) Panigrahi, S. K.; Desiraju, G. R. *Proteins* **2007**, *67*, 128.

35. Aakeröy, C. B.; Seddon, K. R. *Chem. Soc. Rev.* **1993**, *22*, 397.

36. (a) Taylor, R.; Kennard, O. *Acc. Chem. Res.* **1984**, *17*, 320. (b) Steiner, T.; Saenger, W. *Acta Crystallogr., Sect. B.* **1992**, *48*, 819. (c) Pirard, B.; Bandoux, G.; Durant, F. *Acta Crystallogr., Sect. B.* **1995**, *51*, 103.

37. (a) Etter, M. C.; MacDonald, J. C.; Bernstein, J. *Acta Crystallogr., Sect. B.* **1990**, *46*, 256. (b) Etter, M. C. *Acc. Chem. Res.* **1990**, *23*, 120.

38. Corey, J. *Pure Appl. Chem.* **1967**, *14*, 19.

39. Thalladi, V. R.; Goud, B. S.; Hoy, V. J.; Allen, F. H.; Howard, J. A. K.; Desiraju, G. R. *Chem. Commun.* **1996**, 401.

40. For Examples: (a) Reddy, D. S.; Ovchinnikov, Y. E.; Shishkin, O. V.; Struchkov, Y. T.; Desiraju, G. R. *J. Am. Chem. Soc.* **1996**, *118*, 4085. (b) Reddy, D. S.; Craig, D. C.; Desiraju, G. R. *J. Am. Chem. Soc.* **1996**, *118*, 4090. (c) Saha, B. K.; Nangia, A. *Cryst. Growth Des.* **2007**, *7*, 393. (d) Allen, F. H.; Hoy, V. J.; Howard, J. A. K.; Thalladi, V. R.; Desiraju, G. R.; Wilson, C. C.; McIntyre, G. J. *J. Am. Chem. Soc.* **1997**, *119*, 3477. (e) Haynes, D. A.; Chisholm, J. A.; Jonesa, W.; Motherwell, W. D. S. *CrystEngComm.* **2004**, *6*, 584. (f) Nangia, A.; Desiraju, G. R. *Top. Curr. Chem.* **1998**, *198*, 57. (g) Saha,

B. K.; Nangia, A.; Jaskólski, M. *CrystEngComm.* **2005**, *7*, 355. (h) Sarma, J. A. R. P.; Desiraju, G. R. *Cryst. Growth Des.* **2002**, *2*, 93.

41. Briggs, J. M.; Nguyen, T. B.; Jorgensen, W. L. *J. Phys. Chem.* **1991**, *95*, 3315.

42. Leiserowitz, L. *Acta Crystallogr., Sect. B.* **1976**, *32*, 775.

43. For reviews see: (a) Aakeröy, C. B.; Seddon, K. R. *Chem. Soc. Rev.* **1993**, 397. (b) Subramanian, S.; Zawarotko, M. J. *Coord. Chem. Rev.* **1994**, *137*, 357. (c) Krische, M. J.; Lehn J.-M. *Struct. Bonding* **2000**, *96*, 3. (d) Prins, L. J.; Reinhoudt, D. N.; Timmerman, P. *Angew. Chem. Int. Ed.* **2001**, *40*, 2383.

44. For examples: (a) Kolotuchin, S. V.; Thiessen, P. A.; Fenlon, E. E.; Wilson, S. R.; Loweth, C. J.; Zimmerman, S. C. *Chem. Eur. J.* **1999**, *5*, 2537. (b) Chatterjee, S.; Pedireddi, V. R.; Ranganathan, A.; Rao, C. N. R. *J. Mol. Struct.* **2000**, *520*, 107. (c) Holy, P.; Zavada, J.; Zezula, J.; Cisarova, I.; Podlaha, J. *Collect. Czech. Chem. Commun.* **2001**, *66*, 820. (d) Beatty, A. M. *CrystEngComm.* **2001**, *51*, 1. (e) Field, J. E.; Combariza, M. Y.; Vachet, R. W.; Venkataraman, D. *Chem. Commun.* **2002**, 2260. (f) Bhogala, B. R.; Vishweshwar, P.; Nangia, A. *Cryst. Growth Des.* **2002**, *2*, 325.

45. Zhang, X.-L; Chen, X.-M. *Cryst. Growth Des.* **2005**, *5*, 617.

46. Duchamp, D. J.; Marsh, R. E. *Acta Crystallogr., Sect. B.* **1969**, *25*, 5.

47. (a) Ermer, O. *J. Am. Chem. Soc.* **1988**, *110*, 3747. (b) Ermer, O. Lindenberg, L. *Helv. Chim. Acta* **1988**, *71*, 1084. (c) Ermer, O. Lindenberg, L. *Helv. Chim. Acta* **1991**, *74*, 825.

48. Das, D.; Desiraju, G. R. *Chem. Asian J.* **2006**, *1*, 231.

49. For examples: (a) Plaut, D. J.; Lund, K. M.; Ward, M. D. *Chem. Commun.* **2000**, 769. (b) Mak, T. C. W.; Xue, F. *J. Am. Chem. Soc.* **2000**, *122*, 9860. (c) Babb, J. E. V.; Burke, N. J.; Burrows, A. D.; Mahon, M. F.; Slade, D. M. K.

CrystEngComm **2003**, *5*, 226. (d) MacLean, E. J.; Teat, S. J.; Farrell, D. M. M.; Ferguson, G.; Glidewell, C. *Acta Crystallogr., Sect. C.* **2002**, *58*, o470.

50. (a) Vázquez-Campos, S.; Péter, M.; Dong, M. D.; Xu, S. L.; Xu, W.; Gersen, H.; Linderoth, T. R.; Schönherr, H.; Besenbacher, F.; Crego-Calama, M.; Reinhoudt, D. N. *Langmuir* **2007**, *23*, 10294. (b) Jonkheijm, P.; Miura, A.; Zdanowska, M.; Hoeben, F. J. M.; De Feyter, S.; Schenning, A. P. H. J.; De Schryver, F. C.; Meijer, E. W. *Angew. Chem. Int. Ed.* **2004**, *43*, 74. (c) Yagai, S.; Nakajima, T.; Karatsu, T.; Saitow, K.; Kitamura, A. *J. Am. Chem. Soc.* **2004**, *126*, 11500. (d) Kerckhoffs, J. M.; Ishi-i, T.; Paraschiv, V.; Timmerman, P.; Crego-Calama, M.; Shinkai, S.; Reinhoudt, D. N. *Org. Biomol. Chem.* **2003**, *1*, 2596. (e) Thalacker, C.; Würthner, F. *Adv. Funct. Mater.* **2002**, *12*, 209. (f) Fenniri, H.; Deng, B.-L.; Ribbe, A. E. *J. Am. Chem. Soc.* **2002**, *124*, 11064. (g) Lu, J.; Zeng, Q.-D.; Wang, C.; Zheng, Q.-Y. Wan, L. J.; Bai, C. L. *J. Mater. Chem.* **2002**, *12*, 2856. (h) Nangia, A. *Curr. Opin. Solid State Mater. Sci.* **2001**, *5*, 115. (i) Valiyaveettil, S.; Müllen, K. *New J. Chem.* **1998**, 89.

51. (a) Rakotondradany, F.; Sleiman, H. F.; Whitehead, M. A. *THEOCHEM.* **2007**, *806*, 39. (b) Elango, M.; Parthasarathi, R.; Subramanian, V.; Sathyamurthy, N. *J. Phys. Chem. A* **2005**, *109*, 8587.

52. For examples: (a) Cowley, M. J.; Lynam, J. M.; Whitwood, A. C. *Dalton Trans.* **2007**, 4427. (b) Johnson, R. S.; Yamazaki, T.; Kovalenko, A.; Fenniri, H. *J. Am. Chem. Soc.* **2007**, *129*, 5735. (c) Gamez, P.; Reedijk, J. *Eur. J. Inorg. Chem.* **2006**, 29. (d) Ahn. S.; PrakashaReddy, J.; Kariuki, B. M.; Chatterjee, S.; Ranganathan, A.; Pedireddi, V. R.; Rao, C. N. R.; Harris, K. D. M. *Chem. Eur. J.* **2005**, *11*, 2433. (e) Kerckhoffs, J. M. C. A.; van Leeuwen, F. W. R.; Spek, A. L.; Kooijman, K.; Crego-Calama, M.; Reinhoudt, D. N. *Angew. Chem. Int.*

Ed. **2003**, *42*, 5717. (f) Félix, O.; Crego-Calama, M.; Luyten, I.; Timmerman, P.; Reinhoudt, D. N. *Eur. J. Org. Chem.* **2003**, *8*, 1463. (g) Yagai, S.; Karatsu, T.; Kitamura, A. *Chem. Commun.* **2003**, 1844. (h) Highfill, M. L.; Chandrasekaran, A.; Lynch, D. E.; Hamilton, D. G. *Cryst. Growth Des.* **2002**, 15. (i) Bielejewska, A. G.; Marjo, C. E.; Prins, L. J.; Timmerman, P.; de Jong, F.; Reinhoudt, D. N. *J. Am. Chem. Soc.* **2001**, *123*, 7518. (j) Yang, J.; Marendaz, J.-L.; Geib, S. J.; Hamilton, A. D. *Tetrahedron Lett.* **1994**, *35*, 3665. (k) Jetti, R. K. R; Thallapally, P. K.; Xue, F.; Mak, T. C. W.; Nangia, A. *Tetrahedron* **2000**, *56*, 6707. (l) Mascal, M.; Hext, N. M.; Warmuth, R.; Arnall-Culliford, J. R.; Moore, M. H.; Turkenburg, J. P. *J. Org. Chem.* **1999**, *64*, 8479. (m) Mascal, M.; Hext, N. M.; Warmuth, R.; Moore, M. H.; Turkenburg, J. P. *Angew. Chem. Int. Ed.* **1996**, *35*, 2204. (n) Simanek, E. E.; Isaacs, L.; Li, X.; Wang, C. C. C.; Whitesides, G. M. *J. Org. Chem.* **1997**, *62*, 8994. (o) Pedireddi, V. R.; Chatterjee, S.; Ranganathan, A.; Rao, C. N. R. *J. Am. Chem. Soc.* **1997**, *119*, 10867. (p) Timmerman, P.; Vreekamp, R. H.; Hulst, R.; Verboom, W.; Reinhoudt, D. N.; Rissanen, K.; Udachin, K. A.; Ripmeester, J. *Chem. Eur. J.* **1997**, *3*, 1823. (q) Li, X.; Chin, D. N.; Whitesides, G. M. *J. Org. Chem.* **1996**, *61*, 1779. (r) Russell, K. C.; Leize, E.; Van Dorsselaer, A.; Lehn, J. M. *Angew. Chem. Int. Ed.* **1995**, *34*, 209.

53. Shuvalov, R. R.; Burns, P. C. *Acta Crystallogr., Sect. C.* **2003**, *59*, i47.

54. (a) Herbstein, F. H.; Kapon, M.; Reisner, G. M. *J. Inclusion Phenom.* **1987**, *5*, 211. (a) Mathias, J. P.; Simanek, E. E.; Zerkowski, J. A.; Seto, C. T.; Whitesides, G. M. *J. Am. Chem. Soc.* **1994**, *116*, 4316. (b) Mathias, J. P.; Seto, C. T.; Simanek, E. E.; Whitesides, G. M. *J. Am. Chem. Soc.* **1994**, *116*, 1725. (c) Mathias, J. P.; Simanek, E. E.; Whitesides, G. M. *J. Am. Chem. Soc.* **1994**,

116, 4326. (d) Zerkowski, J. A; Seto, C. T.; Whitesides, G. M. *J. Am. Chem. Soc.* **1992**, *114*, 5473. (e) Seto, C. T.; Whitesides, G. M. *J. Am. Chem. Soc.* **1990**, *112*, 6409. (g) Whitesides, G. M.; Simanek, E. E.; Mathias, J. P.; Seto, C. T.; Chin, D. N.; Mammen, M.; Gordon, D. M. *Acc. Chem. Res.* **1995**, *28*, 37, and references cited therein.

56. Ranganathan, A.; Pedireddi, V. R.; Rao, C. N. R. *J. Am. Chem. Soc.* **1999**, *121*, 1752.

57. Katrusiak, A.; Szafrański, M. *Acta Crystallogr., Sect. C.* **1994**, *50*, 1161.

58. (a) Videnova-Adrabinska, V.; Obara, E.; Lis, T. *New J. Chem.* **2007**, 287. (b) Russell, V. A.; Ward, M. D. *J. Mater. Chem.* **1997**, *7*, 1123. (b) Russell, V. A.; Etter, M. C.; Ward, M. D. *J. Am. Chem. Soc.* **1994**, *116*, 1941. (c) Russell, V. A.; Evans, C. C.; Li, W.; Ward, M. D. *Science* **1997**, *276*, 575. (d) Swift, J. A.; Reynolds, A. M.; Ward, M. D. *Chem. Mater.* **1998**, *10*, 4159. (e) Swift, J. A.; Ward, M. D. *Chem. Mater.* **2000**, *12*, 1501. (f) Evans, C. C.; Sukarto, L.; Ward, M. D. *J. Am. Chem. Soc.* **1999**, *121*, 320. (g) Swift, J. A.; Pivovar, A. M.; Reynolds, A. M.; Ward, M. D. *J. Am. Chem. Soc.* **1998**, *120*, 5887.

59. Melendez, R. E.; Sharma, C. V. K.; Zaworotko, M. J; Bauer, C.; Rogers, R. D. *Angew. Chem. Int. Ed.* **1996**, *35*, 2213.

60. Puschner, B.; Poppenga, R. H.; Lowenstine, L. J.; Filigenzi, M. S.; Pesavento, P. A. *J. Vet. Diagn. Invest.* **2007**, *19*, 616.

61. Abrahams, B. F., Hawley, A.; Haywood, M. G.; Hudson, T. A.; Robson, R.; Slizys, D. A. *J. Am. Chem. Soc.* **2004**, *126*, 2894.

62. Adrabinska, V. V.; Tyrk, I. T.; Borowiak, T.; Dutkiewicz, G. *New J. Chem.* **2001**, *25*, 1403.

63. (a) Abrahams, B. F.; Haywood, M. G.; Robson, R. *J. Am. Chem. Soc.* **2005**, *127*, 816. (b) Russell, V. A.; Ward, M. D. *Chem. Mater.* **1996**, *8*, 1654.

64. Caira, M. R.; Nassimbeni, L. R.; Toda, F.; Vujovic, D. *J. Am. Chem. Soc.* **2000**, *122*, 9367.

65. Apel, S.; Lennartz, M.; Nassimbeni, L. R.; Weber, E. *Chem. Eur. J.* **2002**, 3678.

66. Bourne, S. A.; Corin, K. C.; Nassimbeni, L. R.; Toda, F. *Cryst. Growth Des.* **2005**, *5*, 379.

67. Tanaka, K.; Nakashima, A.; Shimada, Y.; Scott, J. L. *Eur. J. Org. Chem.* **2006**, 2423.

68. Kim, J.; Lee, S.-O.; Yi, J.; Kimc, W.-S.; Ward, M. D. *Sep. Purifi. Technol.* **2008**, *62*, 517.

69. Lam, C.-K.; Xue, F.; Zhang, J. P.; Chen, X. M.; Mak, T. C. W. *J. Am. Chem. Soc.* **2005**, *127*, 11536.

70. Han, J.; Yau, C.-W.; Lam, C.-K.; Mak, T. C. W. *J. Am. Chem. Soc.* **2008**, *130*, 10315.

71. Lam, C.-K.; Mak, T. C. W. *Chem. Commun.* **2003**, 2660.

72. (a) West, R. *Oxocarbons*; Ed.; Academic Press: New York, 1980. (b) Leibovici, C. *J. Mol. Struct.* **1972**, *13*, 185. (c) Cerioni, G.; Janoschek, R.; Rappoport, Z.; Tidwell, T. T. *J. Org. Chem.* **1996**, *61*, 6212.

73. (a) Lam, C.-K.; Mak, T. C. W. *Tetrahedron* **2000**, *56*, 6657. (b) Lam, C.-K.; Mak, T. C. W. *Cryst. Eng.* **2000**, *3*, 33.

74. Desiraju, G. R.; Steiner, T. *The Weak Hydrogen Bond in Structural Chemistry and Biology*, Oxford University Press, New York, **1999**.

75. Allen, F. H.; Bird, C. M.; Rowland, R. S.; Raithby, P. R. *Acta Crystallogr., Sect. C.* **1997**, *53*, 696.

76. Holý, P.; Závada, J.; Císařová, I.; Podlaha, J. *Angew. Chem. Int. Ed.* **1999**, *38*, 381.

77. Chang, Y.-L.; West, M.-A.; Fowler, F. W.; Lauher, J. W. *J. Am. Chem. Soc.* **1993**, *115*, 5991.

78. For examples: (a) Said, F. F.; Ong, T.-G.; Bazinet, P.; Yap, G. P. A.; Richeson, D. S. *Cryst. Growth Des.* **2006**, *6*, 1848. (b) Vaidhyanathan, R.; Natarajan, S.; Rao, C. N. R. *J. Mol. Struct.* **2002**, *608*, 123. (c) Braga, D.; Eckert, M.; Fraccastoro, M.; Maini, L.; Grepioni, F.; Caneschi, A.; Sessoli, R. *New J. Chem.* **2002**, *26*, 1280. (d) Vaidhyanathan, R.; Natarajan, S.; Rao, C. N. R. *J. Chem. Soc., Dalton Trans.* **2001**, 699. (e) Andrews, L. C.; Deroski, B. R.; Ricci, J. S. *J. Cryst. Mol. Struct.* **1979**, *9*, 163.

79. Katritzky, A. R.; Rees, C. W. *Comprehensive Heterocyclic Chemistry*; Ed. Bird, C. W.; Cheeseman, G. W. H. Pergamon Press: New York, **1984**; pp 1.

80. For Examples: (a) Kopel, P.; Dolezal, K.; Machala, L.; Langer, V. *Polyhedron* **2007**, *26*, 1583. (b) Iltzsch, M.; Tankersley, K. O. *Biochem. Pharmacol.* **1993**, *46*, 1849. (c) Iltzsch, M.; Tankersley, K. O. *Biochem. Pharmacol.* **1993**, *48*, 781. (d) Henke, K. R.; Robertson, D.; Krepps, M. K.; Atwood, D. A. *Water Res.* **2000**, *34*, 3005.

81. (a) Cutting, W. C. *Handbook of Pharmacology*, 3rd ed., Meredith Publishing Company, New York, **1967**. (b) Sans, R. G.; Chozas, M. G. *Pharmazie* **1988**, *43*, 827. (c) Jovanovic, M. V.; Biehl, E. D. *J. Heterocycl. Chem.* **1987**, *24*, 191.

82. Kakkar, R.; Katoch, V. *Int. J. Quantum Chem.* **1999**, *74*, 327.

83. Slesarev, V. I.; Popov, A. S. *Russ. J. General Chem.* **2002**, *72*, 949.

84. (a) Rebek, J. Jr.; Marshall, L.; Wolak, R.; Parris, K.; Killoran, M.; Askew, B.; Nameth, D.; Islam, N. *J. Am. Chem. Soc.* **1985**, *107*, 7476. (b) Chan, T.-L.; Cui, Y.-X.; Mak, T. C. W.; Wang, R.-J.; Wong, H. N. C. *J. Cryst. Spectrosc. Res.* **1991**, *21*, 297. (c) Bencini, A.; Bianchi, A.; Burguete, M. I.; Dapporto, P.; Doménech, A.; García-España, E.; Luis, S. V.; Paoli, P.; Ramírez, J. A. *J. Chem. Soc., Perkin Trans. 2* **1994**, 569.

85. Kemp, D. S.; Petrakis, K. S. *J. Org. Chem.* **1981**, *46*, 5140.

86. Hirose, T.; Baldwin, B. W.; Wang, Z. H.; Kennard, C. H. L. *Acta Crystallogr., Sect. C.* **1998**, *54*, 1143.

87. Thuéry, P.; Nierlich, M.; Baldwin, B. W.; Aoki, Y.; Hirose, T. *J. Chem. Soc., Perkin Trans. 2* **1999**, 2077.

88. Menger, F. M.; Chicklo, P. A.; Sherrod, M. J. *Tetrahedron Lett.* **1989**, 6943.

89. Bolton, W. *Acta Cryst.* **1963**, *16*, 950.

90. Masoud, M. S.; Ghonaim, A. K.; Ahmed, R. H.; Abou EI-Enein, S. A.; Mahmoud, A. A. *J. Coord. Chem.* **2002**, *55*, 79.

91. Craven, B. M.; Martinez-Carrera, S.; Jeffrey, G. A. *Acta Cryst.* **1964**, *17*, 891.

92. Simonsen, O. *Acta Crystallogr., Sect. C.* **1985**, *41*, 1258.

93. Simonsen, O. *Acta Chem. Scand.* **1997**, *51*, 861.

94. Thaimattam, R.; Reddy, D. S.; Xue, F.; Mak, T. C. W.; Nangia, A.; Desiraju, G. R. *J. Chem. Soc., Perkin Trans. 2* **1998**, 1783.

95. Abashev, G. G.; Vlasova, R. M.; Kartenko, N. F.; Kuzmin, A. M.; Rozhdestvenskaya, I. V.; Semkin, V. N.; Usov, O. A.; Russkikh, V. S. *Acta Crystallogr., Sect. C.* **1987**, *43*, 1108.

96. Usov, O. A.; Burshtein, I. A.; Kartenko, N. F.; Rozhdestvenskaya, I. V.; Vlasova, R. M.; Semkin, V. N.; Abashev, G. G.; Russkikh, V. S. *Acta Crystallogr., Sect. C.* **1991**, *47*, 1851.

97. Weber, G.; Saenger, W. *Acta Crystallogr., Sect. B.* **1980**, *36*, 424.

98. Platts, J. A.; Howard, S. T.; Bracke, B. R. F. *J. Am. Chem. Soc.* **1996**, *118*, 2726.

99. Kolev, T.; Preut, H.; Bleckmann, P.; Radomirska, V. *Acta Crystallogr.,Sect. C.* **1997**, *53*, 805.

100. Sabareesh, V.; Ranganathan, A.; Kulkarni, G. U. *Private Communication* **2000**.

101. Kálmán, A.; Párkányi, L. In *Advances in Molecular Structure Research*; Hargittai, M., Hargittai, I., Eds.; JAI Press: Stamford, Connecticut, **1997**; Vol. 3, pp. 189.

102. A search of the Cambridge Structural Database (Version 5.29) by drawing Kemp's triacid and mono-deprotonated one only yielded 9 hits, excluding metal organic complex and derivative of Kemp's triacid.

103. Smith, G.; Wermuth, U. D.; White, J. M. *Chem. Commun.* **2000**, 2349.

104. Smith, G.; Bott, R. C.; Wermuth, U. D. *Acta Crystallogr.,Sect. C* **2000**, *56*, 1505.

105. Slesarev, I.; Popov, A. S. *Russ. J. General Chem.* **2004**, *74*, 414.

106. Baures, P. W.; Rush, J. R.; Wiznycia, A. V.; Desper, J.; Helfrich, B. A.; Beatty, A. M. *Cryst. Growth Des.* **2002**, *2*, 653.

107. Eggerding, D.; West, R. *J. Org. Chem.* **1976**, *41*, 3904.

108. Pryor, K. E.; Shipps, G. W. Jr.; Skyler, D. A.; Rebek, J. Jr. *Tetrahedron* **1998**, *54*, 4107.

109. Mao, J. G.; Zhang, H. J.; Ni, J. Z.; Wang, S. B.; Mak, T. C. W. *Polyhedron* **1999**, *18*, 1519.

110. *Bruker SMART 5.0 and SAINT 4.0 for Windows NT: Area Dector Control and Intergration Software*, Bruker Analytical X-Ray Systems, Inc.: Madison, Wisconsin, USA, **1998**.

111. *Sheldrick, G. M. SADABS: Program for Empirical Absorption Correction of Area Detector Data*; University of Göttingen: Göttingen, Germany, **1996**.

112. Sheldrick, G. M. *SHELXTL 5.10 for Windows NT: Structure Determination Software Programs*, Bruker Analytical X-Ray Systems, Inc., Madison, Wisconsin, USA, **1998**.

Appendix I. Publications

1. **Han, J.**; Yau, C.-W.; Lam, C.-K.; Mak, T. C. W.*:

"Designed Supramolecular Assembly of Hydrogen-bonded Anionic Rosette Layers"

J. Am. Chem. Soc. **2008**, *130*, 10315.

2. **Han, J.**; Zhao, L.; Yau, C.-W.; Mak, T. C. W.*:

"Hydrogen-bonded Networks Constructed with 5-Nitrobarbiturate"

Cryst. Growth Des. **2008**, in press.

3. **Han, J.**; Mak, T. C. W.*:

"Designed supramolecular assembly of novel rosette layers"

Acta Cryst. **2008**, *A64*, C389.

4. Zhao, L.; Wan, C.-Q.; **Han, J.**; Chen, X.-D.; Mak, T. C. W.*:

"Ancillary Ligands and Spectator Cations as Controlling Factors in the Construction of Coordination and Hydrogen-bonded Networks with the *tert*-Bu−C≡C⊂Ag_n (n = 4, 5) Supramolecular Synthon"

Chem. Eur. J. **2008**, *14*, 10437.

5. Wan, C.-Q.; **Han, J.**; Mak, T. C. W.*:

"Intermolecular S···π Interaction in Sulfanyl-Triazine Derivatives"

New J. Chem. **2009**, DOI: 10.1039/B818344A, in press.

6. Zang, S.-Q.; **Han, J.**; Mak, T. C. W.*:

"Silver(I)-Organic Networks Assembled with the Flexible Prop-2-ynyloxy-benzene Ligand: In situ Re-crystallization and Unusual Silver-Aromatic Interaction"

Organometallics **2008**, submitted.

7. **Han, J.**; Zang, S.-Q.; Mak, T. C. W.*:

"Designed Crystal Structures Based on Deprotonated Kemp's Triacid"

Manuscript in preparation.

Appendix II. Crystallographic Data

Complex	2.1.1	2.1.2	2.1.3	2.1.4	2.1.5
Molecular formula	$2[C(NH_2)^{3+}]\cdot B_4O_9^{2-}\cdot 2H_2O$	$[C(NH_2)_3^+]\cdot H_4B_5O_{10}^-\cdot H_2O$	$2(Et_4N^+)\cdot 2(H_3BO_3)\cdot CO_3^{2-}\cdot 5H_2O$	$[(n\text{-}C_3H_7)_4N^+]\cdot[C(NH_2)_3^+]\cdot CO_3^{2-}\cdot 2B(OH)_3$	$[(n\text{-}Bu_4N^+)]\cdot[C_4O_4H^-]\cdot[H_3BO_3]$
Molecular weight	347.48	296.19	534.26	430.12	415.32
Crystal size (mm)	0.45 × 0.40 × 0.34	0.35 × 0.33 × 0.30	0.32 × 0.25 × 0.20	0.26 × 0.22 × 0.18	0.42× 0.26 × 0.23
Crystal system	Triclinic	Triclinic	Monoclinic	Orthorhombic	Triclinic
Space group	$P\bar{1}$	$P\bar{1}$	$P2_1/c$	*Pnma*	$P\bar{1}$
a (Å)	7.2905(8)	7.5460(8)	14.311(1)	16.024(6)	9.352(4)
b (Å)	8.4129(9)	8.3204(9)	14.544(1)	13.854(5)	9.833(4)
c (Å)	12.502(1)	10.020(1)	15.009(1)	11.651(4)	14.339(6)
α (°)	90.605(2)	85.412(2)	90	90	70.499(9)
β (°)	106.882(2)	85.276(2)	103.211(2)	90	80.495(9)
γ (°)	103.731(2)	85.868(2)	90	90	80.991(9)
V (Å)	710.1(1)	623.6(1)	3040.9(5)	2587(2)	1218.6(9)
Z	2	2	4	4	2
F(000)	364	304	1176	936	452
Density(cal.)(g cm^{-1})	1.625	1.577	1.167	1.105	1 132
Theta range (°)	1.71 to 25.01	2.05 to 25.99	4.87 to 67.80	2.28 to 28.28	1 52 to 25.01
Reflections measured	3648	3720	20987	17137	6620
Index ranges of measured data	$-8 \le h \le 8$ $-10 \le k \le 7$ $-14 \le l \le 14$	$-8 \le h \le 9$ $-10 \le k \le 10$ $-12 \le l \le 9$	$-16 \le h \le 19$ $-19 \le k \le 18$ $-16 \le l \le 20$	$-13 \le h \le 21$ $-18 \le k \le 18$ $-15 \le l \le 15$	$-11 \le h \le 11$ $-11 \le k \le 11$ $-17 \le l \le 14$
Independent reflections	2402 (0.0171)	2435 (0.0174)	7522 (0.0334)	3332 (0.0483)	4261 (0.0350)
Observed reflection	2180	2099	4106	1810	2102
Absorption correction	multi-scan	multi-scan	multi-scan	multi-scan	multi-scan
Relative transmission Factor	0.815	0.700	0.786	0.780	0.806
Data/restraints/parameters	2402/0/224	2435/0/197	7522/0/341	3332/14/149	4261/0/265
Final R indices (obs.)*	$R1$ = 0.0375 w$R2$ = 0.1062	$R1$ = 0.0334 w$R2$ = 0.0940	$R1$ = 0.0528 w$R2$ = 0.1357	$R1$ = 0.0688 w$R2$ = 0.2183	$R1$ = 0.0680 w$R2$ = 0.1718
R indices (all)*	$R1$ = 0.0412 w$R2$ = 0.1128	$R1$ = 0.0391 w$R2$ = 0.0986	$R1$ = 0.1009 w$R2$ = 0.1727	$R1$ = 0.1214 w$R2$ = 0.2621	$R1$ = 0.1343 w$R2$ = 0 1926
Goodness-of-fit index	1.079	1.111	1.004	1.093	1.039
Largest difference peak (eÅ^{-3})	0.388, -0.463	0.178, -0.241	0.401, -0.267	0.534, -0.305	0 404, -0.321

Complex	2.1.6	2.1.7	2.1.8	2.1.9	2.1.10
Molecular formula	$2[(n\text{-}C_3H_7)_4N^+] \cdot 4[CS(NH_2)_2] \cdot [C_4O_2S_2^{2-}] \cdot 2H_2O$	$2[(n\text{-}C_4H_9)_4N^+] \cdot 4[CS(NH_2)_2] \cdot [C_4O_2S_2^{2-}]$	$2[(n\text{-}C_4H_9)_4N^+] \cdot 6[CS(NH_2)_2] \cdot [C_4O_2S_2^{2-}] \cdot H_2O$	$[(n\text{-}C_3H_7)_4N^+] \cdot 2[C(NH_2)_3^+] \cdot [C_4O_2S_2^{2-}]$	$2[(CH_3)_4N^+] \cdot 2[(C_6H_3)_2(COOH)_3(COO^-)] \cdot H_2O$
Molecular weight	857.39	933.56	1103.82	446.71	824.77
Crystal size (mm)	0.45 × 0.42 × 0.33	0.35 × 0.25 × 0.20	0.32 × 0.25 × 0.20	0.39 × 0.30 × 0.23	0.43 × 0.41 × 0.29
Crystal system	Monoclinic	Monoclinic	Triclinic	Orthorhombic	Monoclinic
Space group	$P2_1/n$	$P2_1/c$	$P\bar{1}$	$Pbca$	$P2_1/c$
a (Å)	8.538(1)	23.280(2)	9.112(2)	16.057(2)	13.40(1)
b (Å)	18.329(3)	8.936(1)	12.138(2)	16.991(2)	17.62(1)
c (Å)	15.738(2)	32.670(2)	31.258(5)	19.045(2)	17.98(1)
α (°)	90	90	86.371(3)	90	90
β (°)	100.055(3)	127.935(4)	81.895(3)	90	110.89(2)
γ (°)	90	90	70.821(3)	90	90
V (Å)	2425.1(6)	5360.7(9)	3232.3(8)	5196(1)	3968(5)
Z	4	4	2	8	4
F(000)	932	2040	1200	1952	1736
Density(cal.)(g cm^{-1})	1.174	1.157	1.134	1.142	1.381
Theta range (°)	1.72 to 25.01	1.58 to 25.00	0.66 to 25.01	2.05 to 28.31	1.63 to 25.01
Reflections measured	12508	27510	17542	34381	19239
Index ranges of measured data	$-9 \le h \le 10$ $-21 \le k \le 15$ $-18 \le l \le 18$	$-27 \le h \le 25$ $-10 \le k \le 10$ $-28 \le l \le 38$	$-10 \le h \le 10$ $-12 \le k \le 14$ $-37 \le l \le 33$	$-21 \le h \le 21$ $-22 \le k \le 22$ $-25 \le l \le 18$	$-17 \le h \le 16$ $-10 \le k \le 10$ $-18 \le l \le 12$
Independent reflections	4258 (0.0361)	9440 (0.0490)	11319 (0.0290)	6455 (0.0556)	6817 (0.1081)
Observed reflection	2632	6319	6884	3148	3764
Absorption correction	multi-scan	multi-scan	multi-scan	multi-Scan	multi-scan
Relative transmission Factor	0.706	0.624	0.648	0.781	0.768
Data/restraints/parameters	4258/13/232	9440/0/523	11319/57/599	6455/2/263	6817/6/564
Final R indices (obs.)*	$R1$ = 0.0946 w$R2$ = 0.3051	$R1$ = 0.0554 w$R2$ = 0.1472	$R1$ = 0.0819 w$R2$ = 0.2318	$R1$ = 0.0552 w$R2$ = 0.1513	$R1$ = 0.0885 w$R2$ = 0.2158
R indices (all)*	$R1$ = 0.1334 w$R2$ = 0.3375	$R1$ = 0.0886 w$R2$ = 0.1633	$R1$ = 0.1233 w$R2$ = 0.2742	$R1$ = 0.1273 w$R2$ = 0.2056	$R1$ = 0.1557 w$R2$ = 0.2368
Goodness-of-fit index	1.224	1.074	1.029	1.007	1.042
Largest difference peak (eÅ^{-3})	0.933, -0.493	0.972, -0.660	0.827, -0.579	0.412, -0.333	0.525, -0.552

Complex	2.1.11	2.1.12	2.1.13	2.1.14	2.2.1
Molecular formula	$2[(C_2H_5)_4N^+]\cdot 2[CS(NH_2)_2]\cdot[(C_6H_3)_2(COOH)_2(COO^-)_2]$	$[(CH_3)_4N^+]\cdot[C(NH_2)_3^+]\cdot[(C_6H_3)_2(COOH)_2(COO^-)_2]$	$[(C_2H_5)_4N^+]\cdot[C(NH_2)_3^+]\cdot[(C_6H_3)_2(COOH)_2(COO^-)_2]$	$[(n\text{-}C_3H_7)_4N^+]\cdot[C(NH_2)_3^+]\cdot[(C_6H_3)_2(COOH)_2(COO^-)_2]$	$[(CH_3)_4N^+]\cdot[H_2KTA^-]\cdot H_2O$
Molecular weight	740.97	462.46	518.56	574.67	349.42
Crystal size (mm)	0.32 × 0.28 × 0.22	0.44 × 0.38 × 0.32	0.48 × 0.43 × 0.40	0.49 × 0.45 × 0.27	0.43 × 0.35 × 0.29
Crystal system	Triclinic	Orthorhombic	Monoclinic	Monoclinic	Monoclinic
Space group	$P\bar{1}$	$P2_12_12_1$	$P2_1$	$P2_1/n$	$P2_1/n$
a (Å)	11.7987(5)	10.241(8)	13.121(4)	12.239 (2)	14.7298(9)
b (Å)	11.8892(5)	11.380(8)	10.154(3)	15.769(2)	8.7769(5)
c (Å)	15.3237(6)	19.56(2)	20.248(6)	16.204(2)	15.4286(9)
α (°)	77.779(3)	90	90	90	90
β (°)	75.799(3)	90	95.209(7)	101.315(3)	103.507(4)
γ (°)	72.057(3)	90	90	90	90
V (Å)	1960.8 (1)	2280(3)	2686(2)	3066.7(7)	1939.5(2)
Z	2	4	4	4	4
F(000)	796	976	1064	1232	760
Density(cal.)(g cm^{-1})	1.255	1.347	1.257	1.245	1.197
Theta range (°)	3.95 to 65.86	2.07 to 28.42	1.01 to 26.00	1.82 to 28.35	3.74 to 66.50
Reflections measured	16854	15577	15962	21199	18030
Index ranges of measured data	$-13 \le h \le 13$	$-13 \le h \le 13$	$-16 \le h \le 12$	$-16 \le h \le 16$	$-17 \le h \le 16$
	$-15 \le k \le 15$	$-15 \le k \le 15$	$-12 \le k \le 12$	$-21 \le k \le 20$	$-10 \le k \le 10$
	$-18 \le l \le 26$	$-18 \le l \le 26$	$-24 \le l \le 24$	$-13 \le l \le 21$	$-18 \le l \le 12$
Independent reflections	6274 (0.0360)	5653 (0.0471)	9627 (0.0364)	7634 (0.0419)	3339 (0.0309)
Observed reflection	3509	3509	5954	4415	2985
Absorption correction	multi-scan	multi-scan	multi-scan	multi-scan	multi-scan
Relative transmission Factor	0.868	0.635	0.782	0.781	0.667
Data/restraints/parameters	6274/19/525	5653/0/322	9627/29/725	7634/0/396	3339/0/218
Final R indices (obs.)*	$R1$ = 0.0740	$R1$ = 0.0483	$R1$ = 0.0668	$R1$ = 0.0474	$R1$ = 0.0516
	w$R2$ = 0.2128	w$R2$ = 0.1001	w$R2$ = 0.1834	w$R2$ = 0.1083	w$R2$ = 0.1526
R indices (all)*	$R1$ = 0.0892	$R1$ = 0.0972	$R1$ = 0.1177	$R1$ = 0.0979	$R1$ = 0.0559
	w$R2$ = 0.2314	w$R2$ = 0.1197	w$R2$ = 0.2139	w$R2$ = 0.1373	w$R2$ = 0.1561
Goodness-of-fit index	1.046	1.033	1.002	1.002	1.041
Largest difference peak (eÅ^{-3})	0.606, -0.339	0.207, -0.169	0.548, -0.362	0.194, -0.197	0.259, -0.204

Complex	2.2.2	2.2.3	2.2.4	2.2.5	2.2.6
Molecular formula	$[C(NH_2)_3^+] \cdot [H_2KTA^-]$	$3[(C_2H_5)_4N^+] \cdot 20[C(NH_2)_3^+] \cdot 11[HKTA^{2-}] \cdot [H_2KTA^-] \cdot 17H_2O$	$3[C(NH_2)_3^+] \cdot [KTA^{3-}]$	$[(n\text{-}C_3H_7)_4N^+] \cdot 2[C(NH_2)_3^+] \cdot [KTA^{3-}]$	$[(CH_3)_4N^+] \cdot 2[C(NH_2)_3^+] \cdot [KTA^{3-}] \cdot 2H_2O$
Molecular weight	317.34	4974.77	435.50	561.77	485.59
Crystal size (mm)	0.32 × 0.28 × 0.22	0.38 × 0.25 × 0.18	0.32 × 0.25 × 0.20	0.48 × 0.34 × 0.31	0.40 × 0.39 × 0.38
Crystal system	Monoclinic	Orthorhombic	Tetragonal	Orthorhombic	Orthorhombic
Space group	$P2_1/n$	$P4_2/n$	$R3c$	$Pca2_1$	$Pbcn$
a (Å)	12.720(7)	23.0829(1)	18.156(2)	17.9871(3)	27.246(4)
b (Å)	10.051(5)	23.0829(1)	18.156(2)	18.5681(3)	11.833(2)
c (Å)	13.118(7)	24.5301(2)	11.980(2)	19.2007(2)	16.125(4)
α (°)	90	90	90	90	90
β (°)	114.182(7)	90	90	90	90
γ (°)	90	90	120	90	90
V (Å)	1530(2)	13070.2(1)	3420.0(7)	6412.8(2)	5199(2)
Z	4	2	6	8	8
F(000)	680	5376	1404	2464	2112
Density(cal.)(g cm^{-1})	1.378	1.264	1.269	1.164	1.241
Theta range (°)	1.88 to 28.34	3.25 to 66.60	4.87 to 67.80	3.42 to 67.80	4.07 to 67.82
Reflections measured	10312	86255	14720	35400	96411
Index ranges of measured data	$-9 \le h \le 16$ $-13 \le k \le 13$ $-17 \le l \le 16$	$-27 \le h \le 27$ $-26 \le k \le 24$ $-28 \le l \le 26$	$-21 \le h \le 17$ $-20 \le k \le 21$ $-13 \le l \le 14$	$-14 \le h \le 21$ $-22 \le k \le 22$ $-22 \le l \le 21$	$-32 \le h \le 32$ $-14 \le k \le 14$ $-15 \le l \le 19$
Independent reflections	3791 (0.0360)	11435 (0.0587)	1364 (0.0237)	10699 (0.0503)	4679 (0.0483)
Observed reflection	2823	8189	1352	7184	3997
Absorption correction	multi-scan	multi-scan	multi-scan	multi-scan	multi-scan
Relative transmission Factor	0.730	0.857	0.806	0.781	0.671
Data/restraints/parameters	3791/0/199	11435/9/874	1364/1/92	10699/6/915	4679/0/299
Final R indices (obs.)*	$R1 = 0.0468$ $wR2 = 0.1244$	$R1 = 0.0629$ $wR2 = 0.1607$	$R1 = 0.0288$ $wR2 = 0.0846$	$R1 = 0.0713$ $wR2 = 0.1844$	$R1 = 0.0460$ $wR2 = 0.1312$
R indices (all)*	$R1 = 0.0659$ $wR2 = 0.1388$	$R1 = 0.0915$ $wR2 = 0.1820$	$R1 = 0.0289$ $wR2 = 0.0848$	$R1 = 0.1012$ $wR2 = 0.2144$	$R1 = 0.0530$ $wR2 = 0.1384$
Goodness-of-fit index	1.016	1.030	1.089	1.005	1.038
Largest difference peak (eÅ^{-3})	0.335, -0.326	0.853, -0.390	0.185, -0.095	0.513, -0.189	0.381, -0.278

Complex	2.3.1	2.3.2	2.3.3	2.3.4	2.3.5
Molecular formula	$3[(n\text{-}C_4H_9)_4N^+] \cdot 2[C(NH_2)_3^+] \cdot 3[1,4\text{-}C_6H_4(COOH)(CO_2^-)] \cdot [1,4\text{-}C_6H_4(CO_2^-)_2] \cdot 2H_2O$	$2[C(NH_2)_3^+] \cdot [2,6\text{-}C_{10}H_4(CO_2^-)_2] \cdot 4H_2O$	$2[C(NH_2)_3^+] \cdot [(4\text{-}C_6H_4CO_2^-)_2] \cdot 4H_2O$	$[(CH_3)_4N^+] \cdot 5[C(NH_2)_3^+] \cdot 3[(4\text{-}C_6H_4CO_2^-)_2] \cdot 2.5H_2O$	$4[(n\text{-}C_4H_9)_4N^+] \cdot 2[C(NH_2)_3^+] \cdot 2[C(NH_2)_2{}^+NHCO_2^-] \cdot 3[(4\text{-}C_6H_4CO_2^-)_2] \cdot 8H_2O$
Molecular weight	1543.05	406.41	432.44	1140.24	2160.93
Crystal size (mm)	0.45 × 0.44 × 0.34	0.30 × 0.30 × 0.18	0.42 × 0.37 × 0.25	0.37 × 0.20 × 0.19	0.46 × 0.40 × 0.39
Crystal system	Monoclinic	Monoclinic	Monoclinic	Triclinic	Triclinic
Space group	*Cc*	$P2_1/c$	$P2_1/c$	$P\bar{1}$	$P\bar{1}$
a (Å)	13.186(2)	10.819(2)	11.272(1)	14.541(6)	8.2617(8)
b (Å)	41.500(7)	10.594(2)	10.632(1)	14.909(6)	18.392(2)
c (Å)	16.514(3)	8.998(2)	8.917(1)	14.984(6)	21.110(2)
α (°)	90	90	90	60.937(8)	73.466(2)
β (°)	99.631(4)	110.211(3)	98.928(2)	88.329(9)	82.856(2)
γ (°)	90	90	90	85.395(9)	86.863(2)
V (Å)	8909(3)	967.8(2)	1055.7(2)	2830(2)	3050.5(5)
Z	4	2	2	2	1
F(000)	3368	432	460	1210	1182
Density(cal.)(g cm^{-1})	1.150	1.395	1.360	1.338	1.176
Theta range (°)	0.98 to 25.01	2.01 to 28.38	1.83 to 28.34	1.40 to 25.01	2.15 to 28.40
Reflections measured	23802	6600	7175	15537	15271
Index ranges of measured data	$-15 \le h \le 13$	$-14 \le h \le 13$	$-15 \le h \le 12$	$-10 \le h \le 17$	$-9 \le h \le 9$
	$-49 \le k \le 49$	$-14 \le k \le 13$	$-14 \le k \le 13$	$-17 \le k \le 17$	$-20 \le k \le 21$
	$-17 \le l \le 19$	$-9 \le l \le 12$	$-11 \le l \le 11$	$-17 \le l \le 16$	$-25 \le l \le 23$
Independent reflections	10837(0.0480)	2408 (0.0266)	2618(0.0259)	9952(0.0318)	10581(0.0241)
Observed reflection	6175	1778	1819	5737	6356
Absorption correction	multi-scan	multi-scan	multi-scan	multi-scan	multi-scan
Relative transmission Factor	0.603	0.703	0.811	0.665	0.605
Data/restraints/parameters	10837/2/983	2408/0/136	2618/0/141	9952/0/739	10581/0/685
Final *R* indices (obs.)*	*R*1 = 0.0539	*R*1 = 0.0442	*R*1 = 0.0473	*R*1 = 0.0630	*R*1 = 0.0546
	w*R*2 = 0.1166	w*R*2 = 0.1144	w*R*2 = 0.1248	w*R*2 = 0.1755	w*R*2 = 0.1448
R indices (all)*	*R*1 = 0.1149	*R*1 = 0.0631	*R*1 = 0.0710	*R*1 = 0.1158	*R*1 = 0.0925
	w*R*2 = 0.1487	w*R*2 = 0.1291	w*R*2 = 0.1466	w*R*2 = 0.1988	w*R*2 = 0.1577
Goodness-of-fit index	1.034	1.025	1.064	1.049	1.080
Largest difference peak (eÅ^{-3})	0.346, -0.160	0.339, -0.258	0.501, -0.302	0.619, -0.396	0.596, -0.656

Complex	2.3.6	2.3.7	2.3.8	2.4.1	2.4.2
Molecular formula	$[(n\text{-}C_3H_7)_4N^+] \cdot [C(NH_2)_3^+] \cdot [1,3\text{-}C_6H_4(CO_2^-)_2] \cdot 3H_2O$	$(C_5H_4N^+CH_2COO^-)_2 \cdot 2H_2O$	$[C(NH_2)_3^+] \cdot (C_5H_4N^+CH_2COOH)_2 \cdot CO_3^{2-} \cdot H_2O$	$[(Et_4N^+)] \cdot [C_4N_2O_2H_3S^-] \cdot H_2O$	$[(Et_4N^+)] \cdot [C_4N_2O_2H_3S^-] \cdot 2H_2O$
Molecular weight	464.60	275.25	344.32	291.41	309.43
Crystal size (mm)	0.48 × 0.26 × 0.18	0.32 × 0.25 × 0.23	0.46 × 0.42 × 0.41	0.33 × 0.31× 0.18	0.32 × 0.25 × 0.20
Crystal system	Orthorhombic	Triclinic	Monoclinic	Monoclinic	Monoclinic
Space group	$P2_12_12_1$	$P\bar{1}$	$P2_1/n$	$P2_1$	$P2_1/n$
a (Å)	8.4119(9)	7.708(1)	6.3430(9)	8.262(1)	9.201(1)
b (Å)	15.546(2)	8.345(1)	11.615(2)	11.870(2)	14.761(2)
c (Å)	20.732(2)	9.914(1)	11.018(2)	15.678(2)	12.517(1)
α (°)	90	88.274(3)	90	90.00	90
β (°)	90	86.405(3)	100.118(2)	117.741(4)	94.022(3)
γ (°)	90	74.709(3)	90	90.00	90
V (Å)	2711.1(5)	613.8 (2)	799.1 (2)	1537.4(4)	1695.9(3)
Z	4	2	2	4	4
F(000)	1016	290	364	632	672
Density(cal.)(g cm^{-1})	1.138	1.489	1.431	1.259	1.212
Theta range (°)	1.64 to 25.01	2.06 to 26.00	2.57 to 28.33	2.15 to 28.34	2.14 to 25.99
Reflections measured	15388	3658	5430	10495	9875
Index ranges of measured data	$-9 \le h \le 10$	$-9 \le h \le 9$	$-8 \le h \le 8$	$-11 \le h \le 10$	$-11 \le h \le 10$
	$-18 \le k \le 17$	$-10 \le k \le 10$	$-15 \le k \le 13$	$-15 \le k \le 15$	$-18 \le k \le 16$
	$-18 \le l \le 24$	$-12 \le l \le 6$	$-14 \le l \le 10$	$-20 \le l \le 18$	$-15 \le l \le 14$
Independent reflections	4775 (0.0515)	2394 (0.0217)	1989 (0.0320)	3806 (0.0354)	3336(0.0251)
Observed reflection	2865	1807	1576	2343	2667
Absorption correction	multi-scan	multi-scan	multi-scan	multi-scan	multi-scan
Relative transmission Factor	0.654	0.738	0.707	0.826	0.879
Data/restraints/parameters	4775/0/290	2394/0/188	1989/0/109	3806/0/184	3336/9/230
Final R indices (obs.)*	$R1$ = 0.0460	$R1$ = 0.0570	$R1$ = 0.0473	$R1$ = 0.0576	$R1$ = 0.0680
	w$R2$ = 0.1049	w$R2$ = 0.1677	w$R2$ = 0.1251	w$R2$ = 0.1523	w$R2$ = 0.2277
R indices (all)*	$R1$ = 0.1005	$R1$ = 0.0743	$R1$ = 0.0597	$R1$ = 0.0965	$R1$ = 0.0791
	w$R2$ = 0.1219	w$R2$ = 0.1811	w$R2$ = 0.1343	w$R2$ = 0.1771	w$R2$ = 0.2419
Goodness-of-fit index	0.987	1.109	1.059	1.044	1.097
Largest difference peak (eÅ^{-3})	0.116, -0.147	0.481, -0.421	0.288, -0.198	0.515, -0.365	0.607,-0.309

Complex	2.4.3	2.4.4	2.4.5	2.4.6	2.4.7
Molecular formula	$2[(n\text{-}C_3H_7)_4N^+]\cdot 2[C_4N_2O_2H_3S^-]\cdot 2[CO(NH_2)_2]\cdot 5H_2O$	$[(CH_3)_4N^+]\cdot[C_3N_3S_3H_2^-]$	$[(n\text{-}C_4H_9)_4N^+][C_3N_3S_3H_2^-]\cdot H_2O$	$2[(CH_3)_4N^+]\cdot[C_3N_3S_3H^{2-}]\cdot 5[CO(NH_2)_2]\cdot H_2O$	$[(n\text{-}C_3H_7)_4N^+]\cdot[C_3N_3S_3H_2^-]\cdot[CS(NH_2)_2]$
Molecular weight	869.2	250.40	436.73	641.87	438.73
Crystal size (mm)	0.44 × 0.43 × 0.41	0.39 × 0.38 × 0.24	0.46 × 0.45 × 0.45	0.44 × 0.40 × 0.39	0.33 × 0.24 × 0.21
Crystal system	Monoclinic	Orthorhombic	Triclinic	Monoclinic	Monoclinic
Space group	$P2_1/c$	$Pbca$	$P\bar{1}$	$P2_1/c$	$P2_1/c$
a (Å)	8.653(1)	14.9432(18)	8.863(2)	19.413(5)	17.539(3)
b (Å)	33.371(4)	8.9051(11)	10.086(2)	9.236(2)	8.824(2)
c (Å)	16.779(2)	18.953(2)	15.661(3)	19.308(5)	17.825(2)
α (°)	90.00	90	77.173(4)	90	90.00
β (°)	91.169(2)	90	82.382(4)	110.542(4)	118.908(3)
γ (°)	90.00	90	72.781(4)	90	90.00
V (Å)	4844(1)	2522.0(5)	1300.5(5)	3242(2)	2414.9(6)
	4	8	2	4	4
F(000)	1896	1056	476	1376	944
Density(cal.)(g cm^{-1})	1.192	1.319	1.115	1.315	1.207
Theta range (°)	1.36 to 28.33	2.15 to 27.99	2.15 to 25.01	1.12 to 28.35	1.33 to 28.34
Reflections measured	32834	16176	7108	22065	15954
Index ranges of measured data	$-6 \le h \le 11$	$-19 \le h \le 16$	$-10 \le h \le 10$	$-16 \le h \le 25$	$-23 \le h \le 23$
	$-44 \le k \le 42$	$-11 \le k \le 11$	$-11 \le k \le 11$	$-12 \le k \le 12$	$-10 \le k \le 11$
	$-21 \le l \le 22$	$-25 \le l \le 21$	$-18 \le l \le 11$	$-25 \le l \le 25$	$-23 \le l \le 19$
Independent reflections	12059 (0.0369)	3041 (0.0496)	4546 (0.0212)	8048(0.029)	5970 (0.0468)
Observed reflection	7276	2044	3311	5739	3982
Absorption correction	multi-scan	multi-scan	multi-scan	multi-scan	multi-scan
Relative transmission Factor	0.749	0.712	0.605	0.883	0.668
Data(obs.)/restraints/parameters	12059/0/538	3041/0/127	4546/0/253	8048/0/361	5970/0/243
Final R indices (obs.)*	$R1 = 0.0465$	$R1 = 0.0432$	$R1 = 0.0649$	$R1 = 0.0507$	$R1 = 0.0495$
	$wR2 = 0.1195$	$wR2 = 0.1167$	$wR2 = 0.2092$	$wR2 = 0.1342$	$wR2 = 0.1169$
R indices (all)*	$R1 = 0.0914$	$R1 = 0.0769$	$R1 = 0.0859$	$R1 = 0.0979$	$R1 = 0.0946$
	$wR2 = 0.1432$	$wR2 = 0.1309$	$wR2 = 0.2282$	$wR2 = 0.1373$	$wR2 = 0.1382$
Goodness-of-fit index	1.011	1.072	1.078	1.034	1.020
Largest difference peak (eÅ^{-3})	0.293,-0.210	0.303, -0.263	0.794, -0.189	0.649,-0.441	0.354, -0.301

Complex	2.4.8	2.4.9	2.4.10	2.4.11	2.4.12
Molecular formula	$[(n\text{-}C_3H_7)_4N^+]\cdot[C_3N_3S_3H^{2-}]\cdot[C(NH_2)_3^+]$	$[(n\text{-}C_4H_9)_4N^+]\cdot[C_3N_3S_3H^{2-}]\cdot[C(NH_2)_3^+]$	$[(CH_3)_4N^+]\cdot[(C_4H_2N_3O_5)^-]$	$[(n\text{-}C_3H_7)_4N^+]\cdot[(C_4H_2N_3O_5)^-]\cdot H_2O$	$2[(CH_3)_4N^+]\cdot 2[(C_4H_2N_3O_5)^-]\cdot(NH_2)_2CS$
Molecular weight	421.69	477.79	246.23	376.46	568.59
Crystal size (mm)	0.28 × 0.23 × 0.23	0.32 × 0.26 × 0.24	0.39 × 0.30 × 0.23	0.49 × 0.43 × 0.40	0.49 × 0.45 × 0.21
Crystal system	Monoclinic	Orthorhombic	Monoclinic	Monoclinic	Triclinic
Space group	$P2_1/c$	$P2_12_12_1$	$C2/c$	$P2_1/c$	$P\bar{1}$
a (Å)	8.925(1)	9.4592(9)	25.900(3)	7.909(1)	10.430(2)
b (Å)	28.979(3)	15.025(2)	5.4215(6)	30.211(4)	11.351(2)
c (Å)	8.968(1)	18.973(2)	18.429(2)	17.531(2)	12.093(2)
α (°)	90	90	90	90	108.958(2)
β (°)	91.614(3)	90	124.027(2)	98.182(6)	93.422(3)
γ (°)	90	90	90	90	96.179(3)
V (Å)	2318.5(5)	2696.4(5)	2144.7(4)	4146(1)	1339.2(4)
	4	4	8	8	2
F(000)	912	1040	1040	1632	600
Density(cal.)(g cm^{-1})	1.208	1.177	1.525	1.206	1.410
Theta range (°)	1.41 to 26.00	1.73 to 26.00	1.90 to 27.99	1.79 to 27.98	1.91 to 28.03
Reflections measured	13632	16046	6933	28114	9585
Index ranges of measured data	$-11 \le h \le 10$	$-11 \le h \le 11$	$-34 \le h \le 33$	$-10 \le h \le 10$	$-13 \le h \le 13$
	$-35 \le k \le 35$	$-18 \le k \le 18$	$-7 \le k \le 5$	$-38 \le k \le 39$	$-14 \le k \le 11$
	$-10 \le l \le 11$	$-16 \le l \le 23$	$-24 \le l \le 21$	$-23 \le l \le 20$	$-15 \le l \le 15$
Independent reflections	4534 (0.0562)	5298 (0.0710)	2575 (0.0210)	9862 (0.0367)	6362 (0.0204)
Observed reflection	2698	2819	2126	5176	4244
Absorption correction	multi-scan	multi-scan	multi-scan	multi-scan	multi-scan
Relative transmission Factor	0.918	0.914	0.802	0.821	0.698
Data(obs.)/restraints/parameters	4534/0/235	5298/0/271	2575/0/163	9862/0/485	6362/48/359
Final R indices (obs.)*	$R1$ = 0.0507	$R1$ = 0.0568	$R1$ = 0.0399	$R1$ = 0.0596	$R1$ = 0.0680
	w$R2$ = 0.1119	w$R2$ = 0.1154	$wR2$ = 0.1103	$wR2$ = 0.1755	$wR2$ = 0.2038
R indices (all)*	$R1$ = 0.0983	$R1$ = 0.1306	$R1$ = 0.0488	$R1$ = 0.1145	$R1$ = 0.0949
	w$R2$ = 0.1286	w$R2$ = 0.1446	$wR2$ = 0.1159	$wR2$ = 0.2199	$wR2$ = 0.2316
Goodness-of-fit index	0.973	1.067	1.065	1.027	1.078
Largest difference peak (eÅ^{-3})	0.283, -0.192	0.286, -0.435	0.337, -0.272	0.368, -0.565	0.677, -0.432

Complex	2.4.13	2.4.14	2.4.15	2.4.16	2.4.17
Molecular formula	$2[(C_2H_5)_4N^+]\cdot[(C_4HN_3O_5)^{2-}]\cdot 2(NH_2)_2CS\cdot H_2O$	$[(n\text{-}C_3H_7)_4N^+]\cdot[(C_4H_2N_3O_5)^-]\cdot(NH_2)_2CS\cdot 2H_2O$	$2[(n\text{-}C_4H_9)_4N^+]\cdot 2[(C_4H_2N_3O_5)^-]\cdot(NH_2)_2CS\cdot H_2O$	$[(C_2H_5)_4N^+]\cdot[(C_4H_2N_3O_5)^-]\cdot 2(NH_2)_2CO\cdot 2H_2O$	$[(n\text{-}C_3H_7)_4N^+]\cdot[(C_4H_2N_3O_5)^-]\cdot 2(NH_2)_2CO$
Molecular weight	601.84	470.59	923.23	458.49	478.56
Crystal size (mm)	0.33 × 0.28 × 0.19	0.50 × 0.41 × 0.31	0.55 × 0.41 × 0.34	0.38 × 0.25 × 0.21	0.47 × 0.41 × 0.28
Crystal system	Orthorhombic	Monoclinic	Triclinic	Monoclinic	Monoclinic
Space group	*Pnna*	*Cc*	$P\bar{1}$	$P2_1/c$	$P2_1/n$
a (Å)	14.713(1)	8.579(2)	8.267(2)	10.130(3)	16.363(2)
b (Å)	29.325(3)	17.024(3)	17.553(3)	14.666(5)	8.843(1)
c (Å)	14.992(1)	17.691(3)	20.357(4)	15.268(5)	18.128(3)
α (°)	90	90.00	65.060(4)	90	90
β (°)	90	91.549(4)	81.386(4)	95.243(7)	103.901(2)
γ (°)	90	90.00	78.292(4)	90	90
V (Å)	6468 (1)	2582.8(8)	2615.9(8)	2259(1)	2546.1(6)
	8	4	2	4	4
F(000)	2608	1016	1004	984	1032
Density(cal.)(g cm^{-1})	1.236	1.210	1.172	1.348	1.248
Theta range (°)	1.53 to 28.31	2.30 to 27.99	2.01 to 25.01	1.93 to 28.44	1.51 to 28.27
Reflections measured	43284	8690	14401	15325	16824
Index ranges of measured data	$-19 \le h \le 9$	$-7 \le h \le 11$	$-9 \le h \le 9$	$-8 \le h \le 13$	$-21 \le h \le 13$
	$-38 \le k \le 39$	$-22 \le k \le 22$	$-17 \le k \le 20$	$-18 \le k \le 19$	$-11 \le k \le 11$
	$-20 \le l \le 19$	$-23 \le l \le 23$	$-17 \le l \le 24$	$-19 \le l \le 20$	$-24 \le l \le 24$
Independent reflections	8035 (0.0528)	4706 (0.0227)	9178 (0.0272)	5635 (0.0572)	6304 (0.0281)
Observed reflection	5103	4153	5396	5103	3778
Absorption correction	multi-scan	multi-scan	multi-scan	multi-scan	multi-scan
Relative transmission Factor	0.655	0.718	0.717	0.623	0.790
Data(obs.)/restraints/parameters	8035/0/357	4706/2/289	9178/1/584	5635/0/289	6304/0/307
Final *R* indices (obs.)*	*R*1 = 0.0654	*R*1 = 0.0338	*R*1 = 0.0634	*R*1 = 0.0562	*R*1 = 0.0485
	w*R*2 = 0.1916	w*R*2= 0.0867	w*R*2 =0.1838	w*R*2 = 0.1348	w*R*2 = 0.1308
R indices (all)*	*R*1 = 0.1322	*R*1 = 0.0404	*R*1 = 0.1127	*R*1 = 0.1270	*R*1= 0.0876
	w*R*2 = 0.2524	w*R*2 = 0.0928	w*R*2 = 0.2089	w*R*2 = 0.1645	w*R*2 = 0.1588
Goodness-of-fit index	1.011	1.023	1.079	1.030	1.011
Largest difference peak (eÅ^{-3})	0.607, -0.602	0.175, -0.161	0.430, -0.272	0.449, -0.328	0.303, -0.203

Complex	2.4.18	2.4.19	2.4.20	2.4.21	2.4.22
Molecular formula	$[(n\text{-}C_4H_9)_4N^+]\cdot[(C_4H_2N_3O_5)^-]\cdot(NH_2)_2CO\cdot 2H_2O$	$3[(C_2H_5)_4N^+]\cdot(H^+)[C_3HN_2^-(CO_2^-)(CO_2H)]_2\cdot 8H_2O$	$2[(C_2H_5)_4N^+]\cdot[C_3HN_2^-(CO_2^-)(CO_2H)]\cdot 2[(NH_2)_2CS]$	$[(n\text{-}C_4H_9)_4N^+]\cdot[C_3HN_2H(CO_2^-)(CO_2H)]\cdot[(NH_2)_2CS]\cdot 2H_2O$	$[(n\text{-}C_3H_7)_4N^+]\cdot[C_3HN_2^-(CO_2^-)(CO_2H)]\cdot[C(NH_2)_3^+]\cdot H_2O$
Molecular weight	510.64	844.06	566.83	509.71	418.54
Crystal size (mm)	0.35 × 0.30 × 0.20	0.45 × 0.40 × 0.34	0.28 × 0.25 × 0.20	0.49 × 0.40 × 0.33	0.35 × 0.30 × 0.28
Crystal system	Monoclinic	Monoclinic	Monoclinic	Monoclinic	Orthorhombic
Space group	*Cc*	*C2/c*	$P2_1/n$	$P2_1$	$Pca2_1$
a (Å)	13.272(2)	21.655(2)	12.025(4)	9.470(3)	18.059(7)
b (Å)	13.368(1)	14.531(1)	18.038(6)	16.005(3)	8.222(3)
c (Å)	15.709(2)	15.044(1)	15.050(5)	9.968(3)	31.49(1)
α (°)	90.00	90	90	90	90
β (°)	91.337(2)	91.318(2)	108.795(6)	90.499(4)	90
γ (°)	90.00	90	90	90	90
V (Å)	2786.1(5)	4732.7(8)	3091(2)	1510.7(7)	4675(3)
	4	4	2	2	8
F(000)	1112	1848	1232	1016	1824
Density(cal.)(g cm^{-1})	1.217	1.185	1.218	1.121	1.189
Theta range (°)	2.16 to 28.32	0.98 to 25.01	1.82 to 28.00	2.04 to 28.30	1.29 to 26.00
Reflections measured	9624	13831	20203	10555	26220
Index ranges of measured data	$-16 \le h \le 17$	$-26 \le h \le 17$	$-15 \le h \le 15$	$-12 \le h \le 12$	$-12 \le h \le 12$
	$-16 \le k \le 17$	$-17 \le k \le 17$	$-23 \le k \le 23$	$-21 \le k \le 11$	$-21 \le k \le 11$
	$-20 \le l \le 20$	$-18 \le l \le 18$	$-19 \le l \le 14$	$-12 \le l \le 13$	$-12 \le l \le 13$
Independent reflections	5778 (0.0662)	4653 (0.0433)	7436 (0.0320)	5860 (0.0453)	9075
Observed reflection	4414	2408	5296	3120	5184
Absorption correction	multi-scan	multi-scan	multi-scan	multi-scan	multi-scan
Relative transmission Factor	0.830	0.798	0.806	0.777	0.850
Data(obs.)/restraints/parameters	5778/2/324	4653/0/262	7436/0/338	5860/1/312	9075/1/524
Final *R* indices (obs.)*	*R*1 = 0.0542	*R*1 = 0.0591	*R*1 = 0.0533	*R*1 = 0.0511	*R*1 = 0.0474
	w*R*2 = 0.1403	w*R*2 = 0.1732	w*R*2 = 0.1469	w*R*2 = 0.1048	w*R*2 = 0.0993
R indices (all)*	*R*1 = 0.0677	*R*1 = 0.1153	*R*1 = 0.0811	*R*1 = 0.1171	*R*1 = 0.1040
	w*R*2 = 0.1509	w*R*2 = 0.1998	w*R*2 = 0.1571	w*R*2 = 0.1300	w*R*2 = 0.1270
Goodness-of-fit index	0.960	1.011	1.099	0.994	1.035
Largest difference peak (eÅ^{-3})	0.193, -0.182	0.286, -0.181	0.509, -0.305	0.179, -0.200	0.162, -0.170

*$R1 = \sum \| F_o | - | F_c \| / \sum | F_o |$, $wR2 = [\sum w(F_o^2 - F_c^2)^2 / \sum w(F_o^2)^2]^{1/2}$

Appendix III: Atomic Coordinates, Thermal Parameters, Bonds Lengths and Bond Angles

Available as an electronic file